

AD-A038 299

ILLINOIS UNIV AT URBANA-CHAMPAIGN DEPT OF ELECTRICAL --ETC F/6 17/2.1
TECHNIQUES OF DETERMINING IONOSPHERIC STRUCTURE FROM OBLIQUE RA--ETC(U)
DEC 76 N N RAO, K C YEH, M Y YOUAKIM F19628-75-C-0088

UNCLASSIFIED

UILU-ENG-76-2559

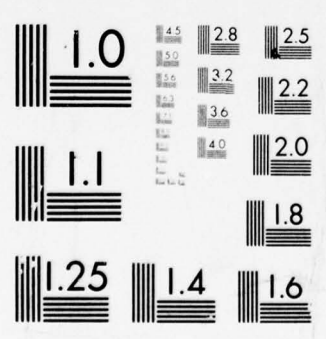
RADC-TR-76-401

NL

1 OF 3
AD
A038 299



OF
038 299



MICROCOPY RESOLUTION TEST CHART
NATIONAL BUREAU OF STANDARDS-1963-A

ADA 038299

RADC-TR-76-401
Final Technical Report
December 1976

17



TECHNIQUES OF DETERMINING IONOSPHERIC STRUCTURE
FROM OBLIQUE RADIO PROPAGATION MEASUREMENTS

Ionosphere Radio Laboratory
Department of Electrical Engineering
University of Illinois at Urbana-Champaign

Approved for public release; distribution unlimited.

ROME AIR DEVELOPMENT CENTER
AIR FORCE SYSTEMS COMMAND
GRIFFISS AIR FORCE BASE, NEW YORK 13441

DDDC
APR 15 1977
RECEIVED

NO. _____
DDDC FILE COPY

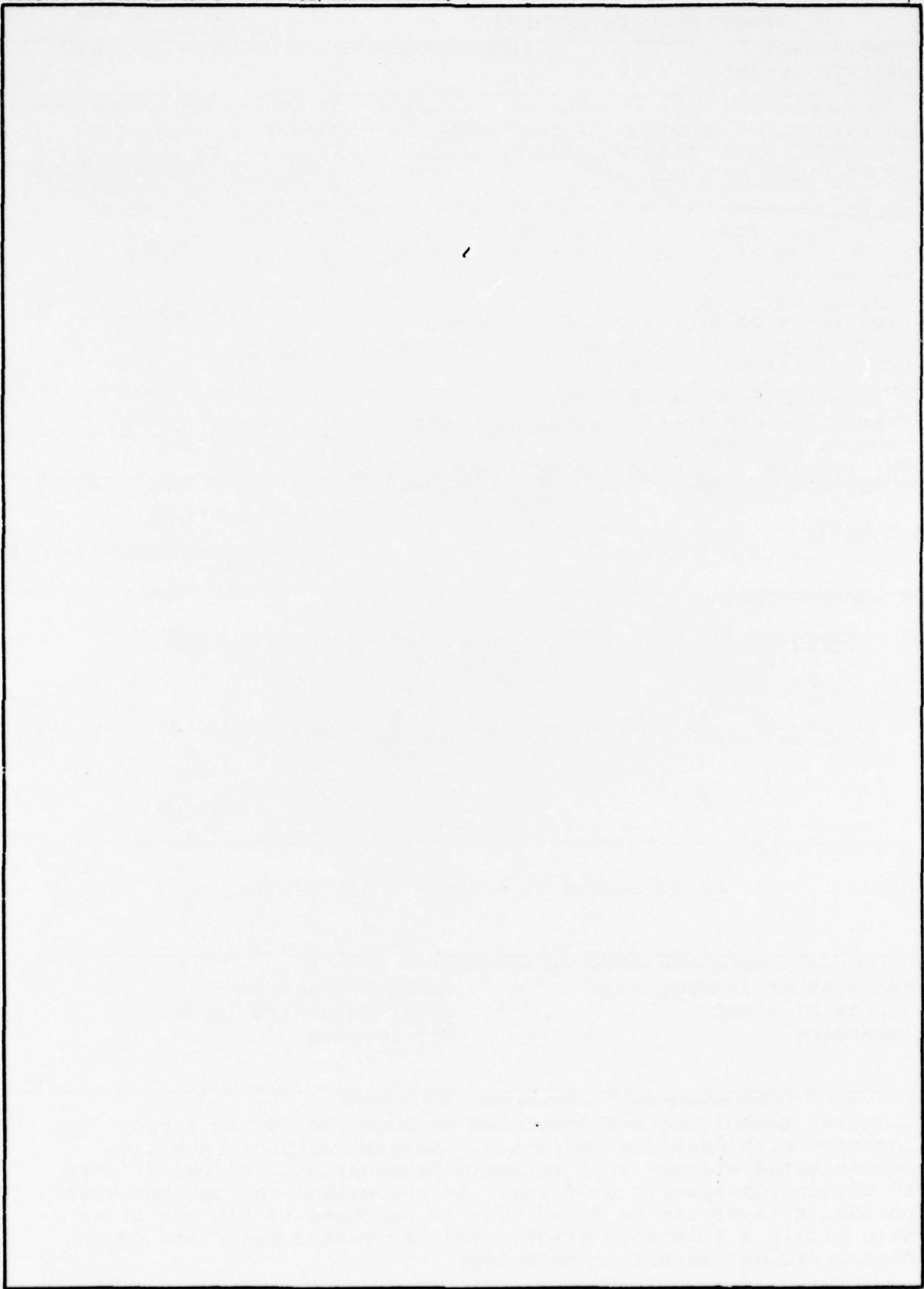
Qualified requesters may obtain additional copies from the Defense Documentation Center. All others should apply to the National Technical Information Service.

Unclassified

SECURITY CLASSIFICATION OF THIS PAGE (When Data Entered)

| REPORT DOCUMENTATION PAGE | | READ INSTRUCTIONS BEFORE COMPLETING FORM |
|---|-----------------------|--|
| 1. REPORT NUMBER RADC-TR-76-401 | 2. GOVT ACCESSION NO. | 3. RECIPIENT'S CATALOG NUMBER |
| 4. TITLE (and Subtitle) TECHNIQUES OF DETERMINING IONOSPHERIC STRUCTURE FROM OBLIQUE RADIO PROPAGATION MEASUREMENTS. | | 5. TYPE OF REPORT & PERIOD COVERED Final, October 1974 through September 1976 |
| 7. AUTHOR(s) N. Narayana/Rao, K. C./Yeh, M. Y./Youakim, K. E. Hoover, P. Parhami, R. E. DuBroff | | 6. PERFORMING ORG. REPORT NUMBER TR No. 59, UILU-ENG-76-2559 |
| 9. PERFORMING ORGANIZATION NAME AND ADDRESS Department of Electrical Engineering University of Illinois at Urbana-Champaign Urbana, Illinois 61801 | | 8. CONTRACT OR GRANT NUMBER(s) F19628-75-C0088 |
| 11. CONTROLLING OFFICE NAME AND ADDRESS Deputy for Electronic Technology (RADC/EREI) Hanscom AFB, MA. 01731 Dr. Terence J. Elkins and Mr. Ming S. Wong | | 10. PROGRAM ELEMENT, PROJECT, TASK AREA & WORK UNIT NUMBERS 61102F 56311601 |
| 14. MONITORING AGENCY NAME & ADDRESS (if different from Controlling Office) <i>11/ Dec 76</i> <i>12/ 282p.</i> | | 12. REPORT DATE December 1976 |
| | | 13. NUMBER OF PAGES 279 |
| | | 15. SECURITY CLASS. (of this report) Unclassified |
| | | 15a. DECLASSIFICATION/DOWNGRADING SCHEDULE |
| 16. DISTRIBUTION STATEMENT (of this Report) A - Approved for public release; distribution unlimited <i>9/ Final rept. Oct 74 - Sep 76,</i> | | |
| 17. DISTRIBUTION STATEMENT (of the abstract entered in Block 20, if different from Report) <i>14/ UILU-Eng-76-2559, TR-59</i> | | |
| 18. SUPPLEMENTARY NOTES Appendix 4 to be published in Radio Science | | |
| 19. KEY WORDS (Continue on reverse side if necessary and identify by block number) backscatter leading edge oblique ionogram homing of a ray quasi-parabolic layer inversion ray tracing | | |
| 20. ABSTRACT (Continue on reverse side if necessary and identify by block number) Computer techniques are developed to home the ray at a specified location with specified accuracy. Several methods have been investigated whereby oblique radio propagation data can be used to obtain ionospheric profiles. In one method the optimum quasi-parabolic layer can be found that is supposed to fit the given data within a tolerable error. Another method makes use of the Backus-Gilbert inversion technique. | | |

SECURITY CLASSIFICATION OF THIS PAGE(When Data Entered)



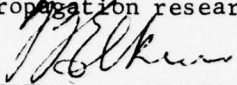
SECURITY CLASSIFICATION OF THIS PAGE(When Data Entered)

EVALUATION

F19628-75-C-0088 - University of Illinois

1. This report is the Final Report on this contract, covering two fiscal years work on the development of mathematical techniques for inversion of oblique ionograms.

2. The work reported is significant from both scientific and applied viewpoints and represents a major contribution to the subject. The techniques developed can and will be applied to the propagation management of operational OTH radars and have other potential applications in HF radio propagation research and technology.


TERENCE J. ELKINS
Contract Monitor
Ionospheric Radio Physics Branch
Electromagnetic Sciences Division

| | | |
|-------|-------------------------------------|-------------------------------------|
| AC | | <input checked="" type="checkbox"/> |
| AFIS | AFIS | <input checked="" type="checkbox"/> |
| EO | EO | <input type="checkbox"/> |
| ENR | ENR | <input type="checkbox"/> |
| J | J | <input type="checkbox"/> |
| BY | DISTRIBUTION/AVAILABILITY STATEMENT | |
| Dist. | Avail. and/or Sale | Dist. |
| A | | |

ACKNOWLEDGMENT

We would like to thank our contract monitors Dr. Terence J. Elkins and Mr. Ming S. Wong for providing us with the ray tracing program and the Air Force model ionosphere, based on which we have carried out our computations. The expert typing is the work of Mrs. Linda Houston.

The financial support of this work was provided by Rome Air Development Center, Deputy for Electronic Technology (ETEI), L G Hanscom Air Force Base, MA., under Contract F19628-75-C0088.

TABLE OF CONTENTS

| | Page |
|---|------|
| 1. Introduction | 1 |
| 2. Homing of the Ray. | 4 |
| 2.1 Introduction. | 4 |
| 2.2 Ground-to-ground homing | 5 |
| 2.2.1 General description. | 5 |
| 2.2.2 Approximate elevation angle - single layer ionosphere | 8 |
| 2.2.3 Approximate elevation angle - multiple layer ionosphere | 16 |
| 2.2.4 Refinement of the elevation angle. . . | 17 |
| 2.2.5 Group path homing. | 23 |
| 2.2.6 Examples and Discussion. | 24 |
| 2.3 Ground-Satellite homing | 37 |
| 2.3.1 Approximate elevation angle. | 37 |
| 2.3.2 Refinement of the elevation angle. . . | 41 |
| 2.3.3 Examples and Discussion. | 43 |
| 2.4 Minimum Group path. | 49 |
| 2.4.1 Chopping technique | 49 |
| 2.4.2 Examples | 53 |
| 2.5 Computer programs | 55 |
| 2.5.1 General description. | 55 |
| 2.5.2 Program listings | 65 |
| 2.6 Discussion. | 66 |
| 3. Analysis of Oblique Propagation Data | 68 |
| 3.1 Introduction. | 68 |
| 3.1.1 Point-to-point oblique ionograms . . . | 68 |
| 3.1.2 Backscatter leading edge | 70 |
| 3.2 The Quasi-parabolic Layer | 73 |
| 3.2.1 The earth-concentric quasi- parabolic layer. | 74 |
| 3.2.2 The eccentric quasi-parabolic layer. . | 76 |
| 3.3 Inversion of point-to-point oblique ionograms | 83 |
| 3.3.1 Sensitivity analysis | 83 |
| 3.3.2 Determination of initial set of parameters | 89 |
| 3.3.3 Inversion of synthesized oblique ionograms. | 92 |
| 3.3.4 Inversion of experimental oblique ionograms. | 102 |
| 3.4 Inversion of backscatter leading edge | 108 |
| 3.4.1 Basic inversion technique. | 108 |
| 3.4.2 Inversion of synthesized QP layer data | 113 |
| 3.4.3 Inversion of synthesized data involving horizontal gradients | 118 |

TABLE OF CONTENTS CONT.

| | Page |
|--|------|
| 3.4.4 Inversion of synthesized data for three-dimensional ionosphere. | 127 |
| 3.4.5 Application of the backscatter inversion technique | 133 |
| 3.5 General consideration of the inversion problem. | 155 |
| 3.6 Conclusions. | 156 |
| 4. Recommendations for Future Work | 157 |
| Appendix 1. | 159 |
| Appendix 2. | 208 |
| Appendix 3. | 211 |
| Appendix 4. | 249 |
| References. | 265 |

LIST OF FIGURES

| Figure | | Page |
|--------|---|------|
| 2.1 | Idealized sketch showing the nature of ground distance dependence on the elevation angle of once reflected ray from a single layer ionosphere | 6 |
| 2.2 | Sketch showing the geometry of the re- flected ray. | 9 |
| 2.3 | Earth geometry for finding the coordinates of the midpoint. | 10 |
| 2.4 | Sketch showing the ground distance - elevation angle curve for a four-layer ionosphere | 18 |
| 2.5 | Sketch illustrating the homing in azimuth. . . | 22 |
| 2.6 | Example 1 illustrating the ground-to- ground homing using the Air Force supplied model ionosphere. The example shows how the initial elevation is determined. | 26 |
| 2.7 | Continuation of the example shown in Fig. 2.6 This shows the refinement procedure in ground distance and azimuth homing using 3D ray tracing | 27 |
| 2.8 | Example 2 illustrating the ground-to-ground homing for rays reflected from a two-layer ionosphere. Note that for a ground range of 1039.36 km, three approximate solutions (indicated by circle A, circle B and circle C) in the elevation angle exist in this case. . | 29 |
| 2.9 | Continuation of Example 2 shown in Fig. 2.8 illustrating the ground distance homing for circle A and circle C using 3D ray tracing. . . | 31 |
| 2.10 | Continuation of Example 2 illustrating azimuthal correction for final homing of the ray on the receiver | 32 |
| 2.11 | Computed initial group path versus elevation angle curve for Example 3. For a specified group path of 2654.08 km two solutions are indicated | 33 |
| 2.12 | Continuation of Example 3 illustrating group path homing for two rays. | 35 |

| Figure | | Page |
|--------|--|------|
| 2.13 | Sketch showing the geometry of ground-satellite homing. | 38 |
| 2.14 | Sketch showing the geometry of satellite-ground homing | 39 |
| 2.15 | Earth geometry for finding the optical elevation angle | 42 |
| 2.16 | Example illustrating ground-to-satellite homing. The plot shows ground distance between the transmitter and the sub-satellite point versus the elevation angle for successive iterations using 3D ray tracing at three frequencies 90 MHz, 170 MHz and 250 MHz | 44 |
| 2.17 | Continuation of example shown in Fig. 2.16 illustrating that no azimuthal correction is needed for homing at all three frequencies. | 46 |
| 2.18 | Example illustrating satellite-to-ground homing for three radio frequencies 70 MHz, 140 MHz and 210 MHz. | 47 |
| 2.19 | Continuation of example shown in Fig. 2.18 illustrating that no azimuthal correction is needed for homing at all three frequencies. | 48 |
| 2.20 | Sketch showing the general behavior of group path versus elevation angle curve . . | 51 |
| 2.21 | Sketch illustrating three possibilities for purpose of finding the minimum group path ray. | 52 |
| 2.22 | Example illustrating the steps in finding the minimum group path ray in a group path versus elevation angle plot. Note the index shifting, equal chopping and final location of the minimum group path to within the tolerance | 56 |
| 2.23 | Another example illustrating the steps in finding the minimum group path ray. | 57 |
| 3.1a | Ray paths for point-to-point oblique ionograms at different frequencies. | 69 |

| Figure | | Page |
|--------|--|------|
| 3.1b | Typical shape of one-hop trace for point-to-point oblique ionogram | 69 |
| 3.2a | Ray paths for backscattered rays at one frequency | 71 |
| 3.2b | Showing that the leading edge of a backscatter ionogram is the tangent curve to a continuum of point-to-point oblique ionograms | 71 |
| 3.3 | The eccentric quasi-parabolic model with its defining parameters | 78 |
| 3.4 | The geometry for computing gradients as a function of ω_t , D | 80 |
| 3.5 | Peak height gradient as a function of D and ω_t | 82 |
| 3.6 | Effect of the f_c (critical frequency parameter (in MHz) | 84 |
| 3.7 | Effect of changing h_o ; the layer base-height (in km). | 85 |
| 3.8 | Effect of changing the layer semi-thickness y_m (in km). | 86 |
| 3.9 | Effect of changing the D parameter (in km). | 87 |
| 3.10 | Effect of varying the ω_t parameter (in degrees). | 88 |
| 3.11 | Determining an initial set of parameters. | 91 |
| 3.12 | Inverting numerically synthesized data. | 95 |
| 3.13 | Synthesized oblique ionograms for Range=1111.7 km and $\omega_t=0^\circ$. The parameter D is successively changed by 500 km. For each D, the remaining three parameters are adjusted so as to force the curve through the three points marked by X. The parameters for the two extreme curves are given above | 96 |

| Figure | | Page |
|---------|--|------|
| 3.14 | Technique for the inversion of real data. The first three data points are adjusted so that the technique in Section 3.3.3 can be employed for minimizing $(\Delta f_4)^2 + (\Delta f_5)^2$ | 100 |
| 3.15 | Method of steepest descent for inverting actual data | 103 |
| 3.16 | Graphical illustration of the least squared error method of backscatter ionogram leading-edge inversion for a Q-P ionosphere. | 110 |
| 3.17 | Nominal electron density profile. | 121 |
| 3.18 | Reconstruction of ground range. | 135 |
| 3.19 | Limitations of information contained in data. | 136 |
| 3.20 | Interpolation procedure | 140 |
| 3.21 | Block diagram of steps involved in backscatter leading edge inversion and application. | 141 |
| A.3.1 | Flow chart for main program | 233 |
| A.3.2 | Flow chart for subroutine FUNCT | 234 |
| A.3.3.a | Flow chart for subroutine BACKS3 (continued next figure). | 235 |
| A.3.3.b | Flow chart for subroutine BACKS3 (continuation of Fig. A.3.3.a). | 236 |
| A.3.4.a | Flow chart for subroutine FSTDFS (continued on next figure) | 237 |
| A.3.4.b | Flow chart for subroutine FSTDFS (continuation of Fig. A.3.4.a). | 238 |
| A.3.5 | Flow chart for subroutine DCAL. | 239 |
| A.3.6 | Flow chart for special functions (square root, log, and \cos^{-1}) | 240 |
| A.3.7 | Sequence of data cards. | 241 |

LIST OF TABLES

| Table | Page |
|--------|---|
| 3.1 | Inversion of synthesized oblique ionograms using the technique in section 3.3.3 98 |
| 3.2 | Inversion of real oblique ionograms, using the technique in section 3.3.3 101 |
| 3.3(a) | Inversion of an actual ionogram. 106 |
| 3.3(b) | Inversion of an actual ionogram. 107 |
| 3.4 | Synthesized noisy backscatter ionogram leading edge data inversion assuming a spherical earth-concentric quasi-parabolic ionosphere model 114 |
| 3.5 | Noisy backscatter leading edge synthesis assuming earth-centered Q-P ionosphere $r_b=6570$ km, $r_m=6720$ km, and $f_c=7.0$ MHz 116 |
| 3.6 | Results of Inversion of the data in Table 3.4, using various numbers of points in E. 117 |
| 3.7 | Inversion of synthesized backscatter leading edge data for an eccentric quasiparabolic layer 119 |
| 3.8 | Group path (km) to leading edge of backscatter ionogram for various linear tilts and gradients. 122 |
| 3.9 | Ground range (km). 123 |
| 3.10 | Height of maximum plasma frequency ($h_m F_2$) (kilometers) 124 |
| 3.11 | Base height of ionosphere (km) 125 |
| 3.12 | Critical frequency ($f_o F_2$) (in MHz) 126 |
| 3.13 | Results of inversion of simulated backscatter ionogram data. 128 |
| 3.14 | Computed minimum group path data and other propagation parameters for transmitter location of $40^\circ N$, $175^\circ W$, and 330° azimuth. 130 |

| Table | Page |
|-------|---|
| 3.15 | Same as Table 3.14 except for 358° azimuth . . . 131 |
| 3.16 | Computed QP layer parameter values and the corresponding ground ranges for 330° azimuth 132 |
| 3.17 | Same as Table 3.16, except for 358° azimuth 132 |
| 3.18 | Group path and ground range versus elevation angle for 16 MHz and for 340° azimuth, using the originally assumed model 137 |
| 3.19 | Same as Table 3.18 except using computed ionosphere 137 |
| 3.20 | Same as Table 3.18 except using the simplified ionospheric model. 142 |
| 3.21 | The effect of varying r_b initial estimate upon inversion of group path into ground range (untilted ionosphere). 144 |
| 3.22 | The effect of varying the initial estimate of critical frequency upon inversion of group path into ground range (untilted ionosphere) 146 |
| 3.23 | The effect of varying layer semithickness upon inversion of group path to ground range (untilted ionosphere) 147 |
| 3.24 | The effect of the initial estimate of r_b (radius to ionospheric base) upon the inversion of group path into ground range 148 |
| 3.25 | The effect of initial estimate of critical frequency (f_c) upon inversion 149 |
| 3.26 | The effect of initial estimate of r_m upon inversion of group path into ground ^m range. Program was allowed to go 40 iterations in computing QPP 150 |
| 3.27 | The effect of varying the layer semithickness upon the inversion of group path to ground range 151 |
| 3.28 | The effect of initial estimate of r_m upon inversion of group path into ground ^m range. Program was allowed to go 80 iterations in fitting QPP. 153 |

| Table | Page |
|-------|---|
| 3.29 | Variance resulting from different values of r_m as affected by iteration number 154 |

1. INTRODUCTION

The use of pulse sounding as an experimental technique in the investigation of the ionosphere can be traced back to Breit and Tuve (1926). These authors invented such a technique to prove the existence of the ionosphere. Modern reviews of these early endeavors can be found in Waynick (1974) and Booker (1974). The improved electronic technology after the Second World War stimulated interest in the possibility of computing the electron density profiles from pulse sounding data whose carrier frequency was swept. While the major emphasis has been towards inverting the vertical sounding data for electron density profiles, there have also been sporadic attempts to devise techniques of obtaining ionospheric structure from oblique sounding data. Our work, reported here, is concerned with this later problem.

Mathematically, the group delay measured experimentally is a nonlinear functional of the electron density profile. As such this is very difficult to solve. Fortunately, for vertical incidence case with the geomagnetic field ignored, the integral can be cast in the form of a convolution integral known as Abel's integral equation which can then be solved, for example, by Laplace transform (Manning, 1947). Once the geomagnetic field effect is introduced or when the propagation path becomes oblique, the convolution integral property is destroyed. The problem becomes much more difficult. The methods that have been devised in the literature are almost all numerical. Ours is no exception. In this connection, the capability of homing the ray at a specified

location with specified tolerance must be established first. This is the subject of Chapter 2. In ray homing we are interested in three configurations: ground-to-ground homing via a reflection from the ionosphere, ground-to-satellite homing via transmission through the ionosphere and satellite-to-ground homing also via transmission through the ionosphere. In each case, the homing is achieved through an iterative procedure whereby the ray lands at a point successively closer to the given location. Several examples are also given to illustrate the method used. The inversion of backscatter ionograms utilizes the values of the minimum group path computed for a given ionospheric profile. It is therefore desirable to have the capability of computing the minimum group path. A chopping method is used to achieve this and two examples are given to illustrate the procedure involved. In order to achieve these capabilities, the Air Force supplied three-dimensional ray tracing program and the associated electron density model are augmented by seven subroutines. These subroutines are fully described and documented with computer listings.

The major objective of this research is to investigate methods whereby oblique radio propagation data can be used to obtain ionospheric profiles. This is contained in Chapter 3. There exist in practice two kinds of oblique propagation data: point-to-point oblique ionograms and backscatter leading edges. The nature of these data and their intuitive limitations are discussed in section 3.1. In many ionospheric propagation studies, the quasi-parabolic layer has been found to give adequate accuracy. Further, such a layer has a relatively small number of parameters (3, consisting of critical frequency, base

height of the ionosphere and the semi-thickness) and, in many cases, the desired expressions can be evaluated analytically. For this reason our inversion is based on finding the optimum quasi-parabolic layer that fits the given data within a tolerable error. After some discussion of the nature and properties of the quasi-parabolic layer in section 3.2, we go directly to the inversion problem. The inversion of a point-to-point oblique ionogram is discussed first (section 3.3), which is then followed by a discussion of backscatter leading edge (section 3.4). The results are given in terms of graphs and tables. In addition to approaches discussed in 3.3 and 3.4, we have also looked into the inversion problem from general considerations (section 3.5 and Appendix 4). This inversion method makes use of the Backus-Gilbert technique and seems to be very promising. Finally, the report is concluded in Chapter 4 with recommendations for future research.

2. HOMING OF THE RAY

2.1 Introduction

Homing of the ray is the main objective of this chapter. Our study deals with the modification of the three dimensional ray tracing program to incorporate the homing features for ground-to-ground, ground-to-satellite, and satellite-to-ground propagation.

Homing of the ray to the required location can be obtained through an iterative procedure by homing first to the ground distance for a fixed value of the azimuthal angle. If the ground distance homing is successful the azimuthal angle of the transmitted ray is then corrected next. This type of iteration requires back and forth transfer from homing in ground distance to homing in azimuthal angle. The iteration stops when the errors are smaller than the prescribed values.

For each of the three configurations studied we present a detailed development of the technique applied to achieve homing of the ray together with some examples. Difficulties encountered during the course of the study are also pointed out. In section 2.2 we discuss the ground-to-ground homing procedure for a single and multiple layer ionosphere. The ground-to-satellite and satellite-to-ground configurations together with examples to illustrate the homing technique are presented in section 2.3. In section 2.4 we discuss the chopping method utilized in finding the minimum group path for a given transmitter location, azimuthal angle, and oblique frequency. A listing of the computer programs developed under this study together with their description is included in section 2.5. Finally, in section 2.6 we discuss the current

accomplishments and outline suggestions towards future improvement and possible additions to the three dimensional ray tracing program.

2.2 Ground-to-Ground Homing

The ground-to-ground homing is the most involved configuration of the homing study. Given the transmitter and receiver coordinates on the Earth's surface, the electron density profile, the oblique transmission frequency we find an initial approximate elevation angle that will home the ray to the receiver via reflection from the ionosphere. This approximate elevation angle is then used as an initial input for the final homing of the ray through the three dimensional ray tracing computer program.

2.2.1 General Description

It is well known that for a given single-layer ionosphere and a given radio frequency the one-hop ground distance, D , as a function of elevation angle, β , has the dependence sketched in Figure 2.1. Several features of this figure are worth noting. Due to spherical geometry, the ground distance has some finite value, D_0 , even when the elevation angle is zero. As the elevation angle increases, the ground distance decreases to a minimum value D_s at β_s . This is the skip distance and consequently the use of subscript s on all quantities related to the skip ray. For $\beta > \beta_s$ the ground distance increases again and approaches to infinity at $\beta = \beta_t$ at which the ray becomes trapped. A figure such as Figure 2.1 suggests the following three possibilities:

- i) For $D < D_s$ the observer is in the shadow region and no ray can reach the observer via reflection from the ionosphere.

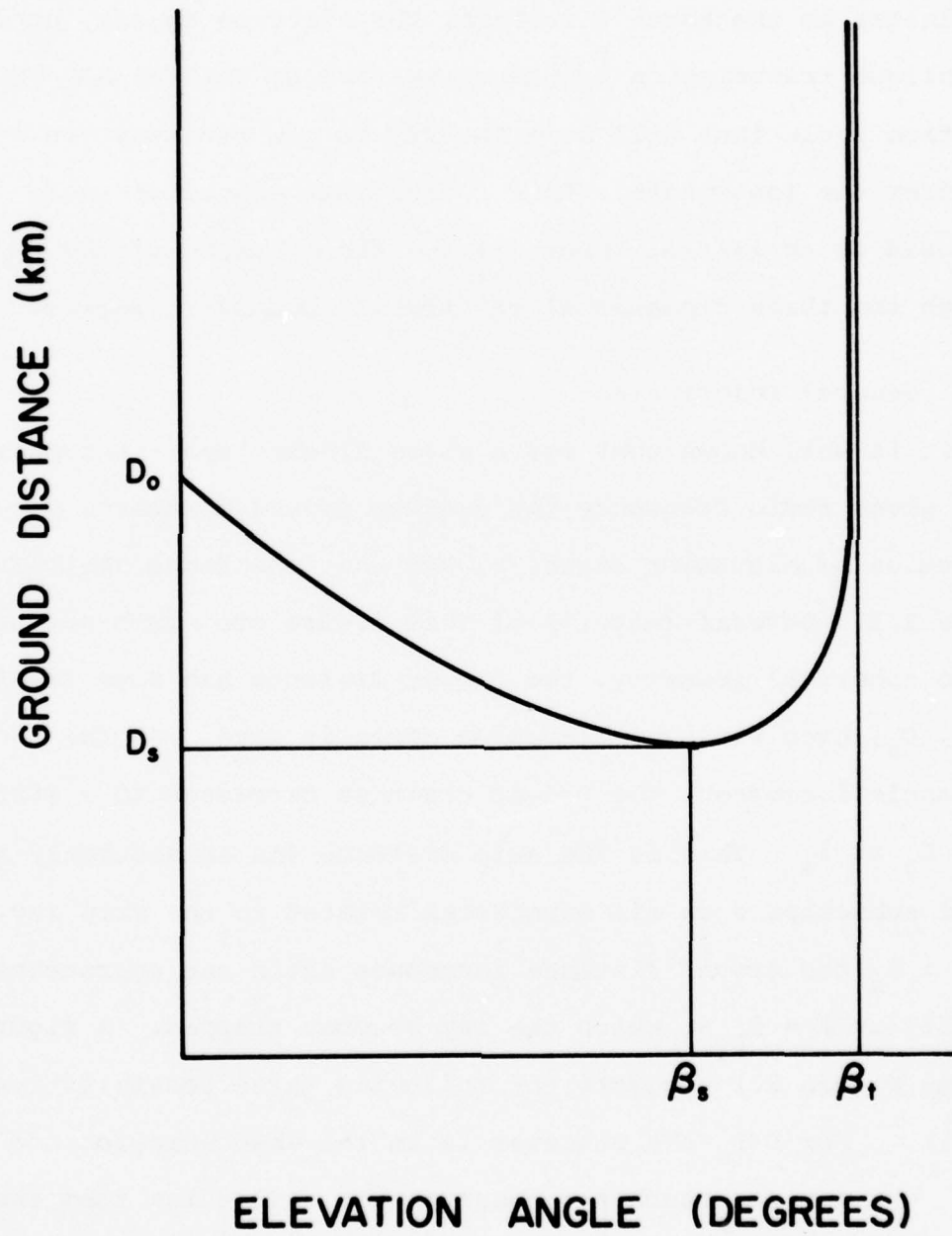


Figure 2.1. Idealized sketch showing the nature of ground distance dependence on the elevation angle of once reflected ray from a single layer ionosphere.

- ii) For $D_0 < D < D_s$ the observer is in the illuminated region within which a low ray and a high ray (Pedersen ray) can reach the observer.
- iii) For $D > D_0$ the low ray is cut off by the earth shadow and only the high ray can reach the observer. Generally, the high ray with an elevation angle β near β_t is very much de-focussed and is very sensitive to elevation angles and small changes in the ionospheric model.

Based upon the above observations, we outline the procedure to obtain an approximate homing elevation angle. This approximate angle is then refined through utilization of the three dimensional ray tracing program.

The given ionosphere at the midpoint of the transmitter and receiver is approximated by segments of a second degree polynomial which for the i^{th} segment has the form

$$N_i(r) = a_i + \frac{b_i}{r} + \frac{g_i}{r^2} \quad r_{i-1} \leq r \leq r_i \quad (2.1)$$

The coefficients are chosen by fitting to the given ionospheric model and making sure that both the density and its derivatives are continuous in going from segment to segment. Using the electron density profile given by (2.1) we find analytic expressions for the ground distance (range) D and the virtual path (group path) P' . Since the trapped rays are known to have ray apogee slightly below the peak of the layer and since the high rays are very sensitive near β_t we let the ray apogee occur at the ionospheric peak as an approximation and find the penetration angle β_p . In general β_p so found is slightly less than β_t . Then, from the range

of elevation angles we calculate the corresponding ground distances and group paths through the analytical expressions, thus generating a table of elevation angles versus ground distance and group path. The ground distance between the transmitter and receiver is compared with the tabulated ground distances. If $D < D_s$ there is no solution; if $D = D_s$ there is possibly one solution; if $D_s < D < D_0$ there are two solutions; and $D > D_0$ there is one solution. The solutions, if they exist, are found by linear interpolation. Once the solutions are found, the approximate elevation angles serve as the initial input in the ray tracing program to eventually home the ray.

2.2.2 Approximate Elevation Angle-Single Layer Ionosphere

The geometry of the ground-to-ground homing problem is shown in Figure 2.2. We assume that the transmitter and receiver coordinates are given in geographic east longitude and north latitude. The ground distance, D_{TR} , between the transmitter and receiver is given by

$$D_{TR} = r_0 \gamma \quad (2.2)$$

where r_0 is the earth radius in km and γ is the angle subtended at the earth center between the transmitter and receiver. Applying the cosine law of spherical trigonometry to Figure 2.3, angle γ is

$$\gamma = \cos^{-1} [\cos \theta_T \cos \theta_R + \sin \theta_T \sin \theta_R \cos (\phi_T - \phi_R)] \quad (2.3)$$

where θ_T, θ_R are the colatitudes, ϕ_T, ϕ_R are the longitudes of

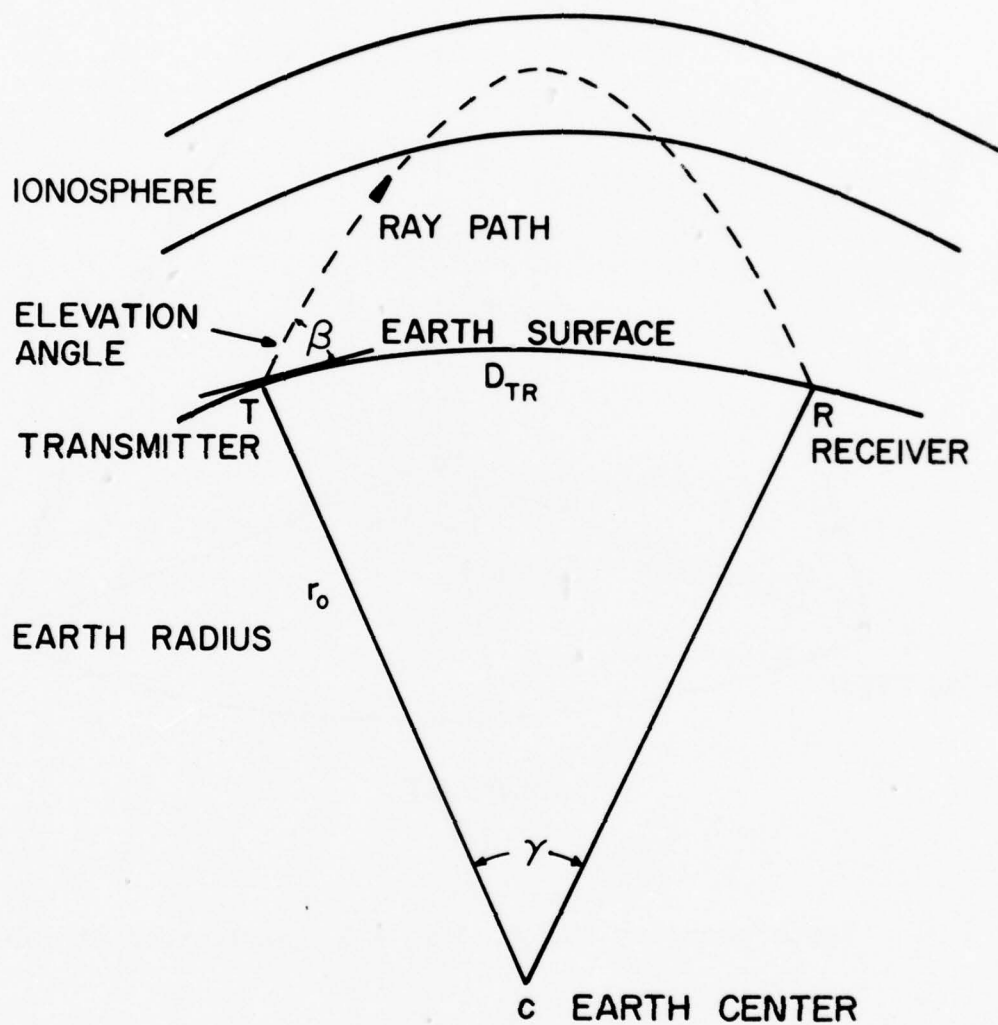


Figure 2.2. Sketch showing the geometry of the reflected ray.

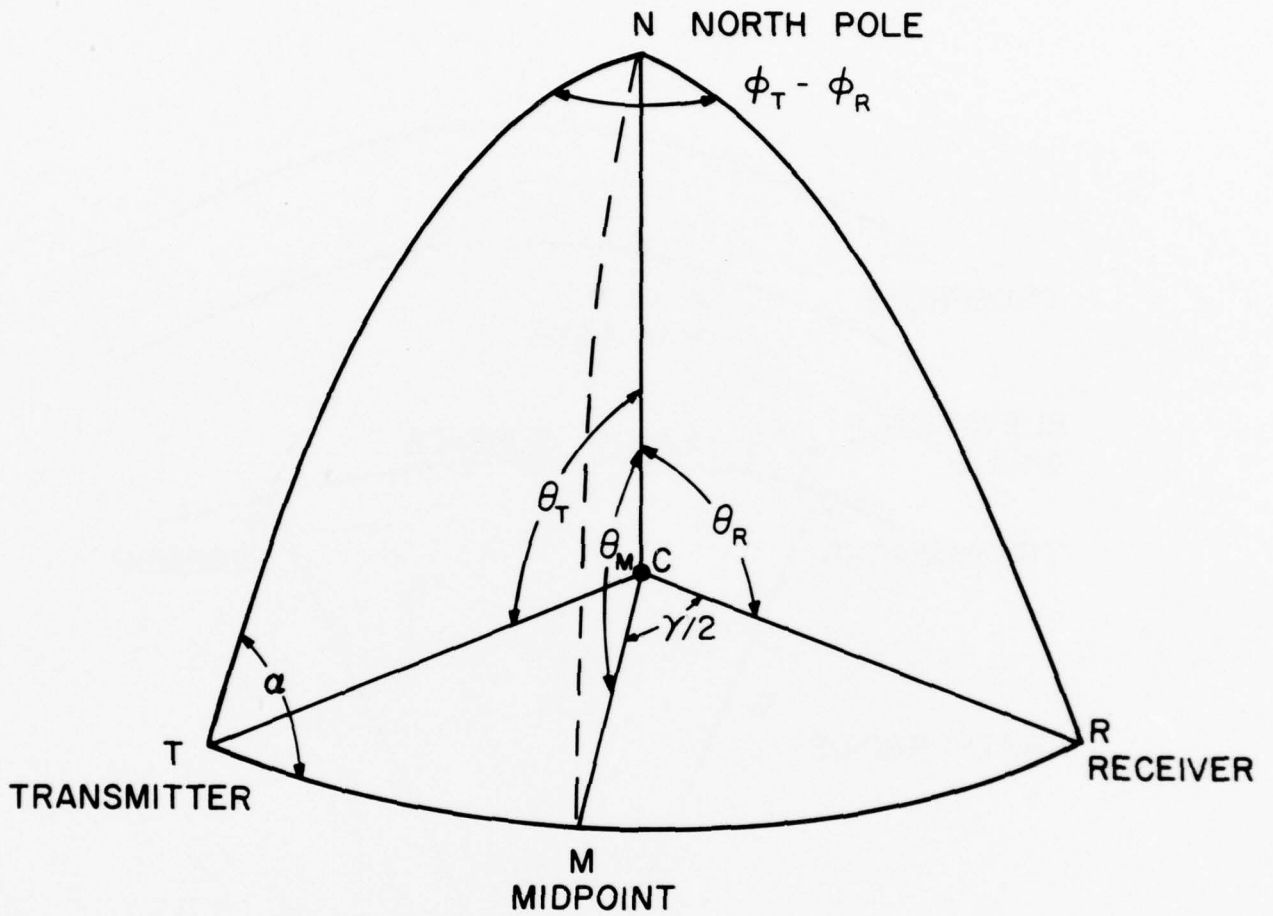


Figure 2.3. Earth geometry for finding the coordinates of the midpoint.

the transmitter and receiver respectively. The coordinates of the midpoint between the transmitter and receiver are then found through the application of the sine and cosine laws of spherical trigonometry to Figure 2.3. From Figure 2.3, the azimuthal angle of the receiver as viewed from the transmitter is

$$\alpha = \sin^{-1} [\sin (\phi_T - \phi_R) \sin \theta_R / \sin \gamma] \quad (2.4)$$

The colatitude of the midpoint, M, is

$$\theta_M = \cos^{-1} [\cos \theta_T \cos \frac{\gamma}{2} + \sin \theta_T \sin \frac{\gamma}{2} \cos \alpha] \quad (2.5)$$

The relative longitude of the midpoint M with respect to the transmitter longitude, $\delta\phi_M$, is given by

$$\delta\phi_M = \sin^{-1} [\sin \alpha \sin \frac{\gamma}{2} / \sin \theta_M] \quad (2.6)$$

The exact longitude of the midpoint M is found by adding or subtracting the relative longitude $\delta\phi_M$ from the transmitter longitude ϕ_T , i.e.

$$\phi_M = \phi_T \pm \delta\phi_M \quad (2.7)$$

If the receiver is located east of the transmitter the positive sign is used otherwise the negative sign is applied. The coordinates of the midpoint thus found are compared with the coordinates of the grid points at which ionospheric models are given. The profile corresponding to the grid point having the smallest difference in coordinates is chosen to represent the profile at the midpoint of the path.

The midpoint profile selected in this manner is approximated by segments of a second degree polynomial which for the i^{th} segment has the form given by (2.1). The coefficients in equation (2.1) are found by making sure that both the density and its derivatives are continuous in going from one segment to another. Each segment value corresponds to the height increment dictated by the composite ionospheric profile. Utilizing equation (2.1) we find analytical expressions for the ground distance D and the group path P' . Neglecting the effects of the Earth's magnetic field and collisions, the ground distance and the group path can be expressed in the form

$$D = 2 \int_{r_0}^{r_t} \frac{r_0^2 \cos \beta_0 dr}{r[r^2 \mu^2 - r_0^2 \cos^2 \beta_0]^{\frac{1}{2}}} \quad (2.8)$$

and

$$P' = 2 \int_{r_0}^{r_t} \frac{r dr}{[r^2 \mu^2 - r_0^2 \cos^2 \beta_0]^{\frac{1}{2}}} \quad (2.9)$$

where r_t is the radial distance from the Earth center to ray apogee, β_0 is the ray elevation angle, and μ is the refractive index of the medium. The refractive index μ and the plasma frequency f_p are related through

$$\mu^2 = 1 - (f_p/f)^2 \quad (2.10)$$

Since the density N is proportional to the square of the plasma frequency, we can substitute (2.1) in (2.10) to obtain

$$\mu_i^2 = 1 - \frac{1}{f^2} \left(a_i + \frac{b_i}{r} + \frac{g_i}{r^2} \right) \quad (2.11)$$

Through substitution of (11) in (8) and (9), the ground distance and the group path can be written in the form

$$D = D_0 + \sum_{i=1}^n D_i + D_f \quad (2.12a)$$

and

$$P' = P'_0 + \sum_{i=1}^n P'_i + P'_f \quad (2.12b)$$

The terms D_0 and P'_0 in (2.12) are evaluated from the earth surface up to the base of the composite ionospheric profile. The terms $\sum_{i=1}^n D_i$ and $\sum_{i=1}^n P'_i$ are evaluated from the base of the composite profile up to layer n just below the layer containing the reflection height. The last terms D_f and P'_f are the contributions from the top of the n^{th} layer up to the reflection height of the ray. Explicitly, the terms in (2.12) are

$$D_0 = 2r_0 \left[\cos^{-1} \left(\frac{r_0 \cos \beta_0}{r_b} \right) - \beta_0 \right] \quad (2.13a)$$

$$P'_0 = 2r_0 \left[\sqrt{(r_b/r_0)^2 - \cos^2 \beta_0} - \sin \beta_0 \right] \quad (2.13b)$$

$$D_i = 2 \int_{r_i}^{r_{i+1}} \frac{r_0^2 \cos \beta_0 dr}{[A_i r^2 + B_i r + G_i]^{\frac{1}{2}}} \quad i=1,2,\dots,n \quad (2.14a)$$

$$P'_i = 2 \int_{r_i}^{r_{i+1}} \frac{r dr}{[A_i r^2 + B_i r + G_i]^{\frac{1}{2}}} \quad i=1,2,\dots,n \quad (2.14b)$$

and

$$D_f = 2 \int_{r_n}^{r_t} \frac{r_o^2 \cos \beta_o \, dr}{[A_n r^2 + B_n r + G_n]^{\frac{1}{2}}} \quad (2.15a)$$

$$P_f' = 2 \int_{r_n}^{r_t} \frac{r \, dr}{[A_n r^2 + B_n r + G_n]^{\frac{1}{2}}} \quad (2.15b)$$

where r_b is the base radius of the composite ionospheric profile, and

$$\begin{aligned} A_i &= 1 - a_i/f^2 \\ B_i &= b_i/f^2 \\ G_i &= g_i/f^2 - r_o^2 \cos^2 \beta_o \end{aligned} \quad (2.16)$$

Analytical expressions for the integrals in (2.14) and (2.15) are readily available from standard integral tables. The resulting analytical expressions together with (2.13) are programmed on the computer under subroutine FITT. Given the elevation angle β_o , the oblique frequency f , and the density profile N , the subroutine FITT calculates the corresponding ground distance and group path.

Since we are seeking all possible homing solutions, we need to generate a table of ground distances versus elevation angles corresponding to the midpoint density profile. Due to the sensitivity of the trapping angle to changes in the ionospheric model we take the penetration angle β_p as the maximum elevation angle possible. The penetration angle β_p is the solution of the equation

$$r_{\max}^2 \mu^2 - r_0^2 \cos^2 \beta_p = 0 \quad (2.17)$$

Therefore, β_p is given by

$$\beta_p = \cos^{-1} \left\{ \frac{r_{\max}}{r_0} [1 - (f_c/f)^2]^{1/2} \right\} \quad (2.18)$$

and the range of elevation angles is

$$0 \leq \beta \leq \beta_p \quad (2.19)$$

The interval in (2.19) is subdivided into 50 subintervals of elevation angles. For each of the resulting 51 elevation angles the ground distance and the group path are computed through subroutine FITT. The generated values of ground distance and group path together with their corresponding elevation angles are assembled in a table. The table is then scanned to locate the two successive entries within which the ground distance between the transmitter and receiver is located. For each pair of entries thus found we perform linear interpolation to locate a possible homing solution within a specified tolerance. We assume that the ground distance and the elevation angle within the two entries are linearly related through

$$D = a + b\beta \quad (2.20)$$

Starting with the two entries of ground distances and their corresponding elevation angles the coefficients a and b are found and a new elevation angle and ground distance are computed. A comparison test is then carried out between the new ground distance and the exact ground distance, D_{TR} . If the difference is

larger than the specified ground distance tolerance, δD , then the procedure of calculating the coefficients in (2.20) utilizing the two closest values of ground distances to D_{TR} and their corresponding elevation angles is repeated until $|D - D_{TR}| \leq \delta D$. The number of interpolations is limited to ten (10) trials for finding the approximate elevation angle, otherwise homing of the ray is said to be not possible. The specified ground distance tolerance, δD , is an input parameter in W(387) of the ray tracing program.

Every possible homing solution of elevation angles is assembled in a table. Then, through the three-dimensional ray tracing program these elevation angles are refined to obtain the corresponding true elevation angles that will home the ray. In some cases true elevation angles are not possible. In either situation a message is printed to show whether or not a homing solution has been achieved. The complete procedure described in this section is simulated on the computer under subroutine HOME.

2.2.3 Approximate Elevation Angle - Multiple Layer Ionosphere

In a single layer ionosphere there are at most two approximate initial elevation angles, one for the low ray and the other for the high ray. In a multiple layer ionosphere, the number of approximate initial elevation angles depends upon the number of layers in the given ionospheric profile. The approximate elevation angle solutions are designated by first layer low or high ray, second layer low or high ray, third layer low or high ray, and fourth layer low or high ray. In our study we selected four as the highest number of layers. This restriction could be removed

with minor modifications on the computer code in subroutine HOME.

Whether the given ionospheric profile is single or a multi-layered one, the procedure of finding the approximate elevation angle is the same as the one described in section 2.2.2. The computer code does not differentiate between single and multi-layered profiles and it is written for a four-layered ionosphere. A sample of the ground distance versus elevation angle curve for a four-layered ionosphere is shown in Figure 2.4.

2.2.4 Refinement of the Elevation Angle

Thus far we have discussed the computation of the approximate elevation angles. In this section we focus our attention on the procedure to refine these approximate elevation angles through actual ray tracing.

Let the exact ground distance between the transmitter and receiver be D_{TR} . Then starting with one of the tabulated approximate elevation angles, β_1 , we trace one ray through the given ionospheric model utilizing the three dimensional ray tracing program. The ground distance corresponding to β_1 is D_1 . Utilizing the table of ground distances and elevation angles generated in the previous section we increment or decrement elevation angle β_1 . The value and sign of the increment depends on the relative location of D_1 with respect to D_{TR} in the ground distance versus elevation angle table. With the new elevation angle β_2 we compute D_2 through the ray tracing program. The ground distance, D_{TR} , must then be located either above D_1 and D_2 , below D_1 and D_2 , or in between D_1 and D_2 . For the cases where D_{TR} is above or below D_1 and D_2 the elevation angles and their corresponding ground

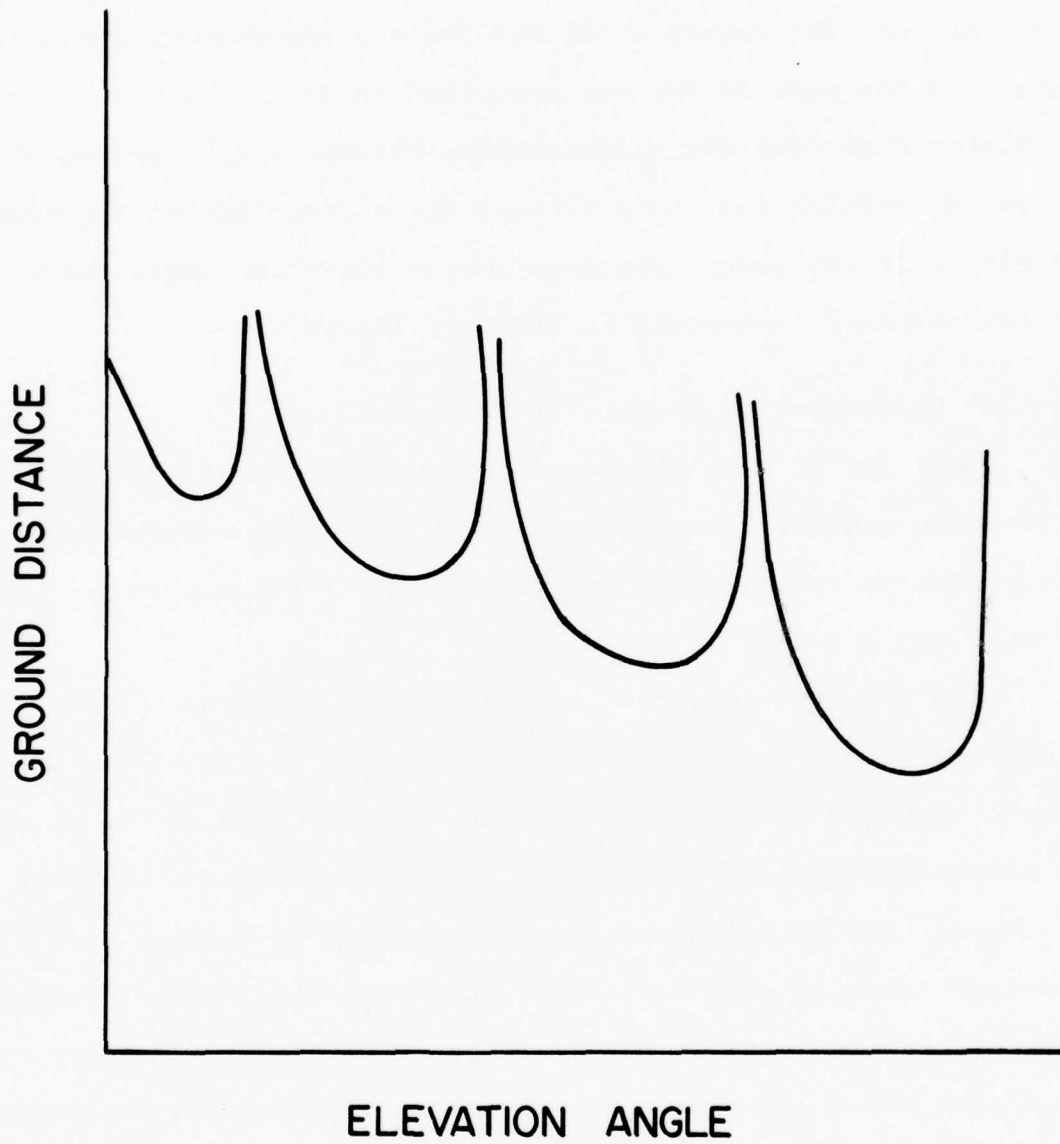


Figure 2.4. Sketch showing the ground distance - elevation angle curve for a four-layer ionosphere.

distances are adjusted through linear interpolation in accordance with equation (2.20) until D_{TR} is either located between D_1 and D_2 or such a condition cannot be achieved. In the latter situation the elevation angle found through (2.20) lies outside the range of elevation angles set for the ray in a multiple layer ionosphere. In the event that D_{TR} cannot be located between D_1 and D_2 , homing of the ray cannot be accomplished and one of the statements 'High angle ray' or 'Discontinuity in the ray traced range - Beta curve or range too close to the skip distance' is printed from subroutine ADJUST.

Let us assume that we can locate D_{TR} between D_1 and D_2 then we can find β_3 through linear interpolation on β_1, D_1, β_2 and D_2 . With β_3 we calculate a new ground distance D_3 . If the difference between D_{TR} and D_3 is less than a specified ground distance tolerance, then β_3 is the desired homing elevation angle except for azimuthal angle corrections. The ground distance tolerance, δD , is an input parameter and is specified in W(387). However, if the difference between D_{TR} and D_3 is greater than δD then we need to correct for the ground distance discrepancy. Since the dependence of the ground distance on the elevation angle is known to be nonlinear, we let

$$D_i = a_0 + a_1\beta_i + a_2\beta_i^2 \quad i=1,2,3 \quad (2.21)$$

The coefficients a_0, a_1 , and a_2 are computed by inverting the matrix resulting from the substitution of ground distances D_1, D_2, D_3 and their corresponding elevation angles $\beta_1, \beta_2, \beta_3$. The new elevation angle is then given by

$$\beta_{\pm} = \frac{1}{2a_2} [-a_1 \pm \sqrt{a_1^2 - 4a_2(a_0 - D_{TR})}] \quad (2.22)$$

If the quantity under the radical sign in (2.22) is negative, then we cannot find an elevation angle and an appropriate message is printed. Equation (2.22) yields two solutions, β_+ and β_- . In order to decide whether β_+ or β_- is the desired elevation angle we set up the following criterion. First, we take the absolute differences between D_{TR} and D_1 , D_2 , D_3 and the resulting three difference values are compared with each other. The elevation angle β_1 , β_2 , or β_3 corresponding to the smallest difference is then selected. The elevation angles β_+ and β_- are then compared with the selected elevation angle. The one yielding the smaller difference is chosen as the new elevation angle i.e. $\beta_4 = \beta_+$ or $\beta_4 = \beta_-$. With β_4 we trace another ray and find D_4 . If the difference between D_{TR} and D_4 is within the specified tolerance δD , then β_4 is the homing angle except for possible azimuthal corrections. However, if the difference between D_{TR} and D_4 is the largest difference then we cannot home the ray and the message 'Discontinuity in the ray traced range-beta curve or range too close to the skip distance' or 'High angle ray' is printed. On the other hand, if D_4 is closer to D_{TR} than any or all of D_1 , D_2 , D_3 then the ground distance D_1 , D_2 , or D_3 yielding the largest absolute difference with D_{TR} is replaced by D_4 and its corresponding elevation angle by β_4 . The procedure starting with equation (2.21) is repeated to find a new elevation angle and a new ground distance. The comparison steps are carried out until the ground distance tolerance criterion is met or a message is printed. The number of allowable tries to find the homing angle is controlled

by an input parameter in W(386).

Once the ground distance tolerance criterion is satisfied a first order elevation angle that will home the ray to the receiver is said to be found except for possible azimuthal deviation correction. The azimuthal deviation is defined as the difference between azimuth of the computed receiving point from the transmitter and the azimuth of the intended receiving point from the transmitter. If the azimuthal deviation of the ray is within the calculated azimuthal tolerance, δA , the homing of the ray is completed. Otherwise, the azimuth of transmission has to be corrected in order to satisfy the azimuthal tolerance condition. The azimuthal tolerance, δA , is computed with the help of Figure 2.5. In Figure 2.5, we show the transmitter T, the receiver R, the computed receiver R', and the angles $\gamma_1, \gamma_2, \gamma_3$ subtended at the earth center opposite arcs TR, TR', and RR' or δD respectively. Applying the cosine law to the spherical triangle TRR' we obtain

$$\cos \gamma_3 = \cos \gamma_1 \cos \gamma_2 + \sin \gamma_1 \sin \gamma_2 \cos \delta A \quad (2.23)$$

If we let $\gamma_1 = \gamma_2 = D_{TR}/r_0$ and $\gamma_3 = \delta D/r_0$, then

$$\cos \delta A = [\cos (\delta D/r_0) - \cos^2 (D_{TR}/r_0)] / \sin^2 (D_{TR}/r_0) \quad (2.24)$$

Since δD is much smaller than r_0 , the argument of the cosine function, $\delta D/r_0$ is very small. Expanding this term and retaining two terms of the expansion, (2.24) takes the form

$$\cos \delta A \approx 1 - \frac{1}{2} \left[\frac{\delta D}{r_0 \sin(D_{TR}/r_0)} \right]^2 \quad (2.25)$$

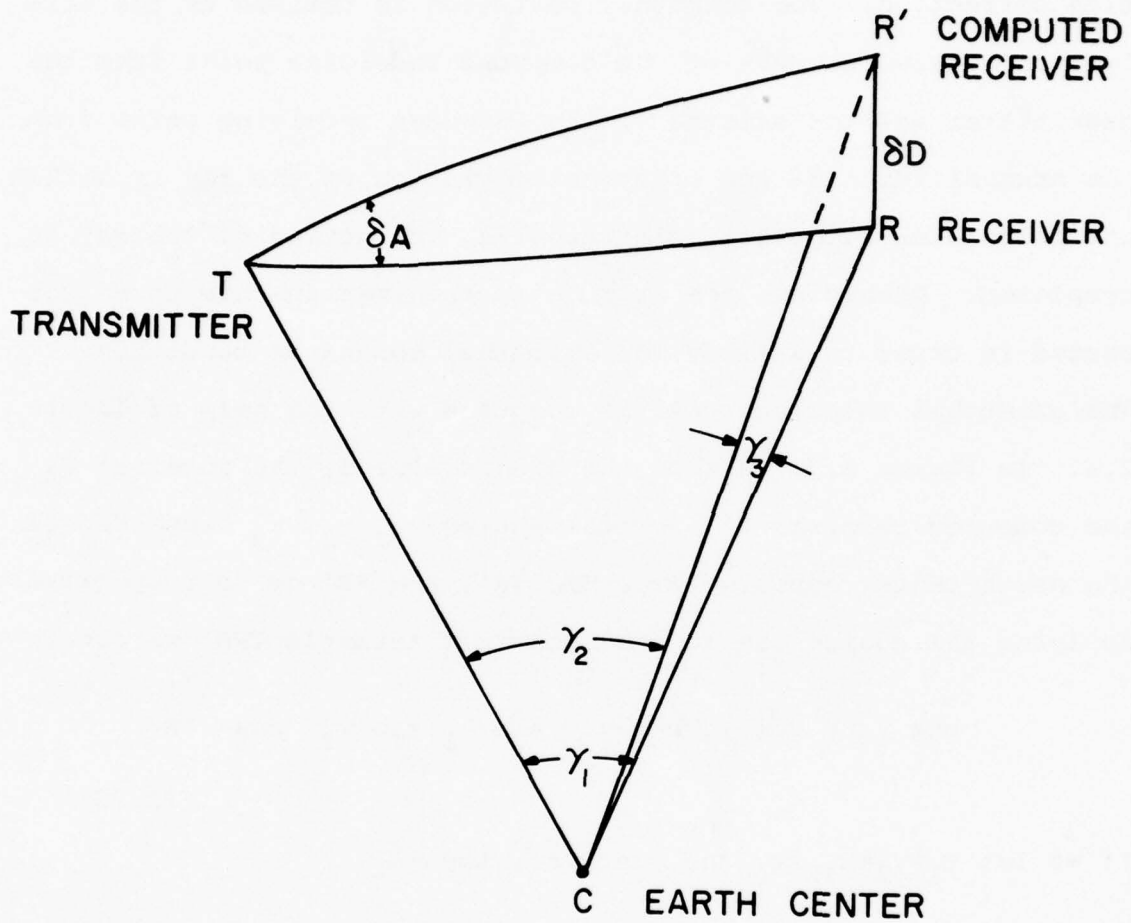


Figure 2.5. Sketch illustrating the homing in azimuth.

Since the azimuthal tolerance δA is also small, we expand the left hand side of (2.25) retaining two terms of the expansion. The resulting expression for δA is

$$\delta A \approx \frac{\delta D}{r_0 \sin (D_{TR}/r_0)} \quad (2.26)$$

For each ray homed in ground distance a comparison test is performed between the ray azimuth and the computed transmitter-receiver azimuth. If the ray azimuthal deviation is within the azimuthal tolerance δA then homing is achieved and control is transferred to another activity within the ray tracing program. However, if the ray azimuthal deviation is larger than δA we adjust the azimuth of transmission by the amount of the ray azimuthal deviation. With a new azimuth of transmission and the same elevation angle we repeat the complete procedure of ground distance homing and find a new homing angle. The ray azimuthal deviation corresponding to this new homing angle is then compared to the azimuthal tolerance, δA . The above steps are repeated until both ground distance tolerance and azimuthal tolerance criteria are satisfied or a message is printed.

2.2.5 Group Path Homing

The capabilities of the three-dimensional ray tracing program was extended to include homing of the group path. The procedure described in the ground-to-ground homing case is also used for the group path homing. The only difference being in the parameters supplied to the ray tracing program through the W-array data input.

The parameters needed to perform group path homing are the transmitter coordinates, the azimuthal angle of transmission, the oblique frequency of transmission and the value of the homed in group path. The homed in group path is supplied through W(394). In the event that group path homing is not desired, then W(394) should be set to zero. An example of group path homing is discussed in the next section.

2.2.6 Examples and Discussion

In the preceding section we discussed in detail the technique through which the ground-to-ground homing of the ray is achieved. In order to illustrate the homing procedure we present three examples. The first example is for a single layer ionosphere, the second example is for a two layered ionosphere, and the third example is for group path homing. In all cases the ray is traced through the Air Force supplied ionospheric model. This model gives the electron density profile on a geomagnetic longitude-geomagnetic colatitude grid spanning from -130°E to -110°E in geomagnetic longitude and 0° to 54° in geomagnetic colatitude. The increments in longitude, colatitude and height are 5° , 3° and 10 km respectively. The base height in all cases is 90 km extending upward to 600 km. Note that these increments are very coarse for accurate ray tracing even with careful interpolation routines. This causes some difficulty as discussed later.

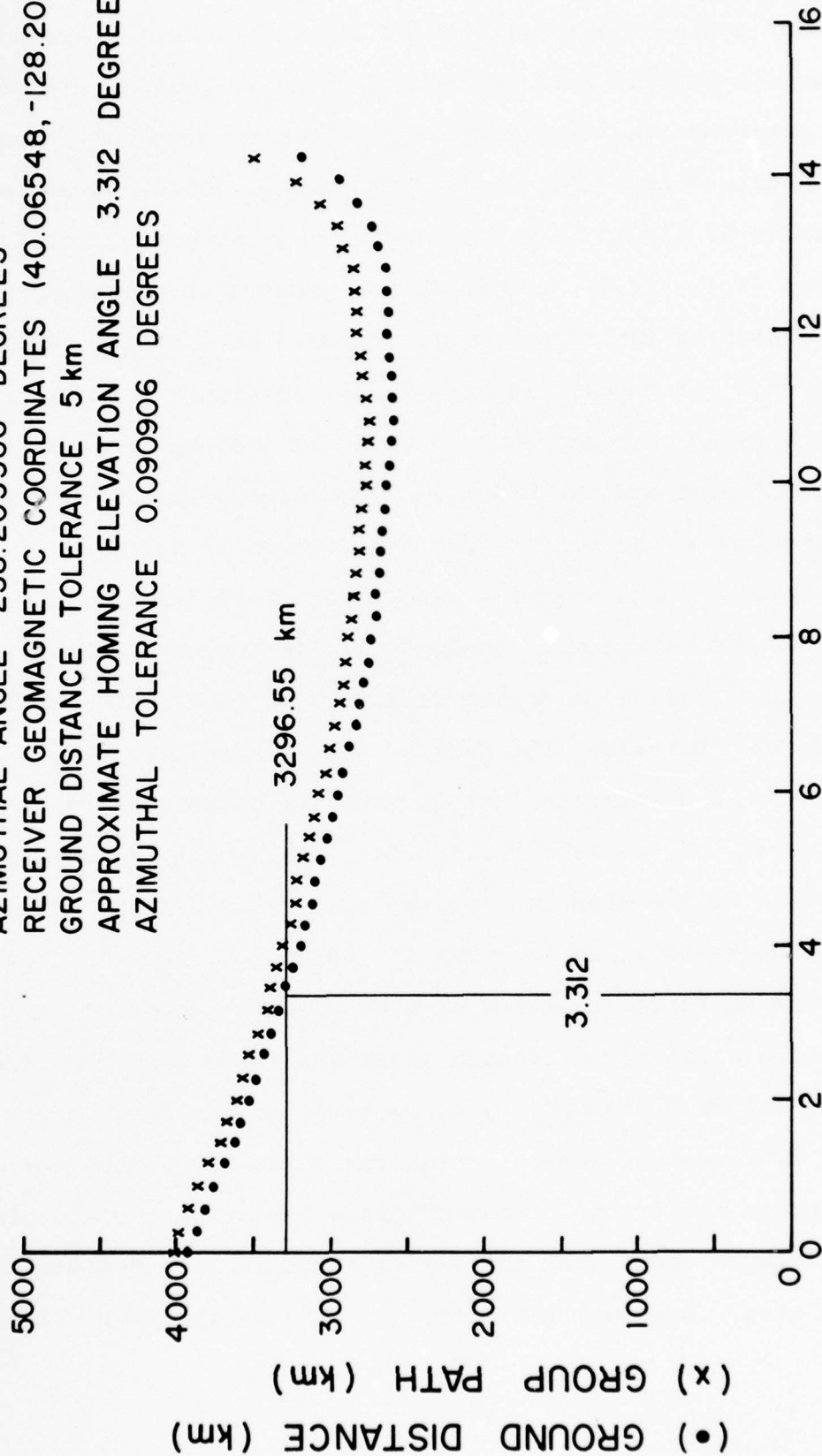
Example 1. Single Layer Ionosphere

Let the transmitter and receiver geographic coordinates be located at (125°W , 78°N) and (185°W , 56°N) respectively. For this

configuration the ground distance $D_{TR} = 3296.55$ km and the azimuthal angle of transmission is 258.2 degrees. Since the ionospheric profile grid points are given in geomagnetic coordinates we transform the transmitter and receiver geographic coordinates to obtain colatitudes of 10.81658 and 40.06548 degrees and longitudes of 114.47052 and 128.20226 degrees east. Utilizing equations (2.4), (2.5), and (2.7) the geographic and geomagnetic coordinates of the midpoint are found to be (-169.81, 69.18) longitude and latitude, (-125.12, 25.33) longitude and colatitude respectively. A comparison between the geomagnetic coordinates of the midpoint and the given ionospheric profile results in the selection of the density profile located at (-125.0, 24.0). For an oblique frequency of transmission of 20 MHz equation (2.18) yields the penetration angle of 14.236 degrees. Then, the interval of elevation angles from zero to 14.236 degrees is divided into 50 intervals. For each of the 51 resulting elevation angles the ground distance and group path are calculated through equations (2.13), (2.14), (2.15) and (2.16) utilizing the density profile of the midpoint located at (-125.0, 24.0). The result of this calculation is shown in Figure 2.6. For the specified ground distance tolerance of 5 km, figure 6 shows that the approximate initial elevation angle was found to be 3.312 degrees.

Figure 2.7 shows the steps taken in the refinement procedure and the eventual homing of the ray. The top portion of Figure 2.7 displays the ground distance versus elevation angle homing steps. The figure shows that the ray is homed in ground distance in the 5th step. However, the bottom portion of the figure also shows

TRANSMITTER (78, -125) RECEIVER (56, -185)
 FREQUENCY 20 MHz
 GROUND DISTANCE 3296.55 km
 AZIMUTHAL ANGLE 258.205566 DEGREES
 RECEIVER GEOMAGNETIC COORDINATES (40.06548, -128.20226)
 GROUND DISTANCE TOLERANCE 5 km
 APPROXIMATE HOMING ELEVATION ANGLE 3.312 DEGREES
 AZIMUTHAL TOLERANCE 0.090906 DEGREES



ELEVATION ANGLE (DEGREES)

Figure 2.6. Example 1 illustrating the ground-to-ground homing using the Air Force supplied model ionosphere. The example shows how the initial elevation is determined.

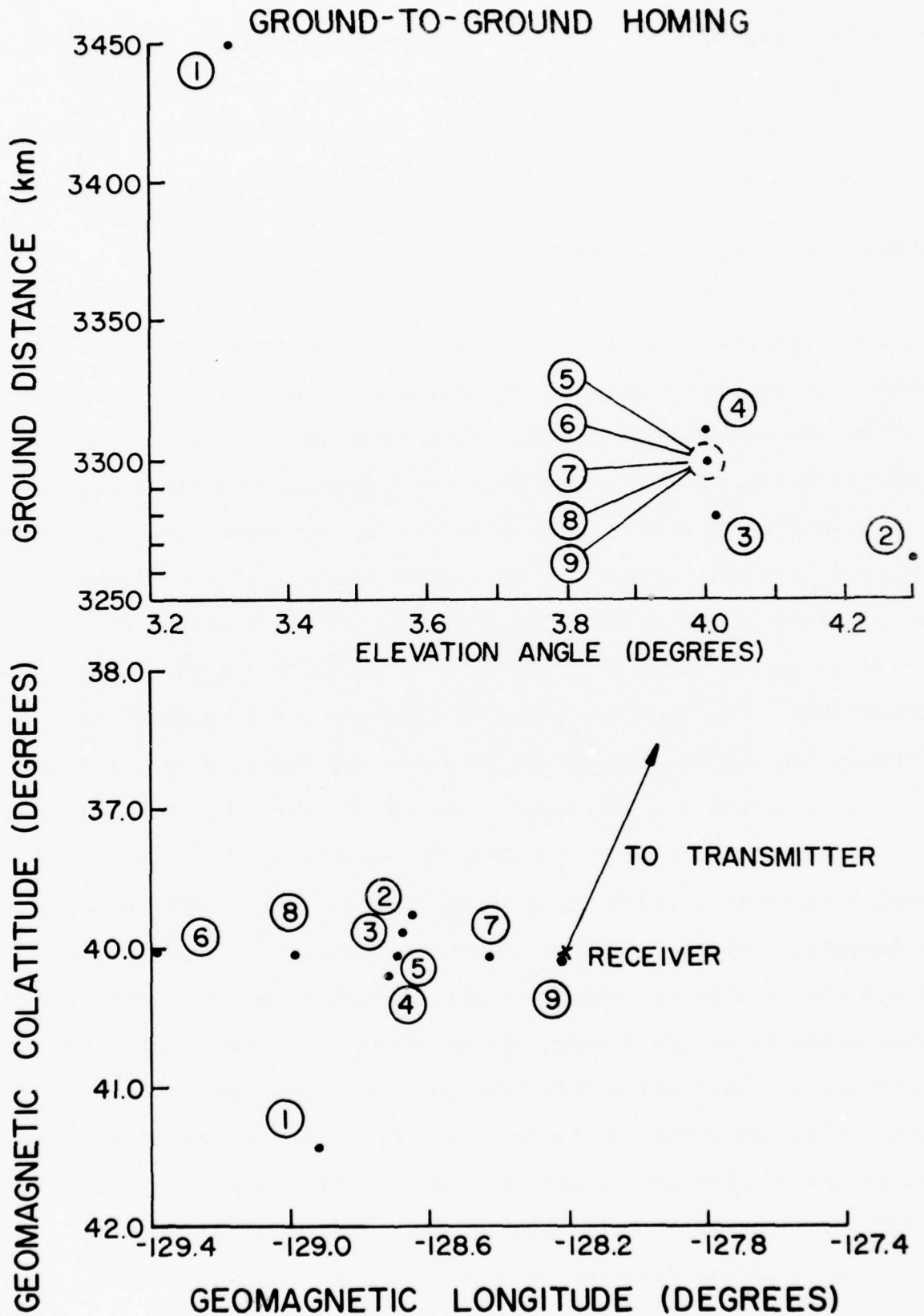


Figure 2.7. Continuation of the example shown in Fig. 2.6. This shows the refinement procedure in ground distance and azimuth homing using 3D ray tracing.

that the azimuthal angle of the ray is not within the calculated tolerance. Prior to final homing of the ray, there were four azimuthal corrections with no ground distance adjustments since for each azimuth the ground distance was homed in.

Example 2. Two Layer Ionosphere

In a single layer ionosphere there are at most two initial homing elevation angles while in a two layer ionosphere there are four initial homing angles. Following example 1 we let the transmitter and receiver geographic coordinates be $(-175.0^{\circ}\text{E}, 68.0^{\circ}\text{N})$ and $(-150.0^{\circ}\text{E}, 72.0^{\circ}\text{N})$ respectively. The ground distance D_{TR} for such a configuration is 1039.36 km and the azimuthal angle of transmission is 53.51 degrees. Upon transformation, the geomagnetic coordinates of the transmitter and receiver are found to be $(-127.7972, 27.21986)$ and $(-114.25255, 19.5317)$ longitude and colatitude. The geographic coordinates and the corresponding geomagnetic coordinates of the midpoint are found to be $(-163.72, 70.43)$ longitude and latitude, $(-122.09, 23.22)$ longitude and colatitude respectively. The density profile at the midpoint is then located at $(-120.0, 24.0)$ longitude and colatitude in the ionospheric profile. For an oblique transmission frequency of 7 MHz the rays do not penetrate the ionosphere and the penetration angle is set to ninety (90) degrees. Upon subdividing the interval of elevation angles from zero to ninety degrees into 50 intervals, the ground distances and group paths of the resulting 51 values of elevation angles are calculated through subroutine FITT. The result of this calculation is shown in Figure 2.8.

For a ground distance tolerance $\delta D=2$ km Figure 2.8 shows that

TRANSMITTER (68, -175) RECEIVER (72, -150.0)
 FREQUENCY 7 MHz
 GROUND DISTANCE 1039.36 km
 AZIMUTHAL ANGLE 53.509872 DEGREES
 RECEIVER GEOMAGNETIC COORDINATES (19.51317, -114.25255)
 GROUND DISTANCE TOLERANCE 2 km
 APPROXIMATE HOMING ELEVATION ANGLES (7.415, 13.093, 20.566)
 AZIMUTHAL TOLERANCE 0.110743 DEGREES

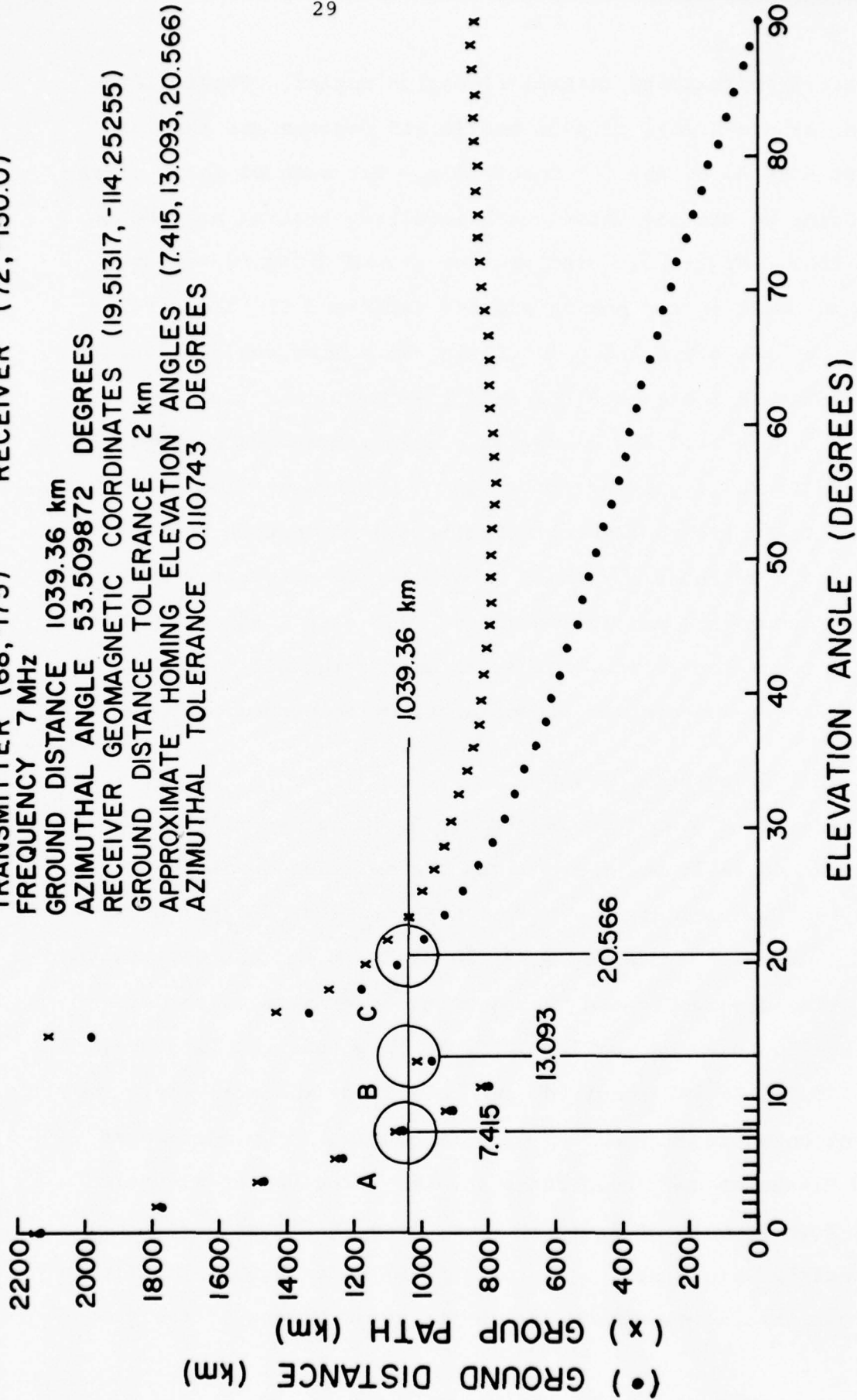


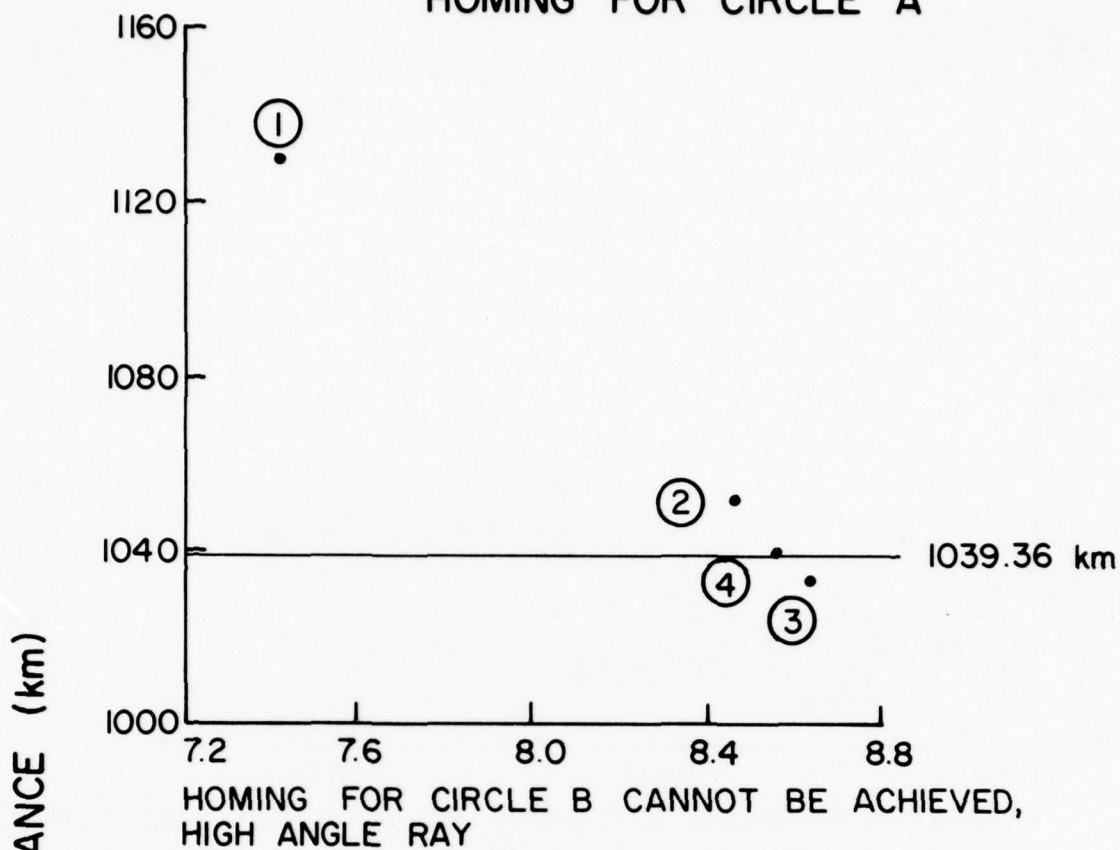
Figure 2.8. Example 2 illustrating the ground-to-ground homing for rays reflected from a two-layer ionosphere. Note that for a ground range of 1039.36 km, three approximate solutions (indicated by circle A, circle B and circle C) in the elevation angle exist in this case.

there are 3 approximate initial elevation angles. These elevation angles are 7.415, 13.093, and 20.566 degrees and they are designated by A, B, and C respectively. For each of these elevation angles we use the three dimensional ray tracing program to refine them. Figure 2.9 displays the ground distance versus elevation angle in the homing process for A and C. The circled numbers are the steps taken to obtain the homing angle. Homing for B cannot be achieved since it corresponds to a high angle ray. In Figure 2.10 the geomagnetic colatitude versus geomagnetic longitude is plotted for A and C. For case A the azimuthal angle of transmission does not require any correction and the homing angle is found by linear interpolation on steps 2 and 3 without recourse to matrix inversion. For case C the azimuthal angle is corrected twice in order to meet azimuthal tolerance criterion corresponding to ground distance tolerance of 2 km.

Example 3. Group Path Homing

Using the transmitter geographic coordinates (-150.0, 78.0) longitude and latitude, the oblique transmission frequency of 12 MHz, and the azimuthal angle of transmission of 209.4 degrees we calculated the coordinates of the midpoint and the penetration angle. The geographic and geomagnetic coordinates of the midpoint are found to be (-164.97, 66.86) longitude and latitude, and (-119.04, 26.59) longitude and colatitude respectively. The penetration angle is found to be 38.9 degrees. The calculated ground distances and group paths for the 51 values of elevation angles from zero to 38.9 degrees are shown in Figure 2.11. For the specified group path value of 2654.08 km in W(394) the figure shows two initial elevation angles for which homing of the group

HOMING FOR CIRCLE A



HOMING FOR CIRCLE C

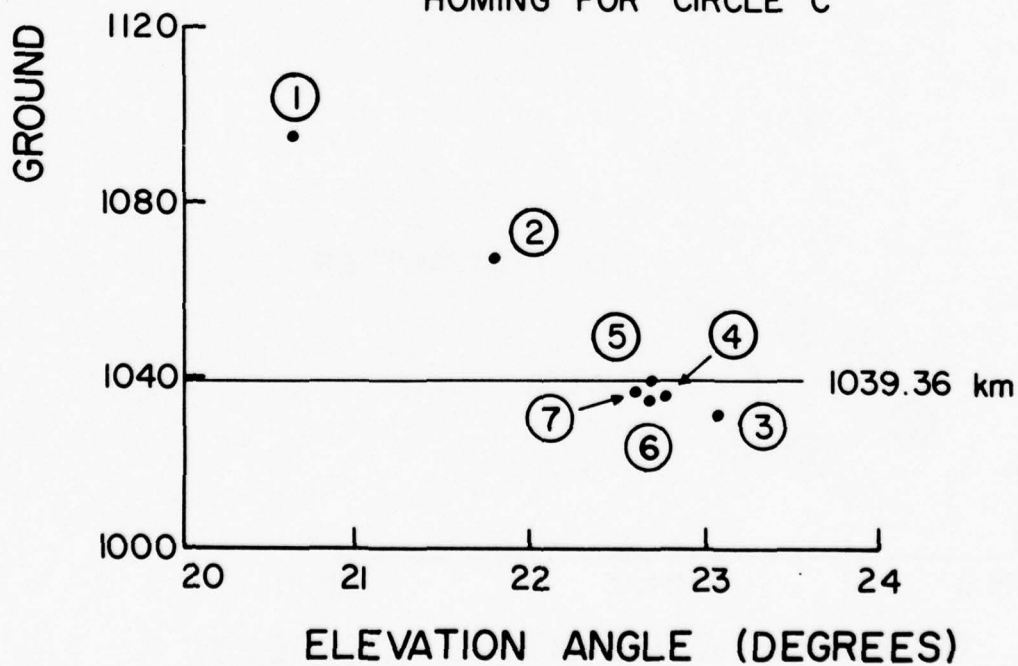


Figure 2.9. Continuation of Example 2 shown in Fig. 2.8 illustrating the ground distance homing for circle A and circle C using 3D ray tracing.

HOMING FOR CIRCLE A

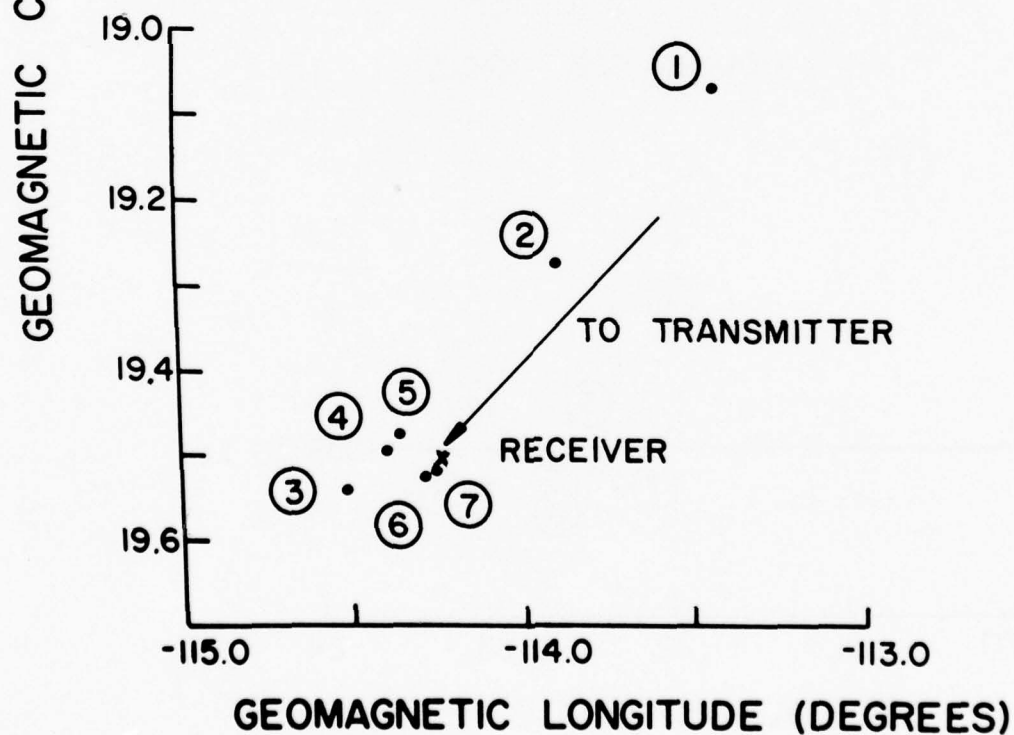
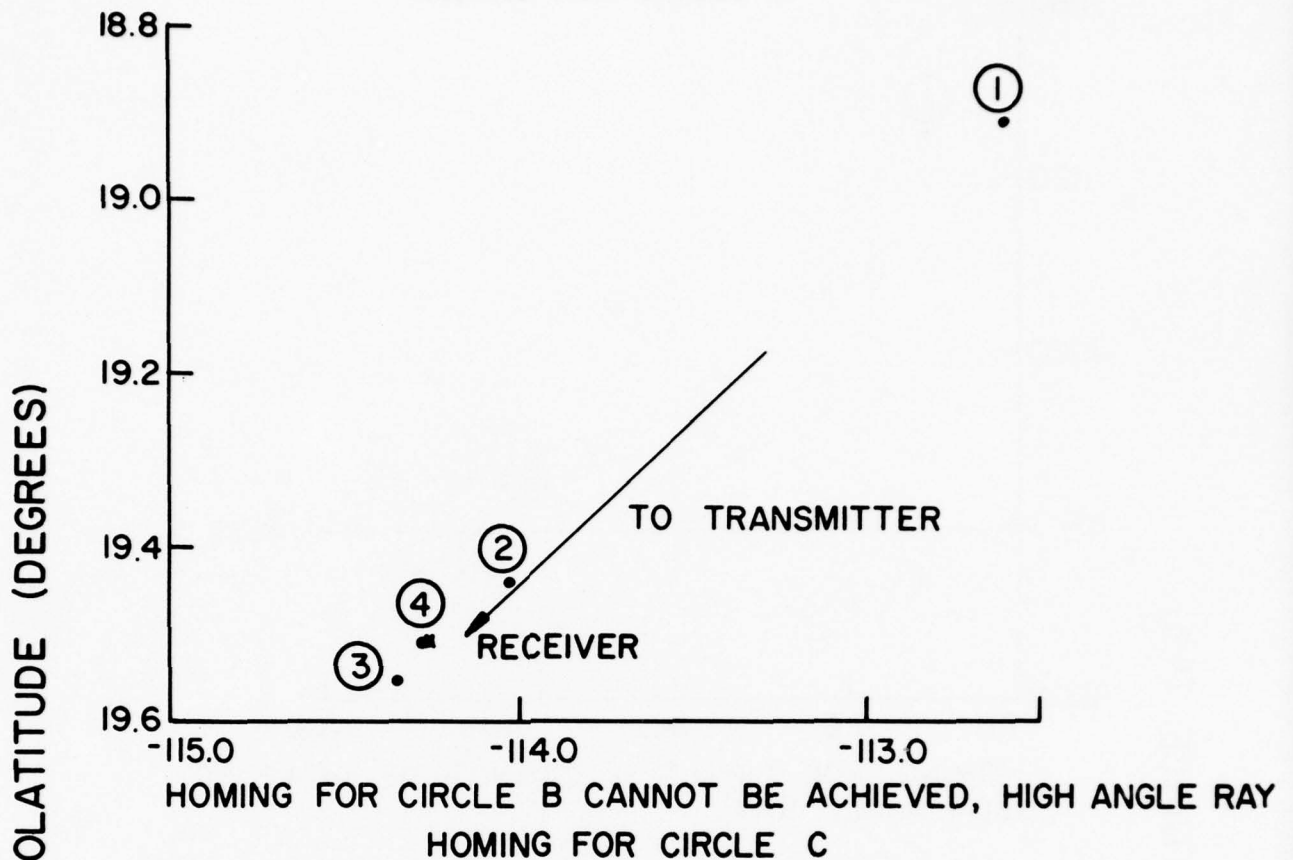


Figure 2.10. Continuation of Example 2 illustrating azimuthal correction for final homing of the ray on the receiver.

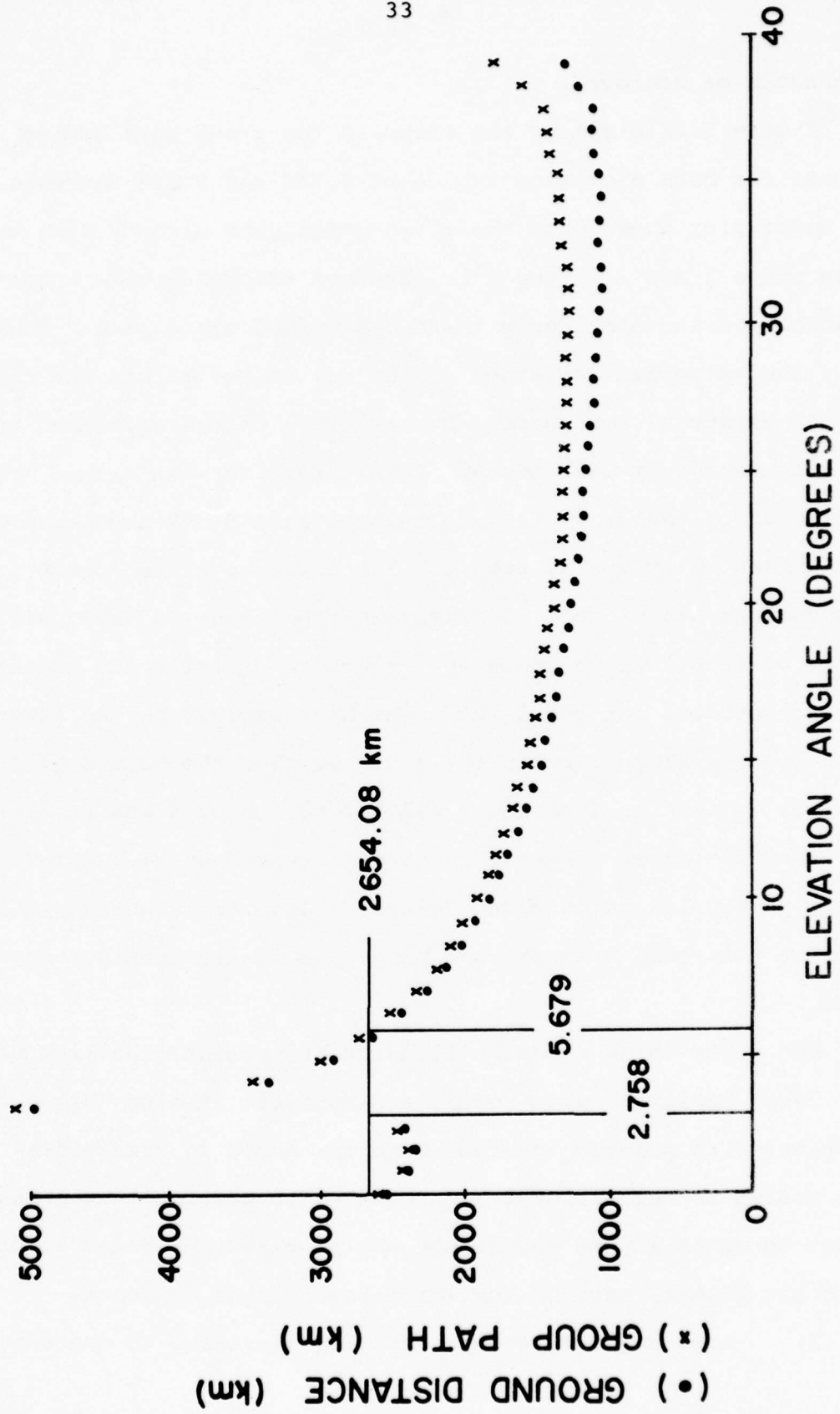


Figure 2.11. Computed initial group path versus elevation angle curve for Example 3. For a specified group path of 2654.08 km two solutions are indicated.

path could be achieved.

Figure 2.12 displays the steps in the group path homing process for both elevation angles of 2.758 and 5.679 degrees. The upper plot shows that the given group path already lies between steps 2 and 3. Step 4 is obtained through linear interpolation and it coincides with the specified group path. However, the azimuthal deviation of the ray is not within the calculated azimuthal tolerance. A correction on the azimuthal angle of transmission yields step 5. Then, starting with step 5 and using increments of the previously calculated ground distances and elevation angles we arrive at step 6. Since the specified group path lies between steps 5 and 6, linear interpolation on them yields values of step 7 which meets the tolerance criteria and homing is thus complete for the first layer high angle. In the lower graph the specified group path is higher than the values of steps 1, 2, 3, 4, and 5. Therefore, all the values of steps 1, 2, 4, and 5 are discarded and only values of steps 3 and 6 are retained. Linear interpolation on these values yields step 7 which satisfies the tolerance criteria and hence the desired homing elevation angle.

The above three examples illustrated successful homing of the ray. When homing is successful, a diagnostic stating that homing is achieved is printed together with the homed in parameters. When homing is not successful, a diagnostic stating that homing cannot be achieved and the reason why it cannot be homed is printed. There are several reasons for which rays cannot be homed.

- i) high angle rays which are too sensitive to ionospheric

GROUP PATH HOMING

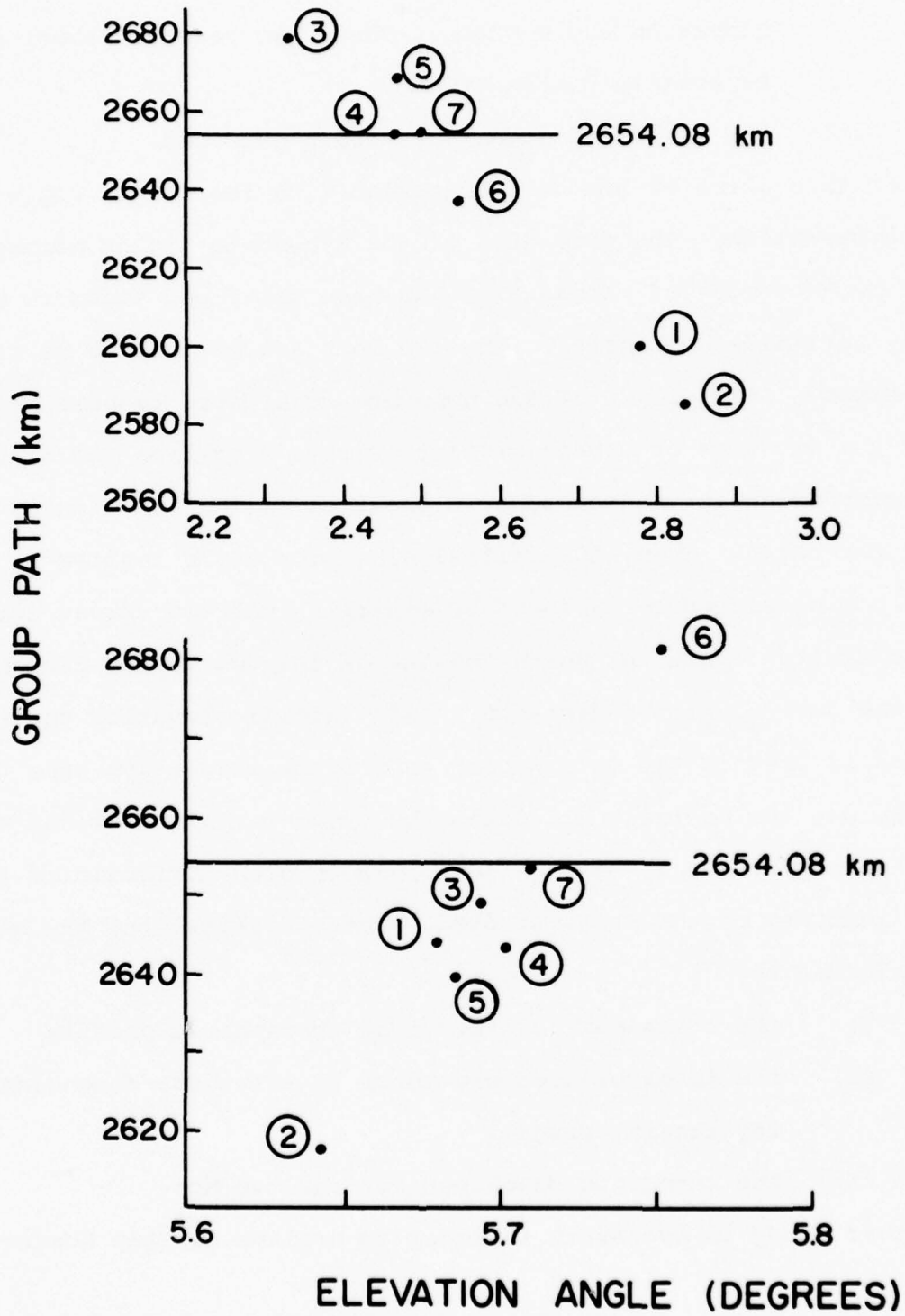


Figure 2.12. Continuation of Example 3 illustrating group path homing for two rays.

parameters and small increments in elevation angles.

- ii) ground distance too close to the skip distance or discontinuity in the ray traced ground distance versus elevation angle curve. These two reasons cannot be separately distinguished.
- iii) the specified number of trials exceeded.

Up to this point we are only concerned with the single hop mode of propagation. The extension of the ground-to-ground homing to the two-hop mode of propagation has been tried and found to be only partially successful. The two hops are assumed to be similar or mixed. Initially, the two hops are considered to be similar and the two sets of ground distance versus elevation angle curves corresponding to the ionospheric profiles at the two midpoints are generated. Then, the initial elevation angle required in the homing procedure is found by searching the two curves for an elevation angle for which the sum of the two ground distances is the desired ground distance. This initial elevation angle if found is used in the same manner as for the single hop case to carry out the homing. Utilizing the above technique we had success in homing for a few cases while we encountered difficulties in the majority of the cases studied. These difficulties may be attributed to

- i) the coarseness of the given ionospheric profile
- ii) the interpolation procedure in the three-dimensional ray tracing program
- iii) the technique developed for the two hop.

Further study is necessary in order to achieve two-hop homing.

2.3 Ground-Satellite Homing

When the transmission frequency is much higher than the critical frequency of the given ionospheric profile the ray penetrates the ionosphere. The geometries of the two possible configurations are shown in Figures 2.13 and 2.14. In Figure 2.13 the transmitter is below the receiver and the configuration is called ground-to-satellite homing. The satellite-to-ground homing configuration is shown in Figure 2.14. In either case our objective is to home the ray to the receiver within a specified ground distance tolerance and a computed azimuthal tolerance. The following discussion is applicable to either configuration.

2.3.1 Approximate Elevation Angle

We assume that the transmitter and receiver coordinates are given in east longitude and latitude north in degrees and their heights above the earth surface in km. Then, to a first approximation we calculate the initial or approximate elevation angle for a straight line path between the transmitter and receiver.

Let $\theta_T, \theta_R, \phi_T, \phi_R$ be the transmitter and receiver colatitudes and longitudes respectively. Compute the cartesian coordinates of the transmitter and receiver through the transformation

$$\begin{aligned} x &= r \sin \theta \cos \phi \\ y &= r \sin \theta \sin \phi \\ z &= r \cos \theta \end{aligned} \tag{2.27}$$

where $r=r_0+h$ and h is the height of the transmitter or receiver above the earth surface. From Figures 2.13 and 2.14, the vectors

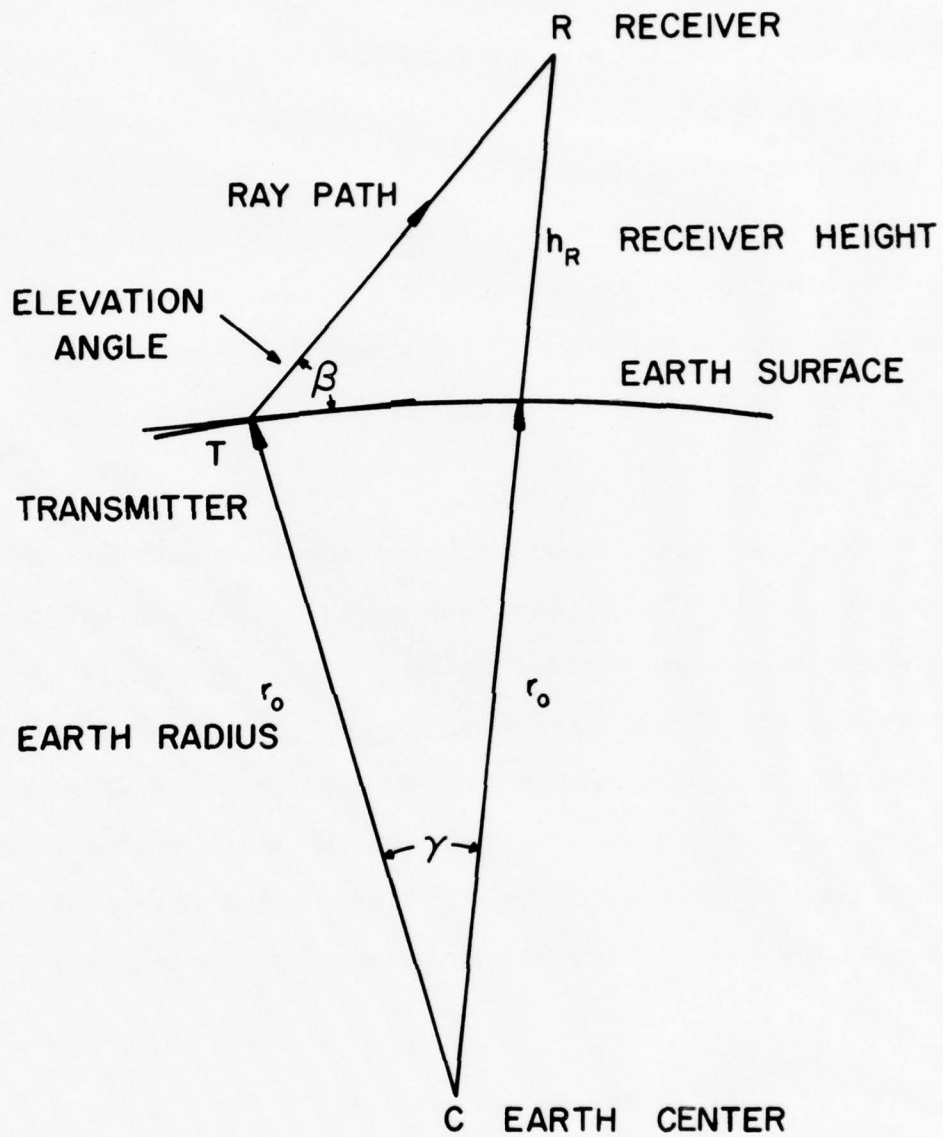


Figure 2.13. Sketch showing the geometry of ground-satellite homing.

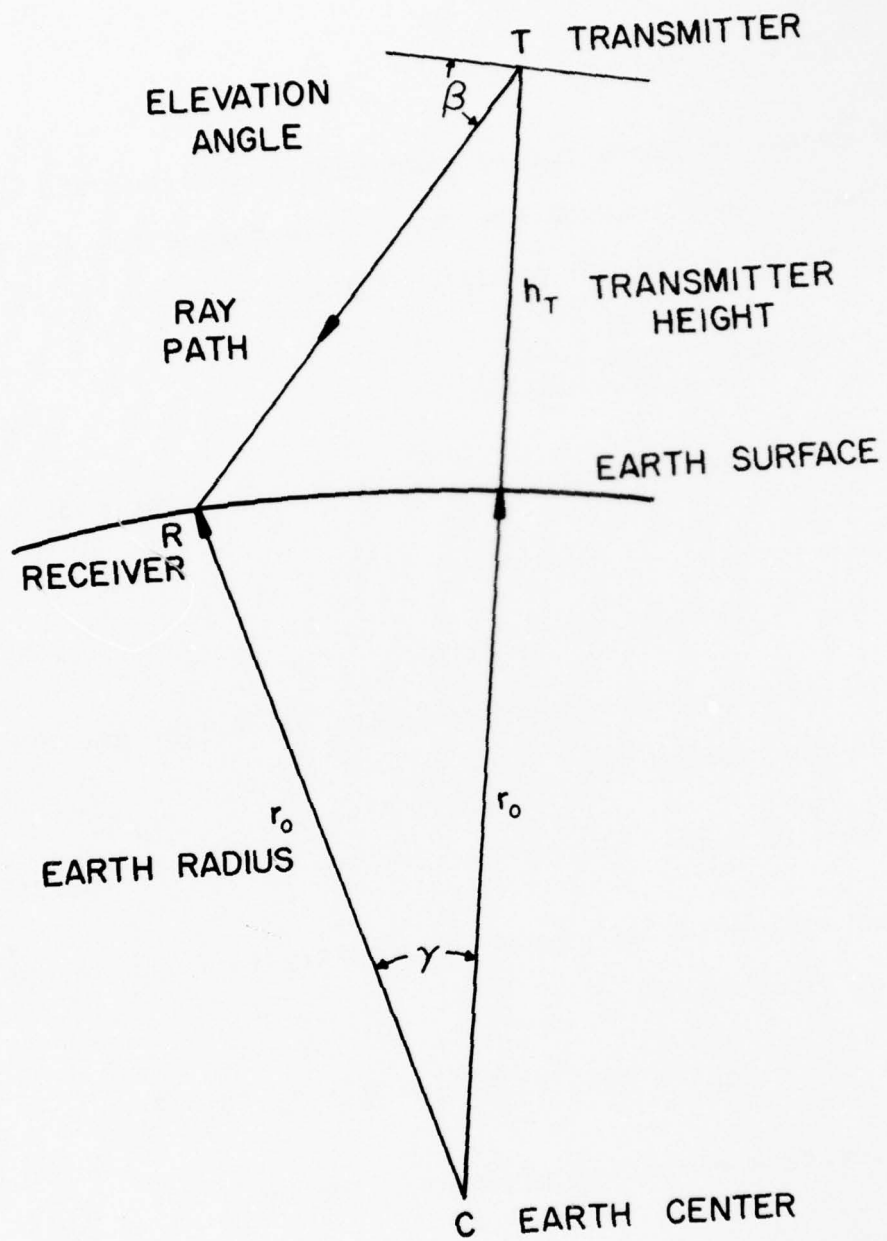


Figure 2.14. Sketch showing the geometry of satellite-ground homing.

\vec{CT} and \vec{CR} are given by

$$\vec{CT} = x_T \hat{i} + y_T \hat{j} + z_T \hat{k} \quad (2.28)$$

$$\vec{CR} = x_R \hat{i} + y_R \hat{j} + z_R \hat{k}$$

Then the ground distance D_{TR} between the transmitter and receiver can be found either through the use of the cosine law equation (2.3) or by taking the dot product of the vectors in (2.28), i.e.

$$\gamma = \cos^{-1} \left[\frac{\vec{CT} \cdot \vec{CR}}{|\vec{CT}| |\vec{CR}|} \right] \quad (2.29)$$

The ground distance D_{TR} projected at the transmitter radius is given by

$$D_{TR} = (r_0 + h_T) \gamma \quad (2.30)$$

In order to find the elevation angle, we define the straight line path by the vector \vec{TR} ,

$$\vec{TR} = \vec{CR} - \vec{CT} \quad (2.31)$$

Applying the cosine law of plane trigonometry to triangle CTR, angle CTR is found to be

$$\sphericalangle CTR = \cos^{-1} [(|\vec{TR}|^2 + |\vec{CT}|^2 - |\vec{CR}|^2) / 2 |\vec{TR}| |\vec{CT}|] \quad (2.32)$$

and the approximate elevation angle is given by

$$\beta = \sphericalangle CTR - \pi/2 \quad (2.33)$$

In the ground-to-satellite case β is positive while in the satellite-to-ground case β is negative. The above procedure is pro-

grammed in subroutine HOMES.

2.3.2 Refinement of the Elevation Angle

In section 2.2.3 we presented in detail the steps used to refine the approximate elevation angle for the ground-to-ground configuration. The refinement of the elevation angle for both the ground-to-satellite and satellite-to-ground is basically the same as that of the ground-to-ground case except for the initial elevation angle increment. The computer code of ADJUST is used for all three configurations. The initial elevation angle increment is only used once upon entry into routine ADJUST.

Starting with the known value $\beta_1 = \beta$ of the approximate straight line path between the transmitter and receiver we trace one ray and obtain the ground distance D_1 . In order to find a new elevation angle β_2 we assume a plane earth geometry and consider the equivalent triangle TRA in Figure 2.15. In this figure, T is the transmitter, R is the equivalent receiver, which, when a perpendicular line is dropped on RC from T, is a distance D km away and which is h km above the foot of the perpendicular point A as shown in Figure 2.15. From triangle TRA, the approximate elevation angle $\tilde{\beta}$ is given by

$$\tan \tilde{\beta} = h/D \quad (2.34)$$

Differentiating both sides of the equation and solving for the approximate initial increment in $\tilde{\beta}$ we obtain the relation

$$\delta \tilde{\beta} \approx \sin \tilde{\beta} \cos \tilde{\beta} \delta D/D \quad (2.35)$$

where $\beta = \beta_1$, $\delta D = D_{TR} - D_1$, and $D = D_{TR}$. Then, with an elevation angle

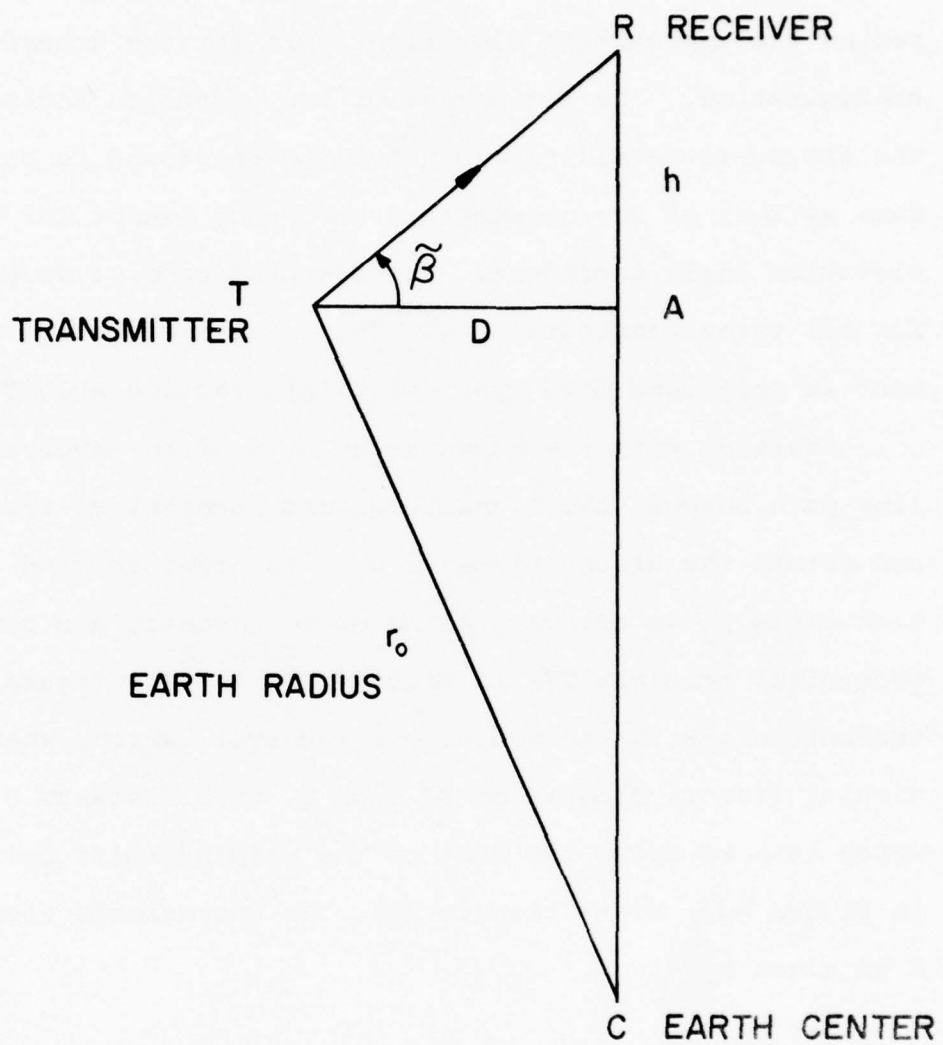


Figure 2.15. Earth geometry for finding the optical elevation angle.

$\beta_2 = \beta_1 + \delta\beta$ we proceed in the same manner as that described in section 2.2.3 to find the true homing elevation angle.

2.3.3 Examples and Discussion

In order to illustrate our homing technique we present two examples, one for ground-to-satellite and the other for the satellite-to-ground case. In both examples we studied the homing technique for the different oblique frequencies. The initial elevation angle is independent of the frequency of transmission. Since the straight line path approximation approaches the true path for high frequencies we expect the initial elevation angle to be very close to the true homing elevation angle.

Example 1. Ground-to-satellite.

Let the transmitter and receiver geographic coordinates be $(-165.0, 72.0)$ and $(-170.0, 56.0)$ longitude and latitude respectively. Also, let the transmitter and receiver heights above the earth surface be 0.0 and 560.0 km respectively. Then, for such a configuration the ground distance at the transmitter radius is 1793.97 km, the azimuthal angle of transmission is 190.1 degrees, and the initial approximate elevation angle is 8.475. The oblique transmission frequencies considered for this example were 90, 170, and 250 MHz. For each of these frequencies and starting with an elevation angle of 8.475 degrees we utilize the ray tracing program through subroutine ADJUST. The result of the calculation is presented in Figure 2.16. From Figure 2.16 we note that as the frequency gets higher the number of steps needed to achieve homing decreases. We also note that neither matrix

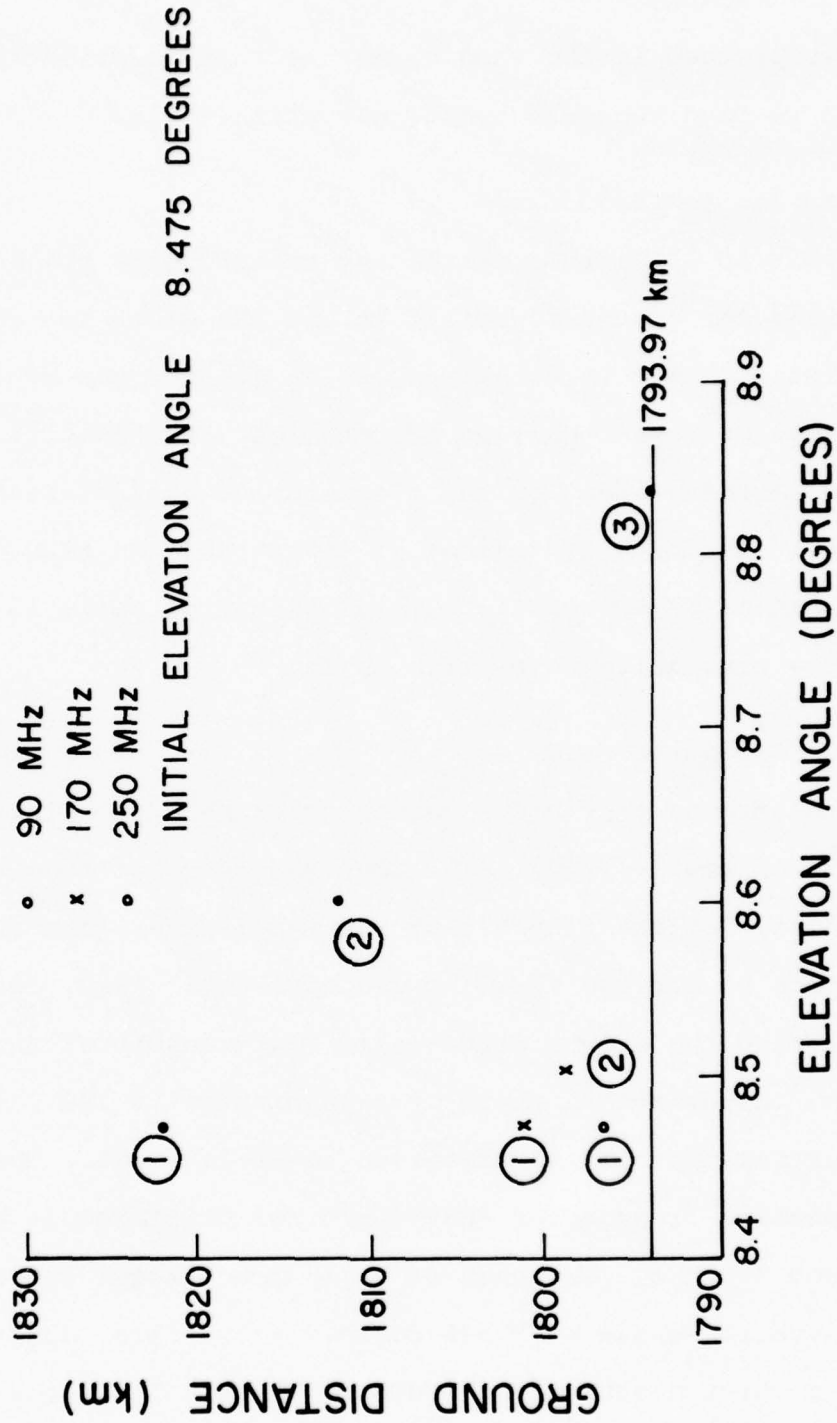


Figure 2.16. Example illustrating ground-to-satellite homing. The plot shows ground distance between the transmitter and the sub-satellite point versus the elevation angle for successive iterations using 3D ray tracing at three frequencies 90 MHz, 170 MHz and 250 MHz.

inversion nor linear interpolation is needed to achieve homing for all three frequencies. In Figure 2.17 the geomagnetic colatitude is plotted versus the geomagnetic longitude to show the homing steps for the three frequencies. For all frequencies the figure shows that no azimuthal correction is needed.

Example 2. Satellite-to-ground

For this example we let the transmitter and receiver be located at (-150.0, 78.0) and (-165.0, 60.0) longitude and latitude respectively. We also let the transmitter and receiver heights above the earth surface be at 550 and 0.0 km. For these geographic coordinates the ground distance at the transmitter radius is 2251.96 km, the azimuthal angle of transmission is 203.87 degrees, and the initial approximate elevation angle is -23.472 degrees. For each of the oblique frequencies 70, 140, and 210 MHz we used routine ADJUST to find the homing elevation angle. Figure 2.18 shows the ground distance versus the elevation for all frequencies together with the number of steps needed to achieve homing. For the 70 and 140 MHz it takes 4 steps while for 210 MHz only 3 steps are needed. One linear interpolation and one matrix inversion are required for the 70 and 140 MHz while one linear interpolation is carried out for 210 MHz. Figure 2.19 displays the geomagnetic colatitude versus geomagnetic longitude for the three frequencies. This figure shows the number of steps along the azimuth of transmission for each frequency. Homing for all frequencies is achieved without azimuthal corrections.

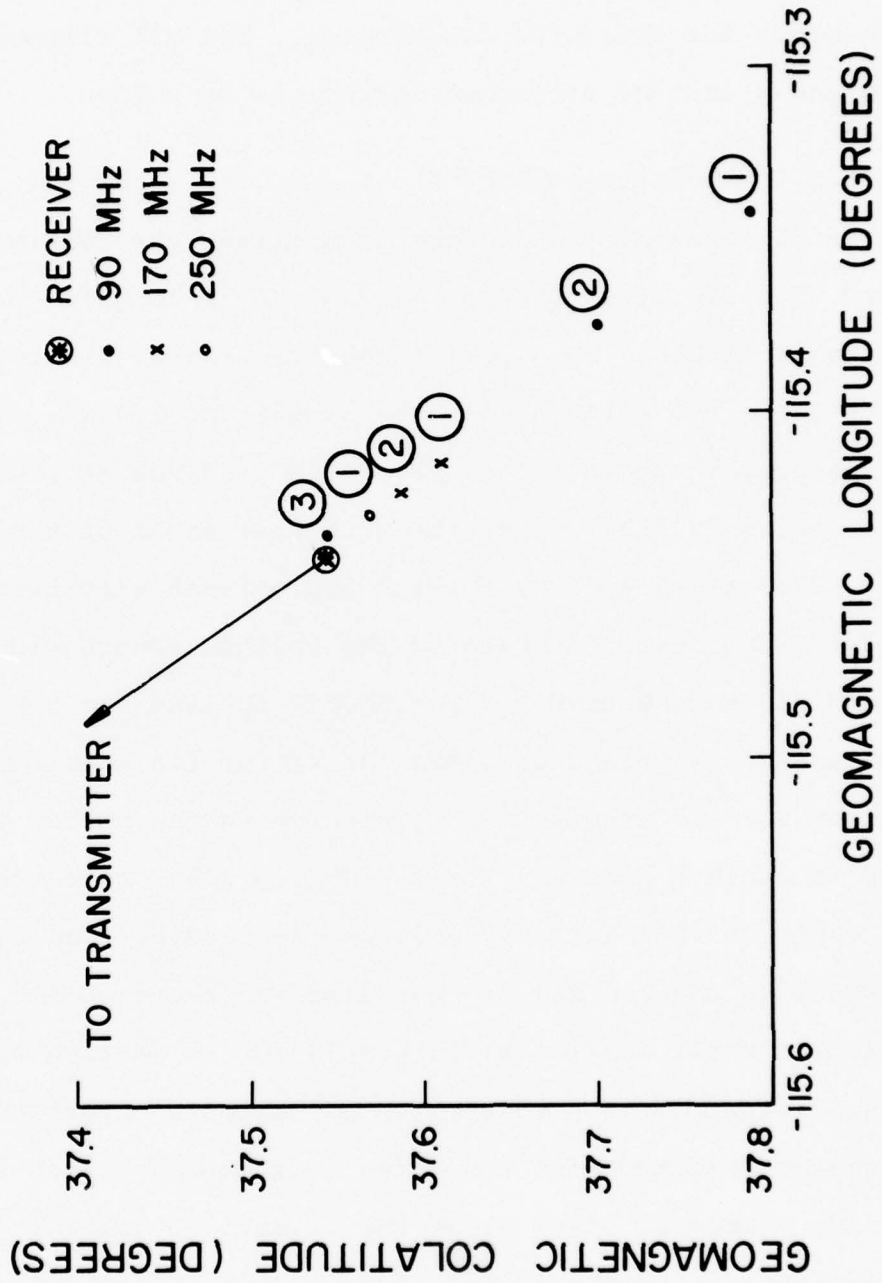


Figure 2.17. Continuation of example shown in Fig. 2.16 illustrating that no azimuthal correction is needed for homing at all three frequencies.

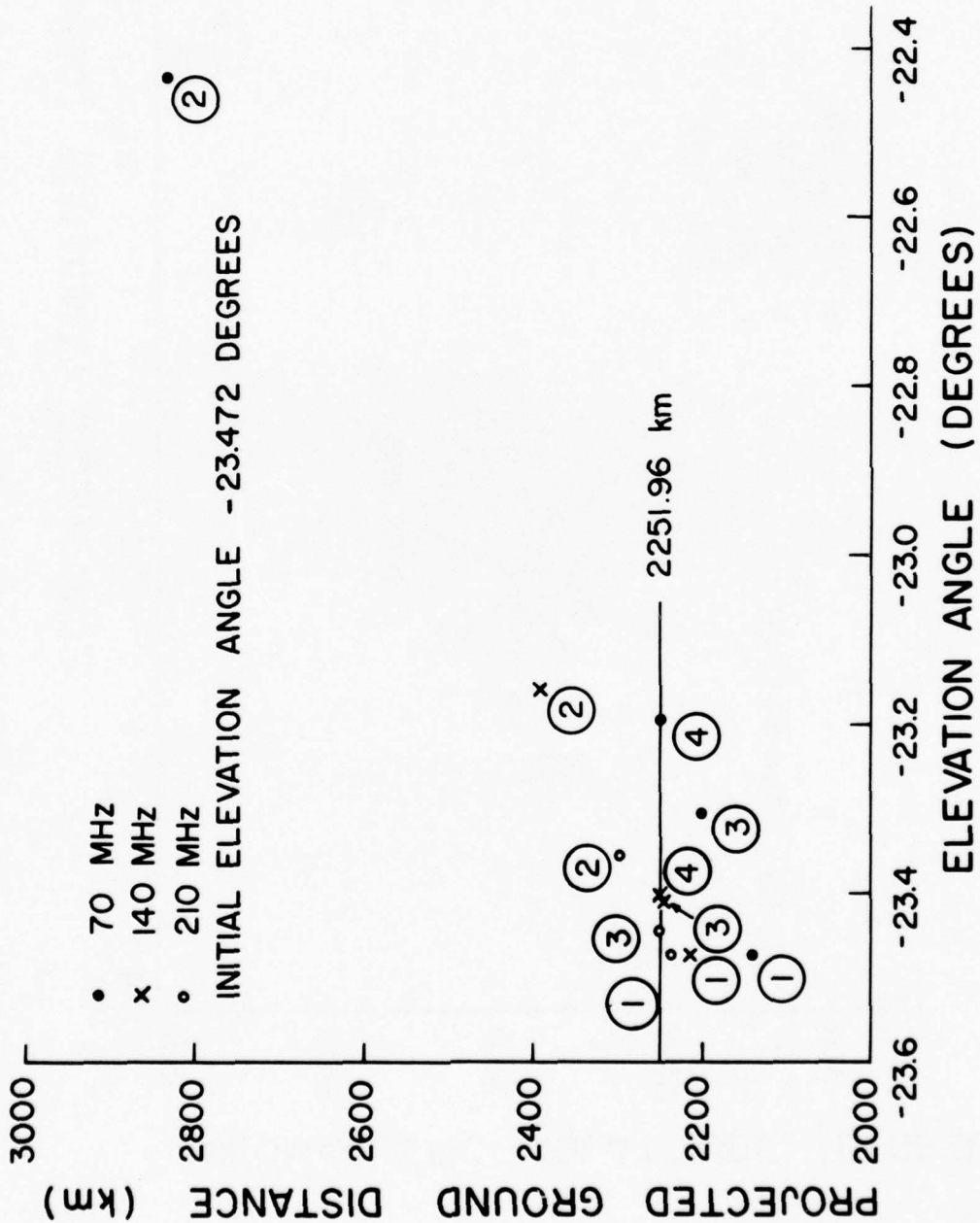
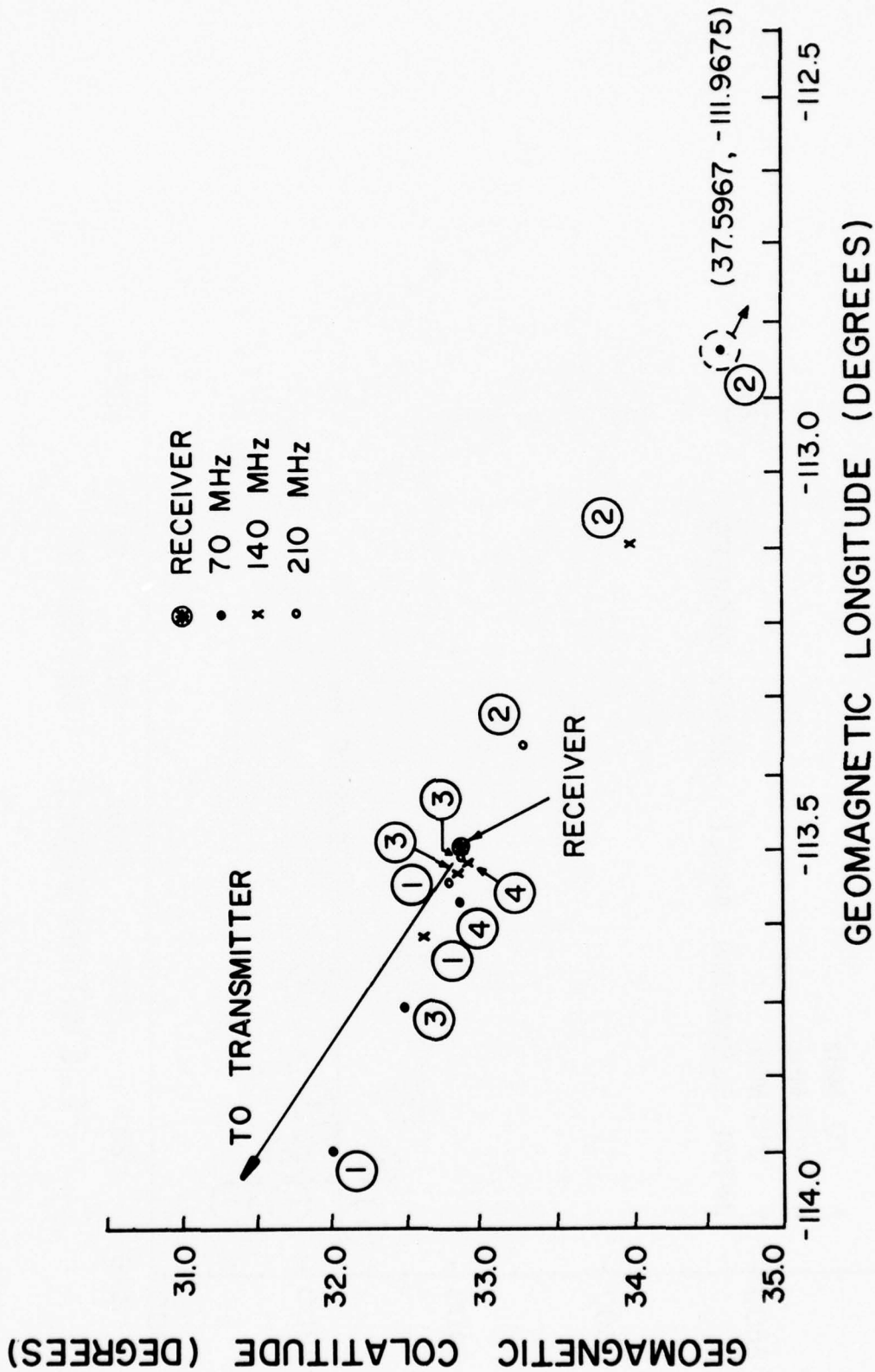


Figure 2.18. Example illustrating satellite-to-ground homing for three radio frequencies 70 MHz, 140 MHz, and 210 MHz.



2.4 Minimum Group Path

The technique of backscatter ionogram inversion utilizes the values of the minimum group path computed for the given ionospheric profile. Therefore, it is necessary to extend the ray tracing program to include the numerical computation of the minimum group path. The complete method is documented in subroutine GROUP M.

2.4.1 The Chopping Method

We assume that the transmitter location, the ionospheric model, the oblique transmission frequency, and the azimuthal angle are given. In addition, the minimum group path tolerance $\delta P'$ is also specified. At the present, the minimum group path tolerance is internally specified with a value of 1 km. With the known transmitter coordinates we can select the closest ionospheric model and find an approximate penetration angle β_p . This approximate angle is found through equation (18). Utilizing the ray tracing program and the given ionosphere we correct the approximate penetration angle until β_1 is just below the penetration condition. Since β_p is approximate we could encounter two main possibilities; either β_p is larger or smaller than the true penetration angle. Very seldom β_p will be equal to the true penetration angle and this situation is included in the cases where β_p is larger or smaller. For the case where β_p is larger than the true penetration angle we successively decrement β_p by one percent i.e. $\beta_{p_i} = 0.99\beta_{p_{i-1}}$, $i=1,2,3,\dots$, and obtain β_1 just below β_p . While in the case where β_p is smaller we successively increment β_p by five percent i.e. $\beta_{p_i} = 1.05\beta_{p_{i-1}}$, $i=1,2,3,\dots$ until the

ray penetrates the ionosphere and then we successively decrement β_p by one percent and obtain β_1 just below β_p .

Associated with β_1 is a group path P_1' . In order to locate the minimum group path we need three points along the group path versus elevation angle curve. The general behavior of this curve is shown in Figure 2.20. Define β_2 and β_3 as ninety five (95) and ninety (90) percent of β_1 and generate their corresponding group path values P_2' and P_3' through ray tracing. A comparison test is then performed on P_1' , P_2' , and P_3' . If $P_1' > P_2' > P_3'$ as in Figure 2.21a we discard β_1 and P_1' , shift indices backward and calculate a new β_3 equal to ninety five (95) percent of the old β_3 . With the new β_3 we generate a new group path P_3' . On the other hand, if $P_1' < P_2' < P_3'$ as in Figure 2.21b we discard β_3 and P_3' , shift indices forward and calculate a new β_1 equal to 105 percent of the old β_1 . With this new β_1 we generate a new group path P_1' . In either case we repeat the comparison tests on P_1' , P_2' , and P_3' until the condition $P_1' > P_2'$ and $P_3' > P_2'$ is satisfied.

Let us assume that we finally arrive at the situation depicted in Figure 2.21c where the condition $P_1' > P_2'$ and $P_3' > P_2'$ is satisfied. Then, in order to decide whether the minimum group path has been found or not we consider the following steps;

Step 1. Utilizing the chopping technique we take β_4 and β_5 at the mid point of the intervals β_1, β_2 and β_2, β_3 respectively. Tracing two rays with β_4 and β_5 we obtain two group paths P_4' and P_5' .

Step 2. If $|P_5' - P_2'| > \delta P'$ then we transfer to actions taken in step 3; otherwise, we have arrived at the minimum group path and a decision is made to select the

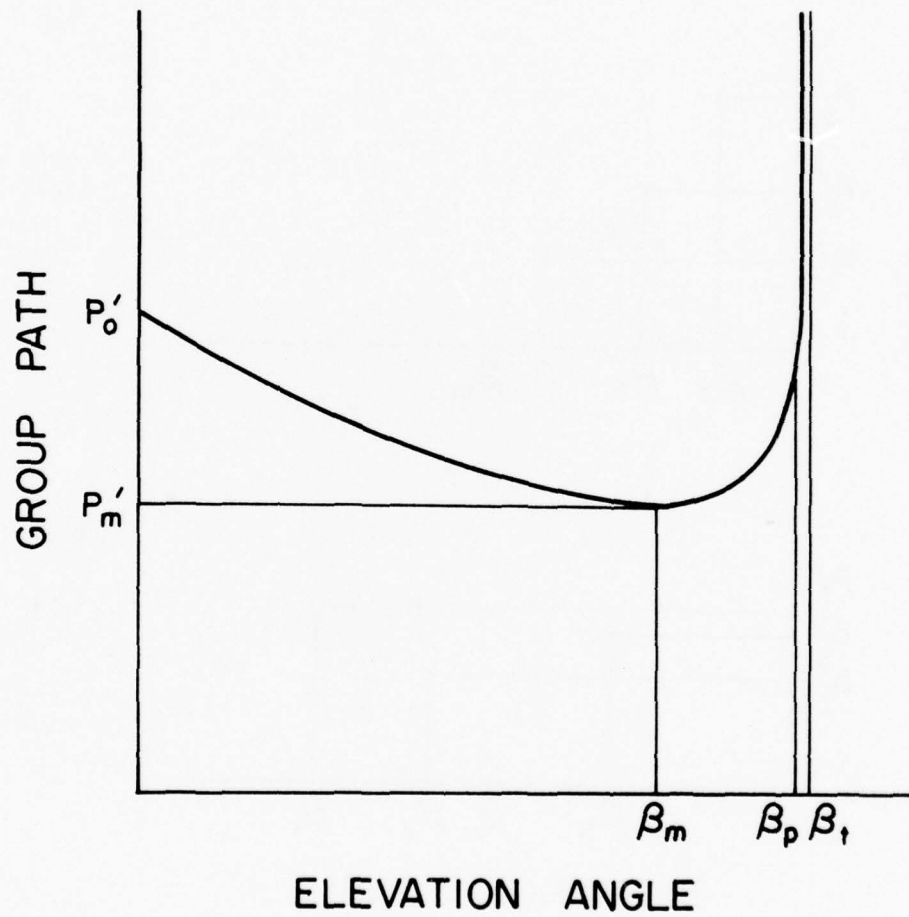


Figure 2.20. Sketch showing the general behavior of group path versus elevation angle curve.

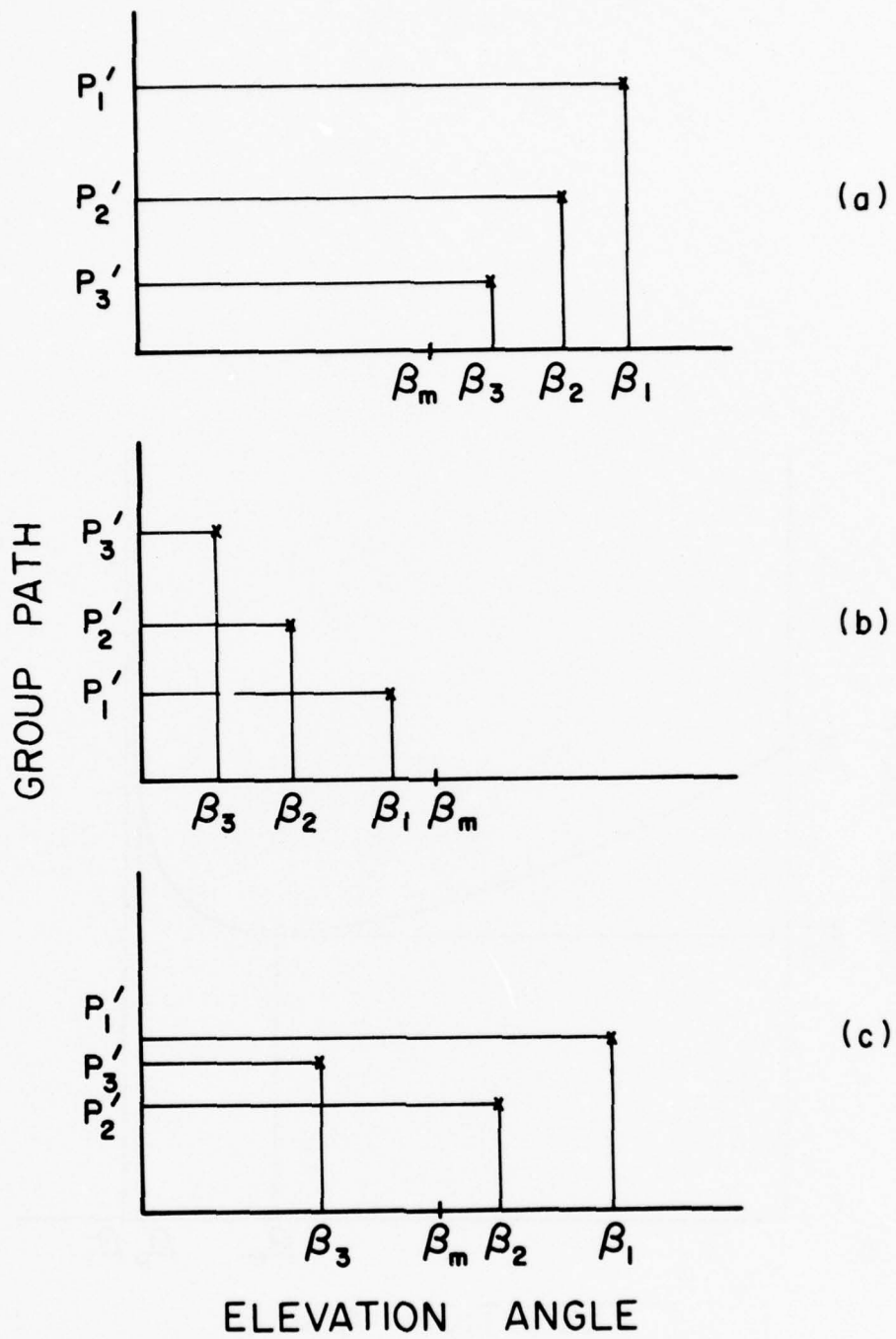


Figure 2.21. Sketch illustrating three possibilities for purpose of finding the minimum group path ray.

smallest of P_2' , P_4' , and P_5' .

- Step 3. If $P_5' > P_2'$ then we concentrate on actions taken in step 4. For $P_5' < P_2'$, the interval given by $P_3' > P_5'$ and $P_2' > P_5'$ is our main concern. In this interval we replace the values of β_1 , β_2 , P_1' , P_2' by the values β_2 , β_5 , P_2' , P_5' respectively and start over from step 1.
- Step 4. If $|P_4' - P_2'| > \delta P'$ then we transfer to actions taken in step 5. Otherwise, we have arrived at the minimum group path and a decision is made to select the smaller of P_2' and P_4' .
- Step 5. If $P_4' > P_2'$ then we concentrate on the interval given by $P_5' > P_2'$ and $P_4' > P_2'$ and replace the values of β_1 , β_3 , P_1' , P_3' by the values β_5 , β_4 , P_5' , P_4' respectively. Otherwise, our main concern is the interval given by $P_2' > P_4'$ and $P_1' > P_4'$. In this interval we replace the values β_2 , β_3 , P_2' , P_3' by the values β_4 , β_2 , P_4' , P_2' respectively. In either case we transfer to step 1 and start over again.

Once the minimum group path is found, control is transferred to the main program to perform a prescheduled activity in accordance with the input data through the W array.

2.4.2 Examples

In order to illustrate the technique of finding the minimum group path we present two examples. Both examples are derived from the same transmitter location at -175 and 40 degrees geographic longitude and latitude respectively. In the first example the azimuthal angle of transmission is 330 degrees and the oblique

frequency of transmission is 12 MHz, while in the second example the azimuthal angle and the oblique frequency are 308 degrees and 10 MHz respectively.

Example 1.

For an oblique frequency of 12 MHz the penetration angle from equation (2.18) is found to be 52.91 degrees. Starting with $\beta_1=52.9$ we generate the group path P_1' through ray tracing. Following the discussion in section 2.4.1 we take 95 and 90 percent of β_1 and define them as β_2 and β_3 . The values of β_2 and β_3 then are given by 50.26 and 47.62 degrees. The corresponding group path values P_2' and P_3' are found to be 1077.37 and 1022.81 km. Since $P_1' > P_2' > P_3'$ we discard β_1 and P_1' and shift the indices backward to obtain $\beta_1=50.26$, $P_1'=1077.37$, $\beta_2=47.62$ and $P_2'=1022.81$. Taking 95% of 47.62 degrees we generate $\beta_3=45.24$ and its corresponding group path $P_3'=995.86$. From the values thus known we still have $P_1' > P_2' > P_3'$. Discarding β_1 and P_1' , taking 95% of 45.24 degrees we obtain the following three sets of values, $\beta_1=47.62$, $P_1'=1022.81$, $\beta_2=45.24$, $P_2'=995.86$, $\beta_3=42.98$, $P_3'=981.11$. Since the condition $P_1' > P_2' > P_3'$ is still satisfied we carry out the same operations as above and arrive at the values $\beta_1=45.25$, $P_1'=995.86$, $\beta_2=42.98$, $P_2'=981.11$, $\beta_3=40.83$, $P_3'=973.56$. Comparison of the group path values reveal that $P_1' > P_2' > P_3'$ is the prevailing condition. Therefore, the next set of values are $\beta_1=42.98$, $P_1'=981.11$, $\beta_2=40.83$, $P_2'=973.56$, $\beta_3=38.79$, $P_3'=973.17$. Since the condition $P_1' > P_2' > P_3'$ is satisfied we carry out the calculations once more and arrive at the situation given by the values $\beta_1=40.83$, $P_1'=973.56$, $\beta_2=38.79$, $P_2'=973.17$, $\beta_3=36.85$, $P_3'=976.87$. An examination

of the group path values shows that the condition $P'_1 > P'_2$ and $P'_3 > P'_2$ is satisfied. Following the chopping method steps we find β_4 and β_5 at the midpoint of the intervals β_1, β_2 , and β_2, β_3 , respectively. With the values of $\beta_4=39.81$ and $\beta_5=37.82$ we find the group path values $P'_4=972.60$ and $P'_5=974.07$. Going to step 2 of the chopping method we find that $|P'_5 - P'_2| > \delta P' = 1$. Therefore, we find the minimum group path, it is either P'_2, P'_4 or P'_5 whichever is the smallest. In this case the minimum group path is given by $P'_4=972.60$ and the elevation angle is $\beta_4=39.81$. Figure 2.22 shows the group path versus elevation angle for the values generated under this example. The test sequence and indices shifting is also displayed on the graph.

Example 2.

In this example we use an azimuthal angle of 308 degrees and an oblique frequency of 10 MHz. The result of the calculation, testing and the value of the minimum group path are displayed in Figure 2.23. The circled numbers beside each point is the sequence calculation number. The table in the figure presents the sequence of operations performed before converging on the minimum group path value. In this example also the chopping technique is applied only once to achieve the final result.

2.5 Computer Programs

During the course of the study we augmented the 3D ray tracing program with six subroutines. They are discussed in the following.

2.5.1 General Description

For each of these subprograms we will be presenting

AZIMUTHAL ANGLE 330 DEGREES
 OBLIQUE FREQUENCY 12 MHz
 GROUP PATH TOLERANCE 1 km

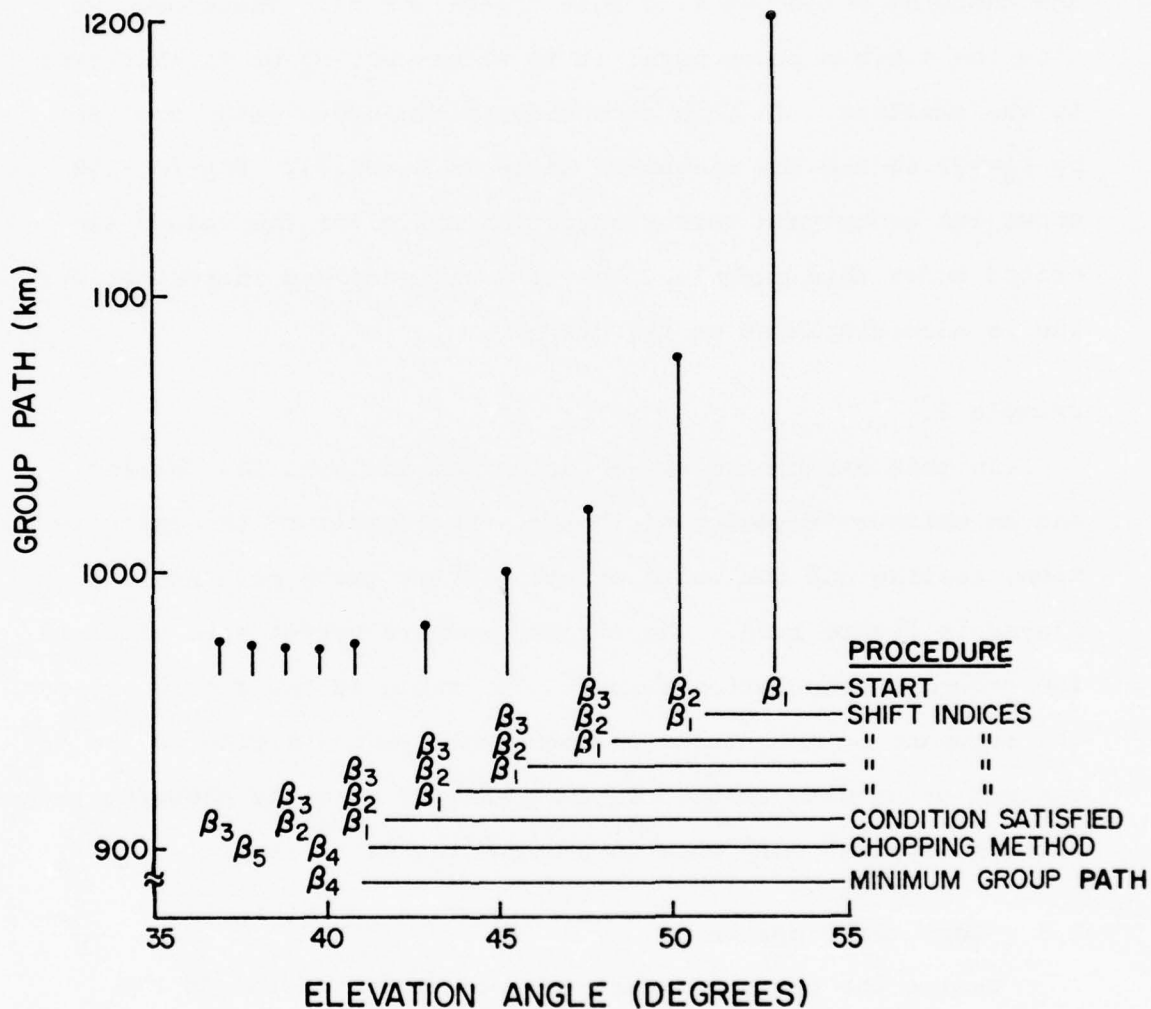


Figure 2.22. Example illustrating the steps in finding the minimum group path ray in a group path versus elevation angle plot. Note the index shifting, equal chopping and final location of the minimum group path to within the tolerance.

a description of their main purpose and the functions they perform.

Prior to describing the subprograms we present a list of the controls needed to successfully run the three dimensional ray tracing program for the homing cases and the minimum group path calculation. These controls are either internal or external allocations in the already existing W-array input data. The internal allocations are equivalence statements in the subprograms and there is no need to specify them. The external allocations are specified by the user in the input data of the W-array. The internal and external allocations of the W-array are:

| W | Description | Internal (In) External (Ex) |
|-----|---|--------------------------------|
| 371 | Control used for penetration conditions | (In) |
| 372 | Geomagnetic colatitude of the ray | (In) |
| 373 | Geomagnetic longitude of the ray | (In) |
| 374 | Local azimuthal deviation of the ray | (In) |
| 375 | Radial distance to the transmitter | (In) |
| 376 | ALPHA | (In) |
| 377 | THO, geomagnetic colatitude of transmitter | (In) |
| 378 | PHO, geomagnetic longitude of transmitter | (In) |
| 379 | Azimuthal deviation of the ray at the transmitter | (In) |
| | 0 regular ray tracing | |
| | 1 ground-to-ground homing | |
| 380 | 2 ground-to-satellite or satellite-to-ground homing | (Ex) |
| | 3 minimum group path | |
| 381 | Geographic East longitude of receiver in degrees | (Ex) |
| 382 | Geographic latitude north of receiver in degrees | (Ex) |

| | | |
|-----|---|------|
| 383 | Height of the ray above the earth surface | (In) |
| 384 | Ground distance computed in PRINTR | (In) |
| 385 | Ground distance computed from the geometry of the problem | (In) |
| 386 | Maximum number of iterations for finding the approximate elevation angle | (Ex) |
| 387 | The tolerance allowed between the ground distance in W(385) and calculated ground distance | (Ex) |
| 389 | Penetration angle used in homing | (In) |
| 390 | Height of the bottom of the ionosphere above earth | (Ex) |
| 391 | Maximum height of the ionosphere above earth | (Ex) |
| 393 | 0 utilizes the given ionospheric profile 1 generates a new ionospheric profile based upon the given quasi-parabolic parameters | (Ex) |
| 394 | Value of the group path used in the group path homing | (Ex) |

Subroutine HOME

Purpose:

The HOME subroutine calculates the initial approximate elevation angle in the ground-to-ground homing for the ground distance and the group path.

Description:

The HOME routine calculates several parameters and generates tables prior to obtaining the final result of initial approximate elevation angles. The azimuthal angle of transmission and the exact ground distance are computed from the given transmitter and receiver coordinates. The midpoint between the transmitter and receiver is found and the electron density profile at this midpoint is extracted from the given ionospheric profile. With

the critical frequency of the midpoint profile and the given oblique frequency of transmission the penetration angle is computed from equation (2.18). Then, the elevation angle interval from zero to this penetration angle is subdivided into 50 intervals thus generating 51 values of elevation angles. For each value of elevation angle in the interval a ground distance and a group path value are calculated from the analytical expressions for a quasi-parabolic density profile. These analytical expressions are programmed in subroutine FITT. Through this procedure a table of elevation angles, ground distances, and group paths is assembled.

The exact ground distance is then compared to the ground distance values in the table. If the exact ground distance is lower or higher than the ground distances in the table, then no approximate elevation angles can be found. However, if the exact ground distance is located between two ground distances in the table, we interpolate linearly to find an approximate elevation angle. Since there might be more than one homing solution we scan through the table and locate all possible elevation angles.

The HOME subroutine is capable of storing approximate elevation angles for a four layered ionosphere. In addition, this subroutine has been mainly written for the single hop mode of propagation. The two hop mixed mode of propagation is already included as described in section 2.2.6.

Subroutine HOMES

Purpose:

The HOMES subroutine calculates the initial approximate ele-

vation angle for a straight line path in the ground-to-satellite and the satellite-to-ground configurations.

Description:

Given the transmitter and receiver coordinates and the oblique transmission frequency subroutine HOMES computes the azimuthal angle of transmission and the ground distance projected at the transmitter radius. Assuming a straight line path between the transmitter and receiver, the approximate elevation angle is found from the triangle in the plane containing the transmitter, the receiver, and the earth center.

Subroutine FITT

Purpose:

Given an elevation angle routine FITT calculates the corresponding ground distance and group path from analytical expressions for a quasi-parabolic density profile.

Description:

Utilizing the analytical expression given by equations (2.13)-(2.16), the electron density profile at the midpoint of the path between the transmitter and receiver, and the oblique frequency of transmission, subroutine FITT computes the ground distance and the group path for a specified elevation angle. The contributions of ground distances and group paths are added up from the transmitter height up to the ray reflection height. The integration step corresponds to the height increment of the electron density profile at the midpoint.

Subroutine RAYINT

Purpose:

Routine RAYINT initializes the ray parameters before any actual ray tracing is performed.

Description:

The code in subroutine RAYINT is extracted from the main subprogram of the ray tracing program to enable the homing and minimum group path procedures to function independently from the main program. With a specified elevation and azimuthal angles this subroutine initializes the ray parameters prior to tracing the ray via subroutine TRACE.

Subroutine ADJUST

Purpose:

The ADJUST subroutine takes the approximate elevation angles for any of the three configurations, ground-to-ground, ground-to-satellite, or satellite-to-ground and modifies them through the ray tracing program to achieve homing.

Description:

Utilizing the initial elevation angle a ray is traced in the ionospheric profile to obtain a ground distance value. Then, the initial elevation angle is incremented or decremented by a small amount depending upon the configuration under consideration. In the ground-to-ground case the initial increment or decrement is found from the table assembled in subroutine HOME, while in the other two cases the initial increment or decrement is found from equation (2.35). Adjusting the initial elevation angle by the initial increment or decrement we obtain a new elevation angle

and a corresponding ground distance through ray tracing. The objective is to locate the exact ground distance between the ground distances of the traced rays. Sometimes, the rays are homed without further calculations and at other times we cannot locate the exact ground distance between the ground distances obtained through ray tracing at which point a message is printed. Let us assume that the exact ground distance lies between the two ground distances obtained from ray tracing. With the two values of elevation angles and their corresponding ground distances we interpolate linearly and find a third elevation angle. Utilizing this third elevation angle we trace another ray to obtain the ground distance. If the ray is not homed in yet, we have three elevation angles and their ground distances. Since the variation between ground distance and elevation angle is nonlinear we fit a second degree polynomial in elevation angle and invert the resulting matrix to find a new elevation angle that will eventually home the ray.

With this elevation angle we trace a ray and find the ground distance. A comparison test on the ground distances will reveal whether or not homing is achieved. In the event that homing is not achieved, the procedure of fitting the second degree polynomial is repeated utilizing the closest three ground distances to the exact ground distance and their corresponding elevation angles. Then, either homing is achieved and no further calculations are needed, or the above procedure is repeated to attain homing. Homing may not be achieved due to discontinuities in the ray-traced ground distance versus elevation angle curve, high angle ray, or that the maximum number of specified trials to find

an elevation angle have been exceeded.

Subroutine GROUPEM

Purpose:

Subroutine GROUPEM calculates the minimum group path for given transmitter coordinates, azimuthal angle of transmission and an oblique transmission frequency.

Description:

With the given transmitter coordinates, the closest density profile is selected from the composite ionospheric profile. From the knowledge of the critical frequency of the selected profile and the oblique frequency of transmission, the penetration angle is computed through equation (2.18). Then, starting with this penetration angle we initialize the ray parameters and trace a ray through the given ionosphere. If the ray penetrates the ionosphere we decrement the elevation angle (penetration angle) by one percent and trace another ray. This procedure is repeated until the ray is reflected and a value for the group path is obtained. There, we take 95 or 90 percent of the resulting elevation angle thus generating two new elevation angles. With these two new elevation angles we trace two rays to obtain their corresponding group path values. The three values of elevation angles and their corresponding group paths describe a curve. This curve may assume three shapes, sloping to the left (most common), sloping to the right (rare) or concave upwards. In the cases where the curve is sloping to the right or left we increment or decrement the elevation angle and trace rays until the shape of the curve is concave upward. For this shape the values

of the group paths are compared with each other to test for the minimum value within a specified 1 km tolerance.

Let us assume that we did not attain the minimum group path value, then we subdivide the two intervals in the curve and obtain two elevation angles, one in each interval, thus generating two additional intervals. Through ray tracing we obtain two values of group paths corresponding to the two new elevation angles. A test is performed between the five group path values and the largest two are discarded retaining only three values and their corresponding elevation angles. Through repeated application of this procedure we converge on the minimum group path value with the specified tolerance of 1 km. This tolerance is imbedded in the subroutine and could be changed to any desired value.

2.5.2 Program Listings

A complete listing of all the programs discussed in this section is given in Appendix 1.

2.6 Discussion

We have modified the three dimensional ray tracing program to include the homing features for ground-to-ground, ground-to-satellite, and satellite-to-ground configurations. In addition, the ray tracing program has been augmented by a chopping technique to find the minimum group path. In the preceding sections we presented in detail the approach and methods utilized in the homing of the ray together with representative examples. We also outlined the purpose and description of each computer sub-program added to the originally supplied AFCRL three dimensional ray tracing program.

The results of our homing approach for the one hop mode of propagation show that homing is almost always achieved provided the input parameters are correctly entered through the input data. We say almost since there are situations where homing of the ray may not be possible. During the course of our study we came across three situations in the ground-to-ground case whereby homing might not be possible. These three situations are

- i) high angle ray
- ii) ground distance too close to the skip distance or discontinuity in the ray traced ground distance versus elevation angle curve.
- iii) number of tries to find an elevation angle is exceeded.

A preliminary investigation of the two mixed hop mode of propagation has been initiated and the technique has been implemented in the HOME subroutine. The application of our technique to achieve homing is only partially successful; the ray was homed in for a few cases while for the majority of the cases tested we

encountered difficulties in homing of the ray. These difficulties may be attributed to the following reasons:

- i) the coarseness of the given ionospheric profile
- ii) the interpolation procedure used in the ray tracing program
- iii) the technique applied to the two hop mode

Through further research, the true nature of the problem could be pinpointed and if need be a sophisticated homing technique for the multi-hop mode of propagation can be developed.

Aside from the homing problems, we have also incorporated a chopping method to find the minimum group path. The results of such a method are quite evident from the examples presented in section 2.4.2. For all the cases studied we have been successful in finding the minimum group path within the specified tolerance. The number of steps needed to obtain the minimum group path decreases as the frequency of transmission gets higher. Once we arrive at the condition whereby the variation of group path versus elevation angle curve is concave upward, the convergence of the chopping method is very fast.

From the results presented in this report and other examples derived from the techniques used in homing of the ray and finding the minimum group path it is quite evident that we have been successful in achieving our objective. The difficulties encountered during the course of this study could be overcome through modification and refinement of the ray tracing program and the ionospheric profile. Such modification and refinement can only be achieved through further research.

3. ANALYSIS OF OBLIQUE PROPAGATION DATA

3.1 Introduction

The goal of this investigation is to devise techniques for inverting h.f. oblique radio propagation data for ionospheric models with horizontal gradients. There are two kinds of oblique propagation data: (a) Point-to-point oblique ionograms, and (b) Backscatter leading edge. In this section, we shall consider briefly the nature of these two types of data and discuss qualitatively their capabilities and limitations in providing information concerning ionospheric models with horizontal gradients.

3.1.1 Point-to-Point Oblique Ionograms

These are traces of group path (P') versus frequency (f) for oblique propagation between two fixed points separated by some distance. Since the end points of the propagation path are fixed, the reflection points of the rays lie in the neighborhood of the midpoint between the transmitter (T) and receiver (R) for the one-hop mode of propagation, irrespective of the frequency, as shown in Fig. 3.1(a). Similarly, for multiple-hop mode of propagation, reflection for each hop occurs in the neighborhood of a single location, for all frequencies capable of propagating in that mode. A typical shape of the oblique ionogram trace for the one-hop mode is shown in Fig. 3.1(b).

It can be easily conjectured from Fig. 3.1(a) that a one-hop mode oblique ionogram is capable of providing an equivalent vertical profile of electron density valid near the midpoint between the transmitter and the receiver, but is not by itself too useful for deriving the horizontal gradients of electron density. How-

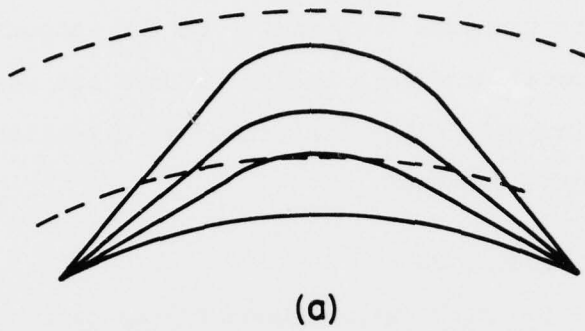


Figure 3.1a. Ray paths for point-to-point oblique ionograms at different frequencies.

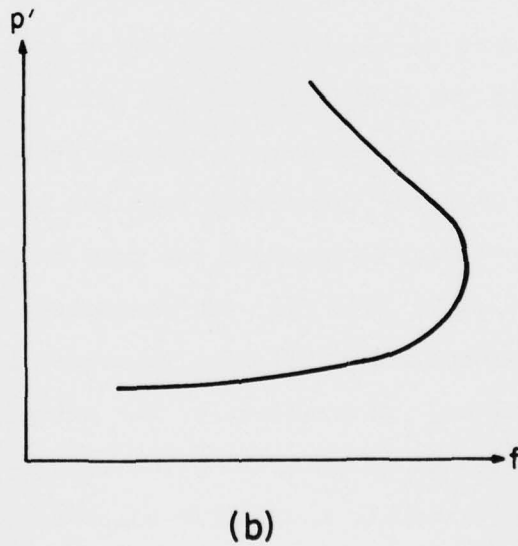


Figure 3.1b. Typical shape of one-hop trace for point-to-point oblique ionogram.

ever, for a particular assumed model with horizontal gradients near the midpoint, it is in principle possible to deduce the parameters so as to achieve a best fit with the experimental ionogram. The use of a two-hop mode trace in addition to the one-hop mode trace would increase the utility of the ionogram for deriving the horizontal gradients but still does not permit their determination continuously along the azimuthal direction from the transmitter to the receiver.

3.1.2 Backscatter Leading Edge

In the case of the backscatter mode of propagation, the transmitter and the receiver are located at about the same location and the time delay of the transmitted signal backscattered from the ground and then received at the receiver is measured as a function of frequency. For a given frequency, many returns are possible corresponding to all elevation angles of transmission and reception within the bandwidths of the transmitting and receiving antennas. There is however a minimum value for the time delay which occurs near the transition from the low angle ray mode of propagation to the high angle ray mode of propagation, as shown in Fig. 3.2(a). Thus for each frequency, a continuum of backscattered returns beginning with the minimum time delay return will be received. Alternatively, the situation can be thought of as a continuum of point-to-point oblique ionograms corresponding to continuously increasing values of ground range of the backscatter location away from the transmitter. Such a continuum of oblique ionograms is shown in Fig. 3.2(b). The tangent curve to these ionograms is the "backscatter leading

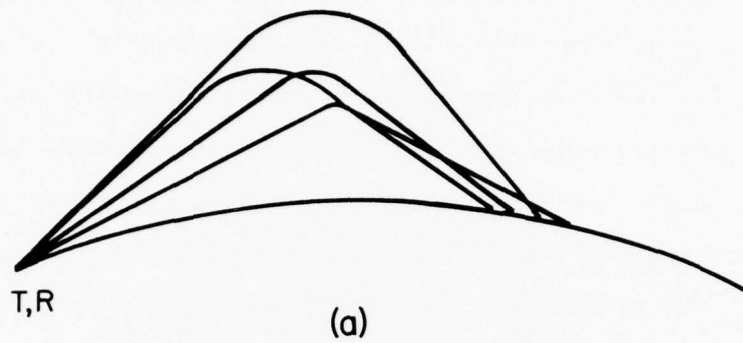


Figure 3.2a. Ray paths for backscattered rays at one frequency.

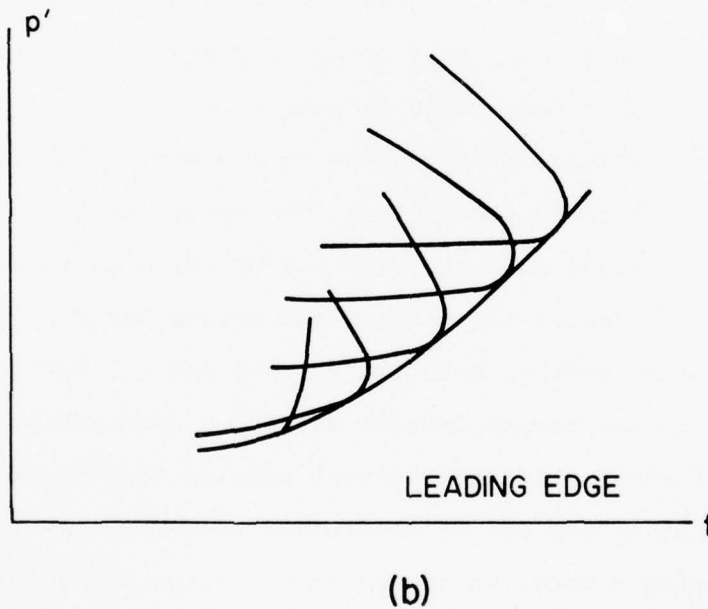


Figure 3.2b. Showing that the leading edge of a backscatter ionogram is the tangent curve to a continuum of point-to-point oblique ionograms.

edge", and is generally the only useful portion of the backscatter ionogram since all the other returns cannot be distinguished from one another, except in the case of high resolution ionograms.

It can now be seen from Fig. 3.2(b) that points along the backscatter leading edge correspond to rays reflecting at continuously increasing distant locations from the transmitter. Hence in principle the backscatter leading edge contains information concerning the horizontal gradients of electron density outward from the transmitter location along the azimuthal direction corresponding to the backscatter ionogram. However to obtain a vertical profile of electron density at any given location, a minimum number of points along an ionogram are required. For example, a quasi-parabolic profile requires a minimum of three points. If we consider three points on the backscatter leading edge, we must select them very close to each other in order to obtain the vertical profile corresponding to a given location. On the other hand, for three such points, the apogee heights of reflection for the corresponding rays do not differ significantly. Hence to increase the separation between the apogee heights of reflection, the points must be selected farther apart. Thus it becomes necessary to compromise between these two conflicting requirements. A further point of interest arising from these requirements is that it may not be profitable to invert the leading edge by employing a model which requires a large number of parameters to describe its vertical profile. This observation is augmented by the fact that simulated backscatter leading edge data using three-dimensional ray tracing indicates that the apogee heights of rays corresponding to points on the leading

edge lie within a narrow range of values. This also makes it impossible for the backscatter leading edge to provide the vertical profile above the maximum apogee height. However, as will be pointed out later, this is not a limitation insofar as the application of the leading edge data is concerned, although it may be a limitation for the purpose of obtaining the complete ionospheric structure up to the layer peak.

Thus in this introductory section, we point out that while the point-to-point oblique ionograms are capable of providing the vertical profile near the midpoint between the transmitter and the receiver, they are not too useful for obtaining horizontal gradients over wide ranges of distance along the line from the transmitter to the receiver. On the other hand, the backscatter leading edge, while unable to provide the vertical profiles above certain heights, is useful for deducing the horizontal gradients over wide ranges of distance along the azimuthal direction from the transmitter corresponding to the backscatter ionogram.

3.2 The Quasi-Parabolic Layer

Since the primary purpose of this investigation is to devise techniques capable of yielding the horizontal gradients of electron density, it can be seen from the discussion in the previous section that it becomes necessary to attach more importance to the backscatter leading edge data than to the point-to-point oblique ionogram data. Hence for selecting a model, the limitation of the leading edge data need to be considered. In view of this, an ionospheric model requiring a small number of parameters to

define its vertical profile is more suitable. Such a model, which is also amenable to analytical solution for the ray path parameters, as compared to numerical ray tracing, is the quasi-parabolic layer model. Hence this section is devoted to the quasi-parabolic layer.

3.2.1 The Earth Concentric Quasi-Parabolic Layer

The quasi-parabolic layer is defined by the variation of electron density N_e with the radial distance r from the center of the earth as given by

$$N_e(r) = \begin{cases} N_m \left[1 - \left(\frac{r-r_m}{Y_m} \right)^2 \left(\frac{r_b}{r} \right)^2 \right] & \text{for } r_b < r < r_m \left(\frac{r_b}{r_b - Y_m} \right) \\ 0 & \text{otherwise} \end{cases} \quad (3.1)$$

where

$N_m = f_c^2/80.6 =$ maximum value of electron density

$f_c =$ critical frequency

$r_m =$ value of r at which N_e is equal to N_m

$r_b =$ value of r at the base of the layer

$Y_m = r_m - r_b =$ semithickness of the layer

The slight modification over the parabolic model, which is defined by ignoring the factor $(r_b/r)^2$ in (3.1), enables the derivation of exact closed form expressions for the ray path parameters for the quasi-parabolic layer (Croft and Hoogasian, 1968), by application of Bouguer's rule for ray tracing in a spherically symmetric layer. For a signal of frequency f and elevation angle

of transmission β , these expressions for the ground range R , and group path P' are given as follows (Rao, 1974; Rao, 1975):

$$R = 2r_0 \left\{ (\gamma - \beta) - \frac{F r_0 \cos \beta}{2\sqrt{C}} \ln \frac{U r_b^2}{W^2} \right\} \quad (3.2)$$

$$P' = 2 \left(1 - \frac{F^2}{A} \right) r_b \sin \gamma - 2r_0 \sin \beta - \frac{BF}{2A^2} \ln \frac{U}{V^2} \quad (3.3)$$

where

$$F = f/f_c$$

$$\gamma = \cos^{-1} \left(\frac{r_0 \cos \beta}{r_b} \right) = \text{elevation angle at the base of the layer}$$

$$r_0 = \text{radius of the earth}$$

$$U = B^2 - 4AC$$

$$V = 2Ar_b + B + 2r_b F \sqrt{A} \sin \gamma$$

$$W = 2\sqrt{C} F r_b \sin \gamma + 2C + B r_b$$

$$A = F^2 - 1 + (r_b/y_m)^2$$

$$B = -2r_m r_b^2 / y_m^2$$

$$C = \left(\frac{r_b r_m}{y_m} \right)^2 - F^2 r_0^2 \cos^2 \beta$$

To find the minimum group path, which is equal to the minimum time delay times the velocity of light in free space, we first note that for a given frequency and for a given set of layer parameters, the elevation angle of transmission corresponding to the minimum group path ray is given by the solution of the equation

$$\begin{aligned}
\frac{\partial P'}{\partial \beta} &= 2 \left(1 - \frac{F^2}{A} + \frac{BF^2}{AV} \right) r_0 \sin \beta \cos \gamma \\
&\quad - 2 \left(1 - \frac{2B F^3 r_0 \sin \beta}{\sqrt{A} U} \right) r_0 \cos \beta \\
&= 0
\end{aligned} \tag{3.4}$$

Recognizing that $\partial P'/\partial \beta$ varies continuously from a large negative value near zero elevation angle to a large positive value near maximum elevation angle corresponding to penetration of the ray through the layer, we can solve (3.4) for β in an iterative manner. The penetration condition occurs for the ray apogee radius equal to $-B/2A$ and hence for the elevation angle of transmission given by

$$\beta_p = \cos^{-1} \left\{ \frac{1}{Fr_0} \left[\left(\frac{r_b r_m}{y_m} \right)^2 - \frac{B^2}{4A} \right]^{\frac{1}{2}} \right\} \tag{3.5}$$

Thus starting with values of β near zero and β_p , the value of β for which $\partial P'/\partial \beta$ is a small specified value can be found in an iterative manner. Substitution of this value of β in (3.2) then gives the value of the minimum group path, P'_{\min} .

In the formulation of the procedures for inversion of the point-to-point oblique ionograms and backscatter leading edges for quasi-parabolic layer parameter, we will find later that the partial derivatives of R and P' with respect to the layer parameters are required. Expressions for these quantities, which can be easily derived from (3.2) and (3.3) are given in the appendix.

3.2.2 The Eccentric Quasi-Parabolic Layer

In papers by Rao (1968, 1973), the ionospheric layer has

been assumed to be still spherical but eccentric with respect to the earth. Figure 3.3 shows the geometry pertinent to such a layer with its center C' displaced by vector \vec{D} from the earth's center C . Assuming quasi-parabolic distribution of electrons in the eccentric layer, the spherical geometry of the system with respect to its own center enables us to use the formulas for the concentric case (Section 3.2.1) with some additional computations introduced by Rao (1968). Thus the eccentric quasi-parabolic layer model, which permits the existence of gradients in the electron density, is completely defined by the following six parameters:

- f_c : critical frequency of the layer
- h_o : vertical distance between the base of the ionosphere and the surface of earth along vector \vec{D}
- Y_m : semi-thickness of the layer
- D : the distance between the centers of the earth and the ionosphere
- ω_t : the angle between the displacement vector \vec{D} and the radius of earth through the transmitter
- α : an angle pertinent to the azimuthal angle of transmission

For simplicity, we assume no gradient lateral to the transmission path ($\alpha = 0$) and the model is then defined by the first five parameters. The consideration of non zero α will not affect the presented techniques and will only add an additional dimension to the problem.

It is essential to have a feel for the type and amount of

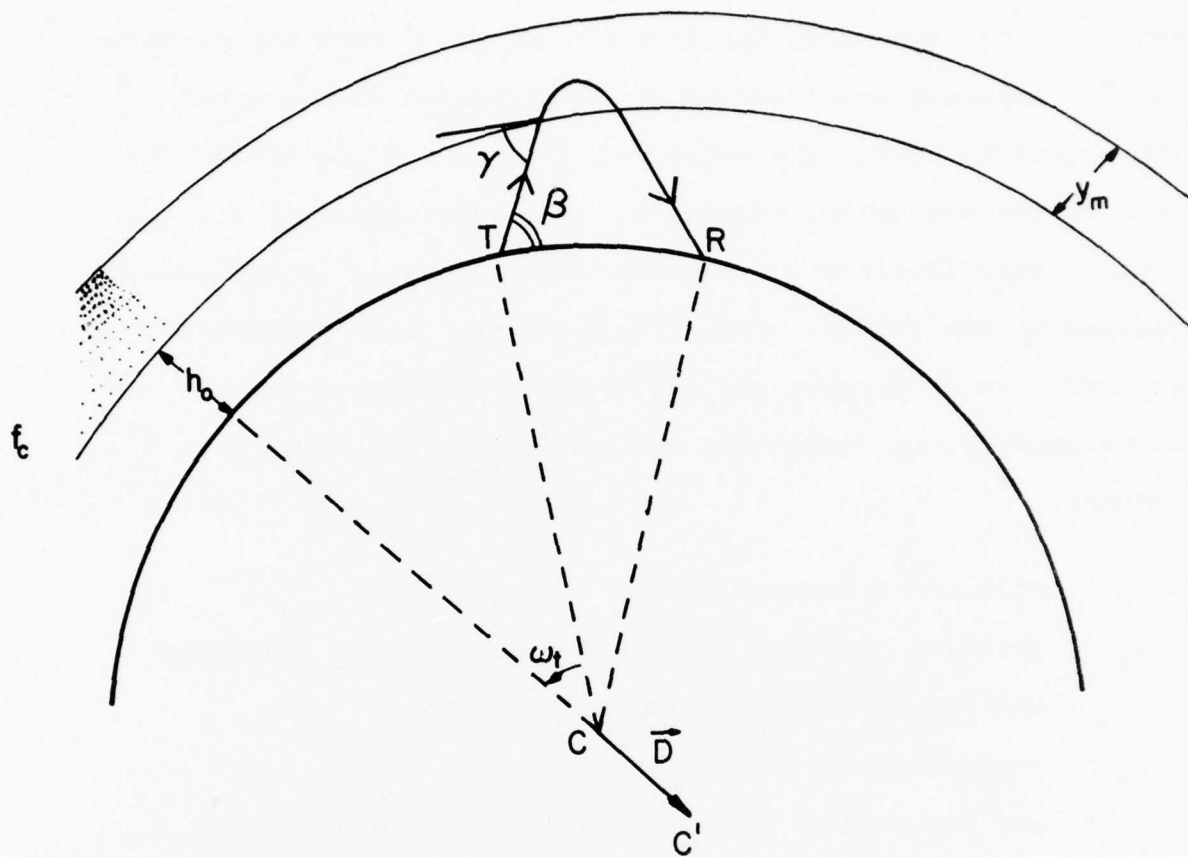


Figure 3.3. The eccentric quasi-parabolic layer with its defining parameters.

the gradients introduced by D and ω_t parameters of the eccentric layer. To accomplish this, we must make a few simplifying assumptions and approximations. The geometry of Figure 3.3 suggests that we have gradients in the base and peak heights of the layer. To obtain realistic relative values for these two gradients, we will assume that the base height of the layer above the transmitter be a constant value for all cases. In Figure 3.4, T and R are the locations of the transmitter and the receiver with M and θ_0 being the location and the angle of their mid-point. The base heights of the layer above T and R are denoted by h'_0 and h''_0 . Expressions can now be derived for the gradients at angle θ_0 (approximately where the reflection takes place).

The equation of the base-height circle can be written as

$$\begin{aligned} (x + D \cos \omega_t)^2 + (y + D \sin \omega_t)^2 &= D^2 + (r_0 + h'_0)^2 \\ &+ 2D(r_0 + h'_0) \cos \omega_t \end{aligned} \quad (3.6)$$

Writing (3.6) in polar coordinates, we get

$$r^2 + 2rD[\cos(\theta - \omega_t)] = (r_0 + h'_0)^2 + 2D(r_0 + h'_0) \cos \omega_t \quad (3.7)$$

Differentiating 3.7 with respect to θ , we have

$$\begin{aligned} 2r \frac{\partial r}{\partial \theta} + 2D \frac{\partial r}{\partial \theta} \cos(\theta - \omega_t) - 2Dr \sin(\theta - \omega_t) &= 0 \\ \frac{\partial r}{\partial \theta} \Big|_{\theta=\theta_0} &= \frac{D \sin(\theta_0 - \omega_t)}{1 + \frac{D}{r} \cos(\theta_0 - \omega_t)} \end{aligned} \quad (3.8)$$

where

$$r' = r_0 + h'_0 \quad \text{for the base height gradient}$$

$$r' = r_0 + h'_0 + y_m \quad \text{for the peak height gradient.}$$

Since, in general $r_0 \gg h'_0$ and y_m , we can assume that the gradient is equal for both base and peak heights ($r' \cong r_0$).

As a typical example, let us assume $\hat{\text{TOR}} = 10^\circ$ corresponding to a ground range of $R = 1111.8$ km ($\theta_0 = 5^\circ$). The gradient given by (3.8) is evaluated for several values of D and ω_t and Fig. 3.5 shows the peak height gradient ($r' = 6370 + 150 + 200 = 6720$ km) as a function of D for several values of ω_t . Figure 3.5 also shows the forbidden regions, characterized by the ionosphere going underground at the receiver. This happens when the gradients are large, forcing the base height of the layer to be less than zero above the receiver ($h''_0 < 0$). The quantity h''_0 can be derived by solving (3.7) for r and setting $\theta = 2\theta_0$. Thus

$$r_0 + h''_0 = -D \cos(2\theta_0 - \omega_t) + \sqrt{D^2 \cos^2(2\theta_0 - \omega_t) + (r_0 + h'_0)^2 + 2D(r_0 + h'_0) \cos \omega_t} \quad (3.9)$$

The above equation can also be used to set an upper limit for h''_0 as well as a lower limit. This will result in a usable region on Fig. 3.5 for the values of D and ω_t .

AD-A038 299

ILLINOIS UNIV AT URBANA-CHAMPAIGN DEPT OF ELECTRICAL --ETC F/6 17/2.1
TECHNIQUES OF DETERMINING IONOSPHERIC STRUCTURE FROM OBLIQUE RA--ETC(U)
DEC 76 N N RAO, K C YEH, M Y YOUAKIM F19628-75-C-0088

UNCLASSIFIED

UILU-ENG-76-2559

RADC-TR-76-401

NL

2 OF 3
AD
A038 299

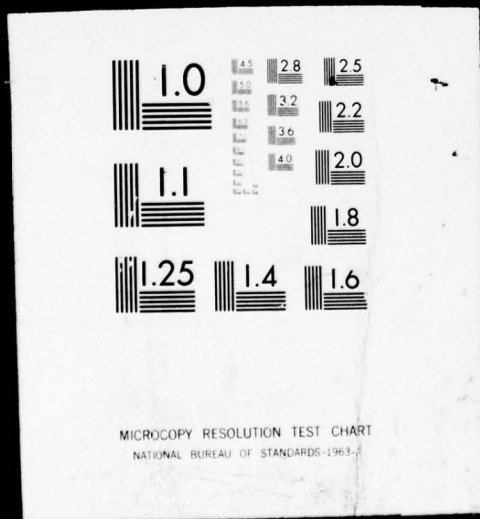


PRINTED

2 OF 3

AD

A038 299



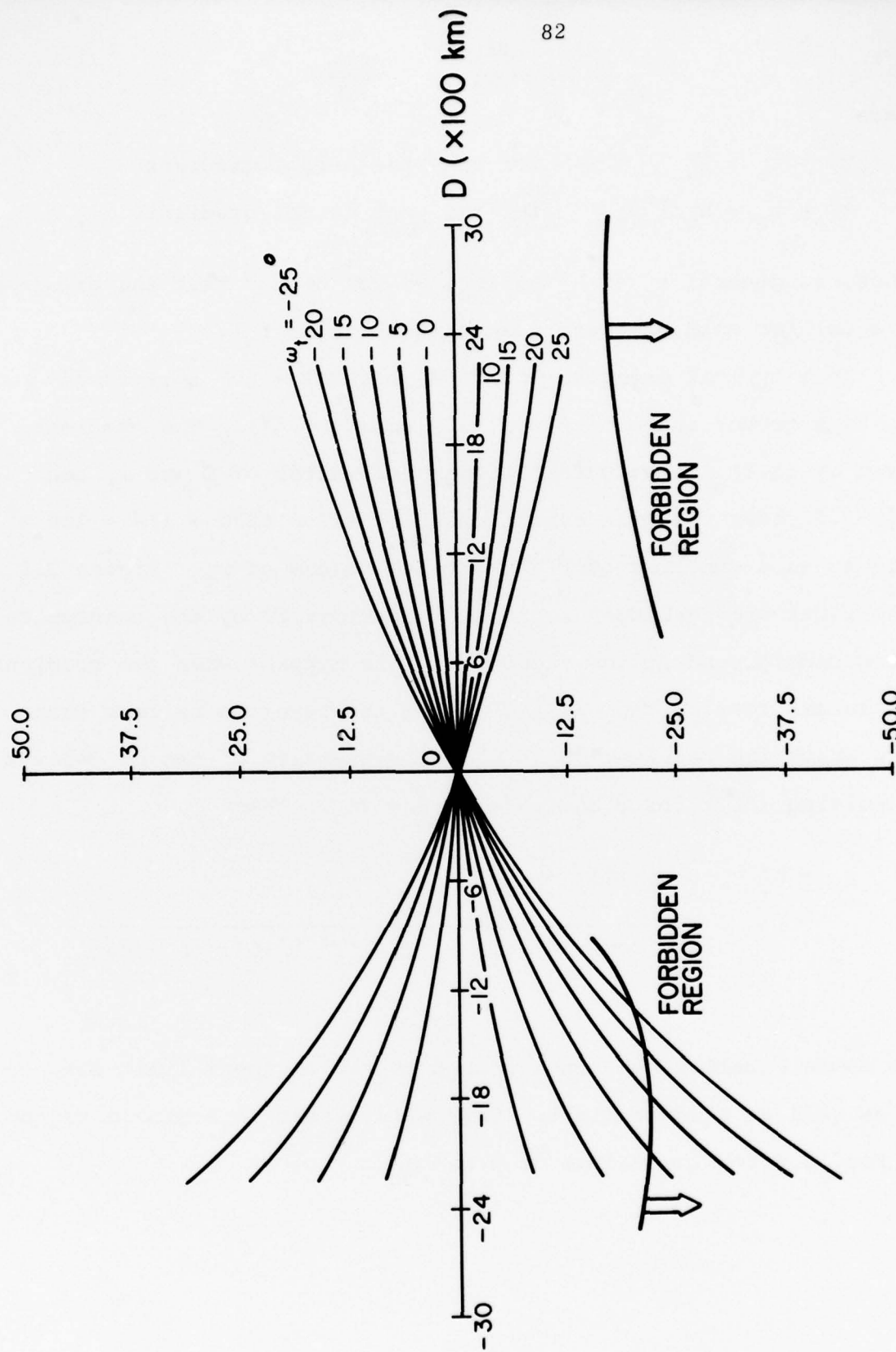


Figure 3.5. Peak height gradient as a function of D and ω_t .

3.3 Inversion of Point-to-Point Oblique Ionograms

In this section, we report our investigation of techniques for inversion of point-to-point oblique ionograms. The inversion of such ionograms for earth-concentric ionospheric layers already exist in the literature. Hence, we consider here their inversion to a layer with horizontal gradients, and in particular the eccentric quasi-parabolic layer discussed in Sec. 3.2.2.

3.3.1 Sensitivity Analysis

First we need to explore the individual behavior of the five parameters of the eccentric Q-P layer model with respect to numerically synthesized oblique ionograms, so that we can devise an efficient numerical procedure for inverting a given oblique ionogram to the model's parameters. In Figs. 3.6-3.10, four of the five parameters are held constant, with the fifth varying over a small range, and the resulting oblique ionograms are plotted. Investigation of these graphs shows that small changes in f_c , h_o , and y_m parameters have a relatively linear effect on their respective ionograms, that is, the curves are shifted by a similar amount for equal changes in each of the three parameters. However, for changes in the gradient parameters (ω_t , D), the shifted ionograms actually tend to converge to a certain curve and do not demonstrate the linear behavior associated with the variation of the first three parameters.

The above conclusion can also be verified from the geometric point of view. Since ω_t is a periodic variable, the constructed ionograms will not be linearly shifted as the ω_t parameter is increased. Also the constructed ionograms can be very insensi-

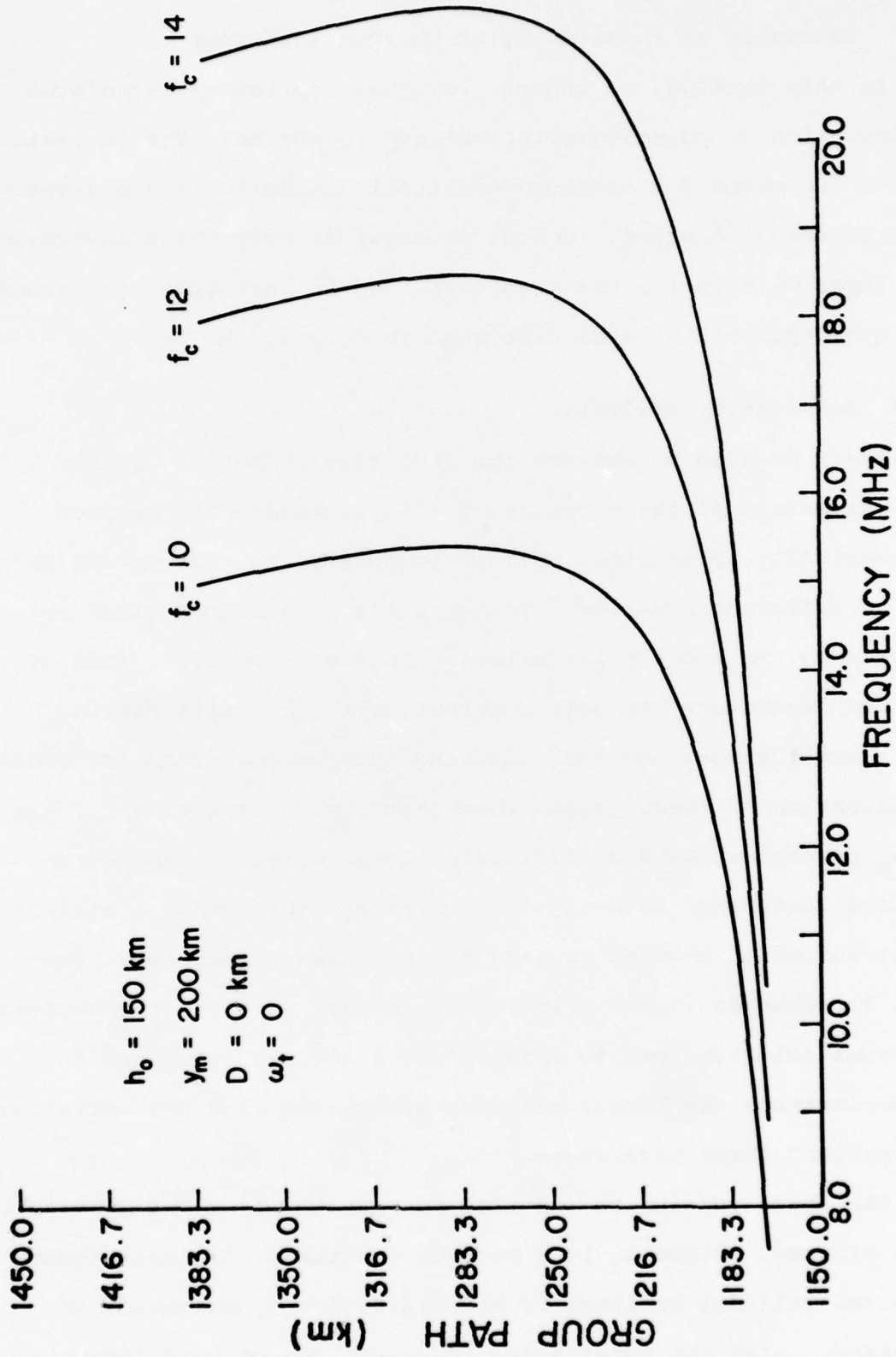


Figure 3.6. Effect of changing the f_c (critical frequency) parameter (in MHz).

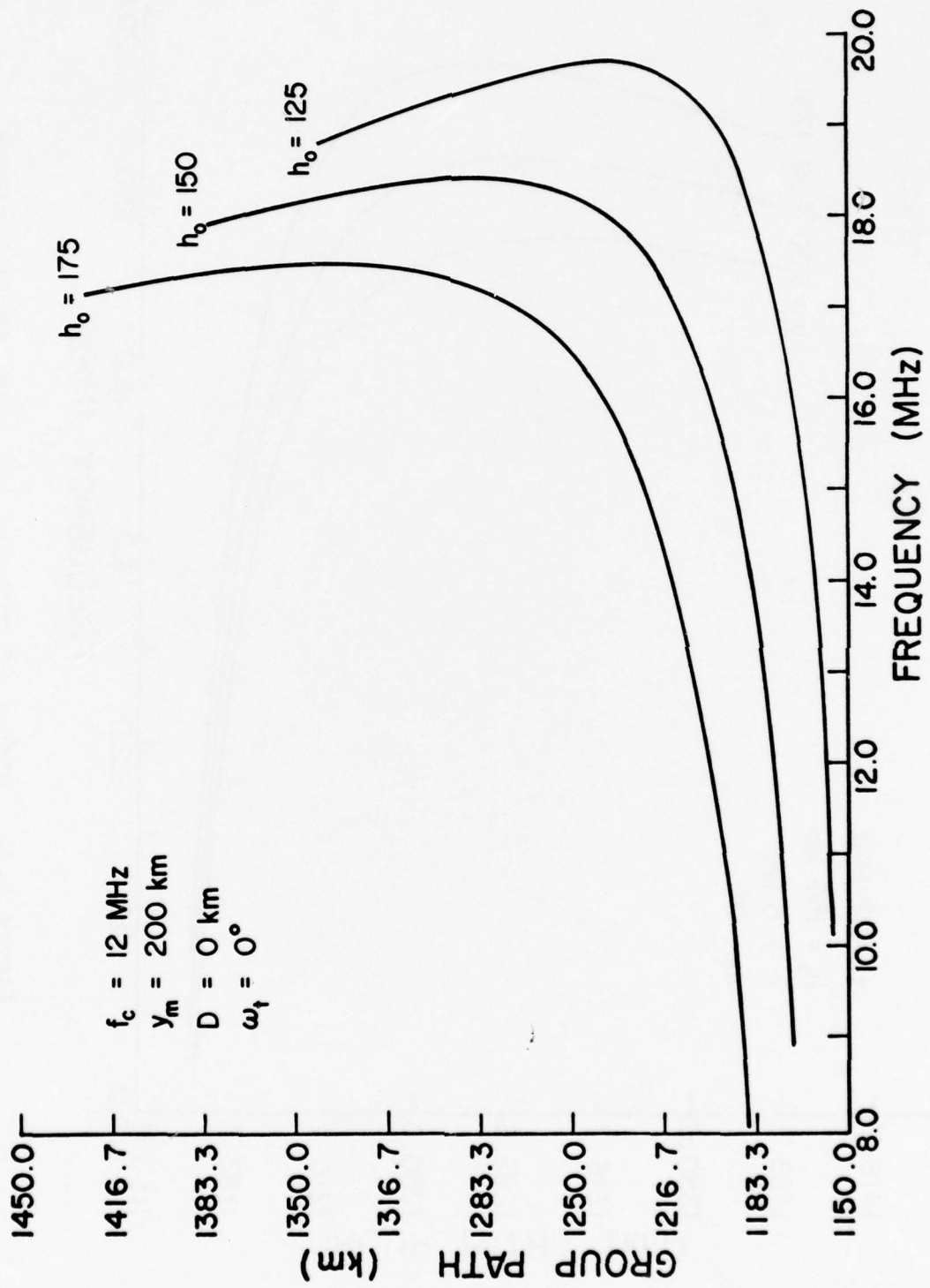


Figure 3.7. Effect of changing h_0 ; the layer base-height (in km).

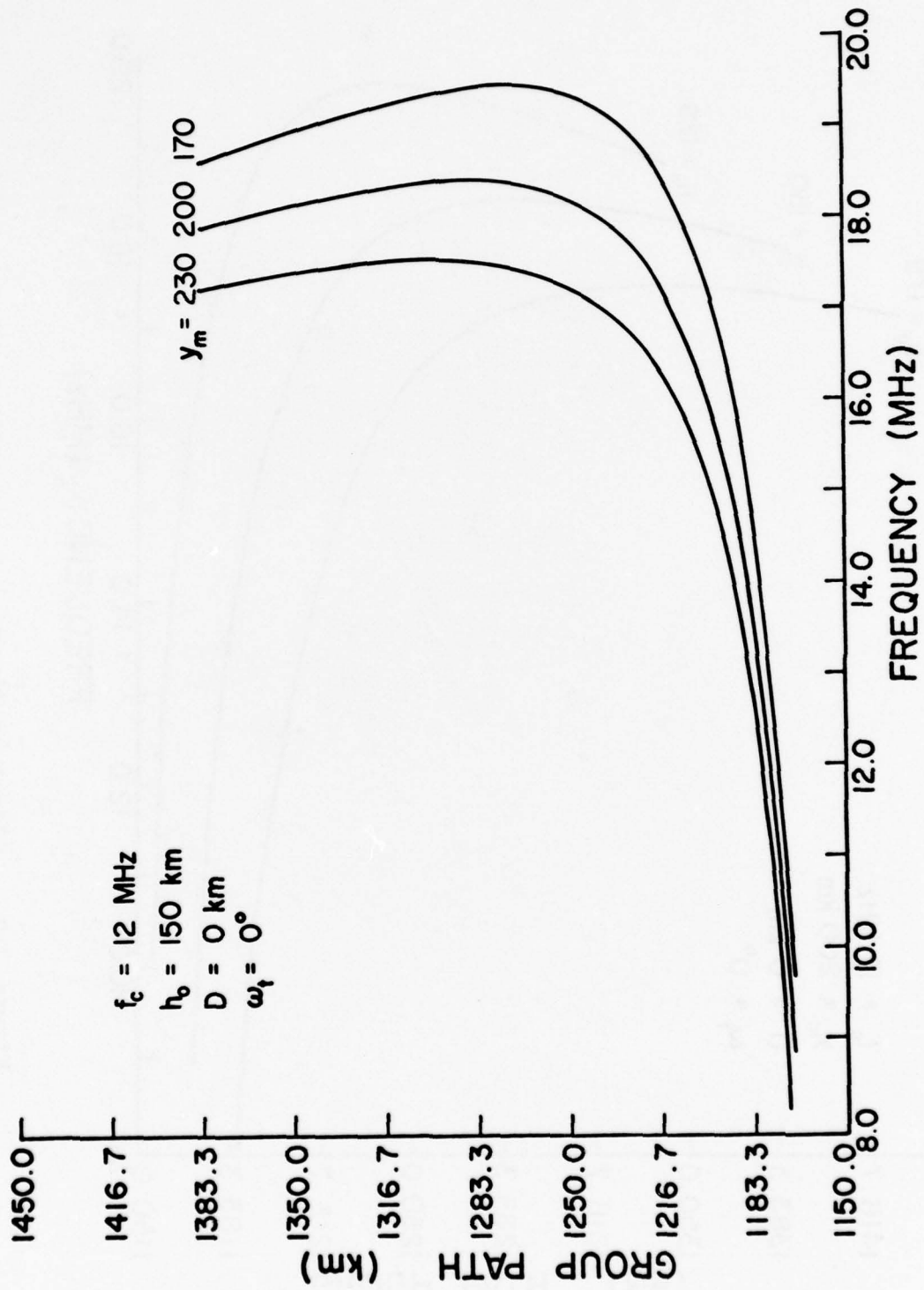


Figure 3.8. Effect of changing the layer semi-thickness y_m (in km).

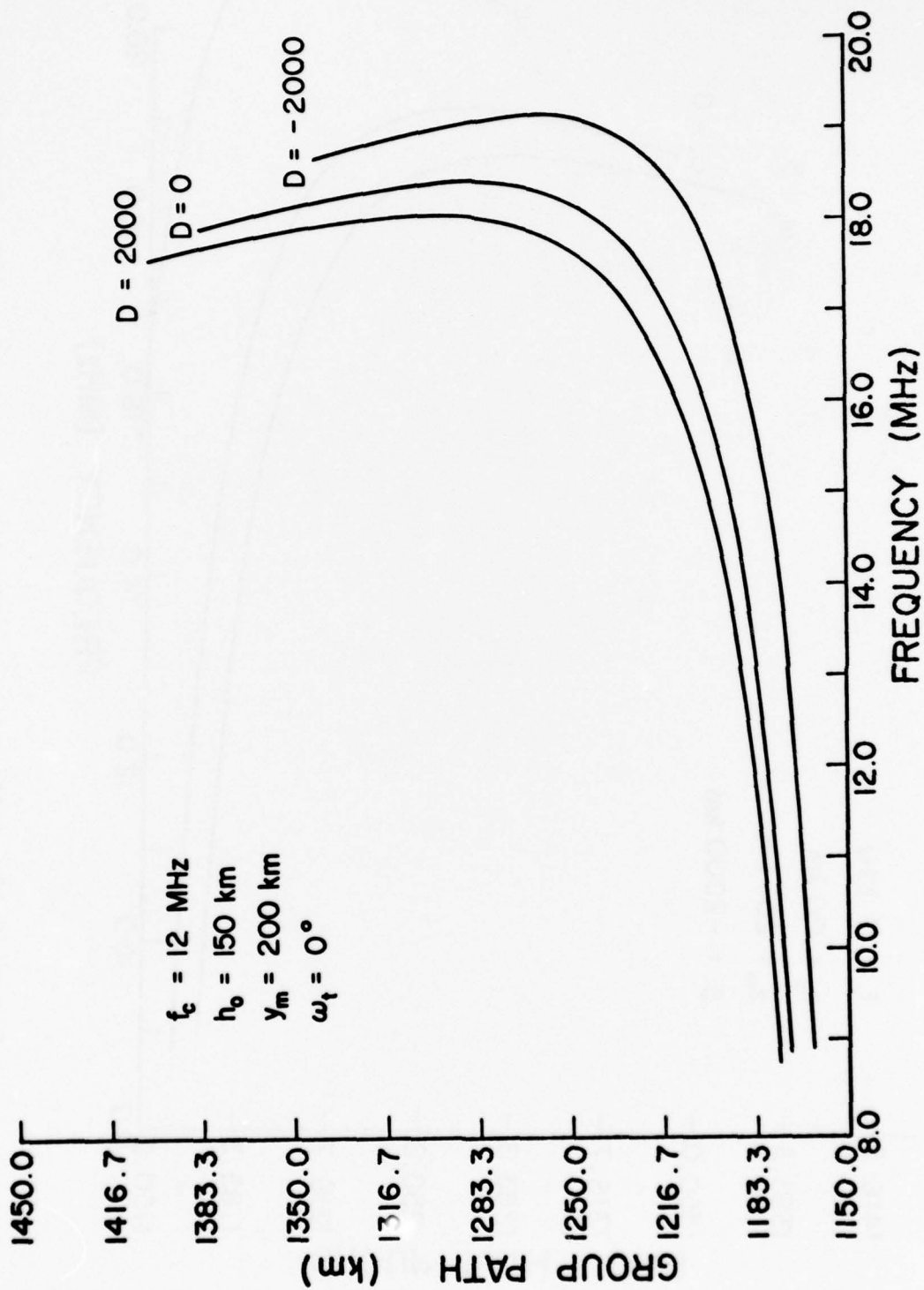


Figure 3.9. Effect of changing the D parameter (in km).

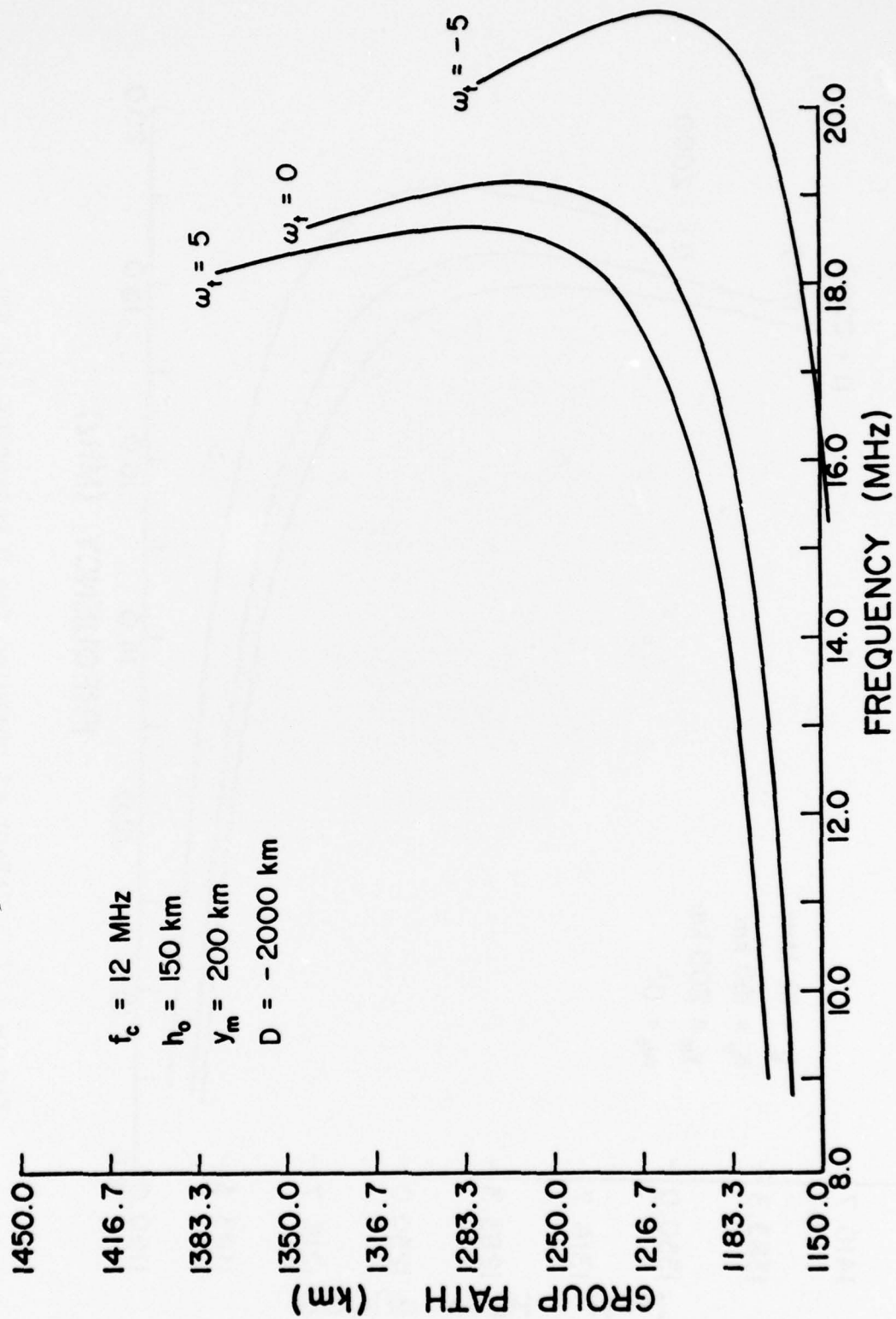


Figure 3.10. Effect of varying the ω_t parameter (in degrees).

tive to changes in D for large values of D (the layer approaches a plane slab) and be highly sensitive for negative D values. These facts tend to suggest that most standard numerical procedures have the potential for inverting for the f_c , h_o , and y_m parameters, but could easily encounter convergence problems when the gradient parameters are introduced.

Rao (1975) successfully inverted an oblique ionogram, using three data points, to the three defining parameters of a concentric quasi-parabolic layer using Newton's iterative technique (this procedure is described and used in Section 3.3.3). An attempt to extend this attractive technique to include two more parameters, D and ω_t , failed because of convergence problems caused by the nonlinear behavior with respect to the gradient parameters. These observations suggest that a slower and more controllable technique is needed to converge to the final solution.

3.3.2 Determination of Initial Set of Parameters

In every complex numerical convergence procedure, it is essential to have a reasonable set of approximate starting values in order to be able to converge to the desired solution. In the present problem we have five data points (frequency-group path pairs) corresponding to five rays with frequencies f_i , group paths P_i' and all having a constant range R . It is desired to find a set of parameters and five elevation angles β_i , so that the reflection of each ray (with frequency f_i and approximate elevation angle β_i) is ensured with small errors in their corresponding group paths and range.

A concentric layer is a practical choice for initial approximation, thus assuming $D = \omega_t = 0$. Using the geometry of Fig. 3.11(a) and applying Martyn's theorem, we can derive approximate expressions for γ_i , the angle of ray at the reflection point and then β_i , the elevation angle:

$$\gamma_i = \sin^{-1} \left[\frac{r_0}{P'_i} \sin \left(\frac{R}{2r_0} \right) \right] \quad (3.10a)$$

$$\beta_i = \pi/2 - \gamma_i - R/2r_0. \quad (3.10b)$$

The critical frequency f_c is chosen to be equal to the highest ray frequency (f_5) to ensure the reflection of all five rays by the modelled ionosphere. Since the zero frequency ray (with group path P'_0), reflects from the base of the layer, the geometry of Fig. 3.11(a) can be used for determining the initial base height h_0 . A linear interpolation of two data points (preferably in the lower frequency region) is made to find an approximate value for P'_0 [Fig. 3.11(b)] and then by using the simple geometry of Figure 3.11(a), h_0 is determined:

$$P'_0 = P'_1 - \left[\frac{P'_2 - P'_1}{f_2 - f_1} \right] f_1 \quad (3.11)$$

$$h_0 = r_0 \cos(R/2r_0) + \sqrt{\frac{P'_0}{4} - r_0^2 \sin^2(R/2r_0)} - r_0. \quad (3.12)$$

Initial value of y_m is not as critical as the other two parameters, we will simply use a physical constraint. Here, we have chosen $y_m = 300 - h_0$ (in kilometers). Using these sets of approximate starting values, we are now ready to consider techniques in order

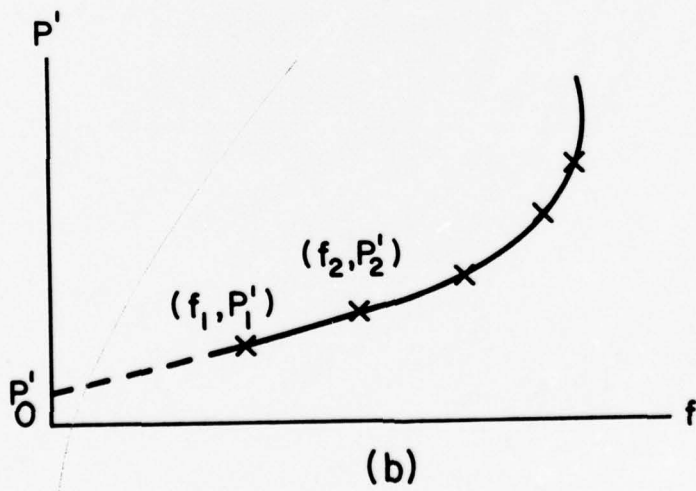
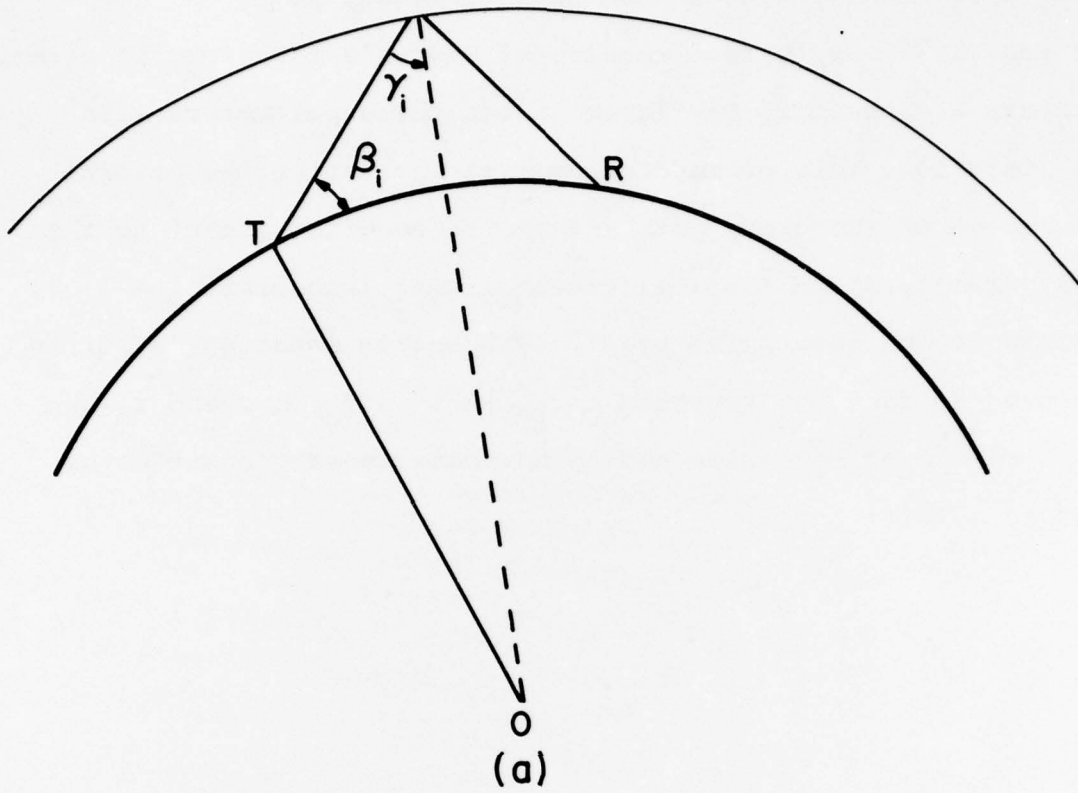


Figure 3.11. Determining an initial set of parameters.

for the solution to converge to an optimal set of parameters.

3.3.3 Inversion of Synthesized Oblique Ionograms

Rao (1975) employed a version of Newton's technique in order to invert a concentric Q-P layer in its three parameters. In each iteration, this procedure requires evaluating the partial derivatives of the group path and the range with respect to the three parameters and three elevation angles (subscript $i = 1, 2, 3$ refers to the data point used). The matrix equation (3.13) is then used to find the required increments in f_c , h_o , and r_m and the three elevation angles and then update these quantities as shown in (3.14):

$$\begin{bmatrix} \Delta f_c \\ \Delta h_o \\ \Delta y_m \\ \Delta \beta_1 \\ \Delta \beta_2 \\ \Delta \beta_3 \end{bmatrix} = \begin{bmatrix} \left(\frac{\partial P'}{\partial f_c} \right)_1 & \left(\frac{\partial P'}{\partial h_o} \right)_1 & \left(\frac{\partial P'}{\partial y_m} \right)_1 & \left(\frac{\partial P'}{\partial \beta} \right)_1 & 0 & 0 \\ \left(\frac{\partial P'}{\partial f_c} \right)_2 & \left(\frac{\partial P'}{\partial h_o} \right)_2 & \left(\frac{\partial P'}{\partial y_m} \right)_2 & 0 & \left(\frac{\partial P'}{\partial \beta} \right)_2 & 0 \\ \left(\frac{\partial P'}{\partial f_c} \right)_3 & \left(\frac{\partial P'}{\partial h_o} \right)_3 & \left(\frac{\partial P'}{\partial y_m} \right)_3 & 0 & 0 & \left(\frac{\partial P'}{\partial \beta} \right)_3 \\ \left(\frac{\partial R}{\partial f_c} \right)_1 & \left(\frac{\partial R}{\partial h_o} \right)_1 & \left(\frac{\partial R}{\partial y_m} \right)_1 & \left(\frac{\partial R}{\partial \beta} \right)_1 & 0 & 0 \\ \left(\frac{\partial R}{\partial f_c} \right)_2 & \left(\frac{\partial R}{\partial h_o} \right)_2 & \left(\frac{\partial R}{\partial y_m} \right)_2 & 0 & \left(\frac{\partial R}{\partial \beta} \right)_2 & 0 \\ \left(\frac{\partial R}{\partial f_c} \right)_3 & \left(\frac{\partial R}{\partial h_o} \right)_3 & \left(\frac{\partial R}{\partial y_m} \right)_3 & 0 & 0 & \left(\frac{\partial R}{\partial \beta} \right)_3 \end{bmatrix}^{-1} \begin{bmatrix} \Delta P'_1 \\ \Delta P'_2 \\ \Delta P'_3 \\ \Delta R_1 \\ \Delta R_2 \\ \Delta R_3 \end{bmatrix} \quad (3.13)$$

$$\begin{aligned}
 [f_c]_{\text{new}} &= [f_c]_{\text{old}} + \Delta f_c \\
 [h_o]_{\text{new}} &= [h_o]_{\text{old}} + \Delta h_o \\
 \dots & \\
 \dots &
 \end{aligned}
 \tag{3.14}$$

where $\Delta P'_i$ and ΔR_i are defined to be the differences between the actual and the computed values of group path and range using the latest values of the parameters.

The iteration in (3.14) is repeated until the errors in the group path and range satisfy a given convergence condition. As mentioned in Section 3.3.1, our attempt to extend this convenient technique to include two more parameters, D and ω_t , failed to result in a stable procedure. However, by employing a bisection search on D and ω_t , and repeating the iteration for every change in these two parameters, the procedure becomes stable. Fig. 3.12 contains the flow chart for such a technique, and for simplicity, it only optimizes D with ω_t constant. This technique can also be demonstrated graphically in Fig. 3.13. Several oblique ionograms are synthesized for different values of the D parameter, satisfying three common data points at all times (step 3.14 is repeated for every value of D). It is clear that by selecting the fourth and the fifth data point in the high frequency region of the ionograms, which is the most sensitive region with respect to the gradient parameters, a bisection search can be used to optimize the values of D and ω_t .

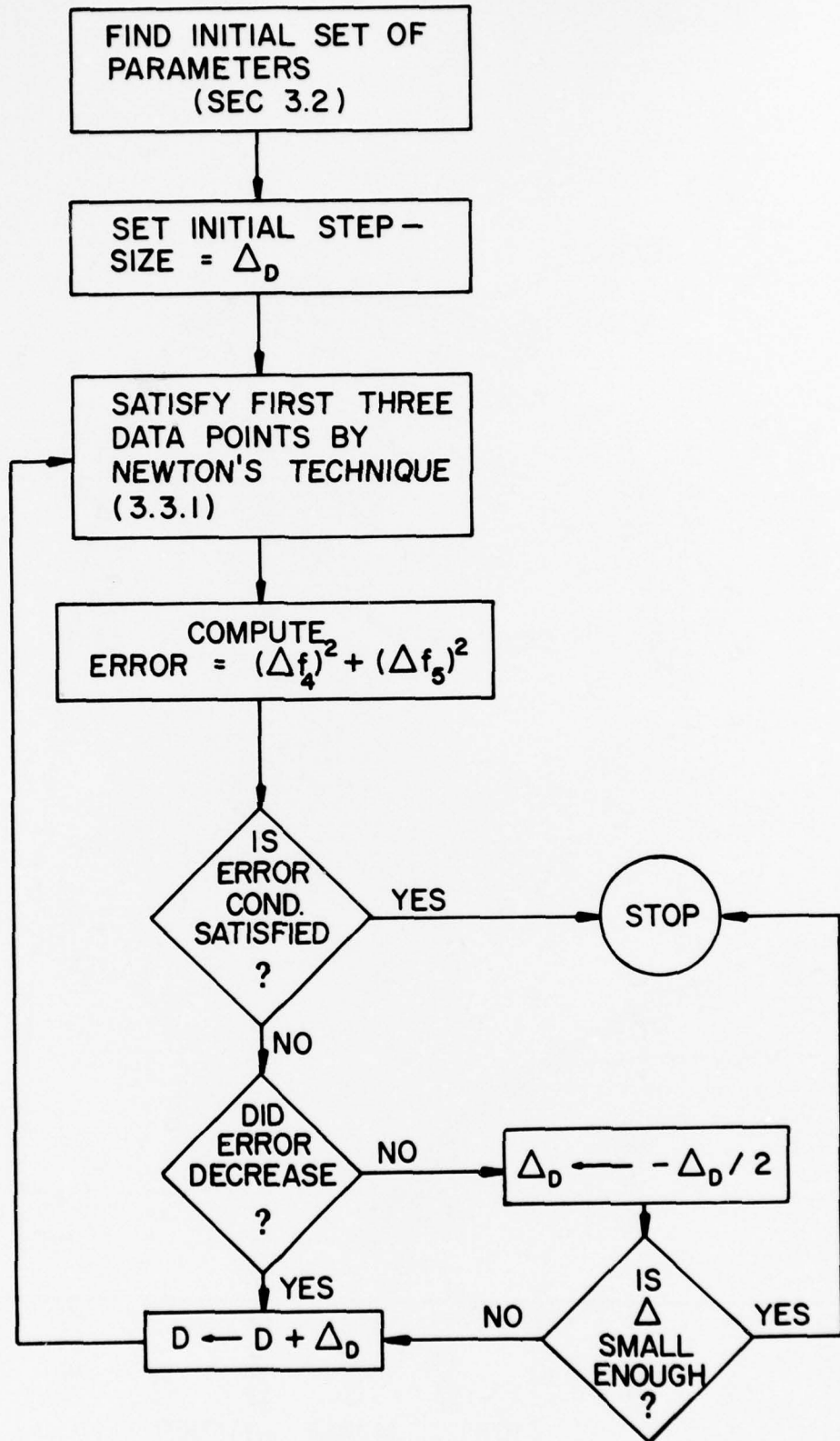
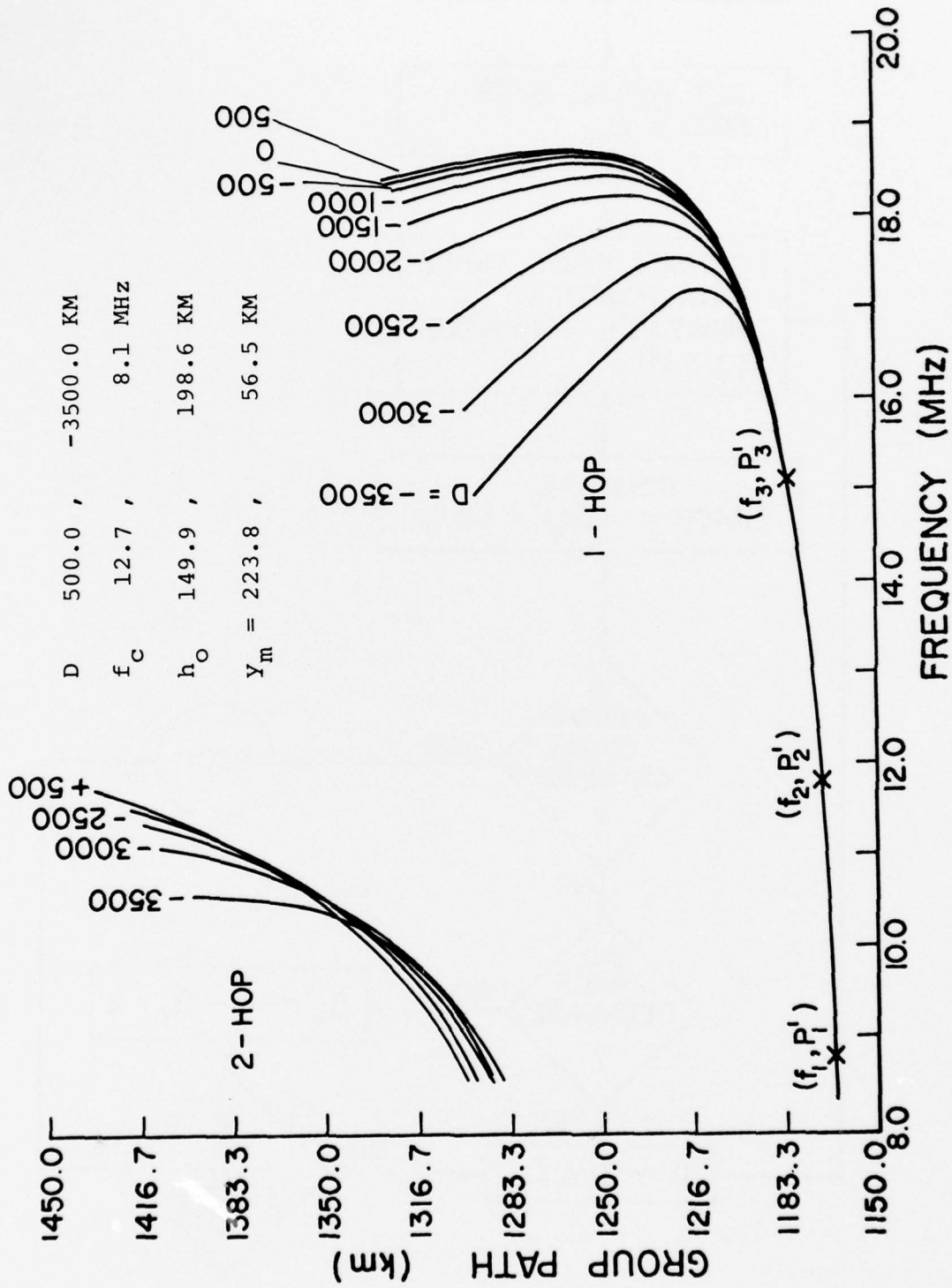


Figure 3.12. Inverting numerically synthesized data.



D 500.0 , -3500.0 KM
 f_c 12.7 , 8.1 MHz
 h_o 149.9 , 198.6 KM
 $Y_m = 223.8$, 56.5 KM

Figure 3.13. Synthesized oblique ionograms for Range = 1111.7 km and $\omega_t = 0^\circ$. The parameter D is successively changed by 500 km. For each D, the remaining three parameters are adjusted so as to force the curve through the three points marked by X. The parameters for the two extreme curves are given above.

The error function used for the bisection search was initially proposed to be:

$$\text{Error} = (\Delta P_4')^2 + (\Delta P_5')^2 \quad . \quad (3.15)$$

However, as apparent from Fig. 3.13, for a given set of parameters, a ray with frequency f_i might penetrate the ionosphere making $\Delta P_i'$ approach infinity. This problem can be solved by considering the ray with group path P_i' and finding the error in its frequency Δf_i (this value is always finite). Based on this explanation, the final error function used in the inversion technique is chosen to be:

$$\text{Error} = (\Delta f_4)^2 + (\Delta f_5)^2 \quad . \quad (3.16)$$

It is important to note that Δf_i ($i = 4, 5$) is defined to be the frequency deviation of the modelled ray, from the actual data value, which has its group path equal to P_i' and the range equal to R (the elevation angle β_i is adjusted so that the error in range vanishes). This technique is completely programmed and simulated on an IBM-360 digital computer, and Table 3.1 contains an example in which a numerically synthesized oblique ionogram is inverted with excellent accuracy to the model's parameters.

TABLE 3.1. Inversion of Synthesized Oblique Ionograms
Using the Technique in Section 3.3.3

Model parameters: $f_c = 12$ MHz
 $h_o = 150$ km
 $y_m = 100$ km
 $D = -2000$ km
 $\omega_t = 0$
Range = 1111.8 km

Synthesized data points used:

| i | 1 | 2 | 3 | 4 | 5 |
|--------|--------|--------|--------|--------|-----------|
| f_i | 12.23 | 19.03 | 22.10 | 23.57 | 24.15 MHz |
| P_i' | 1161.3 | 1173.1 | 1186.3 | 1200.9 | 1217.2 km |

Inversion results:

| | f_c MHz | h_o km | y_m km | D km | ω_t deg | $\Delta f_4^2 + \Delta f_5^2$ (MHz) ² |
|---------------|--------------|-------------|-------------|---------|-------------------|---|
| 1st iteration | 13.07 | 136.4 | 125.3 | 0 | 0 | .031 |
| 2nd iteration | 12.96 | 138.5 | 123.5 | -500 | 0 | .026 |
| 3rd iteration | 12.78 | 141.3 | 119.6 | -1000 | 0 | .018 |
| 4th iteration | 12.48 | 144.9 | 112.3 | -1500 | 0 | .0081 |
| 5th iteration | 11.99 | 150.0 | 99.89 | -2000 | 0 | .00004 |

Since Newton's technique attempts to converge the error to zero, problems can be encountered in case of real data because of the finite errors involved in the final solution. In order to adapt this technique for inversion of real data, a steepest descent method (discussed in detail later in Section 3.3.4) is employed to find an optimal set of starting parameters for three of our data points. Then the group paths of the three rays were computed using the parameters and used to replace the original group path values (Fig. 3.14). These adjusted data points are indeed well behaved and we can continue our procedure as before for minimizing $(\Delta f_4)^2 + (\Delta f_5)^2$. Table 3.2 contains a numerical example for this technique; it must be noted that in this example the fourth and the fifth data points are chosen in the nearly horizontal region of the ionogram, therefore making $\Delta f_4, \Delta f_5$ correspond to a much smaller error in group paths ($\Delta P'_4, \Delta P'_5$).

Because of the two-step optimization involved in inverting real oblique ionograms, the final result is not guaranteed to be optimum. In fact, different combinations of the real data points used in the inversion procedure tend to converge to different sets of parameters (in that case, the combination with the least amount of error is the final solution). Even though the technique converges quite rapidly in the synthesized data case, the computation time becomes an order of magnitude larger for the real data case, which could be considered undesirable.

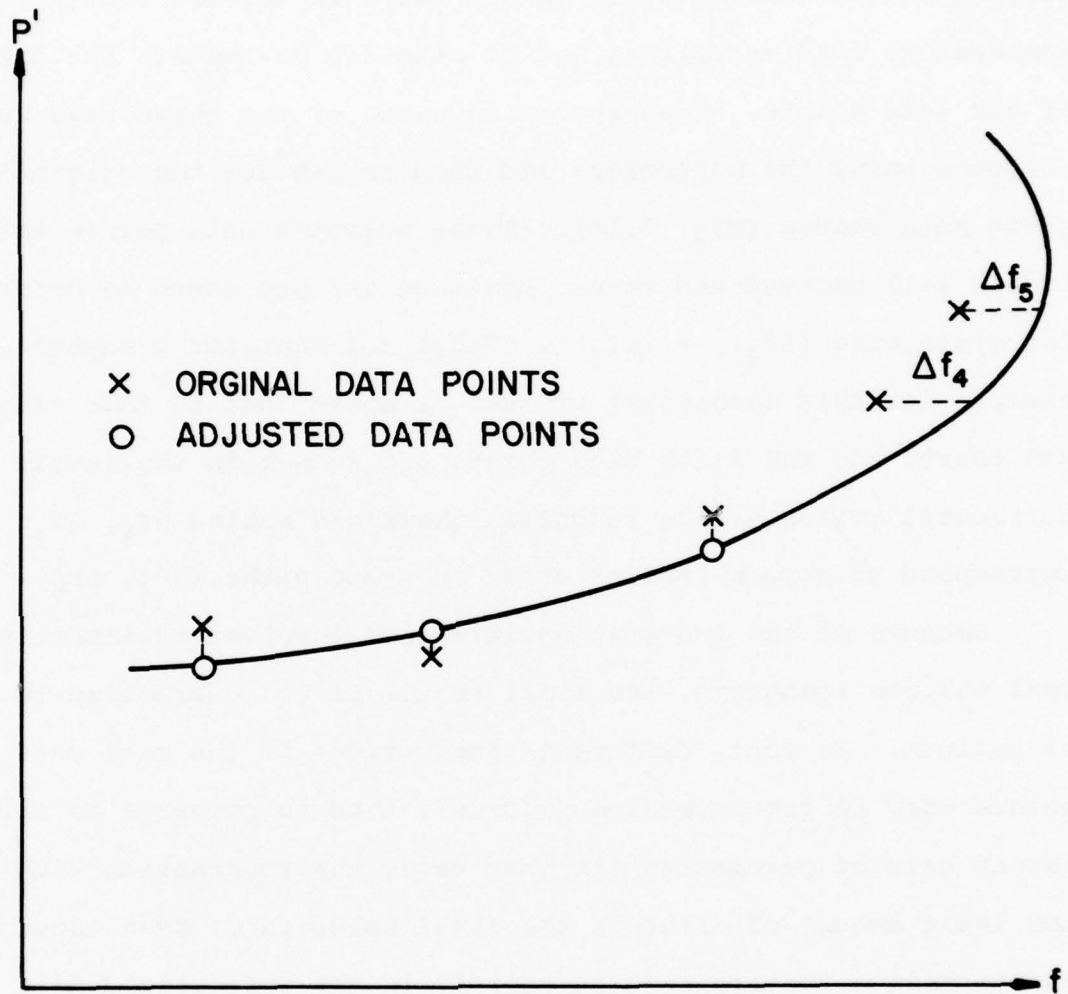


Figure 3.14. A technique for the inversion of real data. The first three data points are adjusted so that the technique in Section 3.3.3 can be employed for minimizing $(\Delta f_4)^2 + (\Delta f_5)^2$.

TABLE 3.2. Inversion of Real Oblique Ionograms,
Using the Technique in Section 3.3.3

Range = 1421.5 km

| | | | | | |
|--|--------|--------|--------|--------|--------|
| Frequency, MHz | 14 | 18 | 22 | 16 | 20 |
| actual (P') km | 1532.0 | 1540.4 | 1556.1 | 1528.5 | 1539.0 |
| adjusted (P') km (after steepest descent) | 1527.0 | 1530.3 | 1559.4 | same | same |

| Parameters | f_c MHz | h_o km | Y_m km | D km | ω_t deg | $(\Delta f_4)^2 + (\Delta f_5)^2$ (MHz) ² |
|--------------|--------------|-------------|-------------|---------|-------------------|---|
| Iteration #1 | 12.87 | 236.7 | 74.2 | 0 | 0 | 26.8 |
| Iteration #2 | 12.73 | 244.6 | 72.1 | -1000 | 0 | 27.4 |
| Iteration #3 | 12.80 | 240.3 | 73.3 | -500 | 0 | 26.6 |
| ⋮ | ⋮ | ⋮ | ⋮ | ⋮ | ⋮ | ⋮ |
| ⋮ | ⋮ | ⋮ | ⋮ | ⋮ | ⋮ | ⋮ |
| ⋮ | ⋮ | ⋮ | ⋮ | ⋮ | ⋮ | ⋮ |
| Iteration #7 | 12.82 | 239.2 | 73.5 | -375 | 0 | 26.2 |

Based on the controllable convergence behavior of the steepest descent method, a different approach to the inversion of real data is proposed and discussed in detail in the following section.

3.3.4 Inversion of Experimental Oblique Ionograms

Actual oblique ionograms are not smooth and nicely behaved as the numerically generated ones. In fact, one can frequently find discontinuities, and other peculiarities on the plots of actual data. Ideal zero error cannot be accomplished when actual data points are used, requiring the optimization of the error function to a minimum value.

It is convenient to approximate the gradient, in the actual data case, by using only one parameter. Referring back to Fig. 3.5, it is apparent that a wide range of gradients can be obtained by holding ω_t at a reasonable value and varying D . In the examples to follow, $\omega_t = 0$ is chosen not only to span a wide range of gradient values by varying D , but also to force h_0 to represent the actual base height value of the layer above the transmitter. The steepest descent method, with its controlled step size is an ideal choice for simultaneous inversion of the remaining four parameters. Figure 3.10 outlines the procedure in a simple flow chart.

Since, in fact, we are finding a best fit curve through the data points, we need not be limited to using five points, and obviously the more data points used the more descriptive the model will be. The error function is chosen to be:

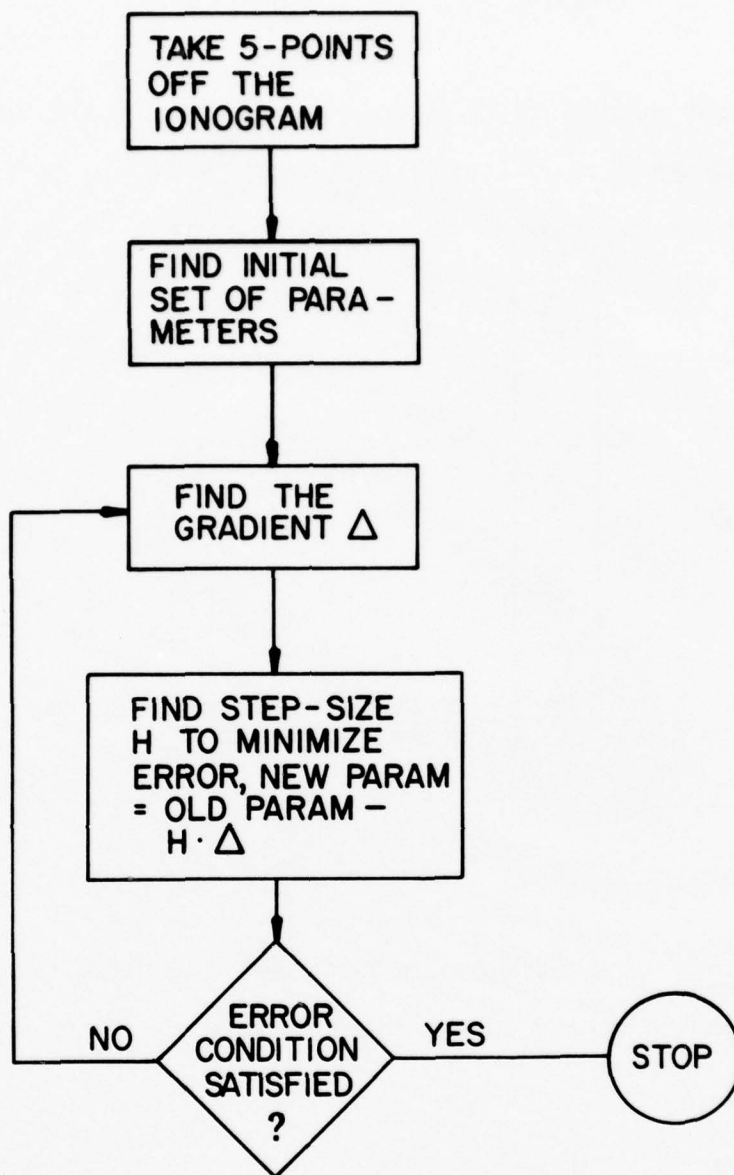


Figure 3.15. Method of steepest descent for inverting actual data.

$$E = \sum_{i=1}^N (\Delta P_i')^2$$

where N is the number of data points and $\Delta P_i'$ is the error in the i^{th} group path as defined in Section 3.3.

The gradient vector Δ is defined to be:

$$[\Delta] = \begin{bmatrix} \frac{\partial f_c}{\partial E} \\ \frac{\partial h_o}{\partial E} \\ \frac{\partial y_m}{\partial E} \\ \frac{\partial D}{\partial E} \end{bmatrix} \quad \text{Evaluated at the current parameter values}$$

The theory of steepest descent uses the fact that continuous functions decrease along the negative of their gradient.

Thus

$$\text{New} \begin{bmatrix} f_c \\ h_o \\ y_m \\ D \end{bmatrix} = \text{Old} \begin{bmatrix} f_c \\ h_o \\ y_m \\ D \end{bmatrix} - H \times [\Delta]$$

where H is a positive scalar step size. For this iteration to be most efficient, we like to choose an H such that the resultant error function from the new parameter is at a minimum. This can be accomplished by simply setting H to zero, and then incrementing it by an interval such that none of the resultant parameters change by more than a specified amount (this ensures a slower but smoother convergence to the final solution not accomplished by the Newton's technique in Section 3.3.3). Error is computed for each value of H and minimized by performing a simple interval halving routine on H . The old parameters are replaced by using the optimal step size H and if the convergence criterion is not met, the gradient is reevaluated and the procedure is repeated. This technique is also programmed on a digital computer and Tables 3.3 and 3.4 contain examples using five data points from actual oblique ionograms.

TABLE 3.3(a). Inversion of an Actual Ionogram

Data points scaled from oblique ionogram (Range = 1421.5 km):

| i | 1 | 2 | 3 | 4 | 5 |
|-------------|------|--------|--------|--------|--------|
| f_i (MHz) | 14. | 16. | 18. | 20. | 22. |
| P_i' (km) | 1536 | 1536.5 | 1540.5 | 1545.3 | 1555.5 |

Inversion results:

| Iteration# | f_c (MHz) | h_o (MHz) | y_m (km) | D(km) | Error = $\sum_{i=1}^5 (\Delta P_i')^2$ |
|------------|-------------|-------------|------------|--------|--|
| 0 | 22.00 | 252.2 | 50.0 | 0.0 | 290.1 |
| 1 | 18.28 | 254.5 | 51.6 | 342.2 | 133.8 |
| 2 | 12.67 | 250.0 | 55.5 | -797.7 | 14.5 |
| 3 | 12.47 | 249.9 | 55.5 | -836.7 | 12.5 |
| 4 | 12.71 | 249.6 | 55.5 | -831.4 | 12.3 |
| . | . | . | . | . | . |
| . | . | . | . | . | . |
| 10 | 12.63 | 249.0 | 55.6 | -803.6 | 11.1 |

The final individual group path errors (in km):

$$\Delta P_1' = 1.17, \quad \Delta P_2' = -1.46, \quad \Delta P_3' = -1.00, \quad \Delta P_4' = -1.11,$$

$$\Delta P_5' = 2.30$$

TABLE 3.3(b) Inversion of an Actual Ionogram

Data points scaled from oblique ionogram: (Range = 1421.5 km):

| i | 1 | 2 | 3 | 4 | 5 |
|-------------|------|--------|--------|--------|--------|
| f_i (MHz) | 14. | 16. | 18. | 20. | 22. |
| P_i' (km) | 1533 | 1539.0 | 1546.2 | 1555.8 | 1566.0 |

Inversion results:

| Iteration # | f_c (MHz) | h_o (km) | y_m (km) | D(km) | Error = $\sum_{i=1}^5 (\Delta P_i')^2$ |
|-------------|-------------|------------|------------|--------|--|
| 0 | 22.0 | 220.0 | 80.0 | 0.0 | 5838.5 |
| 1 | 12.58 | 227.9 | 88.5 | 1237.3 | 20.6 |
| 2 | 12.60 | 227.9 | 88.6 | 1239.1 | 20.5 |
| 3 | 12.59 | 227.9 | 88.5 | 1239.3 | 20.4 |

The final individual group path errors (in km):

$$\Delta P_1' = .49, \quad \Delta P_2' = 1.6, \quad \Delta P_3' = 2.3, \quad \Delta P_4' = 2.5,$$

$$\Delta P_5' = -2.3$$

3.4 Inversion of Backscatter Leading Edge

The most important task of this project is to develop a technique of inversion of the sweep frequency backscatter leading edge data for various azimuthal directions, to an ionosphere varying in three dimensions, which can then be applied for the purpose of other ray path computations. In this section, we report our work on this problem. Several of the results can be found in the various progress reports but not in the order presented here. Here we discuss the solution of the problem in a step-by-step manner and its eventual application to the important problem of finding the ground range for a measured group path for reflection from a target.

3.4.1 Basic Inversion Technique

In a paper by Rao (1974), it has been demonstrated that three data points taken from the leading edge of a backscatter ionogram can be used to obtain the quasi-parabolic layer parameters f_c , r_b , and r_m , corresponding to those three points. Briefly, this method consists of starting with an initial estimate of the layer parameters and then calculating the minimum group paths, P'_{C_i} , corresponding to the three frequencies at which data points are taken from the leading edge. The differences between these computed minimum group path values and the actual minimum group path values, P'_i , from the leading edge are then used in an iterative procedure to obtain a final solution for the quasi-parabolic layer parameters. This final solution is such that the differences between P'_i and P'_{C_i} are less than a certain specified value (theoretically zero).

When the above described procedure was applied to synthesized leading edge data polluted intentionally by adding or subtracting a few kilometers from each of the P'_i values, thereby simulating the actual data case, it was found that in order for the differences between P'_i and P'_{C_i} to go down to less than a small specified value, one or more of the layer parameters often got incremented to physically unrealizable values. The reason for this was found to be that the backscatter leading edges corresponding to quasi-parabolic layer profiles have certain shapes and it is not in general possible to fit a synthesized leading edge exactly through three points on an experimental ionogram. In view of this, the method was modified for use in this work.

The modification involves the minimization of the following sum-squared error function:

$$E(r_b, r_m, f_c) = \sum_{i=1}^3 [P'_{C_i}(r_b, r_m, f_c) - P'_i]^2 \quad (3.17)$$

Fig. 3.16 depicts the strategy graphically. Assume that (f_1, P'_1) , (f_2, P'_2) , and (f_3, P'_3) are the points we have chosen from the backscatter leading edge. As before, we start the procedure with an initial set of layer parameters, which are denoted by $(r_b, r_m, f_c)_0$. Corresponding to these starting parameters is a unique backscatter ionogram leading edge trace $[P'(f)]_0$. We note that the error function E is simply the sum of the squared distances between the ordinates of the $[P'(f)]_0$ curve corresponding to the frequencies f_1, f_2 , and f_3 , and the chosen backscatter ionogram minimum group paths P'_1, P'_2 , and P'_3 . As r_b, r_m , and f_c

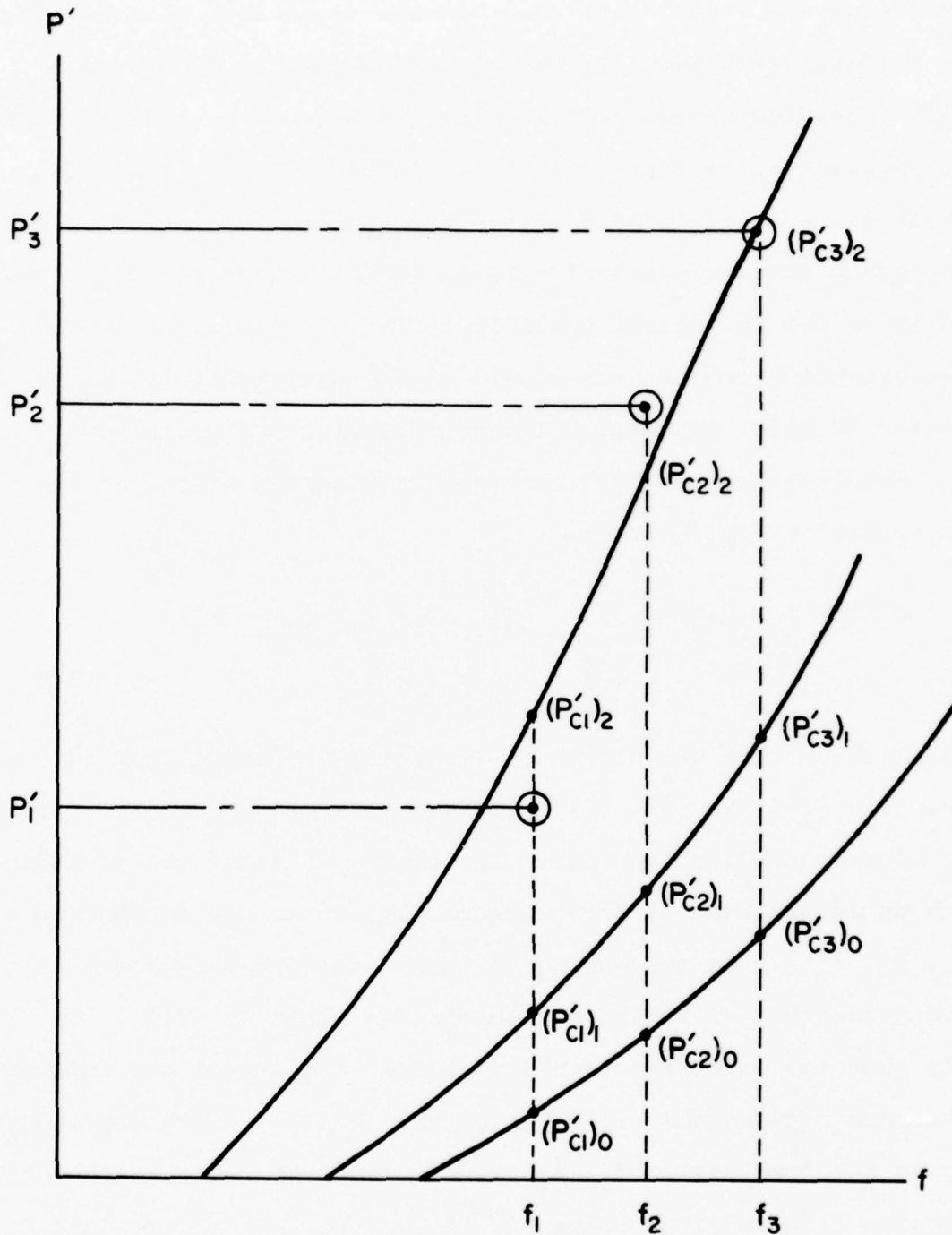


Figure 3.16. Graphical illustration of the least sum-squared error method of backscatter ionogram leading-edge inversion for a Q-P ionosphere.

are varied to minimize E , we see that we are effectively fitting the $P'(f)$ curve to the three data points in the least-squared error sense. Furthermore, the magnitude of the minimum of E provides an indication of the noisiness of the data with reference to a synthetic leading edge. If the data points are from a synthetic curve, computed by assuming the Q-P model, the error E will then be zero.

The error E is in general a nonlinear function of r_b , r_m , and f_c and an iterative method is required to seek its minimum. Numerical minimization techniques are available which seek a local minimum for a given starting point in parameter space. The nonlinear minimization algorithm employed in this study is described by Fletcher and Powell (1963) and is supplied in IBM's scientific subroutine package as subroutine DFMFP. This routine was modified for use with our computer. The Fletcher-Powell method performs, for each iteration step, a linear minimization along a direction determined by the current gradient and an updated estimate of the Hessian. The size of the steps taken through the parameter space as the minimum is sought is proportional to the difference between the current value of the function to be minimized (e), and the user-supplied minimum value (EST), typically taken to be 0.001 km^2 , and inversely proportional to the current magnitude of the function gradient ($|\vec{\nabla}E|$). In this manner, rapid convergence is assured. The minimization procedure is terminated when the function value has not changed by more than a user-specified value (EPS), or if $|\vec{\nabla}E|$ has become less

than EPS. This routine requires an external function subprogram, which supplies DFMP with E and $\vec{\nabla}E$ as the parameters r_b , r_m , and f_c are varied. The components of $\vec{\nabla}E$, which involve derivatives of P' with respect to the layer parameters are calculated using the expressions provided by Rao (1974) and repeated here in the appendix.

Thus far we have discussed the procedure for the inversion of three data points on a backscatter leading edge to Q-P layer parameters. Since each point on the leading edge corresponds to a different ground range, it is obvious that the three points must be chosen fairly close together if horizontal gradients are present. The three data points must correspond to three ionospheric propagation paths which are in such horizontal proximity as to validate the assumption of a locally horizontally uniform ionosphere. These considerations give rise to a method of deriving the horizontal ionization gradients from the leading edge. Three closely spaced points on the leading edge just above the critical frequency at the backscatter sounder site can be used to determine the layer parameters of the ionosphere at a range which is in close proximity to the site. Next, three closely spaced points further up the leading edge can be used to obtain the layer parameters at a greater range than that corresponding to the previous set of data points. In obtaining these layer parameters, the solution for the first set of three data points can be used as the starting solution. A repetition of this process continuously along the leading edge for successive sets of three data points yields the layer parameters as a function

of distance away from the sounder site. This is the technique we employ in the following sections.

3.4.2. Inversion of Synthesized QP Layer Data

The basic technique of inversion of points on the backscatter leading edge for quasi-parabolic layer parameters is tested by simulating the leading edge for assumed QP layer parameters and then polluting the simulated data by adding a few kilometers to one or more of the points. The assumed values of the layer parameters are $r_b=6570$ km, $r_m=6720$ km, and $f_c=5.0$ MHz. Minimum group paths for frequencies of 10, 11, and 12 MHz are synthesized to be $P_1'=1866.1$ km, $P_2'=2133.8$ km, and $P_3'=2441.3$ km, respectively. Table 3.4 shows the results of the test by indicating the errors introduced in P_1' , P_2' , and P_3' and the corresponding solution obtained by inverting the polluted data. For each case, starting values of layer parameters used are $r_b=6500$ km, $r_m=6650$ km, and $f_c=4.0$ MHz. From Table 3.4, it can be seen that even small measurement errors seem to appreciably affect the results of inversion of the leading edge data.

To investigate further the sensitivity of the inversion process to measurement errors, the procedure has been generalized to permit the use of a variable number (N) of data points in the inversion technique, that is, for minimizing the error function E. Leading edge data are synthesized for an earth-concentric QP layer having the parameters $r_b=6570$ km, $r_m=6720$ km, and $f_c=7.0$ MHz and at increments of 0.25 MHz throughout the frequency range of 10.0 to 13.0 MHz. These data are then made noisy by the addition of samples of a random variable uniformly distributed over the interval

TABLE 3.4

SYNTHESIZED NOISY BACKSCATTER IONOGRAM LEADING EDGE DATA INVERSION
 ASSUMING A SPHERICAL EARTH-CONCENTRIC QUASI-PARABOLIC IONOSPHERE MODEL

Synthesized points on backscatter ionogram leading edge:

| Point Number | Frequency (MHz) | Minimum Group Path km |
|--------------|-----------------|-----------------------|
| (1) | 10.0 | 1866.1 |
| (2) | 11.0 | 2133.8 |
| (3) | 12.0 | 2441.3 |

Layer parameters used in synthesis:

$r_b = 6570.0$ km $r_m = 6720.0$ km $f_c = 5.0$ MHz

$r_b = 6500.0$ km $r_m = 6650.0$ km $f_c = 4.0$ MHz

Starting values of layer parameters:

Estimated Minimum Sum-Squared Error (EST) = .001 km²
 Specified Absolute Error (EPS) = .001 km

| Error intro-duced in P_1' (km) | Error intro-duced in P_2' (km) | Error intro-duced in P_3' (km) | Resulting inverted layer parameter r_b (km) | Resulting inverted layer parameter r_m (km) | Resulting inverted layer parameter f_c (MHz) | Value of E (km) ² Minimum |
|----------------------------------|----------------------------------|----------------------------------|---|---|--|--------------------------------------|
| 0 | 0 | 0 | 6570.6 | 6719.2 | 4.993 | .00023 |
| +1 | -1 | +1 | 6621.7 | 6700.0 | 4.743 | .838 |
| -1 | 0 | -1 | 6550.2 | 6759.9 | 5.324 | .240 |
| -1 | 0 | 0 | 6543.9 | 6777.4 | 5.444 | .00593 |
| -1 | -1 | 0 | 6564.0 | 6724.1 | 5.0311 | .09162 |
| 0 | 0 | +1 | 6566.6 | 6721.7 | 5.0105 | .0844 |
| +2 | 0 | 0 | 6625.4 | 6703.3 | 4.782 | .109 |
| 0 | +2 | 0 | 6555.0 | 6749.6 | 5.248 | 1.83 |
| 0 | +2 | +1 | 6535.7 | 6825.1 | 5.772 | .411 |
| 0 | 4 | 0 | 6533.7 | 6853.7 | 5.966 | 6.01 |

-1.0 km to +1.0 km, as illustrated in Table 3.5. These random noise values were chosen to be the rightmost three digits from consecutive entries on a page of the local telephone directory. Using an initial estimate of layer parameters $r_b=6600$ km, $r_m=6700$ km, and $f_c=9.0$ MHz. These data are inverted by using different sets of points, as shown in Table 3.6. It can be seen that the percent error in determining the actual parameters of the QP layer decreases as the number of noisy data points used in the inversion process is increased.

Table 3.5. Noisy Backscatter Leading
 Edge Synthesis -- Assuming Earth-
 Centered Q-P Ionosphere $r_b=6570$ km,
 $r_m=6720$ km, and $f_c=7.0$ MHz

| Point No. | f_i (MHz) | Precise P'_{M_i} (km) | Additive Noise (km) | Noisy P'_{M_i} (km) |
|--------------|----------------|----------------------------|------------------------|--------------------------|
| 1 | 10.00 | 1233.388 | .114 | 1233.502 |
| 2 | 10.25 | 1268.959 | -.096 | 1268.863 |
| 3 | 10.50 | 1304.946 | -.257 | 1304.689 |
| 4 | 10.75 | 1341.369 | -.332 | 1341.037 |
| 5 | 11.00 | 1378.250 | -.576 | 1377.674 |
| 6 | 11.25 | 1415.611 | .945 | 1416.556 |
| 7 | 11.50 | 1453.475 | -.988 | 1452.487 |
| 8 | 11.75 | 1491.867 | .062 | 1491.929 |
| 9 | 12.00 | 1530.814 | -.600 | 1530.214 |
| 10 | 12.25 | 1570.344 | -.760 | 1569.584 |
| 11 | 12.50 | 1610.486 | -.271 | 1610.215 |
| 12 | 12.75 | 1651.272 | +.931 | 1652.203 |

Table 3.6. Results of Inversion of the Data in
Table 3.4, Using Various Numbers of Points in E.

| Number of leading edge pts used | Optimized value of E (km ²) | % error in r _b | % error in r _m | % error in f _c |
|---|---|---------------------------------|---------------------------------|---------------------------------|
| N=3 using points 1, 6, 12 | .17203 | .1040 | .155 | 1.77 |
| N=6 using points 1, 3, 5, 7, 9, 12 | 1.8730 | .052 | .0327 | .659 |
| N=9 using points 1, 2, 4, 5, 7, 8, 10, 11, 12 | 2.3943 | .0472 | .0193 | .129 |

3.4.3 Inversion of Synthesized Data Involving Horizontal Gradients

To investigate the technique of inversion of successive sets of three data points on the leading edge for the horizontal gradients, the eccentric QP layer model discussed in Sec. 3.2.2 is employed. First, for assumed layer parameters of $r_b=6570$ km, $r_m=6720$ km, $f_c=5.0$ MHz, $D=1000$ km, and $\omega_T=0$, data points on the leading edge trace are computed for every 0.5 MHz from 7.0 to 11.0 MHz. Next, the points are grouped in four sets of three, starting with (7.0, 7.5, 8.0), then (8.0, 8.5, 9.0), etc. Each group of three data points is then inverted for the parameters of a concentric QP layer. The first group is inverted by using an arbitrary starting set of layer parameters ($r_b=6500$ km, $r_m=6650$ km, and $f_c=4.0$ MHz). Succeeding groups of data are inverted by starting with the layer parameters obtained for the previous group of data points. The synthesized data as well as the computed layer parameter values are shown in Table 3.7. It can be seen from this table that inverted layer parameters indeed exhibit horizontal gradient. When the magnitude of the gradient in r_b or r_m is compared with that predicted from the model, with the use of Fig. 3.5, they are found to be in good agreement.

For a practical example of the backscatter ionogram leading edge for horizontal gradients, we consider the data supplied by the contract sponsor. These data of minimum group paths are simulated by 3-D ray tracing for models of the ionosphere, derived from ITS-78 predictions by applying various linear tilts and gradients to a median profile. This median profile, shown in

TABLE 3.7.
 INVERSION OF SYNTHESIZED BACKSCATTER LEADING EDGE DATA
 FOR AN ECCENTRIC QUASIPARABOLIC LAYER

| Frequency MHz | P' (km) | Synthesized Data Range (km) | r_b (km) | Computed Layer Parameters r_m (km) | f_c (MHz) | E (km^2) |
|------------------|----------|--------------------------------|------------|---|-------------|------------------------|
| 7.0 | 1219.238 | 1004.889 | 6531.6 | 6660.3 | 4.1614 | .00064 |
| 7.5 | 1323.839 | 1120.756 | | | | |
| 8.0 | 1433.133 | 1238.934 | 6529.7 | 6659.3 | 4.1445 | .00311 |
| 8.5 | 1547.939 | 1360.683 | | | | |
| 9.0 | 1669.278 | 1487.355 | 6526.9 | 6657.3 | 4.1159 | .01730 |
| 9.5 | 1798.458 | 1620.455 | | | | |
| 10.0 | 1937.207 | 1761.826 | 6623.1 | 6652.5 | 4.0570 | .120 |
| 10.5 | 2087.893 | 1913.875 | | | | |
| 11.0 | 2253.933 | 2079.975 | | | | |

Fig. 3.17, is assumed to represent the vertical profile at a range of 3500 km from a backscatter sounder site. A linear increase or decrease of the layer parameters along the sounder boresight is then introduced as follows:

$$(i) \text{ Gradients: } f_o F2 = (f_o F2)_{\text{median}} \pm na$$

$$h_m F2 = (h_m F2)_{\text{median}}$$

$$(ii) \text{ Tilts: } f_o F2 = (f_o F2)_{\text{median}}$$

$$h_m F2 = (h_m F2)_{\text{median}} \pm pb$$

where $n, p=0,1,2,3$ and $a=1 \text{ MHz}/3500 \text{ km}$, and $b=10 \text{ km}/3500 \text{ km}$.

The simulated minimum group values are shown in Table 3.8. The numbers in each box corresponding to one leading edge. Thus we have 31 leading edges.

Each set of leading edge data in table 3.8 are inverted for QP layer profiles along the boresight by considering overlapping sets of the three data points. Thus a set of five data points for the minimum group path yield three sets of QP layer parameters corresponding to different ranges from the sounder location. The inversion results are shown in Tables 3.9 through 3.12, which correspond to the ground range, peak height of the layer, base height of the layer, and the critical frequency of the layer, respectively. These results indicate that while it is difficult to compare quantitatively the gradients with those of the original model in view of the differences in the two vertical profiles, the directions of the gradients are generally determined correctly by this procedure.

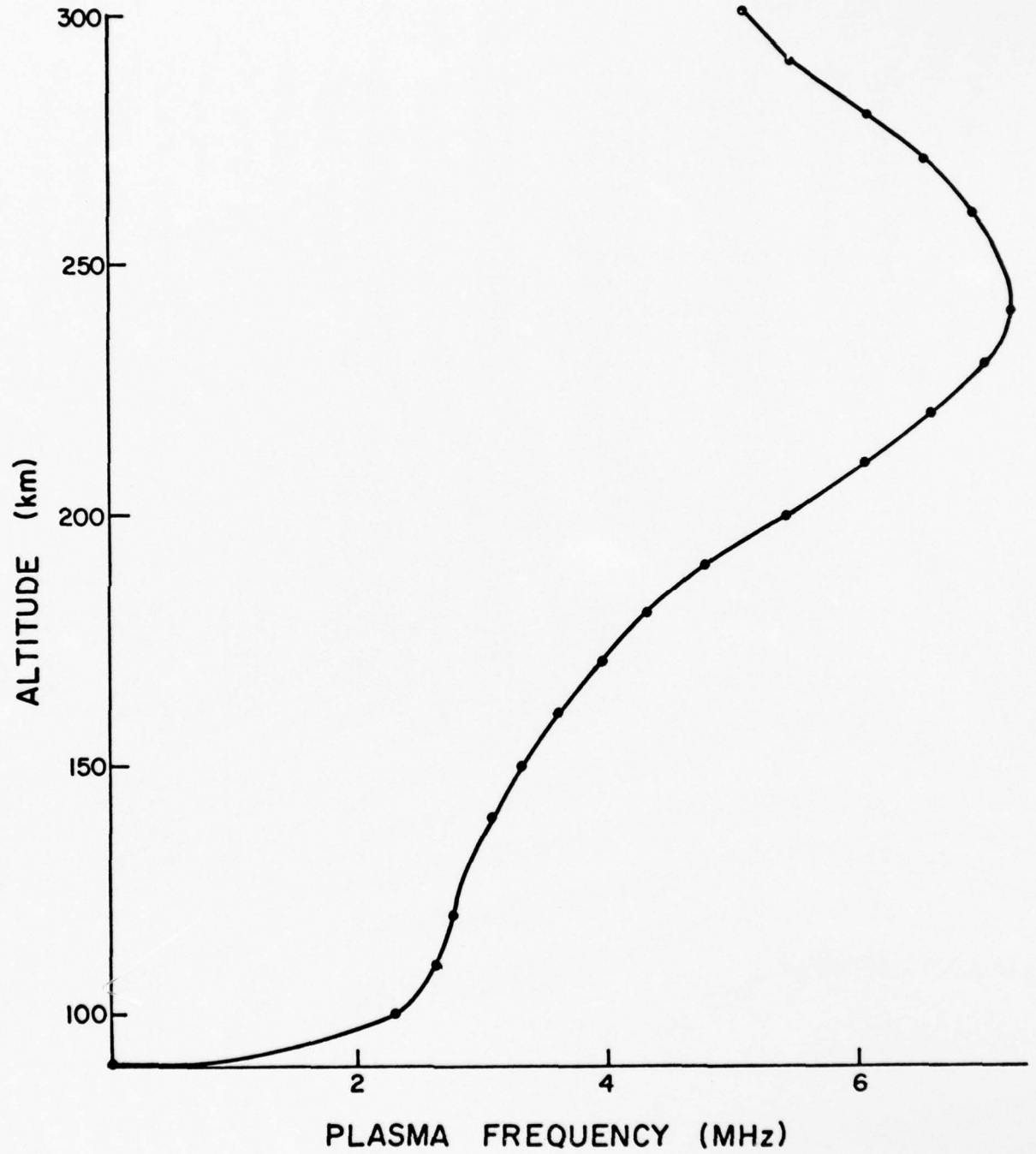


Figure 3.17. Nominal electron density profile.

Table 3.8

Group Path (km) to Leading Edge of Backscatter Ionogram for Various Linear Tilts and Gradients.

| P | | -3 | -2 | -1 | 0 | 1 | 2 | 3 |
|----|----------|------|------|------|------|------|------|------|
| n | | | | | | | | |
| | f=11 MHz | 1036 | 1038 | 1041 | 1044 | | | |
| -3 | 14 | 1388 | 1395 | 1402 | 1409 | | | |
| | 17 | 1815 | 1828 | 1838 | 1852 | | | |
| | 20 | 2398 | 2423 | 2459 | 2499 | | | |
| | 23 | -- | -- | -- | -- | | | |
| | | | | | | | | |
| -2 | 11 | 1025 | 1028 | 1031 | 1033 | | | |
| | 14 | 1364 | 1370 | 1377 | 1384 | | | |
| | 17 | 1766 | 1777 | 1788 | 1802 | | | |
| | 20 | 2288 | 2312 | 2334 | 2372 | | | |
| | 23 | 3128 | 3216 | 3305 | 3395 | | | |
| -1 | 11 | 1015 | 1017 | 1021 | 1023 | | | |
| | 14 | 1343 | 1349 | 1354 | 1361 | | | |
| | 17 | 1724 | 1736 | 1743 | 1755 | | | |
| | 20 | 2194 | 2215 | 2235 | 2264 | | | |
| | 23 | 2855 | 2925 | 2992 | 3044 | | | |
| 0 | 11 | 1005 | 1008 | 1011 | 1014 | 1017 | 1019 | 1021 |
| | 14 | 1322 | 1328 | 1334 | 1338 | 1345 | 1351 | 1357 |
| | 17 | 1685 | 1674 | 1704 | 1715 | 1725 | 1743 | 1761 |
| | 20 | 2114 | 2132 | 2152 | 2184 | 2209 | 2232 | 2254 |
| | 23 | 2698 | 2735 | 2785 | 2848 | 2875 | 2905 | 2930 |
| 1 | 11 | | | | 1004 | 1006 | 1009 | 1012 |
| | 14 | | | | 1320 | 1324 | 1330 | 1336 |
| | 17 | | | | 1677 | 1688 | 1705 | 1718 |
| | 20 | | | | 2110 | 2133 | 2155 | 2176 |
| | 23 | | | | 2679 | 2717 | 2751 | 2787 |
| 2 | 11 | | | | 995 | 998 | 1000 | 1003 |
| | 14 | | | | 1302 | 1307 | 1312 | 1317 |
| | 17 | | | | 1643 | 1654 | 1668 | 1682 |
| | 20 | | | | 2049 | 2069 | 2088 | 2107 |
| | 23 | | | | 2550 | 2584 | 2617 | 2647 |
| 3 | 11 | | | | 987 | 989 | 992 | 994 |
| | 14 | | | | 1284 | 1289 | 1294 | 1299 |
| | 17 | | | | 1611 | 1622 | 1636 | 1648 |
| | 20 | | | | 1993 | 2012 | 2029 | 2047 |
| | 23 | | | | 2449 | 2475 | 2503 | 2531 |

123
Table 3.9

| | | Ground Range (km) | | | | | | |
|----|----------|-------------------|------|------|------|------|------|------|
| P | | -3 | -2 | -1 | 0 | 1 | 2 | 3 |
| n | | | | | | | | |
| -3 | f=14 MHz | 1291 | 1302 | 1310 | 1320 | | | |
| | 17 | 1722 | 1738 | 1751 | 1768 | | | |
| -2 | 14 | 1245 | 1256 | 1268 | 1282 | | | |
| | 17 | 1658 | 1671 | 1684 | 1706 | | | |
| | 20 | 2182 | 2208 | 2229 | 2278 | | | |
| -1 | 14 | 1200 | 1218 | 1221 | 1237 | | | |
| | 17 | 1597 | 1616 | 1622 | 1641 | | | |
| | 20 | 2071 | 2099 | 2113 | 2157 | | | |
| 0 | 14 | 1145 | 1104 | 1173 | 1184 | 1198 | 1220 | 1358 |
| | 17 | 1530 | 1539 | 1563 | 1580 | 1595 | 1625 | 1755 |
| | 20 | 1969 | 2006 | 2018 | 2061 | 2085 | 2113 | 2251 |
| 1 | 14 | | | | 1132 | 1150 | 1178 | 1193 |
| | 17 | | | | 1517 | 1537 | 1569 | 1585 |
| | 20 | | | | 1966 | 1993 | 2024 | 2046 |
| 2 | 14 | | | | 1061 | 1083 | 1122 | 1145 |
| | 17 | | | | 1450 | 1471 | 1508 | 1528 |
| | 20 | | | | 1878 | 1902 | 1937 | 1957 |
| 3 | 14 | | | | 958 | 1006 | 1052 | 1084 |
| | 17 | | | | 1381 | 1404 | 1443 | 1466 |
| | 20 | | | | 1795 | 1816 | 1849 | 1871 |

Table 3.10

Height of Maximum Plasma Frequency
 $(h_m F_2)$
(kilometers)

| p | | | -3 | -2 | -1 | 0 | 1 | 2 | 3 |
|----|----------|--|-----|-----|-----|-----|-----|-----|-----|
| n | | | | | | | | | |
| -3 | f=14 MHz | | 235 | 236 | 239 | 239 | | | |
| | 17 | | 230 | 232 | 220 | 214 | | | |
| -2 | 14 | | 244 | 243 | 247 | 249 | | | |
| | 17 | | 245 | 239 | 238 | 231 | | | |
| | 20 | | 245 | 239 | 236 | 238 | | | |
| -1 | 14 | | 264 | 262 | 260 | 262 | | | |
| | 17 | | 274 | 282 | 258 | 250 | | | |
| | 20 | | 276 | 262 | 258 | 256 | | | |
| 0 | 14 | | 289 | 347 | 283 | 270 | 269 | 249 | 234 |
| | 17 | | 303 | 276 | 290 | 266 | 260 | 263 | 268 |
| | 20 | | 290 | 278 | 277 | 268 | 277 | 307 | 319 |
| 1 | 14 | | | | | 305 | 288 | 269 | 259 |
| | 17 | | | | | 292 | 281 | 286 | 280 |
| | 20 | | | | | 292 | 290 | 311 | 311 |
| 2 | 14 | | | | | 340 | 324 | 302 | 283 |
| | 17 | | | | | 321 | 311 | 305 | 306 |
| | 20 | | | | | 320 | 315 | 328 | 332 |
| 3 | 14 | | | | | 391 | 364 | 336 | 315 |
| | 17 | | | | | 351 | 339 | 330 | 324 |
| | 20 | | | | | 346 | 344 | 356 | 358 |

Table 3.11

| | | Base Height of Ionosphere (km) | | | | | | |
|----|----------|--------------------------------|-------|-------|-------|-------|-------|-------|
| | | -3 | -2 | -1 | 0 | 1 | 2 | 3 |
| n | p | | | | | | | |
| -3 | f=14 MHz | 136.7 | 129.4 | 126.4 | 122.1 | | | |
| | 17 | 142.6 | 135.1 | 142.2 | 139.1 | | | |
| -2 | 14 | 164.5 | 156.8 | 147.7 | 136.6 | | | |
| | 17 | 161.3 | 163.2 | 159.9 | 151.1 | | | |
| | 20 | 160.9 | 163.3 | 169.9 | 135.4 | | | |
| -1 | 14 | 186.7 | 169.5 | 174.7 | 158.9 | | | |
| | 17 | 174.7 | 159.1 | 179.5 | 173.2 | | | |
| | 20 | 174.7 | 177.8 | 202.0 | 156.1 | | | |
| 0 | 14 | 215.9 | 224.1 | 196.3 | 201.1 | 189.3 | 181.7 | 175.7 |
| | 17 | 207.6 | 211.8 | 187.0 | 204.2 | 205.2 | 165.5 | 157.3 |
| | 20 | 225.1 | 169.4 | 213.5 | 182.5 | 167.0 | 148.7 | 150.5 |
| 1 | 14 | | | | 215.4 | 212.3 | 198.9 | 195.5 |
| | 17 | | | | 228.1 | 222.4 | 178.9 | 177.0 |
| | 20 | | | | 205.4 | 194.2 | 168.6 | 166.8 |
| 2 | 14 | | | | 248.9 | 245.0 | 222.4 | 216.1 |
| | 17 | | | | 262.3 | 256.4 | 205.3 | 191.3 |
| | 20 | | | | 231.4 | 226.2 | 191.0 | 187.1 |
| 3 | 14 | | | | 291.4 | 274.2 | 258.1 | 247.7 |
| | 17 | | | | 286.7 | 283.6 | 233.4 | 221.0 |
| | 20 | | | | 258.0 | 251.0 | 218.3 | 210.7 |

Table 3.12

Critical Frequency ($f_0 F_2$)
(in MHz.)

| p | | | -3 | -2 | -1 | 0 | 1 | 2 | 3 |
|----|----------|-------|-------|-------|--------|-------|-------|-------|---|
| n | | | | | | | | | |
| -3 | f=14 MHz | 6.237 | 6.207 | 6.224 | 6.156 | | | | |
| | 17 | 6.140 | 6.158 | 5.872 | 5.725 | | | | |
| -2 | 14 | 6.568 | 6.523 | 6.567 | 6.530 | | | | |
| | 17 | 6.610 | 6.448 | 6.386 | 6.198 | | | | |
| | 20 | 6.613 | 6.447 | 6.334 | 6.316 | | | | |
| -1 | 14 | 7.148 | 7.061 | 7.002 | 7.005 | | | | |
| | 17 | 7.378 | 7.466 | 6.943 | 6.740 | | | | |
| | 20 | 7.413 | 7.072 | 6.873 | 6.856 | | | | |
| 0 | 14 | 7.804 | 9.232 | 7.644 | 7.272 | 7.251 | 6.732 | 6.322 | |
| | 17 | 8.173 | 7.488 | 7.816 | 7.146 | 6.937 | 7.078 | 7.118 | |
| | 20 | 7.814 | 7.614 | 7.444 | 7.265 | 7.400 | 7.830 | 7.990 | |
| 1 | 14 | | | | 8.235 | 7.784 | 7.274 | 7.001 | |
| | 17 | | | | 7.853 | 7.546 | 7.706 | 7.538 | |
| | 20 | | | | 7.937 | 7.868 | 8.184 | 8.125 | |
| 2 | 14 | | | | 9.193 | 8.739 | 8.176 | 7.679 | |
| | 17 | | | | 8.558 | 8.262 | 8.288 | 8.264 | |
| | 20 | | | | 8.713 | 8.547 | 8.763 | 8.782 | |
| 3 | 14 | | | | 10.537 | 9.831 | 9.072 | 8.481 | |
| | 17 | | | | 9.414 | 9.037 | 9.020 | 8.814 | |
| | 20 | | | | 9.450 | 9.378 | 9.595 | 9.559 | |

3.4.4 Inversion of Synthesized Data for Three-Dimensional Ionosphere

For nonzero value of the parameter ω_t , that is, when the transmitter is not situated along the line joining the Earth's center to the center of the ionosphere, the eccentric quasi-parabolic layer provides a three-dimensional variation of the electron density with respect to the transmitter location. Hence when backscatter leading edge data are synthesized for various azimuthal directions from the transmitter, they will all be different. To test the inversion of synthesized data for a three-dimensional ionosphere, leading edges are synthesized by assuming eccentric QP layer parameters of $r_b=6570$ km, $r_m=6720$ km, $f_c=7.00$ MHz, $D=500$ km, and $\omega_T=5^\circ$, and for azimuthal beam headings from 0° to 70° in steps of 10° . The leading edge data for each azimuth is then inverted in the usual manner. The resulting concentric QP layer parameters as a function of range from the transmitter and azimuth are shown in Table 3.13. The entries in each box of this table correspond to values of r_b , r_m , and f_c , respectively. It can be seen that the inversion results do indicate the three dimensional variability of the assumed ionospheric model.

As a further test of the inversion technique, the three-dimensional ionospheric model supplied by the contract sponsor is used and by three-dimensional ray tracing including magnetic field backscatter leading edges are generated for two azimuths (330° and 358°) with the transmitter located at the geographic coordinates of 40° N lat. and 175° long. The generated minimum group path values and other propagation parameters versus fre-

Table 3.13. Results of Inversion of Simulated Backscatter Ionogram Data

Q-P parameters: $r_b=6570$ km $r_m=6720$ km $f_c=7.00$ MHz
 Eccentricity: $|\tilde{D}|=500$ km $\omega_T=5^\circ$

| Approx. Gnd Range km | Azimuthal Beam Heading 0° | 6586.1 | 6583.7 | 6580.1 | 6575.0 | 6568.8 | 6562.8 | 6556.1 |
|----------------------|----------------------------------|--------|--------|--------|--------|--------|--------|--------|
| 630 | 6586.5 | 6586.1 | 6583.7 | 6580.1 | 6575.0 | 6568.8 | 6562.8 | 6556.1 |
| | 6727.7 | 6727.5 | 6726.2 | 6724.4 | 6721.9 | 6719.5 | 6717.1 | 6714.8 |
| | 7.1851 | 7.1794 | 7.1471 | 7.0998 | 7.0339 | 6.9592 | 6.8845 | 6.8024 |
| 1150 | 6564.3 | 6563.9 | 6562.7 | 6560.8 | 6558.4 | 6555.0 | 6551.7 | 6548.3 |
| | 6716.8 | 6716.6 | 6716.1 | 6715.3 | 6714.3 | 6714.4 | 6713.2 | 6712.0 |
| | 6.9146 | 6.9087 | 6.8921 | 6.8659 | 6.8314 | 6.8065 | 6.7601 | 6.7716 |
| 2020 | 6553.7 | 6553.5 | 6552.8 | 6551.5 | 6550.0 | 6548.0 | 6545.8 | 6543.4 |
| | 6711.2 | 6711.1 | 6710.8 | 6710.2 | 6709.6 | 6708.4 | 6707.5 | 6706.5 |
| | 6.7816 | 6.7773 | 6.7651 | 6.7447 | 6.7178 | 6.6825 | 6.6457 | 6.6059 |
| 2170 | 6545.8 | 6545.7 | 6545.1 | 6544.4 | 6543.2 | 6542.4 | 6540.7 | 6537.8 |
| | 6701.1 | 6701.1 | 6700.7 | 6699.6 | 6698.8 | 6690.7 | 6695.7 | 6696.3 |
| | 6.6046 | 6.6006 | 6.5888 | 6.5640 | 6.5383 | 6.4940 | 6.4580 | 6.4383 |

quency are shown in Tables 3.14 and 3.15. To invert these leading edge data, a QP layer is fitted to the actual vertical electron density profile existing above the transmitter location. By using these QP layer parameters as the starting solution, overlapping sets of three data points along the leading edge are inverted for QP layer parameters. In inverting a given set other than the first one, the solution found for the previous set is used as the starting solution. For each set of data inverted, the corresponding ground range is computed and the QP layer parameters are assigned to a location half that distance from the transmitter and along the pertinent azimuth. The layer parameters and the corresponding ranges generated in this manner are listed in Tables 3.16 and 3.17. It can be seen that in this manner, actual experimental backscatter leading edge data for various azimuthal directions from the transmitter location can be inverted for a three dimensional ionosphere specified by QP layer parameters at a set of grid points located along the azimuthal directions.

Table 3.14. Computed minimum group path data and other propagation parameters for transmitter location of 40°N, 175°W, and 330° azimuth.

| Frequency, MHz | Minimum Group path, km | Ground range, km | Apogee height, km |
|-------------------|------------------------------|---------------------|----------------------|
| 10 | 798.35 | 468.81 | 220.26 |
| 11 | 884.79 | 590.29 | 222.25 |
| 12 | 972.60 | 708.63 | 222.02 |
| 13 | 1062.92 | 826.38 | 220.63 |
| 14 | 1155.56 | 929.67 | 223.15 |
| 15 | 1251.66 | 1041.29 | 222.89 |
| 16 | 1349.12 | 1150.64 | 222.91 |
| 17 | 1450.55 | 1261.44 | 223.20 |
| 18 | 1555.26 | 1370.37 | 225.13 |
| 19 | 1665.43 | 1483.68 | 227.10 |
| 20 | 1780.63 | 1604.12 | 227.60 |

Table 3.15. Same as Table 3.14 except for 358° azimuth

| Frequency, MHz | Minimum Group path, km | Ground range, km | Apogee height, km |
|-------------------|------------------------------|---------------------|----------------------|
| 10 | 805.04 | 474.50 | 222.20 |
| 11 | 894.16 | 598.72 | 224.30 |
| 12 | 984.55 | 719.84 | 224.14 |
| 13 | 1077.68 | 840.37 | 222.70 |
| 14 | 1173.13 | 954.99 | 222.23 |
| 15 | 1273.45 | 1062.07 | 225.29 |
| 16 | 1376.13 | 1172.57 | 227.20 |
| 17 | 1483.70 | 1293.45 | 225.99 |
| 18 | 1596.70 | 1417.13 | 224.96 |
| 19 | 1714.86 | 1531.40 | 230.46 |

Table 3.16. Computed QP layer parameter values and the corresponding ground ranges for 330° azimuth

| Range, km | f_c , MHz | r_b , km | r_m , km |
|-----------|-------------|------------|------------|
| 327.56 | 9.2406 | 6556.4 | 6676.2 |
| 377.18 | 9.3493 | 6561.9 | 6679.5 |
| 431.21 | 9.3344 | 6561.2 | 6679.1 |
| 486.87 | 9.2511 | 6557.4 | 6676.4 |
| 531.07 | 9.7489 | 6565.8 | 6694.9 |
| 577.99 | 10.0895 | 6573.9 | 6707.4 |
| 632.21 | 10.1063 | 6574.6 | 6708.0 |
| 689.80 | 10.0427 | 6572.1 | 6705.8 |
| 749.46 | 9.9592 | 6568.2 | 6702.9 |

Table 3.17. Same as Table 3.16 except for 358° azimuth

| Range, km | f_c , MHz | r_b , km | r_m , km |
|-----------|-------------|------------|------------|
| 373.28 | 8.3981 | 6509.2 | 6661.6 |
| 414.73 | 8.9054 | 6519.1 | 6680.1 |
| 461.30 | 9.0253 | 6526.2 | 6681.9 |
| 515.75 | 8.9677 | 6522.8 | 6680.9 |
| 568.43 | 8.9757 | 6523.2 | 6681.1 |
| 619.54 | 9.0693 | 6529.0 | 6682.8 |
| 676.62 | 9.0482 | 6527.7 | 6682.4 |
| 732.96 | 9.2278 | 6528.4 | 6690.8 |

3.4.5 Application of the Backscatter Inversion Technique

It has been pointed out in Sec. 3.1, that while the backscatter leading edge is not capable of providing the ionospheric vertical profiles above certain heights, this is not a limitation in so far as the application of the inversion technique is concerned. In this section, we shall prove this point and provide an explanation for the applicability of the inversion technique despite the limitation for obtaining the complete ionospheric structure. To do this, we consider an important application, which consists of finding the ground range for a given group path (not a minimum group path) at a known frequency, and compare the applicability of the deduced three-dimensional ionosphere by inversion of the leading edge data, relative to that of the originally assumed three-dimensional model.

Referring back to Sec. 3.4.4 in which we presented the result of inversion of synthesized leading edges for two azimuths for the Air Force supplied model, we now trace rays at one frequency (16 MHz) in the original as well as the computed ionospheres for an azimuth of 340° (lying between 330° and 358° corresponding to the inverted backscatter data) and for several elevation angles of transmission. For tracing rays in the computed ionosphere, it should be noted that the rectangular grid of the originally assumed model is uniformly spaced, whereas the grid generated by the inversion of the leading edge data is nonuniformly spaced, in addition to being in azimuth-range space, rather than in the latitude-longitude space. Hence it has become necessary to generate vertical profiles at the uniformly spaced

rectangular grid of points by applying an interpolation procedure to the QP profiles at the grid point in the azimuth-range space. The result of these ray tracings are shown in Tables 3.18 and 3.19, which correspond to the originally assumed model and the computed ionosphere, respectively. The quantity (P'-R) is shown plotted versus P' for the two cases in Fig. 3.18. A comparison of the two curves indicates that the computed ionosphere gives the correct range to within ± 2 km for a wide range of group path values. The discrepancies greater than ± 2 km toward the low end of the curves are attributable to the fact that the region is close to the minimum group path, whereas the discrepancies greater than ± 2 km toward the high end of the curves are attributable to the fact that the region is beyond the range corresponding to the inverted backscatter data.

We shall now provide a simple explanation for the success of the technique in finding the range for a given group path to a good accuracy, despite the fact that the minimum group path rays all reflect from below a certain apogee height, as can be seen from Tables 3.14 and 3.15 and hence cannot yield the vertical profiles above those apogee heights. To do this, we refer to Fig. 3.19 which illustrates the fact that the backscatter ionogram is a continuum of oblique ionograms corresponding to successively increasing values of ground range away from the transmitter. Let us suppose we have found the range corresponding to a particular point A (f_1, P_1') on the leading edge. Then a point B, corresponding to the same group path as that of A but to a frequency $f_2 < f_1$, corresponds to a range greater than that of A. Alternatively, it corresponds to a range corresponding to

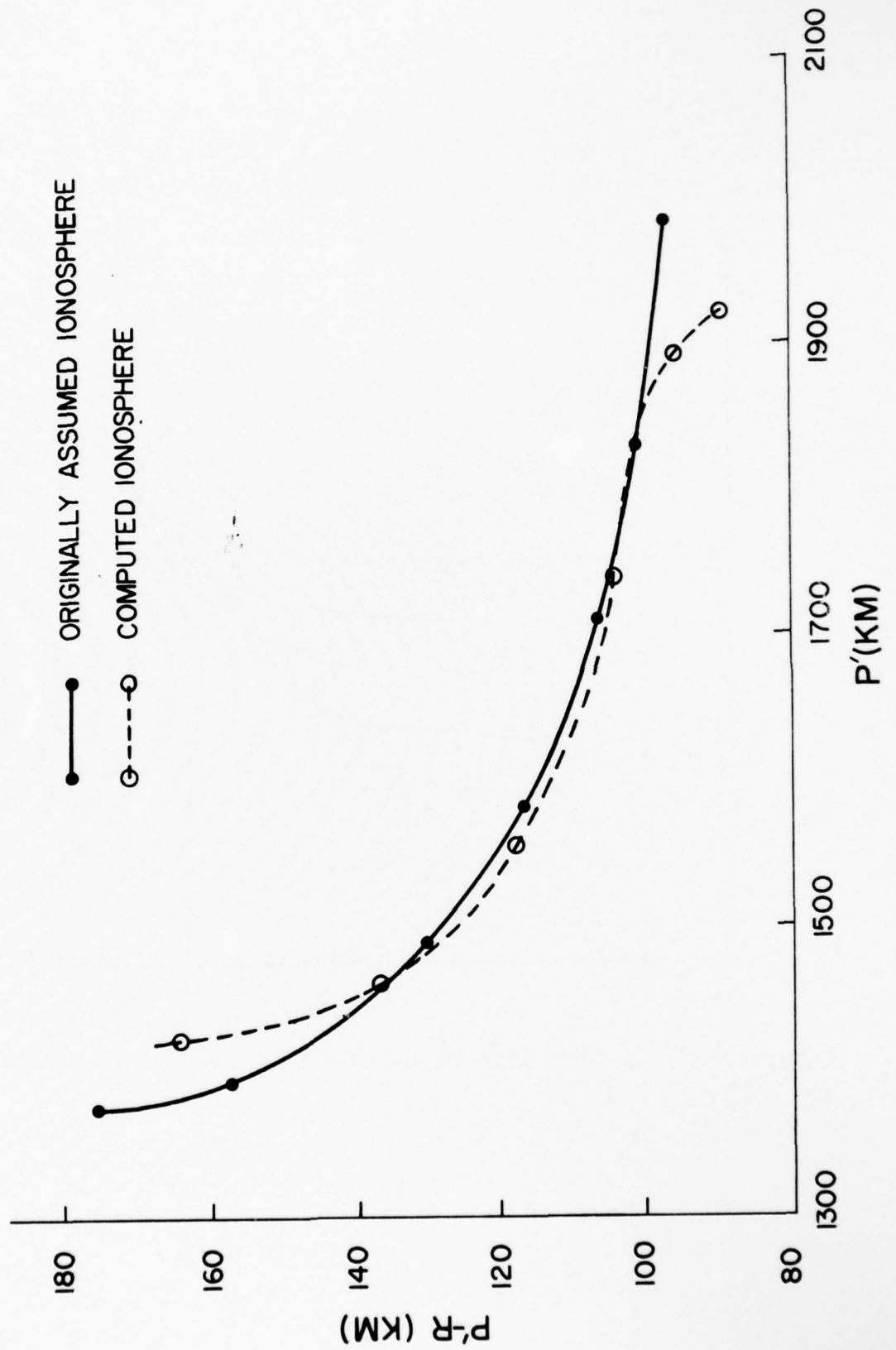


Figure 3.18. Reconstruction of ground range

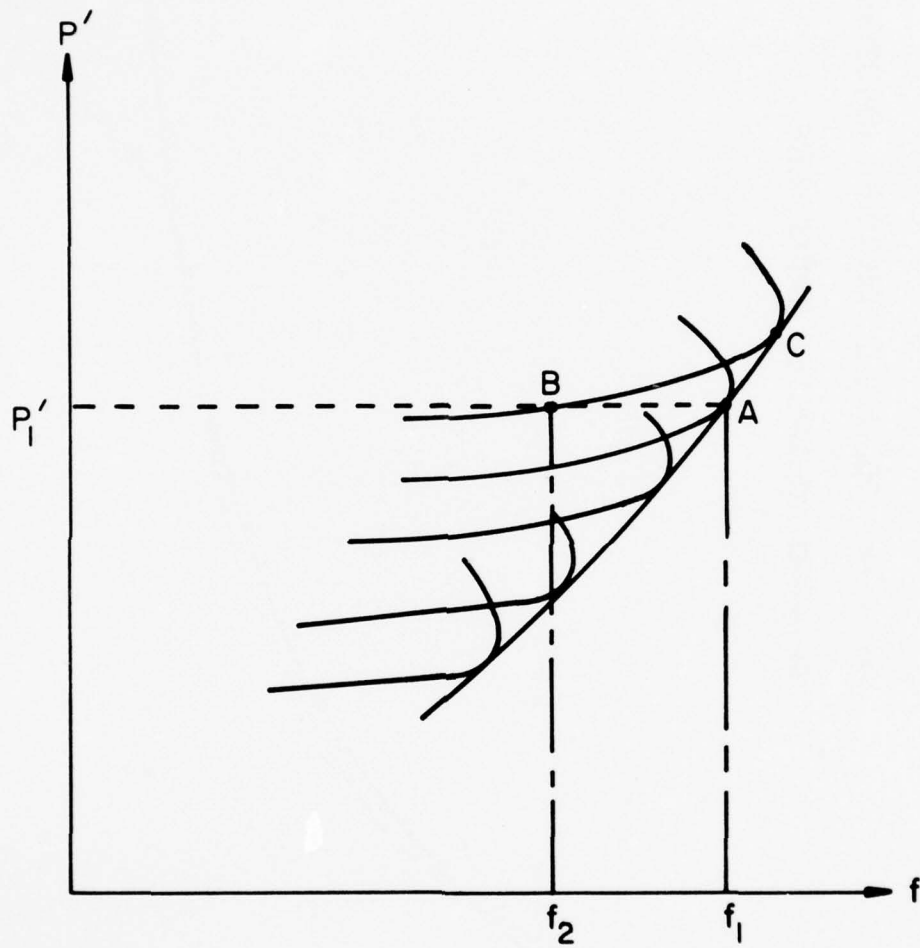


Figure 3.19. Limitations of information contained in data.

Table 3.18. Group path and ground range versus elevation angle for 16 MHz and for 340° azimuth, using the originally assumed model.

| Elevation angle, deg. | Group path P', km | Ground range R, km | (P'-R) km |
|-----------------------|-------------------|--------------------|-----------|
| 10 | 1985.06 | 1888.14 | 96.92 |
| 12 | 1795.51 | 1693.76 | 101.76 |
| 14 | 1661.89 | 1552.97 | 108.92 |
| 16 | 1563.03 | 1444.75 | 118.28 |
| 18 | 1490.80 | 1361.39 | 129.41 |
| 20 | 1435.69 | 1293.32 | 142.37 |
| 22 | 1393.93 | 1236.40 | 157.53 |
| 24 | 1371.43 | 1196.75 | 174.68 |

Table 3.19. Same as Table 3.18 except using the computed ionosphere

| Elevation angle, deg. | Group path P', km | Ground range R, km | (P'-R) km |
|-----------------------|-------------------|--------------------|-----------|
| 14 | 1921.58 | 1833.31 | 88.27 |
| 16 | 1892.55 | 1796.50 | 96.05 |
| 18 | 1725.20 | 1619.59 | 105.61 |
| 20 | 1555.49 | 1437.47 | 118.02 |
| 22 | 1458.60 | 1321.65 | 136.95 |
| 24 | 1422.14 | 1257.31 | 176.83 |

that of a point C on the leading edge, lying above the point A. Hence the ray of frequency f_2 and group path P'_1 reflects below the apogee height corresponding to the point C. Since this argument is true for any point on the low-ray portions of the oblique ionograms, it follows that one can always find the range corresponding to such a point, although the backscatter leading edge is not capable of yielding the ionospheric profile above the apogee heights corresponding to the minimum group path rays.

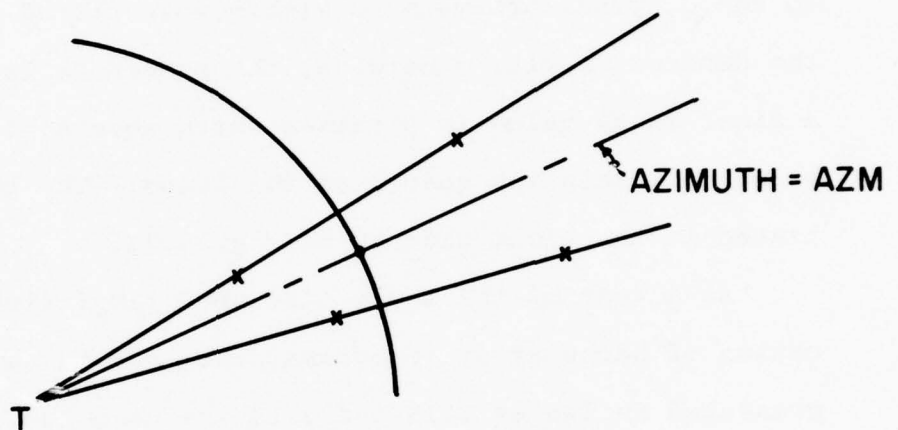
Spurred by the success of the application of the backscatter leading edge inversion technique in the determination of the ground range for a given group path, we decided to combine the inversion problem and the subsequent range determination into one computer program. Thus, provided with the input of backscatter leading edge data for several azimuths and the group path values (non-minimum) at several frequencies for a different azimuth, the program computes the ground ranges. To carry out the range computation, we decided to employ a simple homing technique in conjunction with the exact ray path computation for the concentric QP layer rather than the elaborate three-dimensional ray tracing including the Earth's magnetic field. The details of the entire program are presented in the appendix.

To describe the procedure briefly, first each backscatter leading edge is inverted for a series of QP layer profiles along the corresponding azimuth, in the usual manner. For each specified group path value (P') for which the ground range is to be determined, the program then computes a rough estimate of the range, based on specular reflection at an assumed value of base

height of the ionosphere. By an interpolation procedure involving two azimuths and two ranges along each azimuth as shown in Fig. 3.20, the program then computes the QP layer parameters at half the estimated ground range along the azimuth (α) corresponding to the group path data. Using analytical expressions for ray path parameters and the interpolated QP layer parameters, a ground range value is computed for the specified group path, employing an iterative technique. If this range value is close to the original estimate to within a specified tolerance, it is the desired result; otherwise, the procedure is repeated until a final range value is obtained which agrees with the previous value to within the specified tolerance. The technique is illustrated in the block diagram of Fig. 3.21.

As a test of the above discussed simplified method of application of backscatter ionograms, the leading edge inversion results presented in Tables 3.16 and 3.17 are used to compute the ground ranges for various values of group path for $f=16$ MHz and azimuthal angle of 340° . The results are shown in Table 3.20, which indicates larger errors in (P'-R) than in Table 3.19, but still less than 15 percent of the actual values of (P'-R) given in Table 3.18.

TWO AZIMUTHAL DIRECTIONS
IN WHICH IONOSPHERE HAS
BEEN PROBED BY BSI



x DENOTES POINTS ON SURFACE OF EARTH
FOR WHICH QPP HAVE BEEN DETERMINED
IN ORDER TO DESCRIBE OVERHEAD IONOSPHERE

Figure 3.20. Interpolation procedure.

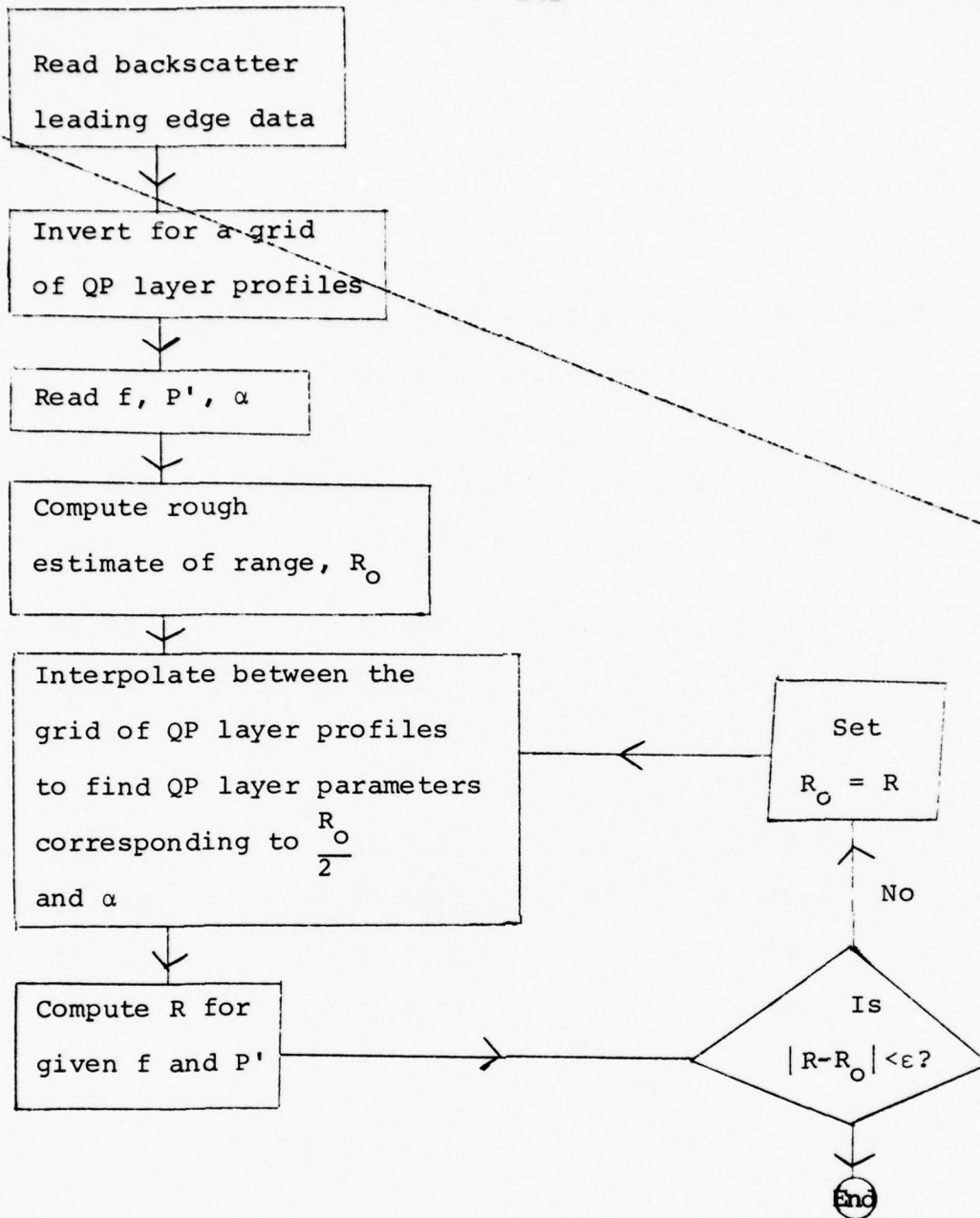


Figure 3.21. Block diagram of steps involved in backscatter leading edge inversion and application.

Table 3.20. Same as Table 3.18 except using the
Simplified Ionospheric Model

| Group path P', km | Ground range R km | (P'-R) km |
|----------------------|----------------------|--------------|
| 1985.06 | 1904.16 | 80.50 |
| 1795.51 | 1707.41 | 88.10 |
| 1661.89 | 1565.75 | 96.14 |
| 1563.03 | 1457.76 | 105.27 |
| 1490.80 | 1375.62 | 115.18 |
| 1435.69 | 1308.68 | 127.01 |
| 1393.93 | 1252.20 | 141.73 |
| 1371.43 | 1216.52 | 154.91 |

3.4.6 Uniqueness of the Application of the Inversion Technique

In this section we will consider the effect of the initial estimate of QPP (QP layer parameters) upon the inversion of group delay into ground range. The motivation for this simulation was to determine the possible effects of the nonuniqueness of the inversion of backscatter ionogram data into ionospheric refractive index. Also we were interested in the reliability of the present technique in providing a reasonably consistent inversion between group delay and ground range, despite the uncertainty involved in the initial estimate of QPP.

The results of this analysis, to date, are presented in the following set of tables. The procedure used in generating these tables was to vary one of the three initial QPP while keeping the other two parameters fixed, and observe the effect of this variation upon the inversion of a fixed value of group path into a computed value of ground range. For our present purposes, we will consider the QPP to consist of the semithickness of the layer (y_m), the height of the base of the ionosphere (h_b), and the critical, or maximum, plasma frequency (f_oF_2). Other parameters such as r_b ($h_b + 6370$ km) and r_m ($y_m + h_b + 6370$ km) may be obtained easily once y_m and h_b are specified. Table 3.21 specifically indicates the effect of varying r_b which is equivalent to varying h_b . The last column illustrates the small variation in the computed ground range thereby induced in the case of an untilted (no horizontal gradient) ionosphere. Table 3.22 demonstrates the effect of varying the initial estimate of the maximum plasma frequency (or critical frequency), and again we

UNTILTED IONOSPHERE

Table 3.21: The Effect of Varying r_b Initial Estimate Upon Inversion of Group Path^b into Ground Range.

| Theoretical Grp. Path (km) | Initial Est. of r_b | Computed Grnd. Range (km) |
|-------------------------------|--------------------------|------------------------------|
| 1700 | 6510 | 1591.89 |
| | 6520 | 1591.26 |
| | 6530 | 1591.93 |
| | 6540 | 1590.95 |
| | 6550 | 1590.53 |
| 1900 | 6510 | 1809.76 |
| | 6520 | 1809.26 |
| | 6530 | 1809.79 |
| | 6540 | 1808.96 |
| | 6550 | 1808.65 |
| 2100 | 6510 | 2020.76 |
| | 6520 | 2020.43 |
| | 6530 | 2020.79 |
| | 6540 | 2020.15 |
| | 6550 | 2019.98 |

see that the effect upon the computed ground range is small. Table 3.23 demonstrates the effect of variations in the initial estimate of r_m while keeping r_b fixed. This corresponds to expansion and contraction of the vertical dimensions of the ionosphere through the variation of y_m . The variation in the computed ground range is somewhat larger than the variation obtained in the previous two tables. Nevertheless, it should be noted that even though r_m is varying by less than 1% from its nominal value of 6610 km, the really significant parameter is the semithickness (y_m) of the ionospheric layer, and this latter parameter is varying over a proportionately larger range--i.e. $r_m = 6600$ km corresponds to a 70 km semithickness, while $r_m = 6620$ km corresponds to a 90 km semithickness.

This type of analysis has also been performed for a tilted ionosphere (an ionosphere with a horizontal gradient). Tables 3.24, 3.25, and 3.26 correspond to Tables 3.21, 3.22, and 3.23 respectively, and in comparing these two sets of tables, it would appear that the inversion of group path into ground range is more sensitive to the variability of the initial QPP in a tilted ionosphere. This effect would seem to be most pronounced in the case of variations of r_m .

We therefore decided to consider the possible causes of the relatively large variation in ground range resulting from the simulated uncertainty in the initial value of r_m . By narrowing the uncertainty in the initial estimate of r_m by a factor of 2, it can be seen that the variability of the ground range

UNTILTED IONOSPHERE

Table 3.22: The Effect of Varying the Initial Estimate of Critical Frequency Upon Inversion of Group Path Into Ground Range.

| Theoretical Grp. Path (km) | Initial Est. of r_b (km) | Computed Grnd. Range (km) |
|-------------------------------|-------------------------------|------------------------------|
| 1700 | 6.75 | 1592.09 |
| | 7.00 | 1591.35 |
| | 7.25 | 1591.93 |
| | 7.50 | 1591.17 |
| | 7.75 | 1591.04 |
| 1900 | 6.75 | 1809.92 |
| | 7.00 | 1809.33 |
| | 7.25 | 1809.79 |
| | 7.50 | 1809.19 |
| | 7.75 | 1809.11 |
| 2100 | 6.75 | 2020.28 |
| | 7.00 | 2020.46 |
| | 7.25 | 2020.79 |
| | 7.50 | 2020.39 |
| | 7.75 | 2020.35 |

UNTILTED IONOSPHERE

Table 3.23: The Effect of Varying Layer Semithickness Upon Inversion of Group Path to Ground Range.

| Theoretical Grp. Path (km) | Initial Est. of r_m (km) | Est. of y_m (km) | Computed Grnd. Range (km) |
|-------------------------------|-------------------------------|-----------------------|------------------------------|
| 1700 | 6600 | 70 | 1590.60 |
| | 6605 | 75 | 1590.56 |
| | 6610 | 80 | 1591.93 |
| | 6615 | 85 | 1592.26 |
| | 6620 | 90 | 1591.96 |
| 1900 | 6600 | 70 | 1808.73 |
| | 6605 | 75 | 1808.67 |
| | 6610 | 80 | 1809.79 |
| | 6615 | 85 | 1810.06 |
| | 6620 | 90 | 1809.81 |
| 2100 | 6600 | 70 | 2020.08 |
| | 6605 | 75 | 2020.14 |
| | 6610 | 80 | 2020.79 |
| | 6615 | 85 | 2020.98 |
| | 6620 | 90 | 2020.80 |

TILTED IONOSPHERE

Table 3.24: The Effect of the Initial Estimate of r_b (Radius to Ionospheric Base) Upon the Inversion of f_b Group Path into Ground Range.

| Theoretical Grp. Path (km) | Initial Est. of r_b (km) | Computed Grnd. Range (km) |
|-------------------------------|-------------------------------|------------------------------|
| 1700 | 6510 | 1584.67 |
| | 6520 | 1583.57 |
| | 6530 | 1586.57 |
| | 6540 | 1586.86 |
| | 6550 | 1583.67 |
| 1900 | 6510 | 1798.66 |
| | 6520 | 1792.39 |
| | 6530 | 1794.79 |
| | 6540 | 1795.77 |
| | 6550 | 1792.42 |
| 2100 | 6510 | 1996.30 |
| | 6520 | 1994.87 |
| | 6530 | 1996.97 |
| | 6540 | 1998.44 |
| | 6550 | 1994.96 |

TILTED IONOSPHERE

Table 3.25: The Effect of Initial Estimate of Critical Frequency (f_c) Upon Inversion.

| Theoretical Grp. Path (km) | Initial Est. of f_c | Computed Grnd. Range (km) |
|-------------------------------|--------------------------|------------------------------|
| 1700 | 6.75 | 1586.41 |
| | 7.00 | 1586.89 |
| | 7.25 | 1586.57 |
| | 7.50 | 1587.24 |
| | 7.75 | 1586.37 |
| 1900 | 6.75 | 1795.11 |
| | 7.00 | 1796.12 |
| | 7.25 | 1794.79 |
| | 7.50 | 1796.61 |
| | 7.75 | 1795.26 |
| 2100 | 6.75 | 1997.62 |
| | 7.00 | 1999.02 |
| | 7.25 | 1996.97 |
| | 7.50 | 1999.62 |
| | 7.75 | 1997.90 |

TILTED IONOSPHERE

Table 3.26: The Effect of Initial Estimate of r_m Upon Inversion of Group Path into Ground^m Range. Program was allowed to go 40 Iterations

| Theoretical Grp. Path (km) | Initial Est. of | | Computed Grnd. Range (km) |
|-------------------------------|-----------------|------------|------------------------------|
| | r_m (km) | y_m (km) | |
| 1700 | 6590 | 60 | 1578.35 |
| | 6600 | 70 | 1582.48 |
| | 6610 | 80 | 1586.57 |
| | 6620 | 90 | 1586.67 |
| | 6630 | 100 | 1590.76 |
| 1900 | 6590 | 60 | 1786.76 |
| | 6600 | 70 | 1790.84 |
| | 6610 | 80 | 1794.79 |
| | 6620 | 90 | 1798.14 |
| | 6630 | 100 | 1801.60 |
| 2100 | 6590 | 60 | 1988.81 |
| | 6600 | 70 | 1992.96 |
| | 6610 | 80 | 1996.97 |
| | 6620 | 90 | 2001.28 |
| | 6630 | 100 | 2005.76 |

TILTED IONOSPHERE

Table 3.27: The Effect of Varying the Layer Semithickness Upon the Inversion of Group Path to Ground Range.

| Theoretical Grp. Path (km) | Initial Est. of r_m (km) | of y_m | Computed Grnd. Range (km) |
|-------------------------------|-------------------------------|-------------|------------------------------|
| 1700 | 6600 | 70 | 1582.48 |
| | 6605 | 75 | 1582.13 |
| | 6610 | 80 | 1586.57 |
| | 6615 | 85 | 1587.62 |
| | 6620 | 90 | 1588.67 |
| 1900 | 6600 | 70 | 1790.84 |
| | 6605 | 75 | 1790.62 |
| | 6010 | 80 | 1794.79 |
| | 6615 | 85 | 1797.08 |
| | 6620 | 90 | 1798.14 |
| 2100 | 6600 | 70 | 1992.96 |
| | 6605 | 75 | 1992.82 |
| | 6610 | 80 | 1996.97 |
| | 6615 | 85 | 2000.16 |
| | 6620 | 90 | 2001.28 |

is also reduced, as shown in Table 3.27. In order to consider the effect of allowing the program to perform a greater number of iterations, we have repeated the calculation of Table 3.26 by doubling the number of iterations which the program uses in computing a final set of QPP. The result is shown in Table 3.28. Although this increase in the number of iterations generally improves the result, this is not always the case, as can be seen in Table 3.29. The significant quantity, σ , denotes the standard deviation of the ground range values from their respective means. For the smaller values of simulated group path, increased iterations produce a smaller standard deviation. For the largest value of group path (2100 km) the standard deviation is actually larger in the case of 80 iterations, as opposed to the case of 40 iterations.

TILTED IONOSPHERE

Table 3.28: The Effect of Initial Estimate of r_m Upon Inversion of Group Path into Ground^m Range. Program was allowed to go 80 Iterations in Fitting QPP.

| Theoretical Grp. Path (km) | Initial Est. of r_m (km) | Est. of y_m (km) | Computed Grnd. Range (km) |
|-------------------------------|-------------------------------|-----------------------|------------------------------|
| 1700 | 6590 | 60 | 1580.18 |
| | 6600 | 70 | 1582.72 |
| | 6610 | 80 | 1586.97 |
| | 6620 | 90 | 1587.40 |
| | 6630 | 100 | 1588.40 |
| 1900 | 6590 | 60 | 1778.40 |
| | 6600 | 70 | 1781.92 |
| | 6610 | 80 | 1788.25 |
| | 6620 | 90 | 1789.21 |
| | 6630 | 100 | 1790.48 |
| 2100 | 6590 | 60 | 1973.34 |
| | 6600 | 70 | 1977.90 |
| | 6610 | 80 | 1986.09 |
| | 6620 | 90 | 1987.49 |
| | 6630 | 100 | 1989.10 |

TILTED IONOSPHERE

Table 3.29: Variance Resulting from Different Values of r_m as Affected by Number of Iterations (IT).

| Theoretical Grp. Path (km) | IT | \bar{D} | σ |
|-------------------------------|----|-----------|----------|
| 1700 | 40 | 1585.37 | 4.45 |
| | 80 | 1585.13 | 3.15 |
| 1900 | 40 | 1794.43 | 5.23 |
| | 80 | 1785.65 | 4.39 |
| 2100 | 40 | 1997.16 | 5.97 |
| | 80 | 1982.78 | 6.10 |

3.5 General Consideration of the Inversion Problem

In the past two sections of this chapter we have presented several techniques that can be applied to deduce the ionospheric structure by using point-to-point oblique ionograms (section 3.3) or backscatter leading edges (section 3.4). In both cases our computations have been carried out for quasi-parabolic profiles. Recently an inversion technique developed in connection with geophysical problems has shown great promise. This technique, known as Backus-Gilbert technique, can be adapted to inverting oblique ionograms of both kinds. The problem has been formulated in a paper "A Method for Inverting Oblique Sounding Data in the Ionosphere" which is attached as Appendix 4. Initial application to the vertical incidence data demonstrates its rapid convergence. The technique has yet to be applied to inverting oblique ionograms. It is desirable to carry out many computations in order to understand the capability, the characteristics and the limitation of this inversion technique. So far the problem has been formulated for inverting either the backscatter leading edge or the oblique ionogram. In both cases spherical stratification is assumed. Details can be found in Appendix 4.

3.6 Conclusions

In conclusion, we have in this section discussed our efforts to devise techniques for the determination of ionospheric structure from oblique radio propagation data. Particular attention was devoted to the problem of obtaining the horizontal gradients. The major findings of the effort are: a) point-to-point oblique ionograms, by themselves, are not very useful for obtaining the horizontal gradients, while b) backscatter leading edge data are capable of providing information concerning the horizontal gradients.

We have provided several examples of inversion of the oblique radio propagation data and even investigated the application of the backscatter technique. We have demonstrated that despite the fact that the inversion technique does not necessarily yield a unique solution for the ionospheric structure, this uncertainty is not an important factor in the application.

4. Recommendations for Future Work

Based on the efforts of our work reported in sections 2 and 3 and the conclusions reached therein, we make the following recommendations for continuing work on this project:

1. Since the backscatter data and the corresponding inversion results involve a grid of points in the azimuth-range space, it is desirable that the electron density model employed in the three-dimensional ray tracing be specified in the azimuth-range space rather than in the latitude-longitude space.

2. The basic inversion techniques of backscatter leading edge data need to be tested by employing simulated data for progressively complicated ionospheres. In this connection, it is necessary that the simulated data points be closely spaced in range, in view of the fact that successive data points correspond to successively increasing values of range away from the transmitter. Hence for the derivation of local horizontal gradients, it is necessary to consider sets of data points, closely spaced in range, and hence in frequency.

3. In addition to the inversion of backscatter leading edge for ionospheric structure, further tests are necessary with regard to the application of the inversion results for computing the ranges for non-minimum group paths. In this connection, it is necessary to have simulated ray tracing data for non-minimum group path rays for the same model ionospheres for which the backscatter leading edges are simulated.

4. The dependence of the inversion result upon the choice of the initial set of layer parameters should be further investigated

with a view to determining how in actual practice, the initial set of layer parameters must be chosen in order to minimize the uncertainty of the inversion technique.

5. The present scheme for homing the ray after one reflection from the ionosphere is very successful as demonstrated by several examples in this report. However, in extending the present scheme to multi-hop modes some difficulties are encountered. Some of these difficulties have been identified: the coarseness of the grid points at which the electron density is given, and inflexibility in the computer program to handle mixed and complex modes. To remove these difficulties requires further refinement of the ray tracing program.

6. Preliminary analysis shows promise in applying the Backus-Gilbert technique to inversion of the oblique propagation data. This technique has been applied to the vertical ionogram and very rapid convergence is obtained. Even though the mathematical formulation for the inversion of oblique data has been carried out, its application to data has yet to be made. One possibility is to choose a model profile (such as piece-wise parabolic profile) for which analytic expressions are available so as to reduce the computation time. Another area of interest is to generalize the Backus-Gilbert technique by including the horizontal gradient. In this latter case the Bouguer's rule is no longer valid, one must reformulate the problem anew.

APPENDIX 1

The computer programs for ray homing are listed in the following pages. These programs are discussed in section 2.5.

| | | |
|----|--|---------|
| | MAXERR=1.E-8 | 0044 |
| | ERATIO=5C. | 0045 |
| | STEF1=1. | 0046 |
| | STPMAX=100. | 0047 |
| | STPMIN=1.E-4 | 0048 |
| | FACTF=0.5 | 0049 |
| | MAXSTP=1000. | 0050 |
| | HCF=1. | 0051 |
| | ELT=0. | 0052 |
| C | | 0053 |
| | 1 CALL REAL W | 0054 |
| C | | |
| | MPRT = C | KV 054 |
| C | | |
| | F=0.0 | |
| | BETA=0.0 | |
| | AZ1=0.0 | |
| | IF (WN.IT.7.) WN=7. | 0056 |
| | IF (WN.GI.12.) WN=12. | 0057 |
| | IF (SKIF.EQ.0.) SKIF=MAXSTP | 0058 |
| | NTYP=2.+FIELD*RAY+0.C1 | 0059 |
| | PRINT 7, ID, NDATE, MODEL, TYPE (NTYP), TYPE2 (NIYE), KOLL | |
| 7 | FORMAT (1E1, 10A4, 2CX, I8/5X, 4 (1X, A4), 2X, 2A4, ' COLLISIONS'/) | |
| | PRINT 8 | 0063 |
| 8 | FORMAT (85H INITIAL VALUES FOR THE W ARRAY -- ALL ANGLES IN RADIAN | 0064 |
| | 1S, ONLY NONZERO VALUES PRINTED/) | 0065 |
| | DO 10 I=1,400 | 0066 |
| | IF (W(I).NE.0.) PRINT 9, I, W(I) | 0067 |
| 9 | FORMAT (I4, E19.11) | 0068 |
| 10 | CONTINUE | 0069 |
| C | LET SUBROUTINES PRINTR AND RAYFIT KNOW THERE IS A NEW W ARRAY | 0070 |
| | PNEWW=1.C | |
| | RNEWW=1.C | |
| C | | 0072 |
| C | INITIALIZE PARAMETERS FOR INTEGRATION SUBROUTINE FKAM | 0073 |
| | N=WN+0.C1 | 0074 |
| | MODE=INTYP +0.01 | |
| | STEP=STEF1 | 0076 |
| | STP=STEF1 | 1/2E/71 |
| | E1MAX=MAXERR | 0077 |
| | E1MIN=MAXERR/ERATIO | 0078 |
| | E2MAX=STFMAX | 0079 |
| | E2MIN=STEMIN | 0080 |
| | FACT=FACTF | 0081 |
| C | | 0082 |
| C | DETERMINE TRANSMITTER LOCATION IN COMPUTATIONAL COORDINATE SYST | 0083 |
| C | (GEOGRAPHIC COORDINATES IF DIPOLE FIELD IS USED) | 0084 |
| | RO=PARTIR*XMTRH | 0085 |
| | SP=SIN (E1AT) | 0086 |
| | CP=SIN (E1I2-PIAT) | 0087 |
| | SINDPH=SIN (LON-ELCN) | 0088 |
| | COSDPH=SIN (E1I2- (LON-ELCN)) | 0089 |
| | SI=SIN (IAT) | 0090 |
| | CI=SIN (E1I2-IAT) | 0091 |
| | ALPHA=ATAN2 (-SINDPH*CP, -COSDPH*CP*SI+SP*CI) | 0092 |
| | THO=ARCCOS (COSIIE*CP*CI+SP*SI) | |
| | PHO=ATAN2 (SINIPH*CI, COSDPH*SP*CI-CP*SI) | 0094 |
| C | THIS PORTION IS ADDED FOR THE HCMING FEATURE. IT READS THE DENSITYUOFI 3 | |
| C | PROFILE FROM ELECTX | UOFI 4 |
| | IF (W(38C).EQ.0.0) GC TO 555 | UOFI 5 |
| | IF (MOREW.EQ.1) GC TO 555 | UOFI 5A |

| | | |
|-----|---|---------|
| | MOREW=1 | UCFI 5B |
| | CALL FIECTX | UCFI 5C |
| C | | 0095 |
| C | LCCE ON FREQUENCY, AZIMUTH ANGLE, AND ELEVATION ANGLE | 0096 |
| 555 | NFFREQ=1 | UOFI 5D |
| | IF (FSTEP.NE.0.) NFREQ=(FFND-PBEG)/FSTEP+1.5 | 0098 |
| | NAZ=1 | 0099 |
| | IF (AZSTEP.NE.0.) NAZ=(AZEND-AZBEG)/AZSTEP+1.5 | 0100 |
| | NBETA=1 | 0101 |
| | IF (ELSTEP.NE.0.) NBETA=(ELEND-ELBEG)/ELSTEP+1.5 | 0102 |
| | DO 50 NF=1, NFREQ | 0103 |
| | F=FBEG+(NF-1)*FSTEP | 0104 |
| | IF (W(380).EQ.0.0) GC TO 55 | UCFI 6 |
| | CALL RCME | UOFI 7 |
| 55 | DO 45 J=1,NAZ | UCFI 9 |
| | IF (W(380).NE.0.0) GC TO 60 | UOFI 10 |
| | AZ1=AZBEG+(J-1)*AZSTEP | 0106 |
| 60 | AZA=AZ1*DEGS | UCFI 11 |
| | GAMMA=PI-AZ1+ALEHA | 0108 |
| | SGAMMA=SIN(GAMMA) | 0109 |
| | CGAMMA=SIN(PID2-GAMMA) | 0110 |
| | DO 40 I=1,NBETA | 0111 |
| | IF (W(380).NE.0.0) GC TO 70 | UCFI 12 |
| | EETA=ELBEG+(I-1)*ELSTEP | 0112 |
| 70 | CBETA=SIN(PID2-EETA) | UCFI 13 |
| C | THIS IS USED FOR THE HOMING FEATURE ONLY | UOFI 14 |
| | IF (W(380).EQ.0.0) GC TO 32 | UCFI 15 |
| | CALL ADJUST | UOFI 16 |
| | MPFT=0 | UOFI 17 |
| | GC TO 50 | UOFI 18 |
| 32 | R(1)=RC | UCFI 19 |
| | R(2)=TE0 | 0115 |
| | R(3)=PEG | 0116 |
| | R(4)=SIN(EETA) | 0117 |
| | R(5)=CEETA*CGAMMA | 0118 |
| | R(6)=CBETA*SGAMMA | 0119 |
| | T=0. | 0120 |
| | RSTART=1. | 0121 |
| | CALL RINDEX | 0122 |
| | EL=EETA*LEGS | 0123 |
| | IF (I.NE.1.AND.NPAGE.LT.3.AND.LINES.IE.17) GC TO 18 | 0124 |
| | NPAGE=0 | |
| | LINES=0 | |
| | PRINT 7, ID(1), ID, NDATE, MCLL, TYPE(NIYP), TYPE2(NTYP), KCLL | 0126 |
| | PRINT 17, F, AZA | 0127 |
| 17 | FORMAT (18X, 11HFREQUENCY =, F12.6, 37H MHZ, AZIMUTH ANGLE OF TRANSMISSION =, F12.6, 4H DEG) | 0128 |
| 18 | NPAGE=NPAGE+1 | 0129 |
| | PRINT 19, EL | 0130 |
| 19 | FORMAT (/31X, 33HELEVATION ANGLE OF TRANSMISSION =, F12.6, 4H DEG/) | 0131 |
| | IF (N2.GT.0.) GC TO 25 | 0132 |
| | CALL FIECTX | 0133 |
| | FN=SIGN(SQRT(ABS(X))*F, X) | 0134 |
| | PRINT 21, FN | 0135 |
| 21 | FORMAT (58HOTRANSMITTER IN EVANESCENT REGION, TRANSMISSION IMPESSIBLE/20H0PLASMA FREQUENCY =, E17.10) | 0136 |
| | GC TO 44 | 0137 |
| 25 | MU=SQRT(N2) | 0138 |
| | R(4)=MU*F(4) | 0139 |
| | R(5)=MU*F(5) | 0140 |
| | R(6)=MU*F(6) | 0141 |
| | | 0142 |
| | | 0143 |

```

DO 28 NN=7,N                                0144
28 R(NN)=C.                                  0145
CALL TRACE                                    0146
C SECND=KLOCK(0)*.001                        0148
C CSEC=TIME
C TIME=SECCND(A)
C DIFF=TIME-OSEC
C PRINT 30, DIFF
30 FORMAT(34X,26HTHIS RAY CALCULATION TCKK ,P8.3,4H SEC ) 0150
C
C NDPRINT IS THE OPTION FOR PRINTING ELEC. DENSITY AND DERIVATIVES
C
C IF(NPRINT.EQ.0) GC TO 370
C
C PRINT ELECTRON DENSITY PROFILE AND THE DERIVATIVES      151 KV 1
C USING APPLETON - HARTREE FORMULA                        151 KV 2
C
C PRINT 331
331 FORMAT (1H1, 48H ELECTRON DENSITY PROFILE AND ITS DERIVATIVES , 151 KV 5
1 40H COURTESY ARCCN CORE. K.VANGURI // , 151 KV 7
2 60H N = C * X, C = 12400*P**2 F IN MHZ, N = EL. PER CC , 151 KV 8
3 40H APPLETON-HARTREE FORMULA / , 151 KV 10
4 60H DN/ER = C * EXPR IN EL/CC/KM / 151 KV 11
5 60H DN/LTH = C * PXPTH * FAD IN EL/CC/DEG / 151 KV 12
6 60H DN/DPH = C * PXEPH * FAD IN EL/CC/DEG / 151 KV 13
7 6X,5HFANGE,5X,6HHEIGHT,1CX,1HN,9X,5HDN/DR,7X,6HDN/DTH,7X, 151 KV 14
8 6HDN/DPH,7X,4BSTEP/ 9X,2HKM,8X,2HKM,6X,5HEL/CC /) 151 KV 15
C
C DC 365 MJ = 1, MPPT 151 KV 25
C PRINT 345, VRANGE (MJ), VHT (MJ), 151 KV 26
2 VN (MJ), VNPF (MJ), VNPIH (MJ), VNPPH (MJ), MJ 151 KV 26
345 FORMAT (1X,F10.4,2X,F10.4,4(2X,F11.4),2X,I5) 151 KV 27
365 CONTINUE 151 KV 28
370 CONTINUE
C MPPT = 0 151 KV 29
C
C IF (NUIEST.EQ.1.AND.CNLY.NE.0..AND.IEOP.EQ.1) GC TO 44 0152
40 CONTINUE 0153
44 IF (FLT.NE.C.) CALL ENDPLT 0154
45 CONTINUE 0155
50 CONTINUE 0156
GO TO 1 0157
END 0158

```

| | | |
|----|---|--------|
| | SUBROUTINE TRACE | 0186 |
| | DIMENSION ROLD(12), DROLD(12) | 0187 |
| | COMMON /FK/ N, STEF, MCDE, E1MAX, E1MIN, E2MAX, E2MIN, FACT, RSTART | 0188 |
| | COMMON /FIN/ N2, PA2(B), TEOIAR, FEOLAR, SPACE, CCLL, FIELD | 0189 |
| | COMMON /TRAC/ GROUND, PERIGE, THERE, MINDIS, UNDER | 0190 |
| | COMMON /FIG/ NTYPE, RNEW, FNEW, SAYBEG, RAYSET, LINES, IHOP, NUTEST, APHT | 0191 |
| | COMMON /XX/ X, XPPE, XPPTH, XPFPH, EXPT, HMAX | 0192 |
| | COMMON /FIAGS/ IFLAG | |
| | COMMON B(12), I, STP, DRDT(12) /WW/ ID(10), WC, W(400) | 0193 |
| | EQUIVALENCE (FARTHR, W(19)), (HS, W(40)), (MAXSTP, W(93)), (SKIP, W(180)) | 0194 |
| | 1, (HCP, W(254)), (PLT, W(272)) | 0195 |
| | EQUIVALENCE (CNLY, W(371)), (STEP1, W(44)) | UOFI 1 |
| | REAL MAXSTP | 0196 |
| | COMPLEX N2, TEOIAR, RECLAR | 0197 |
| | LOGICAL SPACE, HCME, WASNT, PASSED, UNDERG, GROUND, PERIGE, THERE, | 0198 |
| | 1 MINDIS, UNDER | 0199 |
| | CNLY=C.C | UOFI 2 |
| | STEF=STEF1 | UOFI 3 |
| | STP=STEF1 | UOFI 4 |
| | NHCE=HCE+0.01 | 0200 |
| | MAX=MAXSTP+C.01 | 0201 |
| | NSKIP=SKIP+C.C1 | 0202 |
| | RSTART=1. | 0203 |
| | CALL HASEL | 0204 |
| | IF (IFLAG.NE.0) GO TO 50 | |
| | H=R(1)-FARTHR | 0205 |
| | HCMF=DRDT(1)*(H-HS).GF.0. | 0206 |
| | RAYEFG=1. | 0207 |
| | RAYSET=C. | 0208 |
| | CALL PRINTR (EHXMT)) | 0209 |
| | IF (PLT.NE.0.) CALL RAYPT | 0210 |
| | RAYEFG=C. | 0211 |
| C | | 0212 |
| C | LCCE ON NUMBER OF HOPS | 0213 |
| | DO 45 JHOP=1, NHCP | |
| | IHCE=JHCE | |
| | RAYSET=C. | 0215 |
| | NUTEST=C | 0216 |
| | APHT=HS | 0217 |
| | TEOLAR=FEOLAR | 0218 |
| | | 0219 |
| C | LCCE ON MAXIMUM NUMBER OF STEPS PER HOP | 0220 |
| C | DO 28 J=1, MAX | 0221 |
| | IF (ABS(F-HS).GT.AES(APHT-HS)) APHT=H | 0222 |
| | IF (.NOT.SPACE) GO TO 12 | 0223 |
| | CALL REACH | 0224 |
| | IF (IFLAG.NE.0) GO TO 50 | |
| | RSTART=1. | 0225 |
| | IF (IHCE*J.EQ.1) TPOLAR=RECLAR | 0226 |
| | IF (GROUND) GO TO 22 | 0227 |
| | IF (PERIGE) CALL ERINTR (EHPERIGE) | 0228 |
| | IF (THERE) GO TO 40 | 0229 |
| | IF (MINDIS) GO TO 32 | 0230 |
| | IF (PLT.NE.0.) CALL RAYPT | 0231 |
| 12 | DO 13 I=1, N | 0232 |
| | ROLD(I)=F(L) | 0233 |
| 13 | DROLD(L)=DRDT(L) | 0234 |
| | TCLD=I | 0235 |
| | CALL RKAM | 0236 |
| | IF (IFLAG.NE.0) GO TO 50 | |

| | | |
|---|--|------|
| | H=R(1)-EARTH | 0237 |
| | WASNT=.NCT.HCME | 0238 |
| | HCME=DEFT(1)*(H-HS).GE.0. | 0239 |
| | X=(DRDT(1)-DRCID(1))*(T-TCID) | 0240 |
| | SMT=0. | 0241 |
| | IF (X.NE.0.) SMT=0.5*(R(1)-ROLD(1)+0.5*X)**2/ABS(X) | 0242 |
| | UNDRGD=H.LT.0..CR.DRDT(1).GT.0..AND.DRCID(1).LT.0..AND.SMT.GT.H | 0243 |
| | PASSED=(H-HS)*(ROLD(1)-EARTH-HS).LT.0. | 0244 |
| | IF (PASSED.AND.(.NOT.UNDRGD.OR.HS.GT.0.)) GC TO 35 | 0245 |
| | IF (HS.EQ.ROLD(1)-EARTH.AND.DRCID(1)*DEFT(1).LT.0..ANI.HCME) | 0246 |
| | 1 GC TO 39 | 0247 |
| | IF (HCME.AND.WASNT.AND.(.NCT.UNDRGD.CR.HS.GT.0.)) GO TO 17 | 0248 |
| | IF (UNDRGD) GC TO 18 | 0249 |
| | GC TO 23 | 0250 |
| C | | 0251 |
| C | RAY MAY HAVE MADE A CLOSEST APPROACH | 0252 |
| | 17 IF (SMT.GT.ABS(H-HS)) GO TO 36 | 0253 |
| | NUTEST=4 | 0254 |
| | IF (R(5).NE.0..CR.R(6).NE.0.) CALL GRAZE(HS) | 0255 |
| | IF (UNDEF) GO TO 19 | 0256 |
| | IF (NUTEST.EQ.0.) GO TO 36 | 0257 |
| | GO TO 32 | 0258 |
| C | | 0259 |
| C | RAY WENT UNDERGROUND | 0260 |
| | 18 IF (DRDT(1).LT.0.) GC TO 21 | 0261 |
| | 19 UNDEF=.FALSE. | 0262 |
| C | CALL PRINTR(8HUNDERGR) | 0263 |
| | DO 20 L=1,N | 0264 |
| | R(L)=RCL(L) | 0265 |
| | 20 DRDT(L)=IRCLD(L) | 0266 |
| | T=TCLE | 0267 |
| | CALL RINDEX | 0268 |
| | IF (IFLAG.NE.0) GO TO 50 | |
| | 21 CALL EACK UP(0.) | 0269 |
| | 22 R(1)=EARTH | 0270 |
| | R(4)=AES(R(4)) | 0271 |
| | DRDT(1)=ABS(DRDT(1)) | 0272 |
| | RSTART=1. | 0273 |
| | CALL PRINTR(8HGENE FFF) | 0274 |
| | IF (HS.EQ.0.) GC TO 41 | 0275 |
| | H=0. | 0276 |
| | GO TO 25 | 0277 |
| C | | 0278 |
| | 23 IF (DRCID(1).LT.0..AND.DRDT(1).GT.0.) CALL PRINTR(8HPEFIGEE) | 0279 |
| | IF (DRCID(1).GT.0..AND.DRDT(1).LT.0.) CALL PRINTR(8HAPCGEE) | 0280 |
| | IF (DRCID(2)*DRDT(2).LT.0.) CALL PRINTR(8HMAX IAT) | 0281 |
| | IF (DRCID(3)*DRDT(3).LT.0.) CALL PRINTR(8HMAX LONG) | 0282 |
| | DO 24 I=4,6 | 0283 |
| | IF (ROLD(I)*R(I).LT.0.) CALL PRINTR(8HWAVE REV) | 0284 |
| | 24 CONTINUE | 0285 |
| | 25 IF (PLI.NE.0.) CALL RAYELT | 0286 |
| | IF (IFLAG.NE.0) GC TO 50 | |
| | IF (F.GT.HMAX.AND.H.GT.HS.AND.DRDT(1).GT.0.) GO TO 30 | 0287 |
| | IF (MCD(J,NSKIP).EQ.0) CALL PRINTR(8H) | 0288 |
| | 28 CONTINUE | 0289 |
| C | | 0290 |
| C | EXCEEDED MAXIMUM NUMBER OF STEPS | 0291 |
| | NUTEST=2 | 0292 |
| | RAYSET=1. | 0293 |
| | CALL PRINTR(8HMAX STEP) | 0294 |
| | RETURN | 0295 |

| | | | |
|---|----|-----------------------------|--------|
| C | | | 0296 |
| C | | RAY PENETRATED | 0297 |
| | 30 | NUTEST=1 | 0298 |
| | | RAYSET=1. | 0299 |
| | | ONLY=1.0 | UOFI 5 |
| | | CALL PFINTR(8HEENITFAT) | 0300 |
| | | RETURN | 0301 |
| C | | | 0302 |
| C | | RAY MADE A CLOSEST APPROACH | 0303 |
| | 32 | NUTEST=4 | 0304 |
| | | DRDI(1)=C. | 0305 |
| | | RAYSET=1. | 0306 |
| | | CALL PRINTR(8HMIN DIST) | 0307 |
| | | IF (FIT.NE.O.) CALL RAYPLT | 0308 |
| | | IF (IHCF.GE.NHCF) GO TO 45 | 0309 |
| | | IHCF=IHCF+1 | 0310 |
| | | CALL PFINTR (8HMIN DIST) | 0311 |
| | | GO TO 45 | 0312 |
| C | | | 0313 |
| C | | RAY CROSSED RECEIVER HEIGHT | 0314 |
| | 35 | IF (HCME) GO TO 39 | 0315 |
| | 36 | CONTINUE | 0316 |
| C | | CALL PRINTR(8HX RCVRHT) | 0317 |
| | | DO 37 I=1,N | 0318 |
| | | R(L)=RCID(L) | 0319 |
| | 37 | DRDI(L)=IROLD(L) | 0320 |
| | | T=TCID | 0321 |
| | | CALL RINDEX | 0322 |
| | | RSTART=1. | 0323 |
| | 39 | CALL EACK UP(HS) | 0324 |
| | 40 | R(1)=EARTH+HS | 0325 |
| | 41 | RAYSET=1. | 0326 |
| | | CALL PRINTR(8HRCVF) | 0327 |
| | | IF (FLT.NE.O.) CALL RAYPLT | 0328 |
| | 45 | HCME=.TFUF. | 0329 |
| | | RETURN | 0330 |
| | 50 | NUTEST=1 | |
| | | FYTEST=1.0 | |
| | | CALL PRINTR(8H CUT ICN) | |
| | | IFLAG=C | |
| | | RETURN | |
| | | END | 0331 |

| | | | |
|---|--|--|------|
| | | 167 | 0332 |
| | | SUBROUTINE BACK UP(HS) | |
| | | DIMENSION NWORD1(2),NWORD2(2),NWCRD(2) | |
| | | COMMON /FK/ NN,STEP,MCDE,F1MAX,F1MIN,E2MAX,E2MIN,FACT,RSTART | 0333 |
| | | COMMON /TRAC/ GRCOND,FRIGF,THEFF,MINDIS,UNCF | 0334 |
| | | COMMON /FIG/ KTYE,RNEW,ENFW,RAYBEG,RAYSET,IINES,IHOP,NUTEST,APHT | 0335 |
| | | COMMON F(12),I,STP,DRDT(12) /WW/ ID(10),WO,W(400) | 0336 |
| | | EQUIVALENCE (EAFTHR,W(19)),(INTYF,W(41)),(STEP1,W(44)) | 0337 |
| | | REAL INTYF | 0338 |
| | | LOGICAL UNDER | 0339 |
| | | DATA NWCRD1,NWCFD2/4HBACK,4EUF ,4HGFAZ,4HE / | |
| | | STPS=STF | |
| | | NWORD(1)=NWORD1(1) | |
| | | NWCRD(2)=NWCRD1(2) | |
| | | DO 1 I=1,10 | 0340 |
| | | IF (DRDT(1).EQ.C.) GO TO 5 | 0341 |
| | | STEP=- (F(1)-EARTH-PS)/DRDT(1) | 0342 |
| | | STP=SIGN(AMIN1(ABS(STP),ABS(STEP)),STEP) | |
| | | IF (ABS(F(1)-EARTH-HS).LT..5F-4.AN1.STEP.LI.1.) GO TO 5 | 0344 |
| C | | CALL PRINTF(8BECMING) | 0345 |
| | | MCDE=1 | 0346 |
| | | CALL FKAM | 0348 |
| 1 | | CONTINUE | |
| C | | | 0350 |
| | | ENTRY GRIZE | 0351 |
| | | STPS=STF | |
| | | NWORD(1)=NWORD2(1) | |
| | | NWORD(2)=NWORD2(2) | |
| | | DO 2 I=1,10 | 0352 |
| | | IF (DRDT(4).EQ.C.) GO TO 5 | 0353 |
| | | STEP=-F(4)/DRDT(4) | 0354 |
| | | STP=SIGN(AMIN1(ABS(STP),ABS(STEP)),STEP) | |
| | | IF (ABS(R(4)).LE.1.E-6.AN1.STEP.LI.1.) GO TO 5 | 0356 |
| C | | CALL PRINTF(8BECMING) | 0357 |
| | | ROLD=R(1) | 0358 |
| | | MCDE=1 | 0359 |
| | | CALL FKAM | 0361 |
| | | IF (R(1)-EARTH.LT.C.) GO TO 4 | 0363 |
| | | IF ((R(1)-EARTH-HS)*(ROLD-EARTH-HS).LI.C.) GO TO 3 | 0364 |
| 2 | | CONTINUE | 0365 |
| | | GO TO 5 | 0366 |
| 3 | | NUTEST=0 | 0367 |
| | | GO TO 5 | 0368 |
| 4 | | UNDEF=.TRUE. | 0369 |
| 5 | | MODE=INTYF+C.C1 | 0370 |
| | | STEP=STF1 | 0371 |
| | | STP=STF | |
| | | RSTART=1.0 | |
| | | CALL PRINTF(NWCFI) | |
| | | RETURN | 0372 |
| | | END | 0373 |

```

SUBROUTINE RKAM                                0888
C      NUMERICAL INTEGRATION OF DIFFERENTIAL EQUATIONS 0889
CCMCMCN/FLAGS/IFLAG
CCMCMCN /FK/ NN,SPACE,MODE,F1MAX,F1MIN,E2MAX,E2MIN,FACT,RSTART 0890
CCMCMCN Y(12),I,STEP,DYDT(12) /WW/ IC(1C),WC,W(400)
DIMENSION DELY(4,12),BET(4),XV(5),FV(4,12),YU(5,12) 0892
REAL*8 YU
EQUIVALENCE (EASTER,W(19)),(HMIN,W(390)),(HMAX,W(391))
DATA XMM/1.0E-6/
IF (RSTART.EQ.0.) GO TO 1000
LL=1 0894
MM=1 0895
IF (MODE.EQ.1) MM=4 0896
ALPHA=1 0897
EPM=0.0 0898
BET(1)=0.5 0899
BET(2)=0.5 0900
BET(3)=1.0 0901
BET(4)=0.0 0902
R=19.0/270.0 0903
XV(MM)=T 0904
IF (E1MIN.LE.C.) E1MIN=E1MAX/55. 0905
IF (FACT.LE.0.) FACT=0.5 0906
CALL HASEL 0907
IF (MODE.NE.1) STEF=SPACE 0908
IF (IFLAG.NE.0) GO TO 100 0909
DO 320 I=1,NN 0910
FV(MM,I)=DYDT(I) 0911
YU(MM,I)=Y(I) 0912
RSTART=0. 0913
GO TO 1001 0914
1000 IF (MODE.NE.1) GO TO 2000 0915
C 0916
C      RUNGE-KUTTA 0917
DR1=DYDT(1)*STEF
DR2=HMIN+EASTER-Y(1)
IF ((DR1.LT.DR2).AND.(DR2.LT.0.0)) STEP=DR2/DYDT(1)+XMM
DR3=HMAX+EARTH-Y(1)
IF ((DR1.GT.DR3).AND.(DR3.GT.0.0)) STEP=DR3/DYDT(1)+XMM
1001 DO 1034 K=1,4 0918
DC 1350 I=1,NN 0919
DELY(K,I)=STEP*FV(MM,I) 0920
Z=YU(MM,I) 0921
1350 Y(I)=Z+EFFI(K)*DELY(K,I) 0922
T=BET(K)*STEP+XV(MM) 0923
CALL HASEL 0924
IF (IFLAG.NE.0) GO TO 100 0925
DC 1034 I=1,NN 0926
FV(MM,I)=DYDT(I) 0927
DO 1039 I=1,NN 0928
DEL=(DELY(1,I)+2.0*DELY(2,I)+2.0*DELY(3,I)+DELY(4,I))/6.0 0929
YU(MM+1,I)=YU(MM,I)+DEL 0930
MM=MM+1 0931
XV(MM)=XV(MM-1)+STEF 0932
DO 1400 I=1,NN 0933
Y(I)=YU(MM,I) 0934
T=XV(MM) 0935
CALL HASEL 0936
IF (IFLAG.NE.0) GO TO 100
IF (MODE.EQ.1) GO TO 42

```

| | | |
|------|---|------|
| | DO 150 I=1,NN | 0937 |
| 150 | FV (FM,I)=DYDT(I) | 0938 |
| | IF (MM.LE.3) GC TC 1001 | 0939 |
| C | | 0940 |
| | ADAMS-MCULICN | 0941 |
| 2000 | DO 2048 J=1,NN | 0942 |
| | DEL=STEP*(55.*FV(4,I)-59.*FV(3,I)+37.*FV(2,I)-9.*FV(1,I))/24. | 0943 |
| | Y(I)=YU(4,I)+DEL | 0944 |
| 2048 | DELY(1,I)=Y(I) | 0945 |
| | T=XV(4)+STEP | 0946 |
| | CALI HASEI | 0947 |
| | IF (IFIAG.NE.0) GC TC 100 | |
| | XV(5)=T | 0948 |
| | DO 2051 I=1,NN | 0949 |
| | DEL=STEP*(9.*DYDT(I)+19.*FV(4,I)-5.*FV(3,I)+FV(2,I))/24. | 0950 |
| | YU(5,I)=YU(4,I)+DEL | 0951 |
| 2051 | Y(I)=YU(5,I) | 0952 |
| | CALI HASEI | 0953 |
| | IF (IFLAG.NE.0) GC TC 100 | |
| | IF (MCDE.LE.2) GO TO 42 | 0954 |
| C | | 0955 |
| | EFFCR ANALYSIS | 0956 |
| | SSE=0.C | 0957 |
| | DO 3033 I=1,NN | 0958 |
| | EPSIL=R*ABS(Y(I)-DELY(1,I)) | 0959 |
| | IF (MODE.EQ.3.AND.Y(I).NE.C.) EPSIL=EPSIL/AES(Y(I)) | 0960 |
| | IF (SSE.IT.EPSIL) SSE=EPSIL | 0961 |
| 3033 | CONTINUE | 0962 |
| | IF (E1MAX.GT.SSE) GC TC 3035 | 0963 |
| | IF (ABS(STEP).LE.E2MIN) GC TC 42 | 0964 |
| | LL=1 | 0965 |
| | MM=1 | 0966 |
| | STEF=STEF*FACT | 0967 |
| | GC TC 1001 | 0968 |
| 3035 | IF (LL.LE.1.OR.SSE.GE.E1MIN.CF.E2MAX.LE.ABS(STEP)) GO TO 42 | 0969 |
| | LL=2 | 0970 |
| | MM=3 | 0971 |
| | XV(2)=XV(3) | 0972 |
| | XV(3)=XV(5) | 0973 |
| | DO 5363 I=1,NN | 0974 |
| | FV(2,I)=FV(3,I) | 0975 |
| | FV(3,I)=IYDI(I) | 0976 |
| | YU(2,I)=YU(3,I) | 0977 |
| 5363 | YU(3,I)=YU(5,I) | 0978 |
| | STEF=2.C*STEF | 0979 |
| | GO TC 1001 | 0980 |
| C | | 0981 |
| | EXIT ROUTINE | 0982 |
| 42 | LL=2 | 0983 |
| | MM=4 | 0984 |
| | DO 12 K=1,3 | 0985 |
| | XV(K)=XV(K+1) | 0986 |
| | DO 12 I=1,NN | 0987 |
| | FV(K,I)=FV(K+1,I) | 0988 |
| 12 | YU(K,I)=YU(K+1,I) | 0989 |
| | XV(4)=XV(5) | 0990 |
| | DO 52 I=1,NN | 0991 |
| | FV(4,I)=IYDI(I) | 0992 |
| 52 | YU(4,I)=YU(5,I) | 0993 |
| | IF (MODE.LE.2) RETURN | 0994 |
| | E=AES(XV(4)-ALPHA) | 0995 |

IF (E.IE.EPM) GC TO 2000
EPM=F
100 FEIURN
END

C996

0997

C999

```

SUBROUTINE PRINTR(NWHY)
C          PRINTS A LINE EACH TIME IT IS CALLED
DIMENSION G(3,3),G1(3,3),A1(3),E1(3),C1(3)
1,TITLE1(10),TITLE2(10),UNIT(10)
DIMENSION NWHY(2),IPINK(2)
COMMON /CONST/ FI,PIT2,PII2,DEGS,RAI,DUM(3)
COMMON /BK/ N,STEP,MCDE,E1MAX,E1MIN,E2MAX,E2MIN,FACT,RSTART
COMMON /FIN/ N2,MUX,PN2(8),TECLAF(2),POLAR(2),SPACE,COIL,FIFID
COMMON /FLG/ NTYP,RNEWW,FNEWW,RAYBEG,RAYSET,LINES,IHOP,NOTEST,APHT
COMMON B(12),T /WW/ ID(10),WC,W(400)
COMMON /XX/ X,EXEF,EXETH,EXEPH,EXPT,EMAX
COMMON /VERN1/ VN(250),VNPF(250),VNPIH(250),VNPPH(250)
COMMON /VERN2/ VRANGE(250),VHT(250)
COMMON /NDOPT/ NPRINI,KOPT,MPRT
COMMON /EPLI/ SILEG
EQUIVALENCE (IBETA,B(2)),(PHI,R(3))
EQUIVALENCE (P,W(3)),(PICN,W(13)),(ICN,W(14)),(PLAT,W(15)),
1 (LAT,W(16)),(PITA,W(17)),(AZ1,W(18)),(FARTR,W(19)),(XMRH,W(20))
2,(P7,W(280)),(E8,W(281)),(E9,W(282))
EQUIVALENCE (RANGE,W(384)),(AZDEV,W(379)),(H,W(383))
EQUIVALENCE (S2IT,W(372)),(R3LI,W(373)),(AZA,W(374))
REAL N2,ICN,LAT,MCX
DATA A1,E1,C1,1FE,1HN,1HO,1HX,1HF,1HB,1FI,1HI,1HD/
DATA TITLE1(7),TITLE2(7),UNIT(7)/4H PH.,4H PATH,4H KM/
DATA TITLE1(8),TITLE2(8),UNIT(8)/4H ABS,4H CFEN,4H LB/
DATA TITLE1(9),TITLE2(9),UNIT(9)/4H DOE,4H PLER,4H C/S/
DATA IBLNK/2*4H
P7=C.0
P8=C.0
P9=C.0
IF (PNEWW.EQ.C.) GO TO 8
C          NEW W ARRAY -- REINITIALIZE
FNEWW=C.
SPL=SIN(FION-LOK)
CPL=SIN(FID2-(PICN-ICN))
SP=SIN(FIAT)
CP=SIN(FID2-PLAT)
SI=SIN(LAT)
CL=SIN(FIL2-LAT)
G(1,1)=CFI*SP*CI-CP*SI
G(1,2)=SEL*SP
G(1,3)=-SI*SP*CL-CL*CP
G(2,1)=-SPL*CL
G(2,2)=CFI
G(2,3)=SI*SPL
G(3,1)=CI*CP*CFI+SP*SI
G(3,2)=CF*SFI
G(3,3)=-SI*CP*CFI+SP*CI
DENM=G(1,1)*G(2,2)*G(3,3)+G(1,2)*G(3,1)*G(2,3)+G(2,1)*G(3,2)*G(1,3)
1)-G(2,2)*G(3,1)*G(1,3)-G(1,2)*G(2,1)*G(3,3)-G(1,1)*G(3,2)*G(2,3)
G1(1,1)=(G(2,2)*G(3,3)-G(3,2)*G(2,3))/DENM
G1(1,2)=(G(3,2)*G(1,3)-G(1,2)*G(3,3))/DENM
G1(1,3)=(G(1,2)*G(2,3)-G(2,2)*G(1,3))/DENM
G1(2,1)=(G(3,1)*G(2,3)-G(2,1)*G(3,3))/DENM
G1(2,2)=(G(1,1)*G(3,3)-G(3,1)*G(1,3))/DENM
G1(2,3)=(G(2,1)*G(1,3)-G(1,1)*G(2,3))/DENM
G1(3,1)=(G(2,1)*G(3,2)-G(3,1)*G(2,2))/DENM
G1(3,2)=(G(3,1)*G(1,2)-G(1,1)*G(3,2))/DENM
G1(3,3)=(G(1,1)*G(2,2)-G(2,1)*G(1,2))/DENM

```

0493
0494

0496

0497

0498

0499

0500

0501

501 KV 1

501 KV 2

501 KV 3

501 KV 5

501*KV 4

0502

0503

0504

0505

UOFI 1

0506

0512

0513

0514

0515

0516

0517

0518

0519

0520

0521

0522

0523

0524

0525

0526

0527

0528

0529

0530

0531

0532

0533

0534

0535

0536

0537

0538

0539

0540

0541

```

RC=FARTH*XMTRH                                0542
XR=F0*G(1,1)                                   0543
YR=F0*G(2,1)                                   0544
ZR=F0*G(3,1)                                   0545
COSTHR=G(3,1)                                  0546
SINTHR=SIN(ARCCS(COSTHR))                     0547
PHIF=ATAN2(YR,XR)                              0548
ALFH=ATAN2(G(3,2),G(3,3))                     0549
IF (F8.NE.0.) PUNCH 5, F1(NTYP),ID           0550
5  FORMAT (F1,9A8,A7)                          0551
IF (F9.NE.0.) PUNCH 5, C1(NTYP),ID           0552
IF (F7.NE.0.) PUNCH 6, A1(NTYP),ID           0553
6  FORMAT (A1,1X,9A8,A6)                      0554
C
8  IF (RAYEFG.EQ.0.) GO TO 12                 0556
NN=PING(N,9)                                   0557
PRINT 10, (TITLE1(NR),TITLE2(NR),NR=7,NN)    0558
10 FORMAT (61X,7HAZIMUTH/60X,9HDEVIATION,7X,9HELEVATION/20X,15HHEIGHT
1  RANGE,3X,3HESI,3X, 11HCOLAT ICNG,2(5X,12HXMTF LCCAL), 560 KV
2  2X,12HDECLARIZATION,2X,8H GR.PATH,4A4)    561 KV
PRINT 11, (UNIT(NR),NR=7,NN)                 0562
11 FORMAT (16X,2(7X,2HKM),4X,
2  3HDEG, 6(5X,3HDEG),3X,4HREAL,4X,4HIMAG, 563 KV
1  5X,2HKM,1X,2(A6,2X))                     564 KV
12 V=0.
IF (N2.NE.0.) V=(R(4)**2+R(5)**2+R(6)**2)/N2-1. 0566
H=F(1)-FARTH                                  0567
SINTH=SIN(THETA)                              0568
COSTH=SIN(PID2-THETA)                         0569
XP=F(1)*SINTH*SIN(PID2-PHI)-XR               0570
YP=F(1)*SINTH*SIN(PHI)-YR                   0571
ZP=F(1)*COSTH-ZF                              0572
EPS=XP*G1(1,1)+YP*G1(1,2)+ZP*G1(1,3)        0573
ETA=XP*G1(2,1)+YP*G1(2,2)+ZP*G1(2,3)        0574
ZETA=XP*G1(3,1)+YP*G1(3,2)+ZP*G1(3,3)       0575
RCE2 = ETA**2 + ZETA**2                      0576
RCE=SQRT(RCE2)                               0577
RANGE=FC*ATAN2(RCE,F0+EPS)                    UOPI 2
ANGDEG=ATAN2(R(4),SQRT(R(5)**2+R(6)**2))*DEGS 0579
SR=SQRT(RCE2+EPS**2)                         0580
C
C  CHANGES MADE BY ARCCN CORP. BY K.VANGURI 580 KV 1
C
C  STORE THE ELECTRON DENSITY PROFILE AND THE DERIVATIVES 580 KV 2
C  CALCULATE N THE ELECTRON DENSITY IN APLETICN - HARTREE FORMULA 580 KV 3
C  N = 12400*F**2 * X ELECTRONS/CUBIC CM. 580 KV 4
C  IN/CR - EI/CC/KM.
C  IN/ETH - EI/CC/LEG
C  F = FREQUENCY IN MHZ 580 KV 5
C  IN/LEH - EI/CC/LEG
C  DERIVATIVES OF EI. DEN. W.R.T. R,TH,PH ARE COMPUTED BY
C  MULTIPLYING PXP, PXPTH, PXPEH WITH THE CONSTANT C.
C
C  C = 12400.0 * F ** 2 580 KV10
C  MPRT = MERT + 1 580 KV11
C  CALL ELECTX 580 KV12
C  VN(MERT) = 12400.C*F**2 *X 580 KV13
C  VNEP(MERT) = C * PXP 580 KV14
C  VNPTH(MERT) = C * PXPTH * RAD 580 KV15
C  VNEPH(MERT) = C * PXPEH * RAD 580 KV16
C  VRANGE(MERT) = RANGE 580 KV17

```

```

VHT(MPFT) = H 580 KV18
IF(KOFT.EQ.O.AND.NWHY(1).EQ.IBINK(1).AND.NWHY(2).EQ.IBINK(2)) RETU
1RN
C PRINT CCIATITUDE AND LONGITUDE 580 KV21
C R2LT IS COLATITUDE AND R3LT IS LONGITUDE 580 KV22
R2LT = F(2) * DEGS 580 KV23
R3LT = F(3) * DEGS 580 KV24
C
C COMPUTE SIDEQ - ANGLE BETWEEN WAVE NORMAL AND THE MAGNETIC FIELD 580KV27
C ** CALL MAGY FOR OPTICNS 1 + 3. ** CALL TRUPLD FOR OPTION 2. ** 583 V28
CALL TRUPLD OPTION 2
C
IF (SR.GE.1.E-2) GO TO 20 0581
PRINT 15, V,NWHY,H,RANGE, SIDEQ,R2LT,R3LT, 582 KV 1
1 ANGDEG,POLAR,T, (R(I),I=7,NN) 582 KV 2
15 FORMAT (1X,E8.1,1X,2A4,F8.2,1X,F8.2,3F7.1, 23X, 6F8.2,F6.1)
GO TO 40 0584
20 ANGE=ATAN2(FPS,FCF) 0585
EL=ANGE*DEGS 0586
IF (RCF.GE.1.E-2) GO TO 30 0587
PRINT 25, V,NWHY,H,RANGE, SIDEQ,R2LT,R3LT,
1 EL,ANGLEG,POLAR,T, (R(I),I=7,NN) 588 KV 2
25 FCRMAT (1X,E8.1,1X,2A4,F8.2,1X,F8.2,3F7.1, 15X, 7F8.2,F6.1)
GO TO 40 0590
30 ANGA=ATAN2(ETA,2ETA) 0591
ANA=ANGA-PLPH 0592
SINANA=SIN(ANA) 0593
SINPHI=SINANA*SINTHF/SINTH 0594
COSPHI=-SIN(PII2-ANA)*SIN(FID2-(PHI-PHIR))+SINANA*SIN(PHI-PHIR)* 0595
1 COSTHF 0596
AZDEV=180.-AMCE(540.-(AZ1-ANGA)*DEGS,360.) 0597
IF (R(5).NE.O..CR.R(6).NE.C.) GO TO 34 0598
PRINT 33, V,NWHY,H,RANGE, SIDEQ,R2LT,R3LT,
1 AZDEV,EL,ANGLEG,POLAR,T, (R(I),I=7,NN) 599 KV 2
33 FORMAT (1X,E8.1,1X,2A4,F8.2,1X,F8.2,3F7.1,F8.2,7X, 7F8.2,F6.1)
GO TO 40 0601
34 AZA=180.-AMCE(540.-(ATAN2(SINPHI,COSPHI)-ATAN2(F(6),R(5)))*DEGS,
1 360.) 0602
PRINT 35, V,NWHY,H,RANGE, SIDEQ,R2LT,R3LT, 0603
1 AZDEV,AZA,EL,ANGLEG,POLAR,T, (R(I),I=7,NN) 604 KV 2
35 FCRMAT (1X,E8.1,1X,2A4,F8.2,1X,F8.2,4F7.1, 8F8.2,F6.1)
C
C 40 LINES=LINES+1 0606
IF (N.LE.9) GO TO 45 0607
PRINT 42, (R(I),I=10,N) 0608
42 FCRMAT (110X,3F8.2) 609 KV
LINES=LINES+1 0610
45 IF (RAYSH.EQ.O.) RETURN 0611
ELA=BETA*DEGS 0612
IF (H.LE.1.) ANGDEG=ABS(ANGLEG) 0613
C 0614
C 3-D RAYSETS 0615
IF (P8.EQ.O.) GO TO 55 0616
TLCN=LCN*DEGS 0617
IF (TICN.LT.O.) TICN=TLCN+360. 0618
TLAT=LAT*DEGS 0619
IF (TIAT.LT.O.) TIAT=TLAT+360. 0620
AZ=ANGA*DEGS 0621
IF (AZDEV.LE.-100.) AZDEV=AZDEV+360. 0622
IF (AZA.LE.-100.) AZA=AZA+360. 0623

```

| | | |
|---|--|------|
| | PUNCH 50, B1(NTYP), ID(1), XMIER, TLAT, TICN, H, RANGE, AZ, F, IHOP, | 0624 |
| | 1 AZDEV, A2A, FLA, ANGDEG, TPCIPR, ECIAR, NUTEST | 0625 |
| | 50 FORMAT (A1, A3, 2PF6.0, 1P2F4.0, 2PF6.0, 1PF6.0, F5.0, 3PF7.0, I1, 2P4F5.0, | 0626 |
| | 1 1F4F4.C, I1) | 0627 |
| C | | 0628 |
| C | SUFF. FAYSFIS | 0629 |
| | 55 IF (P9.NE.0.) PUNCH 60, C1(NTYP), ID(1), F, IHCP, ELA, (R(I), I=7, 10), | 0630 |
| | 1 T, NUTEST | 0631 |
| | 60 FCRMAT (A1, A3, 3PF7.0, I1, 2PF5.0, CP5P12.4, I3) | 0632 |
| C | | 0633 |
| C | 2-D FAYSFIS | 0634 |
| | IF (NUTEST.NE.0) APET=H | 0635 |
| | IF (P7.NE.0.) PUNCH 70, A1(NTYP), ID(1), F, IHCP, ELA, ANGDEG, T, R(7), | 0636 |
| | 1 RANGE, AEHT, NUTEST | 0637 |
| | 70 FORMAT (A1, 1X, A3, 3PF7.0, I2, 3PF10.5, F9.5, 3F11.4, F12.5, 1X, I1) | 0638 |
| | RETURN | 0639 |
| | END | 0640 |

```

SUBFCUTINE ADJUST
C   A SUBROUTINE TO ADJUST THE ELEVATION ANGLE BETA
C   AZIMUTH TOLERANCE IS SPECIFIED IN KM THEN CONVERTED TO RADIANS
DIMENSION A1(3,3),B1(3),C1(3),DUM1(9)
COMMON/CCNST/ FI,FIT2,FIL2,DEGS,EAD,DUM(3)
COMMON Y(12),T /WW/ ID(10),W0,W(400)
COMMON/DENSC/ DENS(52),HEIT(52),ELRANJ(91,3,2),APROX(8,2,2),FRATIO
1,NMAX,NSTART,JFIAG,NSCL,LEMIN(21),JJJM1
COMMON/RK/ N,STEP,MCDE,DUMY(5),FSTART
COMMON/RIN/ N2,MUX,EN2(8),POLAR(4),SPACE,CCIL,FIELD
COMMON /NDOPT/ NPFINT,KCET,MFFT
REAL N2,MUX,MU
EQUIVALENCE (GRANGF,W(385)),(CRANGE,W(384)),(BETA,W(17)),
1(CCNTRI,W(386)),(TOLERR,W(387)),(AZ1,W(18)),(RC,W(375)),
2(ALPHA,W(376)),(THO,W(377)),(PHC,W(378)),(AZIEV,W(379)),
3(AZA,W(374)),(BETAT,W(389)),(H,W(383)),(P2IT,W(372)),
4(RBIT,W(373)),(FASTER,W(19))
DATA A1(1,1),A1(2,1),A1(3,1)/3*1.0/
C   SET UP THE MAXIMUM HEIGHT FOR GROUND - SATELLITE CASE
IF(NSOL.EC.0) RETURN
NHCE=W(254)+0.1
KNTRI=CCNTRL
RADIUS=EARTH+R(4C)
IF(CRANGF.NE.C.C) GO TO 806
AZTCL=TCIERE/RADIUS
GO TO 807
806 AZTCL=TCIERE/(RADIUS*SIN(CRANGF/RADIUS))
807 DAZTCL=AZTCL*IEGS
PRINT 808,TOLERR,DAZTCL
808 FORMAT(1X,16CRANGF TOLERANCE=,F12.6,3H KM,3X,18HAZIMUTH TOLFRANCE=
1,F12.6,8H DEGREES)
AZ2=AZ1
DC 800 ILL=1,NSCL
INCR=0
CONT=0.0
PRINT 80E
805 FORMAT(1E1)
IF(W(38C).NE.1.C) GO TO 249
PRINT 252,LIL
252 FORMAT(2X,26HEADING FOR SCUTION NUMEEF,I3)
C   SET UP AN INITIAL SLOPE BASED UPON PLANE GEOMETRY CONSIDERATION
C   FOR SATELLITE TO GROUND OR GROUND TO SATELLITE CASES
249 DINCR=-GRANGF/(SIN(ARCOX(ILL,1,1))*CCS(APROX(LIL,1,1)))
IF(W(38C).NE.1.C) GO TO 253
DINCR=C.C
INDEX=ARCOX(ILL,2,1)
IO 254 I=1,NHCE
DINCR=DINCR+(FIFANJ(INDEX,2,I)-FIFANJ(INDEX-1,2,I))/
1(ELFANJ(INDEX,1,I)-ELFANJ(INDEX-1,1,I))
254 CONTINUE
253 CCUNT=C.C
BETA=ARCOX(LIL,1,1)
IF(W(38C).NE.1.C.CR.NHOE.NE.1) GO TO 300
DO 260 I=1,JJJM1
IF(BETA.GT.DBMIN(I+1)) GO TO 260
JJK=I
LEFT=LEMIN(JJK)
BRIGHT=LEMIN(JJK+1)
GO TO 300
260 CONTINUE

```

```

C      ERRCR IN COMPUTING HCMING ANGLE
      PRINT 261
261    FORMAT(2X,39H***ERRCR IN COMPUTING HCMING ANGLE ***)
      GO TO 800
300    CALL RAYINI(AZ1,BETA)
      EL=EETA*LEGS
      AZ3=AZ1*LEGS
      PRINT 55,EL,AZ3
      IF(W(380).NE.1.C.CR.NHCP.NE.1) GO TO 301
      IF(BETA.II.BLEFT.CR.BETA.GT.BRIGHT) GO TO 700
301    CALL TRACE
      PRINT 75,R2LT,R3LT,AZDEV,AZA
75     FORMAT(1X,10PRAY COIAT=,F12.5,2X,9HFAY ICNG=,F12.5,2X,
114HF.AZDEV AT T.=,F12.5,2X,18HICCAL AZDEV AT F.=,F12.5)
      IF(W(394).NE.C.C) CRANGE=1
      IF(ABS(GRANGE-CRANGE).LE.TCIEFE) GO TO 500
      IF(H.GT.(W(40)+0.1).CR.H.IT.(W(40)-0.1)) GO TO 780
      MPRT=0
      E1(1)=CRANGE
      A1(1,2)=EETA
      A1(1,3)=A1(1,2)**2
      IF(INCR.EQ.0) GO TO 310
      DINCR= (E1(1)-E1(2))/(A1(1,2)-A1(2,2))
C      INTERPOLATE LINEARLY IF POSSIBLE
      IF(E1(1).LT.GRANGE.AND.B1(2).LT.GRANGE) GO TO 310
      IF(E1(1).GT.GRANGE.AND.E1(2).GT.GRANGE) GO TO 310
      E=(E1(1)-B1(2))/(A1(1,2)-A1(2,2))
      A=B1(1)-E*A1(1,2)
      BETA=(GRANGE-A)/B
      GO TO 590
C      INCREMENT OR DECREMENT THE APPROXIMATE ELEVATION UTILIZING THE
C      SLOPE OF THE I-E CURVE
310    DIFFR=GRANGE-CRANGE
      EETA=EETA+DIFFR/DINCR
      IF(BETA.GT.0.0.CR.W(380).NE.1.0) GO TO 312
      IF(CCNT.EQ.1.0) GO TO 2100
      EETA=0.0
      CCNT=1.C
312    CALL RAYINI(AZ1,BETA)
      EL=EETA*LEGS
      AZ3=AZ1*LEGS
      PRINT 55,EL,AZ3
      IF(W(380).NE.1.C.CR.NHCP.NE.1) GO TO 311
      IF(BETA.II.BLEFT.CR.BETA.GT.BRIGHT) GO TO 700
311    CALL TRACE
      PRINT 75,R2IT,R3IT,AZDEV,AZA
      IF(W(394).NE.C.C) CRANGE=1
      IF(ABS(GRANGE-CRANGE).LE.TCIEFE) GO TO 500
      IF(H.GT.(W(40)+0.1).CR.H.IT.(W(40)-0.1)) GO TO 780
      MPRT=0
      E1(2)=CRANGE
      A1(2,2)=EETA
      A1(2,3)=A1(2,2)**2
      DINCR= (E1(1)-E1(2))/(A1(1,2)-A1(2,2))
      INCF=INCF+1
C      IF THE GIVEN RANGE IS BETWEEN THE FIRST AND SECOND RANGE THUS
C      COMPUTED , INTERPOLATE LINEARLY ON EETA.
      IF(E1(1).LT.GRANGE.AND.E1(2).LT.GRANGE) GO TO 580
      IF(E1(1).GT.GRANGE.AND.B1(2).GT.GRANGE) GO TO 580
C      INTERPOLATE USING RANGE=A+E*BETA
      E=(E1(1)-B1(2))/(A1(1,2)-A1(2,2))

```

```

A=E1(1)-E*A1(1,2)
BETA=(GRANGE-A)/B
GO TO 590
C INCREMENT OR DECREMENT THE APPROXIMATE ELEVATION UTILIZING THE
C SLOPE OF THE D-B CURVE
580 DIFFR=GRANGE-CRANGE
BETA=BETA+DIFFR/DINCR
IF(BETA.GT.0.0.CR.W(390).NE.1.0) GO TO 581
IF(CCNT.EQ.1.0) GO TO 2100
BETA=0.0
CONT=1.0
581 IF(INCR.GT.KOMBI) GO TO 2000
GO TO 300
590 CALL RAYINT(AZ1,BETA)
EL=BETA*LEGS
AZ3=AZ1*LEGS
PRINT 55,EL,AZ3
IF(W(380).NE.1.0.CF.NHOF.NE.1) GO TO 591
IF(BETA.IT.BLEFT.CR.BETA.GT.BRIGHT) GO TO 700
591 CALL TRACE
PRINT 75,R2LT,R3LT,AZDEV,AZA
IF(W(394).NE.C.0) CRANGE=T
IF(ABS(GRANGE-CRANGE).IE.TCLEFE) GO TO 500
IF(E.GT.(W(40)+0.1).CR.H.IT.(W(40)-0.1)) GO TO 780
MPRT=0
E1(3)=CRANGE
A1(3,2)=BETA
A1(3,3)=A1(3,2)**2
CALL EQSCLV(B1,A1,3,3,1,C1,DUM1,1.0F-8,1FR)
C USE QUADRATIC FORMULA TO COMPUTE BETA
C C1(3)*BETA**2+C1(2)*BETA+C1(1)-GRANGE=0
ARG=C1(2)**2-4.C*C1(3)*(C1(1)-GRANGE)
IF(ARG) 200,210,210
C THE ARGUMENT IS NEGATIVE , NO SOLUTION
200 IF(W(380).EQ.2.0) GO TO 611
PRINT 2010,III
PRINT 610
GO TO 1000
611 PRINT 2011
PRINT 612
612 FORMAT(6X,53HDISCONTINUITY IN THE RAY TRACE RANGE-ELEVATION CURVE
1 )
GO TO 1000
210 BETAP=(-C1(2)+SQRT(ARG))/(2.0*C1(3))
BETAM=(-C1(2)-SQRT(ARG))/(2.0*C1(3))
C FIND THE CLOSEST RANGE
C FIND THE CLOSEST ANGLE TO THE GIVEN RANGE
DIFF1=ABS(GRANGE-E1(1))
DIFF2=ABS(GRANGE-E1(2))
DIFF3=ABS(GRANGE-E1(3))
IF(DIFF1.LT.DIFF2.AND.DIFF1.LT.DIFF3) ANG=A1(1,2)
IF(DIFF2.LT.DIFF1.AND.DIFF2.LT.DIFF3) ANG=A1(2,2)
IF(DIFF3.LT.DIFF1.AND.DIFF3.LT.DIFF2) ANG=A1(3,2)
BETA=BETAM
IF(ABS(ANG-BETAP).LT.ABS(ANG-BETAM)) BETA=BETAP
650 EL=BETA*LEGS
AZ3=AZ1*LEGS
PRINT 55,EL,AZ3
55 FORMAT(/ 5X,33HELEVATION ANGLE OF TRANSMISSION =,F12.6,4H DEG,5X,3
11HAZIMUTE ANGLE OF TRANSMISSION =,F12.6,4H DEG/)
100 COUNT=CCNT+1.0

```

AD-A038 299

ILLINOIS UNIV AT URBANA-CHAMPAIGN DEPT OF ELECTRICAL --ETC F/6 17/2.1
TECHNIQUES OF DETERMINING IONOSPHERIC STRUCTURE FROM OBLIQUE RA--ETC(U)
DEC 76 N N RAO, K C YEH, M Y YOUAKIM F19628-75-C-0088

UNCLASSIFIED

UILU-ENG-76-2559

RADC-TR-76-401

NL

3 OF 3
AD
A038 299

END

DATE
FILMED

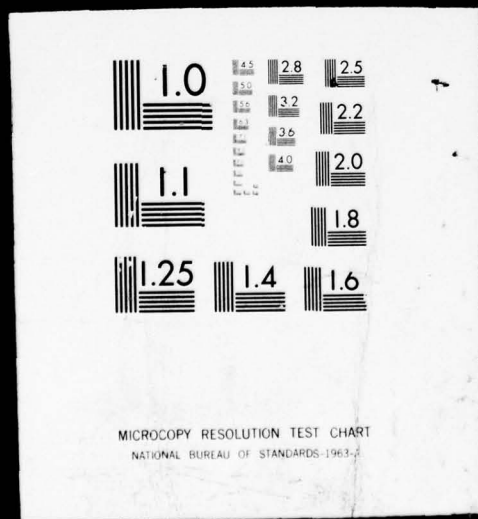
5-77

REFILED

3 OF 3

AD

A038 299



```

IF(CCUNT.GT.CCNTFI) GO TO 2000
CALL RAYINT(AZ1,EETA)
IF(W(38C).NE.1.C.CR.NHCF.NE.1) GO TO 101
IF(EETA.IT.BLEFT.CR.EETA.GT.BRIGHT) GO TO 700
101 CALL TFACE
PRINT 75,R2LT,R3LT,AZEFV,AZA
IF(W(394).NE.C.C) CRANGE=1
C USE THE L-F CURVE TO ADJUST EETA
DIFFR=GRANGE-CRANGE
IF(ABS(DIFFR).IF.TOLERE) GO TO 500
IF(F.GT.(W(40)+C.1).CR.H.IT.(W(40)-0.1)) GO TO 780
MPRT=0
C SELECT THE CLOSEST RANGE TO THE GIVEN RANGE
DIFF1=GRANGE-B1(1)
DIFF2=GRANGE-B1(2)
DIFF3=GRANGE-B1(3)
IF(ABS(DIFF1)-ABS(DIFF2)) 10,20,20
10 IF(ABS(DIFF2)-ABS(DIFF3)) 50,60,60
C REPLACE THE SECCND RANGE AND ELEVATION ANGLE
60 B1(2)=CRANGE
A1(2,2)=EETA
A1(2,3)=A1(2,2)**2
GO TO 150
20 IF(ABS(DIFF1)-ABS(DIFF3)) 50,30,30
C REPLACE THE FIRST RANGE AND ELEVATION ANGLE
30 B1(1)=CRANGE
A1(1,2)=EETA
A1(1,3)=A1(1,2)**2
GO TO 150
C REPLACE THE THIRD RANGE AND ELEVATION ANGLE
50 B1(3)=CRANGE
A1(3,2)=EETA
A1(3,3)=A1(3,2)**2
150 CALL EQSCIV(B1,A1,3,3,1,C1,DUM1,1.0E-8,IER)
C USE QUADRATIC TO COMPUTE BETA
ARG=C1(2)**2-4.0*C1(3)*(C1(1)-GRANGE)
IF(ARG) 160,170,170
C THE ARGUMENT IS NEGATIVE , THERE IS NO SOLUTION
160 IF(W(38C).EQ.2.0) GO TO 162
PRINT 2010,III
PRINT 610
GO TO 1000
162 PRINT 2011
PRINT 612
GO TO 1000
170 BETAP=(-C1(2)+SQRT(ARG))/(2.0*C1(3))
EETAP=(-C1(2)-SQRT(ARG))/(2.0*C1(3))
C FIND THE CLOSEST RANGE
C FIND THE CLOSEST ANGLE TO THE GIVEN RANGE
DIFF1=ABS(GRANGE-B1(1))
DIFF2=ABS(GRANGE-B1(2))
DIFF3=ABS(GRANGE-B1(3))
IF(DIFF1.LT.DIFF2.AND.DIFF1.LT.DIFF3) ANG=A1(1,2)
IF(DIFF2.LT.DIFF1.AND.DIFF2.LT.DIFF3) ANG=A1(2,2)
IF(DIFF3.LT.DIFF1.AND.DIFF3.LT.DIFF2) ANG=A1(3,2)
EETA=EETAP
IF(ABS(ANG-BETA1).LT.ABS(ANG-BETAP)) BETA=EETAP
180 EL=EETA*IEGS
AZ3=AZ1*IEGS
PRINT 55,EL,AZ3
GO TO 1000

```

```

C      CORRECT FOR AZIMUTHAL DEVIATION
500    IF (H.IF. (W(40)+C.1) .AND.H.GE. (W(40)-C.1)) GO TO 502
      GO TO 780
502    AZ4=AZ1-AZDEV*RAD
      IF (ABS(AZ4-AZ2) .LE. AZTOL) GO TO 3000
      INCF=0
      MPRT=0
      AZ5=AZ1+AZDEV*RAD
      AZ1=AZ5
      IF (ABS(AZ5-AZ2) .GT. ABS(AZ4-AZ2)) AZ1=AZ4
      COUNT=0.0
      GO TO 3000
2000   IF (W(380) .EQ. 1.0) PRINT 2010, III
      IF (W(380) .EQ. 2.0) PRINT 2011
2010   FORMAT(/// 2X, 62H*** HOMING CANNOT BE ACHIEVED FOR APPROXIMATE SOL
10UTION NUMBER , I3)
2011   FORMAT(/// 2X, 29H*** HOMING CANNOT BE ACHIEVED )
      PRINT 2020, CCNTFI
2020   FORMAT(6X, 35HIXCEEDING NUMBER OF SPECIFIED TRIES , F5.0)
      GO TO 1000
2100   PRINT 2010, III
      PRINT 2110
2110   FORMAT(6X, 49HTHE RANGE IS HIGHER THAN THE ZERO ELEVATION RANGE )
      GO TO 1000
C      CHECK IF THE DIAGNOSTIC IS FOR A HIGH RAY
700    JJKD2=JJK/2
      JJKR=JJK-JJKD2*2
      IF (JJKR .FC. 0) GO TO 750
C      IT IS NOT A HIGH RAY
      PRINT 2010, III
      PRINT 610
610    FORMAT(6X, 86HDISCONTINUITY IN THE RAY TRACE RANGE-BETA CURVE OR R
1ANGE TOO CLOSE TO THE SKID DISTANCE)
      GO TO 1000
C      IT IS A HIGH ANGLE RAY
750    PRINT 2010, III
      PRINT 755
755    FORMAT(6X, 14HHIGH ANGLE RAY )
      GO TO 1000
780    IF (W(380) .EQ. 1.0) PRINT 2010, III
      IF (W(380) .EQ. 2.0) PRINT 2011
      PRINT 750
790    FORMAT(6X, 52HRAY MISSED THE EARTH OF CONTACT BEACH RECEIVER HEIGHT)
      GO TO 1000
C      WE FOUND AN EXACT SOLUTION
3000   IF (W(380) .EQ. 1.0) PRINT 3010, III
      IF (W(380) .EQ. 2.0) PRINT 3011
3010   FORMAT(/// 2X, 39H*** HOMING ACHIEVED FOR SOLUTION NUMBER , I3)
3011   FORMAT(/// 2X, 19H*** HOMING ACHIEVED )
      PRINT 3020, EI
3020   FORMAT(6X, 11HELEVATION =, F12.6, 2X, 7HDEGREES)
      PRINT 3030, AZ3
3030   FORMAT(6X, 10HAZIMUTH =, F12.6, 2X, 7HDEGREES )
      IF (W(394) .EQ. 0.0) GO TO 3034
      PRINT 3031, CRANGE
3031   FORMAT(6X, 21HHCMEI IN GROUP PATH =, F12.2, 2X, 2HRM)
      GO TO 3039
3034   PRINT 3035, CRANGE
3035   FORMAT(6X, 16HHCMEI IN RANGE =, F12.2, 2X, 2HRM)
      IF (W(380) .EQ. 1.0) GO TO 3039
      PRINT 3036, W(20)

```

```
3036 FORMAT (6X,20HTRANSMITTER HEIGHT =, F9.2,2X,2HKM )  
      PRINT 3037,W(40)  
3037 FORMAT (6X,17HRECEIVER HEIGHT =, F9.2,2X,2HKM )  
3039 PRINT 3040,R211  
3040 FORMAT (6X,33HCOORD IN GEOMAGNETIC LATITUDE =, F12.5,2X,7HDEGREES  
1)  
      PRINT 3050,R311  
3050 FORMAT (6X,32HCOORD IN GEOMAGNETIC LONGITUDE =, F12.5,2X,7HDEGREES)  
1000 W(18)=A22  
800  CONTINUE  
      RETURN  
      END
```

```

SUBROUTINE HCMFS
COMMON/CCNST/ EI,PII2,PID2,DEGS,RAD,DUM(3)
COMMON/DENSC/ DENS(52),HEIT(52),ELRANJ(51,3,2),APROX(8,2,2),FRATIO
1,NMAX,NSTART,JFIAG,NSCL,LEMEN(21),JJJM1
COMMON Y(6) /WW/ ID(10),WC,W(400)
COMMON/DENX/ FH(19,52,5),THETA(19),FGI(52),FHI(5),FRES(4),HL
COMMON/EG2/ LATX,LCNMX,IHTMX
EQUIVALENCE(EAFIHR,W(19)),(TLCN,W(14)),(RLCN,W(381)),(FIAT,W(16)),
1(RLAT,W(382)),(BETA,W(17)),(TFREQ,W(3)),(AZ1,W(18)),(XMIRH,W(20))
EQUIVALENCE(TFANGE,W(385)),(BETAT,W(386)),(PHC,W(378)),(THO,W(377
1))
EQUIVALENCE(PLCN,W(13)),(FIAT,W(15)),(HCF,W(254))
C
SET NMAX TO CNP
NMAX=1
SP=SIN(FIAT)
CP=SIN(FII2-PLAT)
C
TRANSFORM THE RECEIVER COORDINATES TO GEOMAGNETIC COORDINATES
SINDPH=SIN(RLCN-PLCN)
COSDPH=SIN(PID2-(RLCN-FLCN))
SI=SIN(FIAT)
CL=SIN(FII2-RLAT)
GRICN=ATAN2(SINDPH*CL,COSDPH*SP*CL-CP*SI)
GRLAT=ARCCOS(COSDPH*CP*CL+SP*SI)
GRICN=GRICN*DEGS
GRIAT=GFIAT*DEGS
ANGL=ABS(TLCN-RLCN)
ANGT=FII2-TIAT
ANGR=PID2-RLAT
C
USE THE COSINE LAW TO FIND THE ANGLE SUBTENDED AT THE EARTH CENTER
COSIHE=CGS(ANGT)*COS(ANGR)+SIN(ANGT)*SIN(ANGR)*COS(ANGI)
C
COMPUTE THE RANGE
ANGTR=ARCCOS(COSIHE)
TRANSC=EARTH*XMIFH
TRANGE=TFANSC*ANGTR
C
COMPUTE TRANSMITTER COORDINATES
COLAT=FII2-TLAT
XT=TRANSC*COS(TICN)*SIN(CCIAT)
YT=TRANSC*SIN(TICN)*SIN(CCIAT)
ZT=TRANSC*COS(CCLAT)
C
COMPUTE RECEIVER COORDINATES
RECEIC=EARTH*W(40)
COLAT=PID2-RLAT
XR=RECEIC*COS(RICN)*SIN(CCIAT)
YR=RECEIC*SIN(RICN)*SIN(CCIAT)
ZR=RECEIC*COS(CCIAT)
C
COMPUTE THE MAGNITUDES OF CR, CI AND TR
CT=SQRT(XT*XT+YT*YT+ZT*ZT)
CR=SQRT(XR*XR+YR*YR+ZR*ZR)
TR=SQRT((XR-XT)**2+(YR-YT)**2+(ZR-ZT)**2)
C
CALCULATE THE AZIMUTHAL ANGLE
IF(ANGTR.NE.0.0) GC TO 120
AZ1=0.0
IF(TLAT.GT.RLAT) AZ1=PI
GO TO 55
120
SINFTN=SIN(ANGI)*SIN(ANGR)/SIN(ANGTR)
COSFTN=(COS(ANGR)-COS(ANGI)*COS(ANGTR))/ (SIN(ANGT)*SIN(ANGTR))
AZ1=ARCSIN(SINFTN)
IF(SINFTN.LT.0.0) GO TO 45
IF(COSFTN.LT.0.0) AZ1=PI-AZ1
GO TO 50

```

```

45 IF (COSETN.LT.C.C) AZ1=-PI-AZ1
50 IF (TLCN.GT.RLCN) AZ1=PII2-AZ1
C COMPUTE THE ELEVATION ANGLE FROM TRIANGLE TCF
55 ARGUM= (TF**2+CT**2-CR**2)/(2.*TF*CT)
IF (ARGUM.GT.1.0) ARGUM=1.0
IF (ARGUM.LT.-1.0) ARGUM=-1.0
BETA=ARCCS(ARGUM)-PII2
75 NSCI=1
APRCX(1,1,1)=BETA
TLATD=TLAT*DEGS
TICND=TICN*DEGS
PLATD=PLAT*DEGS
RICND=RICN*DEGS
PHO1=PHO*DEGS
THO1=THC*DEGS
PRINT 27
27 FORMAT(1E1)
PRINT 30,TLATD,TLCND,XMIBF
30 FORMAT(1X,44HTHE TRANSMITTER GEOGRAPHIC COORDINATES ARE : ,4X,
14HLAT=,F8.3,2X,5HLONG=,F8.3,2X,7HHEIGHT=,F8.2,3H KM)
PRINT 31,PLATD,PLCND,W(4C)
31 FORMAT(1X,41HTHE RECEIVER GEOGRAPHIC COORDINATES ARE : ,4X,
14HLAT=,F8.3,2X,5HLONG=,F8.3,2X,7HHEIGHT=,F8.2,3H KM)
PRINT 19,EHC1,THO1
19 FORMAT(1X,44HTHE TRANSMITTER GEOMAGNETIC COORDINATES ARE:,2X,5HLCN
1G=,F12.5,3X,6HCLAT=,F12.5)
PRINT 21,GBLON,GBIAT
21 FORMAT(1X,41HTHE RECEIVER GEOMAGNETIC COORDINATES ARE:,2X,5HLONG=,
1F12.5,3X,6HCLAT=,F12.5)
PRINT 32,TRANGE,TFREQ
32 FORMAT(1X,29HRANGE AT TRANSMITTER RADIUS = ,F12.2,2X,2HKM,5X,
127HFREQUENCY OF TRANSMISSION = , F10.4,2X,3HMHZ)
DETA=BETA*DEGS
AZMIH=AZ1*DEGS
PRINT 37,LBETA,AZETH
37 FORMAT(1X,28HTHE INITIAL ELEVATION ANGLE=,F8.3,2X,7HDEGREES,5X,
125HAZIMUTH OF TRANSMISSION = , F12.6,2X,7HDEGREES)
RETURN
END

```

```

SUBROUTINE HCMF
C JFLAG=C MEANS WE CAN FIND AN APPROXIMATE ELEVATION ANGLE.
C =1 MEANS WE CANNOT FIND AN APPROXIMATE ELEVATION ANGLE.
DIMENSION DDMIN(21)
DIMENSION JSOL(2),TEMPR(91,2),NECINT(2),JTEME(21)
REAL*8 A,B,C,LEIT,DANS(52),HAIT ,F1,F2,R3,R4,R5,R6,RE,RI,FJ,DET
REAL*8 A1,B1,C1
COMMON/CCNST/ EI,EI2,PII2,DEGS,FAD,DUM(3)
COMMON/DENSC/ DENS(52),HEIT(52),ELRANJ(91,3,2),APRCX(8,2,2),FRATIO
1,NMAX,NSTART,JFIAG,NSCI,DMIN(21),JJJM1
COMMON Y(6) /WW/ ID(10),WC,W(400)
COMMON/DENX/ FH(19,52,5),THETA(19),HGT(52),PHI(5),FRES(4),HL
COMMON/EG2/ LATX,LCMX,IPTMX
COMMON/CEFF/ A1(52),B1(52),C1(52),HAIT(52),FAFOGE,FAPCGM
EQUIVALENCE (EARTH,W(19)), (TICN,W(14)), (FICK,W(381)), (TLAT,W(16)),
1 (RLAT,W(382)), (ETA,W(17)), (TFREQ,W(3)), (AZ1,W(18))
EQUIVALENCE (TRANGE,W(385)), (BETA1,W(389)), (LIFG,W(387))
EQUIVALENCE (PEC,W(378)), (THO,W(377))
EQUIVALENCE (ELCN,W(13)), (ELAT,W(15)), (FCP,W(254)), (GRCUP,W(394))
DATA INTERV,5C/
C W(380)=1 MEANS HCMING GROUND TO GROUND.
C W(380)=2 MEANS HCMING GROUND TO SATELLITE OR SATELLITE TO GROUND
C W(380)=3 MEANS FIND THE MINIMUM GROUND PATH
NNH=W(380)+.1
GO TO (1200,1300,1400),NNH
C THE MINIMUM GROUND PATH ROUTINE
1400 CALL GRCUM
RETURN
1300 CALL HCMFS
RETURN
1200 RE=FAFFF
C SETUP THE NUMBER OF HOPS
NHCE=HCE+0.1
C SETUP THE FACTORS FOR THE MIDPOINT LOCATION OF EACH HOP DIVISION
HOFF=1.0/(2.0*HCP)
HOPI=-1.0
DO 1 I=1,91
DO 1 J=1,3
DO 1 K=1,2
1 ELRANJ(I,J,K)=C.0
DO 2 I=1,8
DO 2 J=1,2
DO 2 K=1,2
2 APRCX(I,J,K)=C.C
DO 3 I=1,NHOP
3 JSCI(I)=C
C SET UP THE NUMBER OF INTERVALS FOR THE ELEVATION ANGLE.
FRATIO=TFREQ**2
C CHECK IF GROUND PATH HCMING IS NEEDED
IF (W(394).EQ.0.0) GO TO 111
ANGT=PII2-TLAT
ANGIR=GRCUP/EARTH
TRANGE=GRCUP
RANGE=TRANGE/HOF
AZ1=W(263)
GO TO 5000
C CALCULATE THE RANGE BETWEEN TRANSMITTER AND RECEIVER
111 ANGL=ABS(TICN-FICK)
ANGT=PII2-TLAT
ANGR=PII2-RIAT

```

```

C      USE THE CCSINF LAW TO FIND ANGLE SUBTENDED AT EARTH CENTER
      COSFE=CCS (ANGT) *COS (ANGR) +SIN (ANGT) *SIN (ANGR) *COS (ANGL)
      ANGTR=ARCCS (CCSFE)
      TRANGE=ANGTR*(EARTH*W(2C))
C      DIVIDE THE TOTAL RANGE BY THE NUMBER OF HOPS NEEDED.
      RANGE=TRANGE/HCFE
C
C      THIS PORTION OF THE CODE SELECTS A DENSITY PROFILE THAT IS CLOSEST
C      TO THE MID POINT BETWEEN THE TRANSMITTER AND RECEIVER (AVLON,AVLAT)
C      COORDINATES
      IF (ANGTF.NE.0.0)   GC TC 4225
      RTN=C.C
      IF (TLAT.GT.FLAT)   RTN=PI
      GO TC 5000
4225  SINFIN=SIN (ANGL) *SIN (ANGR)/SIN (ANGTF)
      COSFTN=(COS (ANGF) -CCS (ANGT) *CCS (ANGTF)) / (SIN (ANGT) *SIN (ANGTR))
      RTN=ARCSIN (SINRTN)
      IF (SINRTN.LT.C.C)   GC TC 4500
      IF (COSFTN.LT.C.C)   RTN=PI-RTN
      GO TC 5000
4500  IF (CCSFTN.LT.C.C)   RTN=-PI-RTN
5000  DC 8000 JHOP=1,NHCP
      NSOI=0
      HCFI=HCFI+2.0
      COSANG=CCS (HCFI*HCPF*ANGTR)
      SINANG=SIN (HCFI*HCPF*ANGTF)
C      THIS PORTION IS FOR GROUP PATH FINDING
      IF (W(394).EQ.C.C)   GC TC 5005
      AZT=AZ1
      IF (AZT.GT.PI)   AZT=PII2-AZT
      CCSNM=CCS (ANGT) *CCSANG+SIN (ANGT) *SINANG*CCS (AZT)
      AVLATG=PII2-ARCCS (CCSNM)
      TNM=ARCSIN (SIN (AZT) *SINANG/SIN (ARCCS (CCSNM)))
      AVLCNG=IICN+TNM
      IF (AZ1.GT.PI)   AVLCNG=TLCN-TNM
      GO TO 9
5005  COSNM=CCS (ANGT) *CCSANG           +SIN (ANGT) *SINANG           *COS (RTN)
      AVLATG=PII2-ARCCS (CCSNM)
      TNM=ARCSIN (SIN (RTN) *SINANG           /SIN (ARCCS (CCSNM)))
      IF (TLCN-FICN)   4,4,5
4      AVLCNG=IICN+TNM
      AZ1=PII2-RTN
      GO TO 6
5      AVLCNG=IICN-TNM
      AZ1=PII2-RTN
6      CCNTINUE
C
C      TRANSFORM THE MIDPOINT TO GEOMAGNETIC COORDINATES
9      SP=SIN (FIAT)
      CP=SIN (PII2-PIAT)
      SINCPH=SIN (AVLCNG-PICN)
      COSEPH=SIN (PII2-(AVLCNG-FICN))
      SL=SIN (AVLATG)
      CL=SIN (PII2-AVIATG)
      AVLCN=ATN2 (SINCPH*CL,COSEPH*SP*CL-CP*SI)
      AVCLAT=ARCCS (COSEPH*CP*CI+SP*SL)
      IF (W(394).NE.0.C)   GC TO 91
C      TRANSFORM THE RECEIVER COORDINATES TO GEOMETRIC COORDINATES
      SINRPH=SIN (FICN-PICN)
      CCSEPH=SIN (PII2-(FICN-PICN))
      SI=SIN (FIAT)

```

```

CI=SIN(FIC2-RIAT)
GRLCN=ATAN2(SINIPH*CI,CCSDPH*SF*CL-CF*SI)
GRLAT=AFCCS(COSEDPH*CP*CI+SF*SI)
GRICN=CFICN*DEGS
GRLAT=GRIAT*DEGS
C   TEMPORARY PRINTING OF THE MID POINT
91  GCLCNG=AVLONG*DEGS
    GOLATG=AVIATG*DEGS
    AVICND=AVLCN*DEGS
    AVLATD=AVCLAT*DEGS
    PRINT 9911
9911 FORMAT(2X,'MID POINT COORDINATES, GEOGRAPHIC AND GEOMAGNETIC' /)
    PRINT 9912,GCLCNG,GCIATG,AVICND,AVIATG
9912 FORMAT(2X,'GEOGRAPHIC:',2X,'LCNG=',F8.2,2X,'COIAT=',F8.2,2X,'GECMA
1GNETIC:',2X,'LCNG=',F8.2,2X,'COIAT=',F8.2)
    DPHI=ABS(PHI(2)-PHI(1))
    KK=ICNMX
    DO 610 K=1,ICNMX
    DIFF1=ABS(AVLCN-PHI(K))
    IF(DIFF1-DPHI) 620,615,610
615  KK=K
    GO TO 630
620  KK=K
    IF(K.GE.ICNMX) GO TO 630
    DIFF2=ABS(AVLCN-PHI(K+1))
    IF(DIFF2.LT.DIFF1) KK=K+1
    GO TO 630
610  CONTINUE
C   WE CANNOT FIND A LONGITUDE CLOSE ENOUGH TO THE MID POINT.
    WRITE(6,625)
625  FORMAT(1X,82HIF GIVEN DENSITY PROFILE DOES NOT INCLUDE THE MID PO
INT LONGITUDE BETWEEN T AND F)
    GO TO 300
630  DTHETA=ABS(THETA(2)-THETA(1))
    IL=IATMX
    DO 635 I=1,IATMX
    DIFF1=ABS(AVCLAT-THETA(I))
    IF(DIFF1-DTHETA) 645,640,635
640  LL=L
    GO TO 660
645  LL=L
    IF(L.GE.IATMX) GO TO 660
    DIFF2=ABS(AVCLAT-THETA(I+1))
    IF(DIFF2.LT.DIFF1) II=I+1
    GO TO 660
635  CONTINUE
C   CAN NOT FIND A LATITUDE CLOSE ENOUGH TO THE MID POINT
    WRITE(6,650)
650  FORMAT(1X,83HIF GIVEN DENSITY PROFILE DOES NOT INCLUDE THE MID
POINT LATITUDE BETWEEN T AND F)
    GO TO 300
C   EXTRACT THE DENSITY AT THE MID POINT AND THE CORRESPONDING HEIGHT
660  DO 665 I=1,IHIMX
    DENS(I)=PH(LL,I,KK)**2
    DENS(L)=DENS(I)
    HEIT(I)=EGT(L)
665  HEIT(L)=EGT(L)
C   FIND THE HEIGHT ON WHICH THE MAXIMUM DENSITY OCCURS
    DHEIT=HEIT(2)-HEIT(1)
    TEMP=DENS(1)
    NMAX=1

```

```

DC 670 I=2, IHTMX
IF (DENS(I).LE.TIME) GC TO 670
NMAX=L
TEMP=DENS(L)
670 CONTINUE
HMAX=HEIT(NMAX)
FVMAX=SQRT(DENS(NMAX))
C ASSUME AN INITIAL ELEVATION ANGLE OF ZERO
BETAF=C.C
IF (TPREQ-FVMAX) 330, 320, 320
330 BETAT=PII2
GC TO 340
C COMPUTE THE ELEVATION ANGLE FOR A TRAPPED RAY
320 TEMPA=(EARTH+HMAX)*SQRT(1.C-(FVMAX**2/FRATIC))/EARTH
IF (TEMPA-1.0) 321, 321, 400
321 BETAT=AFCCS(TEMPA)
340 TLAT=TIAT*DEGS
TLCND=TIEN*DEGS
RLATD=RLAT*DEGS
RLCND=RLCN*DEGS
PHO1=PHC*DEGS
THO1=TEC*DEGS
PRINT 29
29 FORMAT(1H1)
PRINT 30, TLAT, TLCND, W(20)
30 FORMAT(1X, 44HTHE TRANSMITTER GEOGRAPHIC COORDINATES ARE : , 4X,
14HLAT=, F8.3, 2X, 5HICNG=, F8.3, 2X, 7HHEIGHT=, F8.2, 3H KM)
IF (W(394).NE.C.C) GC TO 301
PRINT 31, RLATD, RLCND, W(40)
31 FORMAT(1X, 41HTHE RECEIVER GEOGRAPHIC COORDINATES ARE : , 4X,
14HLAT=, F8.3, 2X, 5HLONG=, F8.3, 2X, 7HHEIGHT=, F8.2, 3H KM)
301 PRINT 19, PHO1, THO1
19 FORMAT(1X, 44HTHE TRANSMITTER GEOMAGNETIC COORDINATES ARE:, 2X, 5HLCN
1G=, F12.5, 3X, 6HCLAT=, F12.5)
IF (W(394).NE.O.C) GC TO 3211
PRINT 21, GRLCN, GRIAT
21 FORMAT(1X, 41HTHE RECEIVER GEOMAGNETIC COORDINATES ARE:, 2X, 5HICNG=,
1F12.5, 3X, 6HCOIAT=, F12.5)
3211 PRINT 32, TRANGE, TREQ
32 FORMAT(1X, 29HRANGE AT TRANSMITTER RADIUS = , F12.2, 2X, 2HKM, 5X,
127HFREQUENCY OF TRANSMISSION = , F10.4, 2X, 3HMHZ)
NSTART=1
C CALCULATE COEFFICIENTS AND STORE THEM IN ARRAYS A1, B1, C1
87 I=NSTART
J=NSTART+1
K=NSTART+2
L=NSTART+3
IF (NMAX-3) 1000, 1000, 10
C THERE ARE MORE THAN THREE POINTS
10 R1=FE +HAIT(I)
R2=FE +HAIT(J)
R3=FE +HAIT(K)
R4=F3-F2
R5=F3-R1
R6=F1-F2
ED2=2.CED
C CALCULATE THE COEFFICIENT FOR THE FIRST THREE POINTS
DET=R4*R5*R6/(F1*F2*F3)
A=(-R1*R1*R4*DANS(I)+R2*R2*R5*DANS(J)+R3*R3*R6*DANS(K))/(DET*R1*R2
1*R3)
B=(F1*F1*(R3*R3-R2*F2)*DANS(I)-F2*F2*(R3*R3-R1*R1)*DANS(J)-R3*R3*(

```

```

1R1*R1-E2*R2)*DANS (K)) / (DET*R1*R2*R3)
C = (-R1*R4*DANS (I) + R2*R5*DANS (J) + R3*R6*DANS (K)) / DET
DELT = -E / (R3*R3) - DL2*C / (R3**3)
A1 (1) = A
E1 (1) = E
C1 (1) = C
M = 1
DO 73 I=1, NMAX
M = M + 1
RJ = FE + HAIT (I)
RI = FE + HAIT (I - 1)
C CALCULATE THE COEFFICIENT A, E, C
DET = (RJ - RI) ** 2 / ((RI ** 2) * EJ)
A = (FI * RI * (RI - RJ) * DELT + RI * (FI - DL2 * RJ) * DANS (I - 1) + RJ * EJ * DANS (I)) / (DET
1 * RJ * RI ** 2)
B = (FI * (EJ * RJ - RI * RI) * DELT - DL2 * EJ * RJ * (DANS (I) - DANS (I - 1))) / (DET * RI * RJ
1)
C = (FI * (RI - RJ) * DELT + EJ * (DANS (I) - DANS (I - 1))) / DET
DELT = -E / (EJ * RJ) - DL2 * C / (RJ ** 3)
A1 (M) = A
E1 (M) = E
C1 (M) = C
73 CONTINUE
C CALCULATE THE RANGE AND GROUP PATH
CALL FITT (CRF, CGPF, FEATF)
86 CALL FITT (CRT, CGPT, FEAT)
IF (JFLAG.EQ.0) GO TO 88
C DECREMENT THE PENETRATION ANGLE.
FEAT = FEAT - 0.4C * RAD
GO TO 86
C CHECK IF THE TRANSMISSION FREQUENCY IS GREATER THAN FC
88 IF (TFREQ - FVMAX) 92, 92, 89
C CORRECT THE TRAPPING ANGLE FEAT
89 CRT = CRT
CGPT = CGPT
FEAT1 = FEAT
C INCREMENT THE ANGLE BETAT BY 0.1 DEGREE AND CHECK THE SLOPE.
BETAT = FEAT + 0.1C * RAD
CALL FITT (CRT, CGPT, FEAT)
IF (JFLAG.EQ.0) GO TO 95
FEAT = FEAT1
CRT = CRT1
CGPT = CGPT1
GO TO 92
95 IF (CRT.LT.CRT1) GO TO 89
C WE HAVE THE MAXIMUM AND MINIMUM ELEVATION ANGLES AND CORRESPONDING
C RANGES. DIVIDE THE ELEVATION ANGLE RANGE INTO INTERVAL, THE NUMBER
C OF INTERVALS.
92 KINT = INT(FV + 1)
ELRANJ (1, 1, JHCF) = FEATF
ELRANJ (1, 2, JHCF) = CRT
ELRANJ (1, 3, JHCF) = CGPT
ELRANJ (KINT, 1, JHCF) = BETAT
ELRANJ (KINT, 2, JHCF) = CRT
ELRANJ (KINT, 3, JHCF) = CGPT
DINT = (FEAT - BETAT) / INTERVAL
C
C GENERATE THE RANGES CORRESPONDING TO THE INTERVAL VALUES OF THE
C ELEVATION ANGLES.
DO 110 I=2, INTERV
BETAI = (I - 1) * DINT

```

```

CALL FIT1(CR,CGF,EFTAI)
ELRANJ(I,1,JHCF)=EFTAI
ELFANJ(I,2,JHCF)=CR
ELFANJ(I,3,JHCF)=CGF
110 CONTINUE
C LOCATE THE MAXIMA AND MINIMA OF THE ELEVATION-ANGLE CURVE
C INITIALIZE THE VECTOR DEMIN
DO 1110 I=1,21
1110 DEMIN(I)=C.C
TEMP=ELFANJ(1,2,JHCF)**
JJJ=1
JJ=1
DBMIN(JJJ)=ELRANJ(1,1,JHCF)
JTEMP(1)=1
DO 1111 I=2,KINT
GO TO(1112,1113),JJ
1112 IF(ELRANJ(I,2,JHCF).LT.TEMP) GC TO 1118
C REPLACE AND STORE THE ELEVATION ANGLE VALUES
JJ=2
JJJ=JJJ+1
DBMIN(JJJ)=ELRANJ(I-1,1,JHCF)
JTEMP(JJJ)=I-1
GO TO 1118
1113 IF(ELRANJ(I,2,JHCF).GT.TEMP) GC TO 1118
C REPLACE THE INDEX VALUE
JJ=1
JJJ=JJJ+1
DBMIN(JJJ)=ELRANJ(I-1,1,JHCF)
JTEMP(JJJ)=I-1
1118 TEMP=ELFANJ(I,2,JHCF)
1111 CONTINUE
JJJ=JJJ+1
DBMIN(JJJ)=BETAI
JTEMP(JJJ)=KINT
DO 1147 KQ=1,JJJ
1147 DBMIN(KQ)=DBMIN(KQ)*IEGS
PRINT 8733, (DBMIN(KQ),KQ=1,JJJ)
C REMOVE SMALL OSCILLATIONS FROM THE LAYERS OF THE D-E CURVE
C ASSUME 150 KM OSCILLATIONS OR LESS TO BE REMOVED
JJR=1
JJ=1
DO 1130 I=2,JJJ
C RETRIEVE THE INDICES FOR COMPARISON
J1=JTEMP(JJR)
J2=JTEMP(I)
DIFFR=ELRANJ(J1,2,JHCF)-ELRANJ(J2,2,JHCF)
GO TO(1135,1140),JJ
C D-E CURVE SLOPING DOWNWARDS
1135 IF(DIFFR.GT.0.C) GC TO 1137
IF(ELRANJ(J2,2,JHCF).LT.ELRANJ(J1,2,JHCF)) GO TO 1130
DBMIN(JJR)=DBMIN(I)
JTEMP(JJR)=JTEMP(I)
GO TO 1130
1137 IF(ABS(DIFFR).LT.150.0) GC TO 1130
JJ=2
JJR=JJR+1
DBMIN(JJR)=DBMIN(I)
JTEMP(JJR)=JTEMP(I)
GO TO 1130
C D-E CURVE SLOPING UPWARDS
1140 IF(DIFFR.LT.0.C) GC TO 1143

```

```

IF (ELRANJ(J2,2,JHCP).GT.EIFANJ(J1,2,JHCE)) GC TO 1130
DBMIN(JJF)=DBMIN(I)
JTEMP(JJF)=JTEMP(I)
GC TO 1130
1143 IF (ABS(DIFFR).LT.150.0) GC TO 1130
JJ=1
JJR=JJR+1
DEMIN(JJR)=DBMIN(I)
JTEMP(JJR)=JTEMP(I)
1130 CCNTINUE
DO 1146 KQ=1,JJR
1146 DDMIN(KQ)=DEMIN(KQ)*DEGS
PRINT 8733, (DDMIN(KQ),KQ=1,JJR)
JJJM1=JJF-1
PRINT 114
114 FORMAT(2X,21HTHE RANGE-BETA VALUES)
PRINT 115
115 FORMAT(1X,9HPCINT NO.,10X,6HEL DEG,10X,8HRANGE KM,10X,9HG.PATH KM)
L=2
K=3
IF (W(394).EQ.0.C) GC TO 116
L=3
K=2
118 DO 116 I=1,KINT
BETAD=ELRANJ(I,1,JHCE)*DEGS
116 PRINT 117,I,BETAD,ELRANJ(I,L,JHCP),ELRANJ(I,K,JHCP)
117 FORMAT(1X,I6,8X,F12.3,5X,F12.3,7X,F12.3)
C CHECK THE GIVEN RANGE AGAINST THE CALCULATED RANGES TO FIND THE
C NUMBER OF SOLUTIONS.
KFLAG=0
C SET A FLAG EQUAL TO ZERO SO THAT IF THE INTERPOLATION DOES NOT
C CONVERGE WITHIN TEN TRIES, THERE IS NO SOLUTION FOR THAT ANGLE
C (MFLAG)
IF (ELRANJ(1,2,JHCE).LT.RANGE) KFLAG=1
DO 120 I=2,KINT
IF (KFLAG.EQ.1) GC TO 180
C CHECK THE NEXT RANGE IF LARGER THAN GIVEN RANGE
IF (ELRANJ(I,2,JHCE).GT.RANGE) GC TO 120
C INCREMENT NSOL AND HCME THE SOLUTION TO FIND THE APPROXIMATE
C INTERPOLATION ANGLE.
156 IB=(ELRANJ(I,1,JHCP)-ELRANJ(I-1,1,JHCE))/9.C
BETAI=EIFANJ(I-1,1,JHCP)
CR=ELRANJ(I-1,2,JHCE)
MFLAG=C
DO 127 J=1,10
IF (KFLAG.EQ.1) GC TO 129
IF (CR.LT.RANGE) GC TO 128
125 ELRANJ(I-1,1,JHCP)=BETAI
ELRANJ(I-1,2,JHCP)=CR
EETAI=EETAI+DB
CALL FITT(CR,CGE,EETAI)
GO TO 127
128 ELRANJ(I,1,JHCE)=BETAI
ELRANJ(I,2,JHCP)=CR
GO TO 126
129 IF (CR.GT.RANGE) GC TO 128
GO TO 125
127 CCNTINUE
C WE CANNOT FIND A SOLUTION
175 DO 1275 JK=1,JJJM1
JJK=JK

```

```

IF (BETA1.GT.DBMIN (JK) .AND.EETA1.LE.DEMIN (JK+1)) GC TO 1280
1275 CCNTINUE
1280 GO TO (1281,1283,1285,1287,1289,1291,1293,1295),JJK
1281 PRINT 1282
1282 FORMAT(2X,62HCANNCT FIND APPROXIMATE SOLUTION FOR FIRST LAYER LOW
1 ANGLE )
GO TO 171
1283 PRINT 1284
1284 FORMAT(2X,62HCANNCT FIND APPROXIMATE SOLUTION FOR FIRST LAYER HIGH
1 ANGLE )
GO TO 171
1285 PRINT 1286
1286 FORMAT(2X,62HCANNCT FIND APPROXIMATE SOLUTION FOR SECOND LAYER LOW
1 ANGLE )
GO TO 171
1287 PRINT 1288
1288 FORMAT(2X,62HCANNCT FIND APPROXIMATE SOLUTION FOR SECOND LAYER HIGH
1 ANGLE )
GO TO 171
1289 PRINT 1290
1290 FORMAT(2X,62HCANNCT FIND APPROXIMATE SOLUTION FOR THIRD LAYER LOW
1 ANGLE )
GO TO 171
1291 PRINT 1292
1292 FORMAT(2X,62HCANNCT FIND APPROXIMATE SOLUTION FOR THIRD LAYER HIGH
1 ANGLE )
GO TO 171
1293 PRINT 1294
1294 FORMAT(2X,62HCANNCT FIND APPROXIMATE SOLUTION FOR FOURTH LAYER LOW
1 ANGLE )
GO TO 171
1295 PRINT 1296
1296 FORMAT(2X,62HCANNCT FIND APPROXIMATE SOLUTION FOR FOURTH LAYER HIGH
1 ANGLE )
GO TO 171
C USE LINEAR INTERPOLATION RANGE=E+Q*BETA
126 IF (ELRANJ (I-1,1,JHOP).EQ.ELRANJ (I,1,JHCP)) GC TO 175
Q=(ELRANJ (I-1,2,JHOP)-ELRANJ (I,2,JHCP))/(ELRANJ (I-1,1,JHOP)-
1 ELRANJ (I,1,JHCP))
IF (Q.EQ.(.0)) GC TO 175
P=ELRANJ (I-1,2,JHCP)-Q*ELRANJ (I-1,1,JHCP)
BETA1=(RANGE-E)/Q
CALL FITT (CR,CEE,EETA1)
IF (JFLAG) 130,130,175
130 DIFF=RANGE-CR
IF (DIFF) 135,160,145
135 IF (DIFF+LIFG) 140,160,160
140 IF (KFLAG.EQ.1) GC TO 146
136 ELRANJ (I-1,1,JHCP)=EETA1
ELRANJ (I-1,2,JHCP)=CR
MFLAG=MFLAG+1
IF (MFLAG.GE.10) GC TO 175
GO TO 126
145 IF (DIFF-LIFG) 160,160,150
150 IF (KFLAG.EQ.1) GC TO 136
146 ELRANJ (I,1,JHCP)=EETA1
ELRANJ (I,2,JHCP)=CR
MFLAG=MFLAG+1
IF (MFLAG.GE.10) GC TO 175
GO TO 126
C WE HAVE FOUND THE APPROXIMATE ANGLE

```

```

160   NSCI=NSCI+1
      JSOL(JHCE)=NSCI
      APRCX(NSCI,1,JHCF)=EETA1
      APRCX(NSCI,2,JHCF)=I
      EBETA=EETA1*DEGS
      DO 1160 JK=1,JJM1
      JJK=JK
      IF(ETAI.GT.EBMIN(JK).AND.EETA1.IT.EBMIN(JK+1)) GC TO 1170
1160  CONTINUE
1170  GO TO (1171,1172,1175,1177,1179,1181,1183,1185),JJK
1171  PRINT 1172,NSCI,DEETA,CR,CGP
1172  FORMAT(2X,28HAPPROXIMATE SOLUTION NUMBER=,I3,2X,22HFIRST LAYER LO
1W ANGLE ,10H,EL.ANGLE=,F8.3,2X,6HRANGE=,F8.3,2X,7HG.PATH=,F8.3)
      GO TO 171
1173  PRINT 1174,NSCI,DEETA,CR,CGP
1174  FORMAT(2X,28HAPPROXIMATE SOLUTION NUMBER=,I3,2X,23HFIRST LAYER HI
1GH ANGLE ,10H,EL.ANGLE=,F8.3,2X,6HRANGE=,F8.3,2X,7HG.PATH=,F8.3)
      GO TO 171
1175  PRINT 1176,NSCI,DEETA,CR,CGP
1176  FORMAT(2X,28HAPPROXIMATE SOLUTION NUMBER=,I3,2X,23HSECOND LAYER L
1GW ANGLE ,10H,EL.ANGLE=,F8.3,2X,6HRANGE=,F8.3,2X,7HG.PATH=,F8.3)
      GO TO 171
1177  PRINT 1178,NSCI,DEETA,CR,CGP
1178  FORMAT(2X,28HAPPROXIMATE SOLUTION NUMBER=,I3,2X,24HSECOND LAYER HI
1GH ANGLE ,10H,EL.ANGLE=,F8.3,2X,6HRANGE=,F8.3,2X,7HG.PATH=,F8.3)
      GO TO 171
1179  PRINT 1180,NSCI,DEETA,CR,CGP
1180  FORMAT(2X,28HAPPROXIMATE SOLUTION NUMBER=,I3,2X,22HTHIRD LAYER LO
1W ANGLE ,10H,EL.ANGLE=,F8.3,2X,6HRANGE=,F8.3,2X,7HG.PATH=,F8.3)
      GO TO 171
1181  PRINT 1182,NSCI,DEETA,CR,CGP
1182  FORMAT(2X,28HAPPROXIMATE SOLUTION NUMBER=,I3,2X,23HTHIRD LAYER HI
1GH ANGLE ,10H,EL.ANGLE=,F8.3,2X,6HRANGE=,F8.3,2X,7HG.PATH=,F8.3)
      GO TO 171
1183  PRINT 1184,NSCI,DEETA,CR,CGP
1184  FORMAT(2X,28HAPPROXIMATE SOLUTION NUMBER=,I3,2X,23HFOURTH LAYER L
1OW ANGLE ,10H,EL.ANGLE=,F8.3,2X,6HRANGE=,F8.3,2X,7HG.PATH=,F8.3)
      GO TO 171
1185  PRINT 1186,NSCI,DEETA,CR,CGP
1186  FORMAT(2X,28HAPPROXIMATE SOLUTION NUMBER=,I3,2X,24HFOURTH LAYER HI
1GH ANGLE ,10H,EL.ANGLE=,F8.3,2X,6HRANGE=,F8.3,2X,7HG.PATH=,F8.3)
171   IF(KFLAG.EQ.0) III=1
      IF(KFLAG.EQ.1) III=C
      KFLAG=III
      GO TO 120
C     CHECK IF THE NEXT RANGE IS SMALLER THAN GIVEN RANGE
180   IF(ELRANJ(I,2,JEOP).IT.RANGE) GC TO 120
      GC TO 156
120   CONTINUE
280   IF(NSCI.GT.0) GC TO 300
      PRINT 2805
2805  FORMAT(2X,34HTHERE ARE NO APPROXIMATE SOLUTIONS )
      GC TO 300
1000  PRINT 1005
1005  FORMAT(1X,47HTHERE ARE LESS THAN THREE POINTS IN THE DENSITY)
      GC TO 300
400   PRINT 410
410   FORMAT(1X,25HTHE FREQUENCY IS TOO HIGH)
300   CONTINUE
8000  CONTINUE
C     CHECK TO SEE IF IT IS ONE OF MORE

```

```

IF (NHOF.EQ.1) GC TO 12000
C CHECK IF THE HOPS ARE SYMMETRIC WITHIN A CERTAIN TOLERANCE
DO 8050 I=1,NHCF
IF (JSOI (I).EQ.C) GC TO 8050
C THERE ARE SOLUTIONS
GO TO 8060
8050 CONTINUE
C SET THE CONTROL NSOI TO ZERO DEACTING NO SOLUTIONS
NSOI=C
GO TO 12000
C CHECK FOR SYMMETRIC HOPS
8060 NHCF=NHCF-1
DO 8070 I=1,NHCF
IF (JSOI (I).EQ.JSOI (I+1)) GC TO 8070
C THE HOPS ARE NOT SYMMETRICAL
GO TO 8100
8070 CONTINUE
C CHECK IF THE ELEVATION ANGLES ARE CLOSE TO EACH OTHER
KPCINT=JSCL (1)
C ONE DEGREE SEPARATION MAXIMUM
XXJ=1.0*FAD
DO 8080 I=1,KPCINT
HTEMP=AFECX (I,1,1)
DO 8085 J=2,NHCF
IF (ABS (HTEMP-AFECX (I,1,J)).LE.XXJ) GC TO 8085
C THE HOPS ARE NOT SYMMETRIC SINCE THE ELEVATION ANGLES ARE NOT
C CLOSE TO EACH OTHER
GO TO 8100
8085 CONTINUE
8080 CONTINUE
C THE HOPS ARE SYMMETRIC
NSOI=JSCL (1)
GO TO 12000
8100 DO 8120 J=1,NHCF
JJ=1
TEMPR (JJ,J)=ELRANJ (1,2,J)
XJ=JJ*FAD
DO 8110 I=2,KINT
8111 IF (ELRANJ (I,1,J).LT.XJ) GC TO 8110
C INTERPOLATE LINEARLY ON THE RANGE
SLOPE=(ELRANJ (I-1,2,J)-ELRANJ (I,2,J))/(ELRANJ (I-1,1,J)-
1ELRANJ (I,1,J))
CROSS=ELRANJ (I-1,2,J)-SLOPE*ELRANJ (I-1,1,J)
TEMPR (JJ+1,J)=SLOPE*XJ+CROSS
JJ=JJ+1
XJ=JJ*FAD
GO TO 8111
8110 CONTINUE
NPOINT (J)=JJ
8120 CONTINUE
C FIND THE NUMBER OF SOLUTIONS BY COMPARING THE SUM OF THE RANGES/
C HOP WITH THE GIVEN RANGE
ITEMP=NPCINT (1)
DO 8130 I=2,NHCF
IF (NPCINT (I).GT.ITEMP) GC TO 8130
ITEMP=NPCINT (I)
8130 CONTINUE
C RECOPY THE TEMPORARY ARRAYS ONTO THE PERMANENT ONES
DO 8140 I=1,ITEMP
DO 8140 J=1,NHCF
ELRANJ (I,1,J)=(I-1)*FAD

```

```

8140  ELFANJ(I,2,J)=TEMPER(I,J)
      NSCI=0
      SUM1=0.0
      DO 8145 J=1,NHCE
8145  SUM1=SUM1+TEMPER(I,J)
      DO 8150 I=2,ITEMP
      SUM=0.0
      DC 8160 J=1,NHCE
8160  SUM=SUM+TEMPER(I,J)
      IF(SUM.LT.TRANGE.AND.SUM1.LT.TRANGE) GC TC 8149
      IF(SUM.GT.TRANGE.AND.SUM1.GT.TRANGE) GC TC 8149
C     WE FOUND A SOLUTION
      NSCI=NSCI+1
C     INTERPOLATE TO FIND THE APPROXIMATE ELEVATION ANGLE
      SLOPE=(SUM-SUM1)/(ELFANJ(I,1,J)-ELFANJ(I-1,1,J))
      CROSS=SUM1-SLOPE*ELFANJ(I-1,1,J)
      APRCX(NSCI,1,1)=(TRANGE-CROSS)/SLOPE
      APRCX(NSCI,2,1)=I
8149  SUM1=SUM
8150  CCNTINUE
      DO 8771 KQ=1,91
      PR1=ELFANJ(KQ,1,1)*DEGS
      PR2=ELFANJ(KQ,1,2)*DEGS
      PRINT 8734,PR1,ELFANJ(KQ,2,1),PR2,ELFANJ(KQ,2,2)
8734  FORMAT(1X,2F12.3,12X,2F12.3)
8771  CONTINUE
8733  FORMAT(1X,12F8.3)
12000 RETURN
      END

```

```

SUBROUTINE PITT (RANG, GFCUF, ANG)
REAL*8 EARTH, RE, AA, EB, CC, FF, A1, E1, C1, HAIT, ARGUM, X1, X2, X3, R1, R2, X,
1R3, Y1, Y1, XJ, RJ, EETA, CR, CB1, CR2, CR3, CGF, CGF1, CGF2, CGF3
COMMON/CCNST/ E1, E12, E12, DEGS, FAC, DUM(3)
COMMON/DENSC/ DENS(52), HEIT(52), ELRANJ(91, 3, 2), APRCX(8, 2, 2), FRATIO
1, NMAX, NSTART, JFIAG, NSCL, DEMIN(21), JJJM1
COMMON/CCEFF/ P1(52), E1(52), C1(52), HAIT(52), FAFCGF, FAPCGM
COMMON Y(6) /KW/ ID(10), WC, W(400)
EQUIVALENCY (EARTH, W(19))
C CR IS THE CALCULATED RANGE
C NMAX IS THE NUMBER OF POINTS UP TO THE HEIGHT OF MAXIMUM DENSITY
C HEIT IS THE HEIGHT INCREMENTS CORRESPONDING TO THE DENSITY
C DENS IS THE NORMALIZED DENSITY
C CGF IS THE CALCULATED GROUP PATH
C FRATIO IS THE TRANSMISSION FREQUENCY, F, SQUARED.
C BETA IS THE ELEVATION ANGLE
C NSTART IS THE INDEX AT WHICH THE DENSITY HAS A VALUE
SQRT(X) = ISQRT(X)
ALOG(X) = ELOG(X)
ARSIN(X) = DARSIN(X)
ARCCS(X) = DARCCS(X)
CCS(X) = ICCS(X)
SIN(X) = DSIN(X)
AES(X) = DAES(X)
DD1 = 1.010
DD2 = 2.010
DD4 = 4.010
BETA = ANG
FF = FRATIO
EARTH = EARTH
JFIAG = 0
RE = EARTH**2
M = NSTART
C CALCULATE THE RANGE AND GROUP PATH FROM EARTH SURFACE TO THE
C BOTTOM OF THE IONOSPHERE
CR = ABS(EARTH*CCS(BETA) / (HAIT(M) + EARTH))
CR = DD2*EARTH*(ARCCS(CR) - EETA)
CGF = DD2*(SQRT((EARTH+HAIT(M))**2 - (EARTH*CCS(BETA))**2) - EARTH*
1SIN(BETA))
C SET UP THE CONSTANTS AA, EB, CC FOR THE FIRST THREE POINTS
JJ = 1
AA = DD1 - A1(JJ) / FF
EB = -B1(JJ) / FF
CC = -C1(JJ) / FF - (EARTH*CCS(EETA))**2
ARGUM = EE*EE - DD4*AA*CC
I = J + 3
R1 = EARTH + HAIT(M)
R2 = EARTH + HAIT(M+1)
R3 = EARTH + HAIT(M+2)
X1 = AA*B1*R1 + EB*E1 + CC
X2 = AA*B2*R2 + EB*E2 + CC
X3 = AA*B3*R3 + EB*E3 + CC
IF(X1) 400, 400, 52
52 IF(X2) 55, 55, 56
C THE RAY REFLECTED
55 XI = X1
RI = R1
GO TO 305
56 IF(X3) 57, 57, 75
57 YI = X1

```

```

      RI=F1
      GO TO 305
C     CALCULATE THE RANGE
75    IF (CC) 70,60,60
70    CR1=DD2*FE*CCS (ETA) /SQRT (-CC)
      CR2=(FE*F3+DD2*CC) / (ABS (F3) *SQRT (ARGUM))
      CR3=(FB*F1+DD2*CC) / (ABS (F1) *SQRT (ARGUM))
      CR=CR+CF1*(ARSIN (CR2) -ARSIN (CR3))
      GO TO 80
60    CR1=-DD2*RE*CCS (ETA) /SQRT (CC)
      CR2=ABS (DD2*SQRT (CC*X3) /R3+DD2*CC/R3+BE)
      CR3=ABS (DD2*SQRT (CC*X1) /R1+DD2*CC/R1+BE)
      CR=CR+CF1*ALOG (CR2/CR3)
80    CGF1=DD2*(SQRT (X3) -SQRT (X1)) /AA
C     CALCULATE THE GROUP PATH
      IF (AA) 90,100,100
90    CGF2=(DD2*AA*R3+EE) / (SQRT (ARGUM))
      CGF3=(DD2*AA*R1+EE) / (SQRT (ARGUM))
      CGP=CGF+CGF1+BB*(ARSIN (CGF2) -ARSIN (CGF3)) / (AA*SQRT (-AA))
      GO TO 110
100   CGP2=ABS (DD2*SQRT (AA*X3) +LI2*AA*F3+EE)
      CGP3=ABS (DD2*SQRT (AA*X1) +LI2*AA*F1+EE)
      CGP=CGP+CGP1-BB*ALOG (CGP2/CGP3) / (AA**1.5)
C     START THE CALCULATION FOR THE REST OF THE DENSITY PROFILE
110   DO 20 I=1,NMAX
      JJ=JJ+1
C     SET UP THE CONSTANTS AA,BB,CC
120   AA=DD1-A1(JJ)/FF
      FB=-F1(JJ)/FF
      CC=-C1(JJ)/FF-(EAFTHR*CCS (ETA)) **2
      ARGUM=EE*EB-DD4*AA*CC
      RJ=FAFTHR+HAIT (I)
      RI=FAFTHR+HAIT (I-1)
      XJ=AA*RJ*PJ+FE*FJ+CC
      XI=AA*RI*RI+BB*FI+CC
      IF (XI) 300,300,172
172   IF (XJ) 300,300,171
171   IF (CC) 170,160,160
C     CALCULATE THE RANGE UP TO REFLECTION HEIGHT
170   CR1=DD2*FE*CCS (ETA) /SQRT (-CC)
      CR2=(FE*FJ+DD2*CC) / (ABS (FJ) *SQRT (ARGUM))
      CR3=(BB*FI+DD2*CC) / (ABS (FI) *SQRT (ARGUM))
      CR=CR+CF1*(ARSIN (CR2) -ARSIN (CR3))
      GO TO 160
160   CR1=-DD2*RE*CCS (ETA) /SQRT (CC)
      CR2=ABS (DD2*SQRT (CC*XJ) /RJ+DD2*CC/RJ+BE)
      CR3=ABS (DD2*SQRT (CC*XI) /RI+DD2*CC/RI+BE)
      CR=CR+CF1*ALOG (CR2/CR3)
180   CGP1=DD2*(SQRT (XJ) -SQRT (XI)) /AA
C     CALCULATE THE GROUP PATH UP TO REFLECTION HEIGHT
      IF (AA) 190,200,200
190   CGP2=(DD2*AA*RJ+EE) / (SQRT (ARGUM))
      CGF3=(DD2*AA*RI+BB) / (SQRT (ARGUM))
      CGP=CGF+CGP1+EE*(ARSIN (CGF2) -ARSIN (CGP3)) / (AA*SQRT (-AA))
      GO TO 20
200   CGP2=ABS (DD2*SQRT (AA*XJ) +LI2*AA*FJ+EE)
      CGP3=ABS (DD2*SQRT (AA*XI) +DD2*AA*RI+BE)
      CGP=CGP+CGP1-BB*ALOG (CGP2/CGP3) / (AA**1.5)
20    CONTINUE
130   JFLAG=3
      GO TO 400

```

```

300 CONTINUE
    RAFCGF = (-BB + SQRT(ARGUM)) / (DD2*AA)
    RAFCGM = (-BB - SQRT(ARGUM)) / (DD2*AA)
305 IF (CC) 310, 320, 320
310 CR1 = DD2*FE*COS(ETA) / SQRT(-CC)
    CR2 = FID2
    CR3 = (FE*RI + DD2*CC) / (AES(BI) * SQRT(ARGUM))
    CR = CR + CR1 * (CR2 - ARSIN(CR3))
    GO TO 350
320 CR1 = -DD2*FE*COS(BETA) / SQRT(CC)
    CR2 = AES(SQRT(ARGUM))
    CR3 = ABS(DD2*SQRT(CC*XI) / RI + DD2*CC / RI + EB)
    CR = CR + CR1 * ALOG(CR2 / CR3)
350 CGF1 = -DD2*SQRT(XI) / AA
    IF (AA) 360, 370, 370
360 CGF2 = -FID2
    CGF3 = (DD2*AA*RI + BB) / (SQRT(ARGUM))
    CGF = CGF + CGF1 + EB * (CGF2 - ARSIN(CGF3)) / (AA * SQRT(-AA))
    GO TO 400
370 CGF2 = AES(SQRT(ARGUM))
    CGF3 = AES(DD2*SQRT(AA*XI) + DD2*AA*FI + EE)
    CGF = CGF + CGF1 - EB * ALOG(CGF2 / CGF3) / (AA ** 1.5)
400 RANG = CF
    GRUF = CGF
    IF (W(394).EQ.C.C) GO TO 500
    RANG = CGF
    GRUF = CR
500 RETURN
    END

```

```

SUBROUTINE GRCUEN
C   A SUBROUTINE TO COMPUTE THE MINIMUM GRCUE PATH
C   FIRST WE FIND THE PENETRATION ANGLE AND THEN USE CHECKING
C   AND CHOOSING TECHNIQUE TO LOCATE THE MINIMUM WITHIN A GIVEN
C   TOLERANCE IN GRCUE PATH
COMMON/CCNST/ EI,FI12,FI12,DEGS,FAL,IUM(3)
COMMON/FLAGS/IFIAG,IGRT
COMMON Y(12),I,WW/II(10),WC,W(400)
COMMON/DENSC/ DENS(52),HEII(52),FIRANJ(91,3,2),APRCX(8,2,2),FRATIO
1,NMAX,NSTART,JFIAG,NSCI,DEPIN(21),JJJM1
COMMON/DENY/ PH(19,52,5),TEETA(19),EGT(52),FEI(5),FRES(4),HI
COMMON/EG2/ LATEX,LCNMX,LHMX
COMMON/FR/N,STEE,FOIE,ICMY(5),FSTART
COMMON/FIN/XN2,XMUX,PN2(8),ECLAE(4),SEACE,CCIL,FIELD
COMMON/NICPT/ NEFIN,RCFI,PEFT
EQUIVALENCE (EARTH,W(19)),(F,W(3)),(AZ1,W(18)),(BETA,W(17)),
1 (ONLY,W(371)),(AZA,W(263))
EQUIVALENCE (PEO,W(378)),(THC,W(377))
NSCI=0
C   SELECT THE LONGITUDE COORDINATE OF DENSITY
DPHI=AES(PHI(2)-PHI(1))
KK=ICNMX
DO 110 K=1,LCNMX
DIFF1=AES(PH0-PHI(K))
IF(DIFF1-DPHI) 120,115,110
115  KK=K
GO TO 130
120  KK=K
IF(K.GE.ICNMX) GO TO 130
DIFF2=AES(PH0-PHI(K+1))
IF(DIFF2.LT.DIFF1) KK=K+1
GO TO 130
110  CONTINUE
C   PRINT THE ERROR MESSAGE
PRINT 125
125  FORMAT(2X,'CANNOT FIND A LONGITUDE CLOSE TO THE TRANSMITTER')
GO TO 400
C   SELECT THE CLATITUDE COORDINATE OF DENSITY
130  ITHETA=AES(THETA(2)-THETA(1))
IL=IATEX
DO 135 I=1,IATEX
DIFF1=AES(THC-THETA(I))
IF(DIFF1-ITHETA) 145,140,135
140  II=I
GO TO 160
145  II=L
IF(II.GE.IATEX) GO TO 160
DIFF2=AES(THC-THETA(II+1))
IF(DIFF1.LT.DIFF2) II=II+1
GO TO 160
135  CONTINUE
C   PRINT THE ERROR MESSAGE
PRINT 150
150  FORMAT(2X,'CANNOT FIND A CLATITUDE CLOSE TO THE TRANSMITTER')
GO TO 400
C   EXTRACT THE DENSITY
160  DC 165 I=1,LHMX
165  DENS(I)=PH(LL,I,KK)
TEMP=DENS(1)
DO 170 I=2,LHMX

```

```

IF (IENS(I).LE.TFME) GO TO 170
NMAX=L
TEMP=DENS(L)
170 CONTINUE
HMAX=FGT(NMAX)
FC=DENS(NMAX)
WRITE(6,24) F
24 FORMAT(1X,'THE TRANSMISSION FREQUENCY=',F12.5,' MHZ')
TOIGRF=1.0
C TEMPERATURE ALLOCATION OF AZIMUTH IN W (263)
AZ1=AZA
C COMPUTE THE ELEVATION ANGLE FOR A TRAPPED RAY
TEMFA=(EARTH*HMAX)*SQRT(1.0-(FC/F)**2)/EARTH
IF (TFMA-1.0) 10,10,900
10 BETAR=ARCOS(TEMFA)
20 EETA1=EETA
C INITIALIZE THE RAY PARAMETERS AND TRACE THE RAY
CALL RAYINT(AZ1,EETA1)
BETA=BETA1
EL=EETA*LEGS
AZM=AZ1*LEGS
WRITE(6,25) EL,AZM
25 FORMAT(1X,'ELEVATION ANGLE OF TRANSMISSION=',F12.6,' DEG',5X,
1'AZIMUTH ANGLE OF TRANSMISSION=',F12.6,' DEG')
CALL TRACE
MPRT=0
IF (IGRT.NE.0) GO TO 950
C CHECK FOR PENETRATION
IF (ONLY.EQ.0.0) GO TO 30
BETAR=C.95*BETA
GO TO 20
C STORE THE VALUES
30 GROUP1=1
C TAKE 95% OF INITIAL TRAPPING ANGLE
EETA2=C.95*BETA
CALL RAYINT(AZ1,EETA2)
BETA=BETA2
EL=EETA*LEGS
WRITE(6,25) EL,AZM
CALL TRACE
MPRT=0
IF (IGRT.NE.0) GO TO 950
GROUP2=1
C TAKE 90% OF INITIAL TRAPPING ANGLE
EETA3=C.90*BETA
EETA1=EETA3
CALL RAYINT(AZ1,EETA3)
BETA=BETA3
EL=EETA*LEGS
WRITE(6,25) EL,AZM
CALL TRACE
MPRT=0
IF (IGRT.NE.0) GO TO 950
GROUP3=1
C CHECK FOR THE SHAPE OF THE CURVE
40 IF (GROUP3.LT.GROUP2) GO TO 80
C SLICING TOWARDS THE RIGHT TO GROUP 2
50 IF (GROUP2.LT.GROUP1) GO TO 200
C SLICING TOWARDS THE RIGHT; FIND A NEW PENETRATION ANGLE
C INCREMENT EETA BY 5%
BETAR=1.05*BETA

```

```

60  CALL RAYINT (A21,EETA2)
    BETA=EETA2
    EL=EETA*LEGS
    WRITE (6,25) EL,AZM
    CALL TRACE
    MPRT=0
    IF (IGRT.NE.0)  GO TO 950
C   CHECK FOR PENETRATION
    IF (CNLY.GT.0.C)  GO TO 70
C   INTERCHANGE THE VALUES
    BETA3=EETA2
    EETA2=EETA1
    EETA1=EETA3
    GROUP3=GFCUP2
    GROUP2=GFCUP1
    GRCUP1=1
    GO TO 50
C   RAY PENETRATED INCREMENT THE ANGLE BY 1%
70  EETA2=C.99*EETA1
    GO TO 60
C   SLOPING TOWARDS THE LEFT
80  BETA1=C.95*EETA1
    CALL RAYINT (A21,BETA1)
    BETA=BETA1
    EL=EETA*LEGS
    WRITE (6,25) EL,AZM
    CALL TRACE
    MPRT=0
    IF (IGRT.NE.0)  GO TO 950
    EETA1=EETA2
    EETA2=EETA3
    EETA3=EETA1
    GRCUP1=GFCUP2
    GROUP2=GFCUP3
    GRCUP3=1
    GO TO 40
C   WE FOUND A SMALL VALUE GFCUP2 INCLUDED BETWEEN TWO LARGER VALUES
C   GROUP1 AND GFCUP3
C   USE THE CHOP METHOD ON EITHER SIDE OF GFCUP2
200 BETA5=BETA3+0.5*(EETA2-EETA3)
    BETA4=EETA2+0.5*(EETA1-EETA2)
    CALL RAYINT (A21,BETA4)
    BETA=BETA4
    EL=EETA*LEGS
    WRITE (6,25) EL,AZM
    CALL TRACE
    MPRT=0
    IF (IGRT.NE.0)  GO TO 950
    GRCUP4=1
    CALL RAYINT (A21,EETA5)
    EETA=EETA5
    EL=BETA*LEGS
    WRITE (6,25) EL,AZM
    CALL TRACE
    MPRT=0
    IF (IGRT.NE.0)  GO TO 950
    GRCUP5=1
C   CHECK IF IT IS WITHIN THE TOLERANCE
    IF (ABS(GROUP5-GROUP2).GT.TCLGRF)  GO TO 210
    IF (GROUP4.LI.GFCUP5)  GO TO 350
    GO TO 300

```

```

C      CHECK THE LEFT SIDE
210    IF (GROUPE5.GT.GRCUE2) GO TO 220
C      REPLACE THE LEFT SIDE VALUES
      EETA1=EETA2
      EETA2=EETA5
      GROUPE1=GFCUE2
      GRCUE2=GFCUE5
      GO TO 200
C      CHECK IF IT IS WITHIN THE TOLERANCE
220    IF (ABS(GFOUP4-GFOUP2).LE.TCLGRE) GO TO 230
C      CHECK THE RIGHT SIDE
      IF (GROUPE4.GT.GRCUE2) GO TO 240
C      REPLACE THE RIGHT SIDE VALUES
      EETA3=EETA2
      EETA2=EETA4
      GROUPE3=GFCUE2
      GROUPE2=GFOUP4
      GO TO 200
C      REPLACE THE MIDDLE PORTION
240    EETA3=EETA5
      EETA1=EETA4
      GROUPE3=GFCUE5
      GROUPE1=GFCUE4
      GO TO 200
C      WE FOUND THE LEFT SIDE MINIMUM VALUE OF GROUP PATH
300    IF (GROUPE5.GT.GFCUE2) GO TO 305
      GROUPE2=GFCUE5
      EETA2=EETA5
305    WRITE (6,307)
307    FORMAT (/,1X,'***'//)
      WRITE (6,310)
310    FORMAT (1X,'THE LEFT SIDE      ,MINIMUM GROUP PATH AND ITS ANGLE ARE
1.')
      BETAD=EETA2*DEGS
      WRITE (6,320) BETAD,GFCUE2
320    FORMAT (1X,'ELEVATION ANGLE=',F9.4,2X,'MINIMUM GROUP PATH=',F9.4)
      WRITE (6,307)
      GO TO 400
C      WE FOUND THE RIGHT SIDE MINIMUM VALUE GROUP PATH
350    IF (GFOUP4.GT.GFCUE2) GO TO 355
      GROUPE2=GFCUE4
      EETA2=EETA4
355    WRITE (6,307)
      WRITE (6,360)
360    FORMAT (1X,'THE RIGHT SIDE      ,MINIMUM GROUP PATH AND ITS ANGLE ARE
1.')
      BETAD=EETA2*DEGS
      WRITE (6,320) BETAD,GFCUE2
      WRITE (6,307)
400    RETURN
900    WRITE (6,910)
910    FORMAT (1X,'THE ARGUMENT OF ARCOS IS GREATER THAN ONE')
      GO TO 400
950    IGRT=0
      GO TO 400
      END

```

```

SUBROUTINE PROFIL
C   A ROUTINE TO GENERATE A NEW DENSITY PROFILE
DIMENSION AZT(5),RBMFCD(20,5,4),PR(2,3),R(3),NF(5)
COMMON /IENX/ FF(19,52,5),THETA(19),HGT(52),PHI(5),FRES(4),HL
COMMON /EG1/ DTH(2),DPH(2),DHT(2),DITH,DIFF,LIHT,THZC,PHIZC,HTZC
COMMON /EG2/ IATMX,LCNMX,IHIMX
COMMON /CCNST/ FI,PII2,PII2,DEGS,FAL,DUM(3)
COMMON Y(12),T,STE,DEDT(12) /WW/ ID(10),WO,W(400)
EQUIVALENCE (EAFTHR,W(19)),(FLOH,W(13)),(PLAT,W(15)),(TLOH,W(14)),
1 (TLAT,W(16)),(AIPH,W(376)),(TCLAT,W(377)),(TLOH,W(378))
C   AZIMUTH TOLERANCE
AZTCL=10.*RAD
C   CONVERT THE ANGLES TO RADIANS
DO 40 I=1,LATMX
40  THETA(I)=THETA(I)*RAD
DO 50 I=1,LCNMX
50  PHI(I)=PHI(I)*RAD
C   READ THE NUMBER OF AZIMUTH AND THE NUMBER OF POINTS IN EACH
C   AZIMUTH
READ(5,100) N,(NF(I),I=1,N)
100  FORMAT(6I10)
C   READ THE AZIMUTH ANGLES
READ(5,110) (AZI(I),I=1,N)
110  FORMAT(8F10.0)
C   READ RB,FM,FC,AND D FOR EACH AZIMUTH
DO 130 J=1,N
NF1=NF(J)
READ(5,120) ((FEMFCI(I,J,K),K=1,4),I=1,NF1)
120  FORMAT(4F10.0)
130  CONTINUE
C   LOCATE THE CLOSEST RANGE TO THE TRANSMITTER
TEST=RBMFCD(1,1,4)
K1=1
K2=1
DO 160 I=1,N
NF1=NF(I)
DO 165 I1=1,NF1
IF(RBMFCI(I1,I,4).GE.TEST) GO TO 165
K1=I1
K2=I
TEST=RBMFCD(I1,I,4)
165  CONTINUE
160  CONTINUE
C   GENERATE THE NEW DENSITY PROFILE IN ALL THE SPACE
RB=RBMFCI(K1,K2,1)
RM=RBMFCI(K1,K2,2)
FC=RBMFCI(K1,K2,3)
YM=FM-FE
DO 170 K=1,LCNMX
DO 170 J=1,LATMX
DO 170 I=1,LHTMX
PH(J,I,K)=0.0
RT=FARTH+HGT(I)
FACT=((RT-RM)*FE/(YM*RT))**2
IF(FACT.GT.1.0) GO TO 170
PH(J,I,K)=SQRT(FC**2*(1.0-FACT))
170  CONTINUE
C   FIND THE MAXIMUM RANGE AND SET THE LIMIT
TEST=RBMFCD(1,1,4)
DO 145 I=1,N

```

```

NP1=NP(I)
DO 140 I1=1,NF1
IF (REMFCD(I1,I,4).LE.TEST) GC TC 140
TEST=REMFCD(I1,I,4)
140 CONTINUE
145 CCNTINUE
RANGEL=TEST+100.0
C PRINT INPUT DATA
PRINT 1230,N,(NF(I),I=1,N)
1230 FORMAT(1X,'N=',I3,5(' NF=',I4))
PRINT 1231,(AZT(I),I=1,N)
1231 FORMAT(1X,'AZIMUTHS=',5(F8.2,3X))
DO 1233 J=1,N
NP1=NP(J)
PRINT 1232,AZT(J)
1232 FORMAT(1X,'AZIMUTH=',F8.2)
PRINT 1234,((REMFCD(I,J,K),K=1,4),I=1,NF1)
1234 FORMAT(1X,'RE=',F8.2,' RM=',F8.2,' FC=',F8.2,' TC=',F8.2)
1233 CONTINUE
PRINT 1235, FANGEL,ALPH
1235 FORMAT(1X,'MAXIMUM RANGE=',F8.2,' ALPH=',F14.7)
C GO THROUGH THE GRID POINTS AND TRY TO IDENTIFY THE GIVEN DATA
DO 400 K=1,LCNMX
TNE=ABS(TLONG-PHI(K))
DO 380 J=1,LATMX
C FIND THE AZIMUTH OF ONE POINT P(J,K)
ANGTCE=CCS(TCLAT)*CCS(THETA(J))+SIN(TCLAT)*SIN(THETA(J))*CCS(TNE)
ALPHA=ARCCS(ANGTCE)
SINPTN=SIN(TNE)*SIN(THETA(J))/SIN(ALPHA)
COSPTN=(COS(THETA(J))-CCS(TCLAT)*CCS(ALPHA))/(SIN(TCLAT)*
1SIN(ALPHA))
AZP=ARSIN(SINPTN)
IF(SINPTN.LT.C.C) GC TC 210
IF(COSPTN.LT.C.C) AZP=PI-AZP
GO TO 220
210 IF(CCSEFN.LT.C.C) AZP=-PI-AZP
220 IF(TLCNG.GT.PHI(K)) AZP=PI2-AZP
RANGEP=FAFTR*ALPHA
P1=PHI(K)*DEGS
P2=THETA(J)*DEGS
P3=AZP*DEGS
PRINT 1450,RANGEP,P3,P2,P1
1450 FORMAT(1X,'RANGE=',F8.2,' AZIMUTH=',F8.2,' COLAT=',F8.2,
1' LONG=',F8.2)
C CHECK IF THE AZIMUTH AZP OF P IS WITHIN THE LIMITS OF GIVEN
C AZIMUTHS PLUS TOLERANCE
AZ1=AZT(1)*RAD-ALPH-AZTCL
AZN=AZT(N)*RAD-ALPH+AZTCL
IF(AZP.GE.AZ1.AND.AZP.LE.AZN) GC TC 240
C THE AZIMUTH OF P IS OUT OF RANGE
GO TO 380
C CHECK IF THE RANGE IS OUTSIDE THE MAXIMUM GIVEN RANGE + TOLERANCE
C OF 100FE
240 IF(FANGPE.GT.FANGEL) GO TO 380
C LOCATE TWO AZIMUTHAL ANGLES FOR P
KK=N
DO 260 I=1,N
AZT1=AZT(I)*RAD-ALPH
IF(AZP.GT.AZT1) GO TO 260
KK=I
GC TC 265

```

```

260 CCNTINUE
265 KKK=KK-1
   IF (KK.EQ.1) KKK=KK+1
C   COMPUTE THE GEOMAGNETIC AZIMUTHS
   AZT1= AZT (KK) *RAD-ALPH
   AZT2= AZT (KKK) *RAD-ALPH
C   SEARCH FOR THE CLOSEST TWO   VALUES OF GROUND RANGES TO GROUND
C   RANGE OF F
   II=1
   TEST=RANGEP
   I=KK
270 NF1=NF (I)
   K1=NF1
   DO 290 I1=1,NF1
   IF (RBMFCD (I1,I,4) .LT. TEST) GC TO 290
   K1=I1
   GO TO 295
290 CONTINUE
C   INTERPOLATE LINEARLY FOR THE VALUES OF FE, FM, FC
295 K2=K1-1
   IF (K1.EQ.1) K2=K1+1
   DO 300 M=1,3
   SLOPE= (RBMFCD (K1,I,M) - RBMFCD (K2,I,M)) / (RBMFCD (K1,I,4) -
1 RBMFCD (K2,I,4))
   CRCSS=RBMFCD (K1,I,M) - SLOPE * RBMFCD (K1,I,4)
   FR (II,M) = CRCSS + SLOPE * FANGFE
300 CCNTINUE
   IL=II+1
   I=KKK
   IF (II.LE.2) GC TO 270
C   FIND THE DIFFERENCE IN AZIMUTHAL ANGLES AND COMPUTE THE VALUES OF
C   FB, RM, FC AT THE POINT F
   ANG1F=AZT1-AZF
   ANG2F=AZF-AZT2
   ANG12=AZT1-AZT2
   DO 310 M=1,3
310 F (M) = (ANG2F * RR (1,M) + ANG1F * RR (2,M)) / ANG12
C   R (1) CONTAINS FE, R (2) CONTAINS FM, R (3) CONTAINS FC
C   COMPUTE VALUES OF FC AT DIFFERENT HEIGHTS
   YM=F (2) - F (1)
   DO 340 I=1,IHTMX
   FH (J,I,K) = 0.0
   RT=EARTRF+HGT (I)
   FACT= ((RT-R (2)) * R (1) / (YM * RT)) ** 2
   IF (FACT.GT.1.0) GC TO 340
   FH (J,L,K) = SQRT (R (3) ** 2 * (1.0 - FACT))
340 CCNTINUE
380 CCNTINUE
400 CCNTINUE
C   PREPARE ANGLES IN DEGREES FOR PRINTING
   DO 420 I=1,LOPMX
420 PHI (I) = PHI (I) * DIGN
   DO 440 I=1,IATMX
440 THETA (I) = THETA (I) * DIGN
   RETURN
   END

```



```

C      EXIT IF LIMITS EXCEED.
C
      IF (LCNMX - 5) 125,125,135
125 IF (LATMX - 19) 130,130,135
130 IF (LHTMX - 52) 150,150,135
135 WRITE (IY,140) ICMNX,LATMX,LHTMX
140 FORMAT (1X,35H PARAMETERS OUTSIDE THE LIMITS: //
      1 10X,41H MAXIMUM NUMBER OF LONGITUDE PLANES = ,15 , /
      2 10X,41H MAXIMUM NUMBER OF LATITUDE SECTORS = ,15 , /
      3 10X,41H MAXIMUM NUMBER OF HEIGHT LAYERS = ,15 //)
      STCF
150 CONTINUE
C
C      SETUP UNIFORM SPHERICAL GRID.
C
      DO 151 J = 1,IHTMX
151 HGT(J) = HTZC + FICAT(J-1) * DLHT
      DO 152 L = 1,LATMX
152 THETA(L) = THZC + FICAT(L-1) * DLTH
C
C      READ FREQ. DATA PLANES OF SIZE=(LATMX X IHTMX) FOR EACH LONGITUDE
C
      DO 169 KPH = 1,ICNMX
      PHI(KPH) = PHIZC + FICAT(KPH-1) * DLPH
C
      REAL (IX,160) ((PH(I,J,KPH),I=1,LATMX),J=1,IHTMX)
160 FORMAT(15F5.2,5X)
169 CONTINUE
      IF(W(393).GT.C.C) CALL PRCFIL
C
C
C      WRITE OUT DATA PLANES: (IONOSPHERE GRID MODEL)
C
      WRITE (IY,202)
202 FORMAT(1H1,47H PREPARED BY ARCCN CORP. WAKEFIELD, MASS. 01860,
      4 3X, 21HTEL: (617) 245-3404 , ' AUG. 1973. '//)
      WRITE(IY,203) ICMNX,LATMX,LHTMX,NAME,PHIZC,THZC,HTZO,DLPH,DLTH,DLHTELE
203 FORMAT (1X,48H UNIFORM GRID PARAMETERS : //
      11X,8HLICNMX = ,16,4X,8HLATMX = ,16,4X,8HLHTMX = ,16,4X,5HNAME=,A5, //
      21X,8HPHIZO = ,F9.2,1X,8HTHZO = ,F9.2,1X,8HFTZO = ,F9.2, //
      31X,8HDLPHC = ,F9.2,1X,8HDLTH = ,F9.2,1X,8HDLHT = ,F9.2, // )
      WRITE (IY,202)
      WRITE (IY,210) (THETA(I),I=1,LATMX)
210 FORMAT ( 2X, 12HICNG. HGT. , 20F6.1 , //)
      WRITE (IY,235)
C
C
      DO 240 K = 1,LCNMX
      DO 230 J = 1,LHTMX
      WRITE (IY,220) PHI(K), HGT(J) , (PH(L,J,K),I=1,LATMX)
220 FORMAT (1X, 2F6.1, 1X, 20F6.2)
230 CONTINUE
      WRITE (IY,235)
235 FORMAT (1X)
240 CONTINUE
C
C      CONVERT ALL ANGLES INTO RADIANS
C
      DO 245 K = 1,LCNMX
245 PHI(K) = PHI(K) * RAD
C

```

| | | | |
|-----|---|------|-----|
| | DO 250 L = 1, IATMX | EIE | 120 |
| 250 | THETA(L) = THETA(L) * RAD | EIE | 121 |
| C | | EIE | 122 |
| | DIPH = DIPH * RAD | EIE | 123 |
| | DLTH = DLTH * RAD | EIE | 124 |
| | PHIZO = PHIZO * RAD | EIE | 125 |
| | THZO = THZO * RAD | EIE | 126 |
| C | | EIE | 127 |
| C | CALCULATE PHI, THETA, HEIGHT DIFFERENCES | EIE | 128 |
| C | | EIE | 129 |
| | DTH(1) = 0.5 / (ILTH*DLTH) | EIE | 130 |
| | DPH(1) = 0.5 / (DLFF*DIPH) | EIE | 131 |
| | DHT(1) = 0.5 / (ILBT*DLHT) | EIE | 132 |
| | DTH(2) = -2.0 * DTH(1) | EIE | 133 |
| | DPH(2) = -2.0 * DPH(1) | EIE | 134 |
| | DHT(2) = -2.0 * DHT(1) | EIE | 135 |
| C | | EIE | 136 |
| C | ADDED FOR THE HOMING FEATURE ONLY | UCFI | 1 |
| | IF(W(380).NE.C.C) RETURN | UOFI | 2 |
| 300 | CONTINUE | EIE | 137 |
| C | | EIE | 138 |
| | HL = R(1) - EARTH | EIE | 139 |
| | FREQS = F * F | EIE | 140 |
| | X = C.0 | EIE | 141 |
| | EXFH = C.0 | EIE | 142 |
| | PXFTH = C.0 | EIE | 143 |
| | PXPFH = C.0 | EIE | 144 |
| C | | EIE | 145 |
| C | FIND THETA SECTOR AND INDEX LL | EIE | 146 |
| C | | EIE | 147 |
| | LL = IFIX (((TH - THZO) / DLTH) + 1.00001) | EIE | 148 |
| | IF((TH.LT.(THZO-1.E-06)).OR.(TH.GT.(THETA(LATMX)+1.E-06))) GOTO 320 | EIE | 149 |
| | IF (LL - 1) 320, 310, 310 | EIE | 150 |
| 310 | IF (LL - IATMX) 330, 325, 320 | EIE | 151 |
| 320 | CONTINUE | EIE | 152 |
| C | | EIE | 153 |
| | LL = LL+100 | EIE | 154 |
| | GO TO 4000 | EIE | 155 |
| 325 | LL = IATMX - 1 | EIE | 156 |
| 330 | CONTINUE | EIE | 157 |
| C | | EIE | 158 |
| C | FIND PHI PLANE AND INDEX KK | EIE | 159 |
| C | | EIE | 160 |
| | KK = IFIX (((PH - PHIZO) / DIPH) + 1.00001) | EIE | 161 |
| | IF((PH.LT.(PHIZO-1.E-06)).OR.(PH.GT.(PHI(LCNMX)+1.E-06))) GOTO 350 | EIE | 162 |
| | IF (KK - 1) 350, 340, 340 | EIE | 163 |
| 340 | IF (KK - ICMX) 360, 355, 350 | EIE | 164 |
| 350 | CONTINUE | EIE | 165 |
| C | | EIE | 166 |
| | KK = KK+100 | EIE | 167 |
| | GO TO 4000 | EIE | 168 |
| 355 | KK = ICMX - 1 | EIE | 169 |
| 360 | CONTINUE | EIE | 170 |
| C | | EIE | 171 |
| C | FIND HEIGHT LAYER AND INDEX JJ | EIE | 172 |
| C | | EIE | 173 |
| | JJ = IFIX (((HI - HTZO) / DLHT) + 1.00001) | EIE | 174 |
| | IF (JJ - 1) 380, 370, 370 | EIE | 175 |
| 370 | IF (JJ - IHTMX) 510, 380, 380 | EIE | 176 |
| 380 | CONTINUE | EIE | 177 |
| C | | EIE | 178 |

| | | | |
|------|---|----------|-----|
| | HMAX = HGT (LHTMX) | ELF | 179 |
| | GO TO 999 | ELF | 180 |
| C | | ELF | 181 |
| C | PRINT EFFCR MESSAGES EFFCRF EXIT. | ELF | 182 |
| C | | ELF | 183 |
| 4000 | ANG1 = TH * DEGS | ELF | 184 |
| | ANG2 = PH * DEGS | ELF | 185 |
| | X = 1.0 | ELF | 186 |
| | FXPF = 1.0 | ELF | 187 |
| | FXPTH = 1.0 | ELF | 188 |
| | HMAX=HGT (LHTMX) | ELF**189 | |
| | R(1)=FAFTHR+HMAX | ELF**190 | |
| | IFLAG = 1 | ELF | 191 |
| | IGRT=1 | | |
| | WRITE (IY,4444) ANG1,ANG2,II,KK,IFLAG | ELF | 192 |
| 4444 | FORMAT (//1X,36HANGLES OUTSIDE RANGE OF IONOSPHERE /16X, | ELF | 193 |
| | 16HIPPIT=,F7.1,3X,4HEHI=, F7.1, / 1X, | ELF | 194 |
| | 2 15HINDICES ARE ,6H II = ,17,3X,4H KK=,17,6HIFLAG=, I5) | ELF | 195 |
| C | | ELF | 196 |
| | GO TO 999 | ELF | 197 |
| C | | ELF | 198 |
| C | 510 CONTINUE | ELF | 199 |
| C | | ELF | 200 |
| C | INTERPOLATE FOR F(TH,HL,PH) USING THE INDICES LI,KK,JJ | ELF | 201 |
| C | | ELF | 202 |
| C | CALL INTER(LI,KK,JJ) | ELF | 203 |
| C | | ELF | 204 |
| C | COMPUTE X FROM X=(ELASMA FREQ/F) **2, FL. IEN.= 12400 (X) | ELF | 205 |
| C | | ELF | 206 |
| | X = FRES(1) / FFECS | ELF | 207 |
| | FXPF = FRES(2) / FFECS | ELF | 208 |
| | FXPTH = FRES(3) / FFECS | ELF | 209 |
| | FXPFH = FRES(4) / FFECS | ELF | 210 |
| C | | ELF | 211 |
| | IFLAG = C | ELF | 212 |
| C | | ELF | 213 |
| 999 | RETURN | ELF | 214 |
| | END | ELF | 215 |

APPENDIX 2

This appendix contains expressions for the partial derivatives of the ground range (R) and the group path (P') with respect to the elevation angle of transmission (β) and the quasi-parabolic layer parameters (f_c, r_m, r_b), required in the inversion of point-to-point oblique ionograms and backscatter leading edges:

$$\begin{aligned} \frac{\partial R}{\partial \beta} = & 2r_o \left(\frac{r_o \sin \beta}{r_b \sin \gamma} - 1 \right) \\ & + \frac{F r_o^2 \cos \beta}{\sqrt{C}} \left[\frac{4\sqrt{C} F r_o \sin \beta \cot \gamma}{W} + F^2 r_o^2 \sin 2\beta \left(\frac{4}{W} + G \right) \right. \\ & \left. + \tan \beta \ln \left(\frac{U r_b^2}{W^2} \right) \right] \end{aligned} \quad (\text{A.1})$$

$$\begin{aligned} \frac{\partial R}{\partial f_c} = & \frac{F^2 r_o^2 \cos \beta}{\sqrt{C} f_c} \left[2 F r_o^2 \cos^2 \beta \left(\frac{4}{W} + G \right) - \frac{8CF}{U} \right. \\ & \left. + \frac{1}{F} \ln \left(\frac{U r_b^2}{W^2} \right) - \frac{4\sqrt{C} r_b \sin \gamma}{W} \right] \end{aligned} \quad (\text{A.2})$$

$$\frac{\partial R}{\partial r_m} = \frac{F r_o^2 \cos \beta}{\sqrt{C} r_m y_m} \left[B r_b r_m G - 2 B y_m \left(\frac{B}{U} - \frac{r_b}{W} \right) + \frac{4B}{U} (B r_m + C) \right] \quad (\text{A.3})$$

$$\begin{aligned} \frac{\partial R}{\partial r_b} = & \frac{2r_o^2 \cos \beta}{r_b^2 \sin \gamma} \\ & + \frac{Fr_o^2 \cos \beta}{\sqrt{C} r_b y_m} \left[\frac{4\sqrt{C} F r_b y_m \operatorname{cosec} \gamma}{W} - \frac{4B}{U} (Br_m + C) \right. \\ & \left. - \frac{2By_m}{W} (r_m + y_m) - Br_m^2 G - 2y_m \right] \end{aligned} \quad (A.4)$$

In Eqs. (A.1) - (A.4),

$$\begin{aligned} W &= 2\sqrt{C} Fr_b \sin \gamma + 2C + Br_b \\ G &= \frac{4A}{U} + \frac{1}{2C} \ln \left(\frac{Ur_b^2}{W^2} \right) + \frac{2Fr_b \sin \gamma}{\sqrt{C} W} \end{aligned}$$

$$\begin{aligned} \frac{\partial P'}{\partial f_c} = & \left[4 - \frac{4F^2}{A} - \frac{2B(F^2 + A)}{AV} \right] \frac{F^2 r_b \sin \gamma}{A f_c} \\ & + \frac{BF}{f_c A^{3/2}} \left[\frac{1}{2} \left(1 - \frac{3F^2}{A} \right) \ln \frac{U}{V^2} \right. \\ & \left. - \frac{4F^2 (C - Ar_o^2 \cos^2 \beta)}{U} - \frac{4F^2 r_b}{V} \right] \end{aligned} \quad (A.5)$$

$$\begin{aligned}
\frac{\partial P'}{\partial r_m} &= \frac{BF}{r_m y_m A^{3/2}} \left[\left(2 + \frac{B}{V} \right) \frac{F r_b \sin \gamma}{\sqrt{A}} \right. \\
&\quad + B \left(\frac{3}{4A} \ln \frac{U}{V^2} + \frac{2(A r_m r_b + C)}{U} + \frac{2 r_b}{V} \right) \\
&\quad \left. + (r_m + r_b) \left(\frac{1}{2} \ln \frac{U}{V^2} + \frac{B^2}{U} - \frac{B}{V} \right) \right] \tag{A.6}
\end{aligned}$$

$$\begin{aligned}
\frac{\partial P'}{\partial r_b} &= 2 \left(1 - \frac{F^2}{A} + \frac{BF^2}{AV} \right) \operatorname{cosec} \gamma \\
&\quad - \frac{BF}{r_b y_m A^{3/2}} \left[\left(2 + \frac{B}{V} \right) \frac{F r_b \sin \gamma}{\sqrt{A}} + \left(r_m + \frac{3B}{4A} \right) \ln \frac{U}{V^2} \right. \\
&\quad \left. + \frac{2B(A r_m^2 + B r_m + C)}{U} - \frac{2y_m (A r_b + B)}{V} \right] \tag{A.7}
\end{aligned}$$

APPENDIX 3

The computer program for the inversion of backscatter ionograms by utilizing the quasi-parabolic model is listed in the subsequent pages. In addition, this appendix contains a complete set of flow charts (with the exception of subroutine FMFP, which was written from the standard IBM scientific subroutine package), and a description of the input/output formats.

```

1 NAME MAIN
1 EQUIP=CARDRE,PRINTE,CARDPU;
  DIMENSION F(20),RBC(20),RMC(20),FCC(20),RANGEC(20),GPATHC(20),
1 FC(5,2),RB(5,20),RM(5,20),RANGE(5,20),GPATH(5,20),N(5),AZ(10)
  DIMENSION FMID(20)
202 CONTINUE
  READ 1,TLAT,TLONG,FCS,HO,YM,NAZ,IND
10 FORMAT(5F10.2,I1,9X,I1)
40 FORMAT(19X,6F10.2)
  RO=637.
  RBS=RO+HC
  RMS=RBS+YM
  I=1
25 FORMAT(I2)
50 READ 2,AZ(I),NUMTOT,NPTS
20 FORMAT(F10.2,I2,8X,I2)
  CALL BACKS3(NUMTOT,NPTS,RBS,RMS,FCS,RBC,RMC,FCC,FMID,RANGEC,
1 GPATHC,NC,1)
30 FORMAT(5F10.2)
  PRINT 35,(FCC(J),RBC(J),RMC(J),RANGEC(J),GPATHC(J),J=1,NC)
35 FORMAT(5X,5F10.4)
  N(I)=NC
  DO 60 J=1,NC
  FC(I,J)=FCC(J)
  RB(I,J)=RBC(J)
  RM(I,J)=RMC(J)
  RANGE(I,J)=RANGEC(J)
60 GPATH(I,J)=GPATHC(J)
  I=I+1
  IF (I-NAZ) 70,70,80
70 FC=FC(I)
  RBS=RBC(I)
  RMS=RMC(I)
  GO TO 50
80 IF (IND)180,85,180
85 READ 1,FW,AZM,GPM
  IF (FW)201,202,203
203 CONTINUE
  CALP=(6370.*6370.+6470.*6470-GPM*GPM/4.)/(2.*6370.*6470.)
  DEST=ACOSF(CALP)*6370.*2.
  PRINT 4,FW,AZM,GPM,DEST
  IF (NAZ-1)204,204,205
205 CONTINUE
  DO 100 K=1,NAZ
  IF (AZM-AZ(K)) 110,110,100
100 CONTINUE
110 FACTOR=(AZM-AZ(K-1))/(AZ(K)-AZ(K-1))
  N1=N(K)
  N2=N(K-1)
112 DO 120 J=1,N1
  IF (DEST-RANGE(K,J)) 130,130,120
120 CONTINUE
130 FACT=(DEST-RANGE(K,J-1))/(RANGE(K,J)-RANGE(K,J-1))
  FC1=FC(K,J-1)+FACTOR*(FC(K,J)-FC(K,J-1))
  RB1=RB(K,J-1)+FACTOR*(RB(K,J)-RB(K,J-1))
  RM1=RM(K,J-1)+FACTOR*(RM(K,J)-RM(K,J-1))
  PRINT 4,FC1,RB1,RM1
  DO 140 J=1,N2

```

```
IF (DEST-RANGE(K-1,J)) 150,150,140
140 CONTINUE
150 FACT=(DEST-RANGE(K-1,J-1))/(RANGE(K-1,J)-RANGE(K-1,J-1))
FC2=FC(K-1,J-1)+FACT*(FC(K-1,J)-FC(K-1,J-1))
RB2=RB(K-1,J-1)+FACT*(RB(K-1,J)-RB(K-1,J-1))
RM2=RM(K-1,J-1)+FACT*(RM(K-1,J)-RM(K-1,J-1))
PRINT 40,FC2,RB2,RM2
FC1=FC2+FACTOR*(FC1-FC2)
RBI=RB2+FACTOR*(RBI-RB2)
RMI=RM2+FACTOR*(RMI-RM2)
200 CONTINUE
PRINT 40,FC1,RBI,RMI
DTOL=1.
GPTOL=.1
CALL DCAL(FC1,RBI,RMI,FW,GPM,D,GRTOL)
PRINT 40,FW,AZM,GPM,DEST,D
IF (ABS(F(D-DEST)-DTOL) 170,170,160
160 DEST=D
IF(NAZ-1)204,204,112
170 PRINT 40,FW,AZM,GPM,D
GO TO 80
180 CONTINUE
READ 200, KGO
200 FORMAT(I10)
IF(KGO)201,202,201
201 CALL EXIT
204 N1=N(NAZ)
DO 206 J=1,N1
IF(DEST-RANGE(1,J))207,207,206
206 CONTINUE
207 FACT=(DEST-RANGE(1,J-1))/(RANGE(1,J)-RANGE(1,J-1))
FC1=FC(1,J-1)+FACT*(FC(1,J)-FC(1,J-1))
RBI=RB(1,J-1)+FACT*(RB(1,J)-RB(1,J-1))
RMI=RM(1,J-1)+FACT*(RM(1,J)-RM(1,J-1))
GO TO 200
END
```

PAGE 001

```
H      NAME A2
H      EQUIP=CARDRE,PRINTE,CARDPU;
      FUNCTION FOGX(ARG)
C*****SURR FOGX CHECKS TO MAKE SURE WE ARE NOT TAKING THE NATURAL LOG OF A
C*****NEG NUMBER...IF WE ARE IT FLAGS THE ERROR BY SETTING FOGX = 9999.
C*****THE INVALID ARGUMENT IS PRINTED OUT WITH AN ERROR MSG.
      IF(ARG)10,20,20
10     CONTINUE
      PRINT 15,ARG
15     FORMAT(29H LOGF ENTERED WITH NEG ARG = , E13.7)
      FOGX=9999.
      GO TO 30
20     FOGX=LOGF(ARG)
30     RETURN
      END
```

```

4     NAME AS
4     EQUIP=CARDRE,PRINTE,CARDPU
      SUBROUTINE FSTDFS(FW,FC,HB,YM,DGRT,GP,DGPDFC,DGPDRM,DGPDRB,RANGE,
      $DDFG)
C*****THIS SUBR COMPUTES THE MIN TIME DELAY TRACE(MIN GROUP PATH VS FREQ) OF A
C*****EARTH-CENTRIC Q-P IONOSPHERE LAYER AS WELL AS THE DERIVATIVES OF THE
C*****THE GROUP PATH WRT RB, RM AND FC. IT IS A HOPEFULLY MORE RAPID VERSION OF
C*****SURR DIFFS, WHICH DID NOT USE NEWTONS METHOD TO FIND THE ELEVATION ANGLE B
C*****BETA WHICH MINIMIZES THE GROUP PATH FUNCTION
C
C*****CALLING SEQUENCE
C***** FW=(INPUT) FREQ OF TRANSMISSION (MHZ)
C***** FC=(INPUT) CRITICAL FREQUENCY OF Q-P LAYER (IN MHZ)
C***** HB=(INPUT) BASE HEIGHT OF Q-P LAYER (IN KM)
C***** YM=(INPUT) SEMITHICKNESS OF Q-P LAYER (KM)
C***** DGRT=(INPUT) TOLERANCE OF GROUP PATH WRT ELEVATION ANGLE , BETA USED IN
C***** FINDING MINIMUM GROUP PATH IN KM/RAD
C***** GP=(OUTPUT) MIN GROUP PATH (KM)
C***** DGPDFC=(OUTPUT) DERIV OF MIN GROUP PATH WRT FC
C***** DGPDRM=(OUTPUT) DERIV MIN GROUP PATH WRT RM
C***** DGPDRB=(OUTPUT) DERIV MIN GROUP PATH WRT RB
C***** RANGE=(OUTPUT) GROUND RANGE OF BACKSCATTER PT OF MIN GROUP RAY
C
      R0=6370.
      R02=R0*R0
      RB=R0+HB
      RB2=RB*RB
      RM=RB+YM
      RM2=RM*RM
      YM2=YM*YM
      F=FW/FC
      F2=F*F
      RBYM2=RB2/YM2
      A=F2-1.+RBYM2
      SQA=SQROO(A)
      IF(SQA-9999.)50,950,50
C*****
950  NERPT=1
C*****
      GO TO 090
50   CONTINUE
      B=2.*RM*RBYM2
C*****NOW SET SOME CONSTANTS UP FOR FURTHER USE IN THE ITERATION LOOP
C*****THESE CONSTS HAVE NO SIGNIFICANCE IN THE 1974 PAPER BY NNR
      CON1=2.*A*RB*B
      CON2=2.*RB*F*SQA
      B2=B*B
      F2A=F2/A
      CON3=2.*R0*(1.-F2A )
      CON4=(B*F2A )*2.*R0
      CON5=4.*B*F2*F*R02/SQA
      CON6=R0/RB
      CON7=8.*A*F2*R02
C*****BETPEN IS THE PENETRATION FLEVATION ANGLE (BETA MUST BE BETWEEN 0
C*****AND BETPEN)
      SQROOX=SQROO(RM2*RBYM2-B2/(4.*A))
      IF(SQROOX-9999.)75,960,75
C*****

```

```

960  NERPT=2
C.....
    GO TC 900
75   CONTINUE
    BETPEN= ((1./(F*R0))*SORO0X)
    BETPEN = ACOSCK(BETPEN)
    IF(BETPEN-9999.)90,970,90
C.....
970  NERPT=3
C.....
    GO TC 900
90   CONTINUE
C.....INITIALIZE BETA, THE ELEVATION ANGLE OF THE GROUP RAY PUT THE INITIAL GUES
C.....RIGHT IN THE MIDDLE OF THE RANGE OF POSSIBLE BETA VALUES,
    BETA=BETPEN*.5
C.....ITERATE HERE FOR NEW VALUES OF BETA (AT STATEMENT 100) WHICH MINIMIZE
C.....THE GROUP PATH AT A GIVEN OPERATING FREQ FW (USING NEWTONS METHOD)
    NTRY=100
    ITERCT=0
100  SINBET=SIN(BETA)
    ITERCT=ITERCT+1
C.....IF WE HAVE TRIED TO FIND BETA SUCH THAT GP IS MINIMIZED TO WITHIN
C.....DGPT OF ZERO 100 TIMES LETS GIVE UP
    IF(ITERCT-NTRY)150,150,140
140  PRINT 145,DGPT,NTRY
145  FORMAT(//,48H FSTDIF ROUTINE CANNOT MINIMIZE DGPDB TO WITHIN ,
    $F5.3,10H KM AFTER ,I3,6H TRIES ,//)
    PRINT 147 ,BETA,DGPDB
147  FORMAT(8H BETA = ,F572.9H DGPDB = ,F10.5)
    RETURN
150  CONTINUE
    COSBET=COS(BETA)
    COSBE2=COSBET*COSBET
    C=RB*Y*M2*RM2-F2*R02*COSBE2
    COSGAM=R0*COSBET/RB
    GAMMA=ACOSCK(COSGAM)
    IF(GAMMA-9999.)165,971,165
C.....
971  NERPT=4
C.....
    PRINT 972,BETA,BETPEN,ITERCT
972  FORMAT(8H BETA = ,E12.5,5X,10H BETPEN = ,E12.5,5X,10H ITERCT = ,I4)
    $)
    GO TC 900
165  CONTINUE
    SINGAM=SINF(GAMMA)
    COTGAM=COSGAM/SINGAM
    V=CON1*CON2*SINGAM
    V2=V*V
    U=B2-4.*A*C
    U2=U*U
    F1=(CON3*CON4/V)
    G2=2.*R0*CON5*SINBET/U
    DGPDB=F1*SINBET*COTGAM-G2*COSBET
C.....BRANCH OUT OF NEWTON ITERATION LOOP HERE WHEN BETA IS FOUND WHICH
C.....MINIMIZES DGPDB TO WITHIN TOLERANGE DGPT (IN KM/RAD )
    IF(ABS(DGPDB)-DGPT)800,350,350
350  CONTINUE

```

```

SQROOY=SQROO(1.-(CON6*COSBET)**2.)
IF(SQROOY-9999.)375,973,375
*****
973  NERPT=5
*****
PRINT 972,BETA,BETPEN,ITERCT
GO TO 900
375  CONTINUE
DGAMDB=SINBET*CON6/SQROOY
DCOTDB=-DGAMDB/(SINGAM*SINGAM)
DVNB=CON2*CONSGAM*DGAMDB
DF1DB=(CON4/V2)*DVNB
DUDB=-CON7*COSBET*SINBET
DF2DB=CON5*(COSBET/U-(SINBET/U2)*DUDB)
DGPDB2=DF1DB*SINBET+COTGAM*F1*(COSBET*COTGAM+SINBET*DCOTDB)
S=DF2DB*COSBET+G2*SINBET
BETA=BETA-DGPDB/DQPDB2
*****IF BETA HAS BEEN INCREMENTED TO A NEG VALUE BY NEWTONS METHOD WE BETTER SE
*****BETTER SET BETA BACK TO A LITTLE ABOVE 0 OR WE MIGHT HAVE TROUBLES LATER 0
IF(BETA)400,400,500
400  BETA=.0001
500  IF(BETPEN-BETA)600,600,700
600  BETA=BETPEN-.0001
*****CHECK TO ENSURE NEWTONS METHOD IS NOT CAUSING US TO OVERSTEP THE
*****PENETRATION ELEVATION ANGLE BOUNDARY. IF SO SET BETA BACK TO LITTLE BELOW
*****BETPEN
700  GO TO 100
800  CONTINUE
*****AT STATEMENT 800 THE ELEVATION ANGLE BETA CORRESPONDING TO THE MINIMUM GRO
*****GROUP PATH HAS BEEN COMPUTED BY SOLVING FOR THE VALUE OF BETA WHICH FORCES
*****DGPDB TO 0. NOW WE CAN COMPUTE THE MINIMUM GROUP PATH GPM
UV2LOG=FOGX(U/V2)
IF(UV2LOG-9999.)850,974,850
*****
974  NERPT=6
*****
GO TO 930
850  CONTINUE
BFA32=P*F/(A*SQA)
GPM=CON3/CON6*SINGAM-2.*R0*SINBET
S=(BFA32*.5)*UV2LOG
GP=GPM
DPDFC1=2.*CON3/R0-2.*B*(F2+A)/(A*V)
DPDFC2=F2*RB*SINGAM/(A*FC)
DPDFC3=BFA32/FC
DPDFC4=.5*(1.-3.*F2A)*UV2LOG-4.*F2*(C-A*R02*COSB2)/U
S=4.*F2*RB/V
DGDRC=DPDFC1*DPDFC2+DPDFC3*DPDFC4
DPDRM2=.75/A*UV2LOG+2.*(A*RM*RB*G)/U+2.*RB/V
DPDRM1=BFA32/(RM*YM)
DPDRM3=(2.*B/V)*F*RB*SINGAM/SQA+B*DPDRM2+(RM+RB)*(S*UV2LOG+B2/U-B/V)
S/V)
DGDRC=DPDRM1*DPDRM3
DPDRB1=(CON3+CON4/V)/(R0*SINGAM)
DPDRB2=-BFA32/(RB*YM)*((2.*B/V)*F*RB*SINGAM/SQA+(RM+.75*B/A)*UV2LO
SG+2.*B*(A*RM2+B*RM+C)/U+2.*YM*(A*RB*B)/V)
DGDRC=DPDRB1+DPDRB2
SQC=SQROO(C)

```

```
IF(SQC-9999.)875,975,875
C.....
975  NERPT=7
C.....
      GO TO 980
475  CONTINUE
      R1=2.*SQC*RB*F*SINGAM*2.*C+B*RB
      R12=R1/R1
      W=FOGX(U*RB2/R12)
      R3=.5*F*RO*COSEBET*W/SQC
      RANGE=2.*RO*(GAMMA-BETA-R3)
      BDEG=BETA*57.2985
      RETURN
900  FC=-ABS(F)
      PRINT 980,NERPT
980  FORMAT(1X,100(1H)),/,30H FETDFS ERROR AT POINT NUMBER ,I2,/,1X,
      $100(1H))
      PRINT 985,FW,FC,HB,YM,DGPT
985  FORMAT(1X,5E15.7)
      RETURN
      END
```

```

H NAME A4
H EQUIP=CARDRE,PRINTE,CARDPU,
  SURROUTINE FUNCT(N,ARG,VAL,GRAD)
  DIMENSION ARG(3),GRAD(3),FBSMES(50),PBSMES(50),GPC(50),DGPC(50,3)
  DIMENSION RAN(50),BTA(50)
  COMMON FBSMES,PBSMES,DT,NPTS,RAN,BTA,GPCMID
C
C*****SUBROUTINE FUNCT TO BE USED BY BACKS3 BACKSCATTER IONOGRAM INVERSION
C*****ROUTINE. IT EVALUATES THE SUM SQUARED ERROR AND ITS GRADIENT AS A
C*****FUNCTION OF Q-P LAYER PARAMETERS RB, RM, FC,
C
C*****CALLING SEQUENCE.....
C*****N=(INPUT) CONTROL PARAMETER
C***** IF N=3 FUNCTION NORMALLY, RETURN VALUE OF ERROR FUNCTION AND ITS
C***** GRADIENT
C*****ARG=(INPUT) 3 ELEMENT ARRAY OF LAYER PARAMETERS
C***** ARG(1)=RB
C***** ARG(2)=RM
C***** ARG(3)=FC
C*****VAL -(OUTPUT)VALUE OF ERROR FUNCTION E CORRESPONDING TO CURRENT VALUE OF
C***** ARG
C*****GRAD=(OUTPUT) 3 ELEMENT ARRAY WITH
C***** GRAD(1)=DE/DRB
C***** GRAD(2)=DE/DRM
C***** GRAD(3)=DE/DFC
C*****END OF INPUT SEQUENCE*****
C
FC=ARG(3)
HB=ARG(1)-6370.
YM=ARG(2)-ARG(1)
C*****HERE N=3 AND WE WILL EVALUATE E AND GRAD OF E
C*****FIRST INITIALIZE VALUES FOR SUBSEQUENT SUMMING OPERATION
40 SUMF=0
  SUMDRB=0
  SUMDRM=0
  SUMDFC=0
  NMID=NPTS/2+1
  DO 50 I=1,NPTS
C*****FSTDFS CALLED TO EVALUATE MIN GROUP PATH AND ITS DERIVS WRT RB,RM,FC AS A
C*****FUNCTION OF FBSMES(I), THE ITH TRANSMISSION FREQ
  FBSM=FBSMES(I)
  ITRY=0
  CALL FSTDFS(FBSM,FC,HB,YM,DT,GPC(I),DGPC(I,1),DGPC(I,2),
  SDGPC(I,3),RA,BT)
  RAN(I)=RA
  BTA(I)=BT
C*****CATCH AND STORE THE FINAL VALUE OF THE GROUP PATH CORRESPONDING TO THE MID
C*****BACKSCATTER LEADING EDGE POINT
  IF(I=NMID)46,47,46
47 GPCMID=GPC(I)
46 CONTINUE
C NUMERICAL ERROR FLAGGED IF FC NEGATIVE . IF SO ABORT JOB BY MAKING N
C NEGATIVE AND RETURNING TO MAINLINE VIA SUBR FMFP
  IF(FC)42,45,45
42 N=3
  ARG(1)=A1SV
  ARG(2)=A2SV
  ARG(3)=A3SV

```

```
VAL=VALSV
G1SV=GRAD(1)
G2SV=GRAD(2)
G3SV=GRAD(3)
RETURN
45 CONTINUE
ERR=GPC(I)-PBSMES(I)
ERSQ=ERR*ERR
SUMF=SUMF+ERSQ
SUMDRB=SUMDRB+ERR*DGPC(I,3)
SUMDRM=SUMDRM+ERR*DGPC(I,2)
50 SUMDFC=SUMDFC+ERR*DGPC(I,1)
C*****NOTE SUMF NOW CONTAINS SUM SQUARED ERROR
C*****GRAD CONTAINS THE GRADIENT OF THE SUM SQUARED ERROR
VAL=SUMF
GRAD(1)=2.*SUMDRB
GRAD(2)=2.*SUMDRM
GRAD(3)=2.*SUMDFC
C
C*****
C***** NOTE THAT AT THIS POINT IT MEAY BE DESIRABLE TO INSERT PRINT OUT STATEMEN
C*****TO OUTPUT ARG, VAL,GRAD,RANGE,AND BDEG TO OBSERVE CONVERGENCE OF THE ERROR
C*****FUNCTION TO A MINIMUM AS FMFP DOES ITS STUFF.....
C*****ALRO PRINTING OUT RANGE AND BDEG GIVES US SOME INDICATION OF WHERE WE ARE
C*****SAMPLING THE IONOSPHERE IN THE CASE OF HORIZONTAL GRADIENTS
C*****
C
A1SV=ARG(1)
A2SV=ARG(2)
A3SV=ARG(3)
VALSV=VAL
G1SV=GRAD(1)
G2SV=GRAD(2)
G3SV=GRAD(3)
200 RETURN
END
```

```

H NAME AM
H EQUIP=CARDRE,PRINTE,CARDPU;
  SUBROUTINE FMFP(N,X,F,G,EST,EPS,LIMIT,IER,H)
C
C   DIMENSIONED DUMMY VARIABLES
C   DIMENSION H(1),X(1),G(1)
C
C   COMPUTE FUNCTION VALUE AND GRADIENT VECTOR FOR INITIAL ARGUMENT
CALL FUNCT(N,X,F,G)
IF(N)54,100,100
100 CONTINUE
C
C   RESET ITERATION COUNTER AND GENERATE IDENTITY MATRIX
IER=0
KOUNT=0
N2=N*N
N3=N2+N
N31=N3+1
1 K=N31
DO 4 J=1,N
  H(K)=1.
  NJ=N-J
  IF(NJ)5,5,2
2 DO 3 L=1,NJ
  KL=K+L
3 H(KL)=.
4 K=KL+1
C
C   START ITERATION LOOP
5 KOUNT=KOUNT +1
C
C   SAVE FUNCTION VALUE, ARGUMENT VECTOR AND GRADIENT VECTOR
OLDF=F
DO 9 J=1,N
  K=N+J
  H(K)=G(J)
  K=K+N
  H(K)=X(J)
C
C   DETERMINE DIRECTION VECTOR H
K=J+N3
T=0.
DO 8 L=1,N
  T=T-G(L)*H(K)
  IF(L-J)6,7,7
6 K=K+N-L
  GO TO 8
7 K=K+1
8 CONTINUE
9 H(J)=T
C
C   CHECK WHETHER FUNCTION WILL DECREASE STEPPING ALONG H.
DY=0.
MNRM=0.
GNRM=0.
C
C   CALCULATE DIRECTIONAL DERIVATIVE AND TESTVALUES FOR DIRECTION
  VECTOR H AND GRADIENT VECTOR G.

```

```

FMFP 20
FMFP 30
FMFP 40
FMFP 50
FMFP 60
FMFP 70
FMFP 80
FMFP 90
FMFP 100
FMFP 110
FMFP 120
FMFP 130
FMFP 140
FMFP 150
FMFP 160
FMFP 170
FMFP 180
FMFP 190
FMFP 200
FMFP 210
FMFP 220
FMFP 230
FMFP 240
FMFP 250
FMFP 260
FMFP 270
FMFP 280
FMFP 290
FMFP 300
FMFP 320
FMFP 330
FMFP 340
FMFP 350
FMFP 360
FMFP 370
FMFP 380
FMFP 390
FMFP 400
FMFP 410
FMFP 420
FMFP 430
FMFP 440
FMFP 450
FMFP 460
FMFP 470
FMFP 480
FMFP 490
FMFP 500
FMFP 510
FMFP 520
FMFP 530
FMFP 540

```

| | | |
|-----|--|----------|
| | DO 10 J=1,N | FMFP 550 |
| | HNRM=HNRM+ABSF(H(J)) | FMFP 560 |
| | GMRM=GMRM+ABSF(G(J)) | FMFP 570 |
| | 10 DY=DY+H(J)*G(J) | FMFP 580 |
| C | | FMFP 590 |
| C | REPEAT SEARCH IN DIRECTION OF STEEPEST DESCENT IF DIRECTIONAL | FMFP 600 |
| C | DERIVATIVE APPEARS TO BE POSITIVE OR ZERO. | FMFP 610 |
| | IF(DY)11,51,51 | FMFP 620 |
| C | | FMFP 630 |
| C | REPEAT SEARCH IN DIRECTION OF STEEPEST DESCENT IF DIRECTION | FMFP 640 |
| C | VECTOR H IS SMALL COMPARED TO GRADIENT VECTOR G. | FMFP 650 |
| | 11 IF(HNRM/GMRM-EPS)51,51,12 | FMFP 660 |
| C | | FMFP 670 |
| C | SEARCH MINIMUM ALONG DIRECTION H | FMFP 680 |
| C | | FMFP 690 |
| C | SEARCH ALONG H FOR POSITIVE DIRECTIONAL DERIVATIVE | FMFP 700 |
| | 12 FY=F | FMFP 710 |
| | ALFA=2.*(EST-F)/DY | FMFP 720 |
| | AMBDA=1. | FMFP 730 |
| C | | FMFP 740 |
| C | USE ESTIMATE FOR STEPSIZE ONLY IF IT IS POSITIVE AND LESS THAN | FMFP 750 |
| C | 1. OTHERWISE TAKE 1. AS STEPSIZE | FMFP 760 |
| | IF(ALFA)15,15,13 | FMFP 770 |
| | 13 IF(ALFA-AMBDA)14,15,15 | FMFP 780 |
| | 14 AMBDA=ALFA | FMFP 790 |
| | 15 ALFA=0. | FMFP 800 |
| C | | FMFP 810 |
| C | SAVE FUNCTION AND DERIVATIVE VALUES FOR OLD ARGUMENT | FMFP 820 |
| | 16 FX=FY | FMFP 830 |
| | DX=DY | FMFP 840 |
| C | | FMFP 850 |
| C | STEP ARGUMENT ALONG H | FMFP 860 |
| | DO 17 I=1,N | FMFP 870 |
| | 17 X(I)=X(I)+AMBDA*H(I) | FMFP 880 |
| C | | FMFP 890 |
| C | COMPUTE FUNCTION VALUE AND GRADIENT FOR NEW ARGUMENT | FMFP 900 |
| | CALL FIINCT(N,X,F,G) | FMFP 910 |
| | FY=F | FMFP 920 |
| | IF(N)54,101,101 | |
| 101 | CONTINUE | |
| C | | FMFP 930 |
| C | COMPUTE DIRECTIONAL DERIVATIVE DY FOR NEW ARGUMENT. TERMINATE | FMFP 940 |
| C | SEARCH, IF DY IS POSITIVE. IF DY IS ZERO THE MINIMUM IS FOUND | FMFP 950 |
| | DY=0. | FMFP 960 |
| | DO 18 I=1,N | FMFP 970 |
| | 18 DY=DY+G(I)*H(I) | FMFP 980 |
| | IF(DY)19,36,22 | FMFP 990 |
| C | | FMFP1000 |
| C | TERMINATE SEARCH ALSO IF THE FUNCTION VALUE INDICATES THAT | FMFP1010 |
| C | A MINIMUM HAS BEEN PASSED | FMFP1020 |
| | 19 IF(FY-FX)20,22,22 | FMFP1030 |
| C | | FMFP1040 |
| C | REPEAT SEARCH AND DOUBLE STEPSIZE FOR FURTHER SEARCHES | FMFP1050 |
| | 20 AMBDA=AMBDA*ALFA | FMFP1060 |
| | ALFA=AMBDA | FMFP1070 |
| C | END OF SEARCH LOOP | FMFP1080 |
| C | | FMFP1090 |
| C | TERMINATE IF THE CHANGE IN ARGUMENT GETS VERY LARGE | FMFP1100 |

```

      IF (HARM*AMBDA-1.E10)16,16,21
C
C      LINEAR SEARCH TECHNIQUE INDICATES THAT NO MINIMUM EXISTS
21 IER=2
      RETURN
C
C      INTERPOLATE CUBICALLY IN THE INTERVAL DEFINED BY THE SEARCH
C      ABOVE AND COMPUTE THE ARGUMENT X FOR WHICH THE INTERPOLATION
C      POLYNOMIAL IS MINIMIZED
22 T=0.
23 IF (AMBDA)24,36,24
24 Z=3.*(FX-FY)/AMBDA+DX+DY
      ALFA=MAX1F (ABSF(Z),ABSF(DX),ABSF(DY))
      DALFA=7/ALFA
      DALFA=DALFA+DALFA-DX/ALFA+DY/ALFA
      IF (DALFA)51,25,25
25 W=ALFA*SQRT(DALFA)
      ALFA=(DY+W-Z)*AMBDA/(DY+2.*W-DX)
      DO 26 I=1,N
26 X(I)=X(I)+(T-ALFA)*H(I)
C
C      TERMINATE, IF THE VALUE OF THE ACTUAL FUNCTION AT X IS LESS
C      THAN THE FUNCTION VALUES AT THE INTERVAL ENDS. OTHERWISE REDUCE
C      THE INTERVAL BY CHOOSING ONE END-POINT EQUAL TO X AND REPEAT
C      THE INTERPOLATION. WHICH END-POINT IS CHOSEN DEPENDS ON THE
C      VALUE OF THE FUNCTION AND ITS GRADIENT AT X
      CALL FUNCT(N,X,F,G)
      IF (N) 56,102,102
102 CONTINUE
      IF (F-FX)27,27,28
27 IF (F-FY)36,36,28
28 DALFA=1.
      DO 29 I=1,N
29 DALFA=DALFA+G(I)*H(I)
      IF (DALFA)30,33,33
30 IF (F-FY)32,31,33
31 IF (DX-DALFA)32,36,32
32 FX=F
      DX=DALFA
      T=ALFA
      AMBDA=ALFA
      GO TO 23
33 IF (FY-F)35,34,35
34 IF (DY-DALFA)35,36,35
35 FY=F
      DY=DALFA
      AMBDA=AMBDA-ALFA
      GO TO 22
C
C      COMPUTE DIFFERENCE VECTORS OF ARGUMENT AND GRADIENT FROM
C      TWO CONSECUTIVE ITERATIONS
36 DO 37 J=1,N
      K=N+J
      H(K)=G(J)-H(K)
      K=N+K
37 H(K)=X(J)-H(K)
C

```

```

FMFP1110
FMFP1120
FMFP1130
FMFP1140
FMFP1150
FMFP1160
FMFP1170
FMFP1180
FMFP1190
FMFP1200
FMFP1210
FMFP1220
FMFP1230
FMFP1240
FMFP1250
FMFP1260
FMFP1270
FMFP1280
FMFP1290
FMFP1300
FMFP1310
FMFP1320
FMFP1330
FMFP1340
FMFP1350
FMFP1360
FMFP1370
FMFP1380
FMFP1390
FMFP1400
FMFP1410
FMFP1420
FMFP1430
FMFP1440
FMFP1450
FMFP1460
F=FP1 70
FMFP1480
FMFP1490
FMFP1500
FMFP1510
FMFP1520
FMFP1530
FMFP1540
FMFP1550
FMFP1560
FMFP1570
FMFP1580
FMFP1590
FMFP1600
FMFP1610
FMFP1620
FMFP1630
FMFP1640
FMFP1650
FMFP1660

```

| | | |
|---|--|----------|
| C | TERMINATE, IF FUNCTION WAS NOT DECREASED DURING LAST ITERATION | FMFP1670 |
| | IF(OLDF-F+EPS)51,38,38 | FMFP1680 |
| C | | FMFP1690 |
| C | TEST LENGTH OF ARGUMENT DIFFERENCE VECTOR AND DIRECTION VECTOR | FMFP1700 |
| C | IF AT LEAST N ITERATIONS HAVE BEEN EXECUTED, TERMINATE, IF | FMFP1710 |
| C | BCTM ARE LESS THAN EPS | FMFP1720 |
| | 38 IER=0 | FMFP1730 |
| | IF(KOUNT=N)42,39,39 | FMFP1740 |
| | 39 T=0. | FMFP1750 |
| | Z=0. | FMFP1760 |
| | DO 40 J=1,N | FMFP1770 |
| | K=N+J | FMFP1780 |
| | W=H(K) | FMFP1790 |
| | K=K+N | FMFP1800 |
| | T=T+ABS(F(H(K))) | FMFP1810 |
| | 40 Z=Z+W*W(K) | FMFP1820 |
| | IF(HNRM-EPS)41,41,42 | FMFP1830 |
| | 41 IF(T=EPS)55,55,42 | |
| C | | FMFP1850 |
| C | TERMINATE, IF NUMBER OF ITERATIONS WOULD EXCEED LIMIT | FMFP1860 |
| | 42 IF(KOUNT=LIMIT)43,50,50 | FMFP1870 |
| C | | FMFP1880 |
| C | PREPARE UPDATING OF MATRIX H | FMFP1890 |
| | 43 ALFA=0. | FMFP1900 |
| | DO 47 J=1,N | FMFP1910 |
| | K=J+N3 | FMFP1920 |
| | W=0. | FMFP1930 |
| | DO 46 L=1,N | FMFP1940 |
| | KL=N+L | FMFP1950 |
| | W=W+H(KL)*H(K) | FMFP1960 |
| | IF(L=J)44,45,45 | FMFP1970 |
| | 44 K=K+N-L | FMFP1980 |
| | GO TO 46 | FMFP1990 |
| | 45 K=K+1 | FMFP2000 |
| | 46 CONTINUE | FMFP2010 |
| | K=N+J | FMFP2020 |
| | ALFA=ALFA+W*H(K) | FMFP2030 |
| | 47 H(J)=W | FMFP2040 |
| C | | FMFP2050 |
| C | REPEAT SEARCH IN DIRECTION OF STEEPEST DESCENT IF RESULTS | FMFP2060 |
| C | ARE NOT SATISFACTORY | FMFP2070 |
| | IF(Z=ALFA)48,1,48 | FMFP2080 |
| C | | FMFP2090 |
| C | UPDATE MATRIX H | FMFP2100 |
| | 48 K=N31 | FMFP2110 |
| | DO 49 L=1,N | FMFP2120 |
| | KL=N2+L | FMFP2130 |
| | DO 49 J=L,N | FMFP2140 |
| | NJ=N2+J | FMFP2150 |
| | H(K)=H(K)+H(KL)+H(NJ)/Z=H(I)+H(J)/ALFA | FMFP2160 |
| | 49 K=K+1 | FMFP2170 |
| | GO TO 4 | FMFP2180 |
| C | END OF ITERATION LOOP | FMFP2190 |
| C | | FMFP2200 |
| C | NO CONVERGENCE AFTER LIMIT ITERATIONS | FMFP2210 |
| | 50 IER=1 | FMFP2220 |
| | RETURN | FMFP2230 |
| C | | FMFP2240 |

| | | |
|-----|--|----------|
| C | RESTORE OLD VALUES OF FUNCTION AND ARGUMENTS | FMFP2250 |
| 51 | DO 52 J=1,N | FMFP2260 |
| | K=N2+J | FMFP2270 |
| 52 | X(J)=H(K) | FMFP2280 |
| | CALL FUNCT(N,X,F,G) | FMFP2290 |
| | IF(N)56,103,103 | |
| 103 | CONTINUE | |
| C | | FMFP2300 |
| C | REPEAT SEARCH IN DIRECTION OF STEEPEST DESCENT IF DERIVATIVE | FMFP2310 |
| C | FAILS TO BE SUFFICIENTLY SMALL | FMFP2320 |
| | IF(GRM-EPS)55,55,53 | FMFP2330 |
| C | | FMFP2340 |
| C | TEST FOR REPEATED FAILURE OF ITERATION | FMFP2350 |
| 53 | IF(IER)56,54,54 | FMFP2360 |
| 54 | IER=-1 | FMFP2370 |
| | GOTO 1 | FMFP2380 |
| 55 | IER=0 | FMFP2390 |
| | PRINT 57,KOUNT | |
| 57 | FORMAT(//,22H FMFP CONVERGED AFTER ,I4,11H ITERATIONS ,//) | |
| 56 | RETURN | FMFP2400 |
| | END | FMFP2410 |

```

H     NAME A6
H     EQUIP=CARDRE,PRINTE,CARDPU;
      SUBROUTINE BACKS3(NUMTOT,NPTX,RBSTRT,RMSTRT,FCSTRT,RBB,RMM,FCC,
      FMID,RANMID,GPTHMD,NUSED,PRNTSW)
      DIMENSION X(3),G(3),H(32)
      DIMENSION FBSMES(50),PBSMES(50)
      DIMENSION RAN(50),BTA(50),RBB(20),RMM(20),FCC(20),FMID(20)
      DIMENSIONRANMID(20),GPTHMD(20)
      COMMON FBSMES,PBSMES,DT,NPTS,RAN,BTA,GPCMID
C*****
C*****THIS IS SUBROUTINE FOR THE MIN SUM SQUARED ERROR NOISY BACKSCATTER LEADING
C*****EDGE INVERSION PROCEDURE...
C*****DESCRIBED IN QUARTERLY REPORTS 3,4,5 OF DR. YEH AND DR. RAO S AIR FORCE
C***** (AFCL) CONTRACT NUMBER F 19628-75-C-0088, 1975-1976
C
C
C
C
C     SUBROUTINE INPUT PARAMETERS FOLLOW.....
C
C     NUMTOT=TOTAL NUMBER OF POINTS SCALED FROM IONOGRAM BACKSCATTER LEADING
C           EDGE WHICH ARE TO BE INVERTED IN GROUPS OF NPTS
C     NPTS=NUMBER OF POINTS IN EACH GROUP OF DATA THAT WILL BE SUCCESSIVELY INV
C
C           FOR EXAMPLE...TO PROCESS 12 BACKSCATTER IONOGRAM PTS BY INVERTING
C           OVERLAPPING GROUPS OF 4 POINTS AT A TIME, WE LET NUMTOT=12AND
C           NUMGRP=4.
C
C           NOTE THAT THE STARTING SET OF ESTIMATED LAYER PARAMETERS IS USED
C           IN INVERTING THE FIRST SET OF BACKSCATTER LEADING EDGE POINTS. EACH
C           SUBSEQUENT SET USES THE IMMEDIATELY PRECEDING SOLUTION AS THE
C           STARTING POINT.
C
C     RBSTRT=STARTING VALUE RB IN KM
C     RMSTRT=STARTING VALUE RM IN KM
C     FCSTRT=STARTING VALUE FC IN MHZ
C
C     OUTPUT PARAMETER DEFNS.....
C     RBB=VECTOR OF RB PARAMETERS OBTAINED FROM THE SUCCESSIVE INVERSION OF THE
C           SETS OF NPTS POINTS
C     RMM=VECTOR OF RM PARAMETERS
C     FCC=VECTOR OF FC PARAMETERS
C     FMID=VECTOR OF THE FREQUENCIES CORRESPONDING TO THE MIDDLE BACKSCATTER
C           LEADING EDGE POINT IN THE SUCCESSIVE SETS OF NPTS POINTS
C     RANMID=VECTOR OF RANGES IN KM
C     GPTHMD=VECTOR OF GROUP PATHS IN KM
C     NUSED=NUMBER OF SETS OF NPTS POINTS SUCCESSFULLY INVERTED FROM
C           BACKSCATTER LEADING EDGE
C     PRNTSW=J=DO NOT PRINT INTERMEDIATE RESULTS
C     PRNTSW=1=PRINT INTERMEDIATE RESULTS
C
C*****DESCRIPTION OF DATA DECK TO BE READ IN BY SUBROUTINE
C
C*****PARAMETER CARD DESCRIPTION IN 4F10.5 FORMAT
C*****DT IS THE TOLERANCE IN THE DERIV OF THE MINIMUM GROUP PATH WITH RESPECT
C***** TO BETA, TYPICALLY SET TO .05 KM/RAD.
C***** EST = ESTIMATED MIN VALUE OF SUM-SQUARED ERROR FUNCTION E (IN SQ KM)

```

```

C***** UPON WHICH THE MINIMIZATION PROCEDURE BASES ITS STEPSIZE
C***** EPS=TOL TO WHICH MINIMUM IS TO BE COMPUTED (SUBR FMFP USES IT TO DETERM
C***** WHEN TO TERMINATE MINIMIZATION ITERATIONS)
C***** LIMIT=MAXIMUM NUMBER OF ITERATIONS ALLOWED IN MINIMIZATION ITERATION
C***** LOOP BEFORE GIVING UP
C

```

```

      NPTS=NPTX
      X(1)=RRSTRT
      X(2)=RMSTRT
      X(3)=FCSTRT
C***** X(1)=STARTING VALUE RB IN KM
C***** X(2)=STARTING VALUE RM IN KM
C***** X(3)=STARTING VALUE FC IN MHZ
      READ 1,DT,EST,EPS,XLIMIT
10    FORMAT(4F10.5)
      LIMIT=XLIMIT
      NUMSET=NUMTOT-NPTS+1
      NUMED=NUMSET
      JARRAY=1
      DO 101 ICT=1,NUMSET
C*****SAVE STARTING VALUES IN CASE WE WANT TO ABORT ATTEMPT AND TRY AGAIN
      XSV1=X(1)
      XSV2=X(2)
      XSV3=X(3)
C*****KT=0 INDICATES FIRST ATTEMPT AT MINIMIZATION
      KT=0
      ESTSVE=EST
C*****FIRST INITIALIZE FUNCT BY READING IN
C*****IN AND PRINT OUT THE NUMPT POINTS SCALED OFF LEADING EDGE OF BS IONOGRAM
C*****AS WELL AS READ IN THE TOLERANCE TO WHICH THE MIN GROUP PATH IS FOUND IN
C*****SUBROUTINE FSTDIF AND THE NUMBER OF IONOGRAM PTS USED IN DEFINING THE ERRO
C*****ERROR FUNCTION E. IN SUBROUTINE FUNCT...
      IF(PRNTSW)119,121,119
119   CONTINUE
      PRINT 12, DT
C*****DT IS THE TOLERANCE OF DERIV OF GROUP PATH WRT BETA (KM/RAD)
C*****FOR USE IN FSTDIF ROUTINE WHEN IT COMPUTES THE MIN GROUP PATH
12    FORMAT(/,54H1TOLERANCE OF DERIV OF GROUP PATH WRT BETA (KM/RAD) =
      $      ,F5.3//)
C*****NPTS IS THE NUMBER OF POINTS SCALED FROM LEADING EDGE OF B S IONOGRAM
C*****FOR USE IN EVALUATING THE SUM SQUARED ERROR FCN
      PRINT 13,NPTS
121   CONTINUE
13    FORMAT(/, 61H NUMBER OF SCALED IONOGRAM POINTS TO BE USED IN ERROR
      $ FCN = ,I2)
      IF(ICT -1)130,125,130
125   READ 16,(FBSMES(I),PBSMES(I),I=1,NPTS)
C*****HERE THE LEADING EDGE POINTS ARE READ IN
16    FORMAT (2F10.5)
      GO TO 150
130   DO 145 IND=2,NPTS
      FBSMES(IND-1)=FBSMES(IND)
145   PBSMES(IND-1)=PBSMES(IND)
      READ 16,FBSMES(NPTS),PBSMES(NPTS)
150   CONTINUE
      IF (PRNTSW)151,201,151
151   CONTINUE
      PRINT 17

```

```

17  FORMAT(53H MEASURED POINT ON BACKSCATTER IONOGRAM LEADING EDGE ,
      $/,9X,14HFREQUENCY (MHZ) ,4X,6X,15HGROUP PATH(KM) )
      PRINT 19,(FBSMES(I),PBSMES(I),I=1,NPTS)
19  FORMAT(/,11X,F8.3,19X,F8.3,/)
      PRINT 20,X(1),X(2),X(3),EST,EPS,LIMIT
20  FORMAT( 26H STARTING VALUE RB (KM) = ,F8.4,8X,
      $25H STARTING VALUE RM(KM) = ,F8.4,8X,
      $27H STARTING VALUE FC (MHZ) = ,F8.6,/,
      $37H ESTIMATE OF MIN SUM SQUARED ERROR = ,F10.5,/,
      $27H EXPECTED ABSOLUTE ERROR = ,F10.8,/,
      $32H MAXIMUM NUMBER OF ITERATIONS = ,I4////)
      N=3
      CALL FUNCT(N,X,VAL,G)
      PRINT 21,VAL,G
21  FORMAT(33H INITIAL SUM SQUARED ERROR (E) = , E12.5,/,
      $9H DEDRB = ,E12.5,5X,
      $9H DEDRM = ,E12.5,5X,
      $9H DEDFC = ,E12.5,/)
201  CONTINUE
      N=3
      OLDMIN=99999.
C*****THIS BUSINESS ABT OLDMIN HAS TO DO WITH NUMERICAL ERROR PROB IN FSTDIF SUB
C*****SEE STATEMENT 2600 TO SEE WHAT I AM TALKING ABOUT
C*****FMFP IS THE NONLINEAR MINIMIZATION ROUTINE FOUND IN IBM SCIENTIFIC SUBR
C*****SUBROUTINE PACKAGE. IT INTERNALLY CALLS FUNCT TO PERFORM SUCCESSIVE
C*****EVALUATIONS OF THE SUM SQUARED ERROR FUNCTION AND ITS GRADIENT
22  CALL FMFP(N,X,FMIN,G,EST,EPS,LIMIT,IER,H)
C*****IF NUMERICAL ERRORS SUCH AS SORT (NEG NUMBER), LOG(LESS THAN 0), OR
C*****ACOS(GREATER THAN 1) WERE FLAGGED IN THE EVALUATION OF FUNCT, N IS
C*****NEGATED AND SO WE TEST FOR THIS ERROR CONDITIP= UPON EXIT FROM FMFP
      IF(N)25,27,27
25  PRINT 26,KT,EST
26  FORMAT(///30H NUMERICAL ERRORS ON TRY NR = ,I2,16H WITH EST MIN =
      $ = ,F7.5,///)
      KT=KT+1
C*****SET N BACK TO +3
      N=-N
      CALL FUNCT(N,X,FMIN,G)
C*****EVALUATE FMIN ON BASIS OF PARTIALLY ITERATED PARAMETERS JUST BEFORE NUMERI
C*****NUMERICAL PROBLEMS WERE ENCOUNTERED
      IF(OLDMIN-FMIN)2610,2610,2600
2600  SOLN1=X(1)
      SOLN2=X(2)
      SOLN3=X(3)
      SVMIN=FMIN
      GSV1=G(1)
      GSV2=G(2)
      GSV3=G(3)
      OLDMIN=FMIN
2610  CONTINUE
C*****IF THIS IS 7TH TRY GIVE UP ENTIRELY
      IF(KT=7)260,270,270
C*****IF NUMERICAL ERRORS, ALTER EST, WHICH WILL DECREASE THE STEP SIZE AND TRY
C*****TRY AGAIN, FIRST GO BACK TO ORIGINAL STARTING SOLUTION
260  IF(FMIN-EST)262,262,261
C*****IF OUR ESTIMATE WAS TOO SMALL INCREASE IT
261  EST=EST*10.
      GO TO 263

```

```

C*****IF OUR ESTIMATE WAS TOO LARGE DECREASE IT
262 EST=EST/10.
263 CONTINUE
      X(1)=X*V1
      X(2)=X*V2
      X(3)=X*V3
C*****NOW GO BACK TO 22 AND TRY AGAIN
      GO TO 22
270 PRINT 271
271 FORMAT(///,57H WILL GIVE UP TRYING TO INVERT THIS DATA AFTER 7 ATTE
      SMPYS,/)
      PRINT 275
275 FORMAT(100(1HS),/,106H WILL USE LAST VALUES OF ITERATED PARAMETERS
      $ BEFORE NUMERICAL PROBLEM OCCURRED=-NOTE FMFP DID NOT CONVERGE,/,
      $,100(1HS),/)
      X(1)=SOLN1
      X(2)=SOLN2
      X(3)=SOLN3
      FMIN=SVMIN
      G(1)=G*V1
      G(2)=G*V2
      G(3)=G*V3
      GO TO 28
27 CONTINUE
C
C*****IER=0, A VALID MINIMUM WITHIN THE SPECIFIED TOLERANCE (EPS) WAS FOUND BY F
C*****FMFP
C*****IER=1, A MINIMUM WAS NOT FOUND IN THE SPECIFIED (LIMIT) NUMBER OF ITERATIO
C*****IER=-1, IMPLIES ERROR IN GRADIENT CALCULATION
C*****IER=2, LINEAR SEARCH CANNOT FIND MINIMUM
C
      IF (PRNTSW)301,401,301
301 CONTINUE
      IGOTO=IER+2
      GO TO(30,32,34,36),IGOTO
32 PRINT 33
33 FORMAT(///,60H VALID MINIMUM FOUND BY FMFP WITHIN SPECIFIED TOLERANCE EPS
      $NCE EPS )
      GO TO 38
30 PRINT 33
31 FORMAT(///,35H ERROR IN FMFP GRADIENT CALCULATION )
      GO TO 38
34 PRINT 35,LIMIT
35 FORMAT(///,86H ERR FCN COULD NOT BE MINIMIZED WITHIN THE SPECIFIED
      $ NR (LIMIT) OF ITERATIONS I LIMIT = ,I5)
      GO TO 38
36 PRINT 37
37 FORMAT(///,45H LINEAR SEARCH IN FMFP COULD NOT FIND MINIMUM)
38 CONTINUE
C*****PRINT INVERTED LAYER PARAMETERS AS WELL AS MINIMUM VALUE OF SUM-SQUARED
C*****ERROR FUNCTION
      PRINT 40,X,FMIN ,G
40 FORMAT(///,29H ITERATED VALUE OF RB (KM) = ,F6.2, 5X,
      $29H ITERATED VALUE OF RM (KM) = ,F6.2, 5X,
      $30H ITERATED VALUE OF FC (KHZ) = ,F8.4,/,
      $25H MIN SUM SQUARED ERROR = ,F10.5,/,
      $9H DEDRB = ,E12.5,5X,9H DENRM = ,E12.5,5X,9H DEDFC = ,E12.5)
      PRINT 51

```

```

50  FORMAT(//104H RANGE AND ELEVATION ANGLES CORRESPONDING TO THE NPTS B
    $ BACKSCATTER LEADING EDGE POINTS USED IN INVERSION ,/)
60  PRINT70,(I,FBSMES(I),RAN(I),BTA(I),I=1,NPTS)
70  FORMAT(3H F(,I2,4H) = ,F7.4,4H MHZ,5X,23HMIN GROUP RANGE (KM) = ,
    $F9.3,5X,30HMIN GROUP ELEV ANGLE (DEG) = ,F6.3)
401  CONTINUE
C*****HERE WE SAVE THE RESULTS OF THE PRESENT NPTS INVERSION
    RB(JARRAY)=X(1)
    RMM(JARRAY)=X(2)
    FCC(JARRAY)=X(3)
    NMIDL=NPTS/2+1
    FMID(JARRAY)=FBSMES(NMIDL)
    RANMID(JARRAY)=RAN(NMIDL)
    GPTHMD(JARRAY)=GPCMID
    JARRAY=JARRAY+1
100  CONTINUE
    EST=ESTSVE
101  CONTINUE
C*****PRINT OUT SUMMARY OF THE INVERTED BACKSCATTER IONOGRAM POINTS
    PRINT 700,NUSED,NPTS
700  FORMAT(14I,/,/,100(1H*),/,50H SUMMARY OF THE BACKSCATTER LEADING EDG
    $GE INVERSION,/,1X,12,8H SETS OF,12,44H OVERLAPPING SETS WERE SUCCE
    $$$SIVELY INVERTED,///)
    PRINT 710
710  FORMAT(84H      RB (KM)      RM(KM)      FC (MHZ)      FREQ (MHZ)      RANGE (KM)
    $ (KM)      MIN GROUP PATH (KM)  /)
    PRINT 720,(RBB(J),RMM(J),FCC(J),FMID(J),RANMID(J),
    $GPTHMD(J),J=1,NUSED)
720  FORMAT(2X,F9.3,1X,F10.3,F10.3,3X,F10.3,4X,F10.3,9X,F10.3)
    RETURN
    END

```

```

I NAME A7
I EQUIP=CARDRE,PRINTE,CARDPU;
  SUPRCUTINE DCAL(FC,RB,RM,FW,GP,D,GPTOL)
  RO=637.
  SINBET=(RB*RB-RO*RO-GP*GP/4.)/(RO*GP)
  BETA=ASINF(SINBET)
  BETA=0.0001
20 COSBET=COSF(BETA)
  SINBET=SINF(BETA)
  F=FW/FC
  FF=F*F
  YM=RM-RB
  RBYM2=RB*RB/(YM*YM)
  A=FF-1.+RBYM2
  B=-2.*RM*RBYM2
  C=RBYM2*RM*RM-FF*RO*RO+COSRET*COSBET
  U=R*B-4.*A*C
  GAM=ACOSF((RO/RB)*COSBET)
  SINGAM=SINF(GAM)
  COGAM=COSF(GAM)
  COTGAM=COSGAM/SINGAM
  SQA=SQRTF(A)
  V=2.*A*RB+B+2.*RB*F*SQA*SINGAM
  GPC=2.*(1.-FF/A)*RB*SINGAM-2.*RO*SINBET-(B*F/(2.*A*SQA))*LOGF
1(U/(V*V))
  IF (ABS(GPC-GP)-GPTOL) 100,100,50
50 DGPDB=2.*(1.-FF/A+R*FF/(A*V))*RO*SINBET*COTGAM
  I=2.*(1.-(2.*R*F*FF*RO*SINBET)/(SQA*U))*RO*COSBET
  PRINT 40,FW,GP,BETA,GPC,DGPDB,FC,RB,RM
40 FORMAT(6X,8F10.2)
  BETA=BETA+(GP-GPC)/DGPDB
  SINBET=SINF(BETA)
  GO TO 20
100 SQC=SQRTF(C)
  W=2.*SQC*F*RB*SINGAM+2.*C+R*RB
  D=(GAM,BETA)-(F*RO*COSBET/(2.*SQC))*LOGF(U*RB*RB/(W*W))
  D=2.*RO*D
  RETURN
  END

```

```
H NAME AR
H EQUIP=CARDRE,PRINTE,CARDPU;
  FUNCTION SQROO(ARG)
```

C

```
C*****SUBROUTINE SQROO CHECKS TO SEE IF WE ARE TRYING TO TAKE THE SQRT OF A NEG
C*****NUMBER. IF WE SO THEN AN ERROR CONDX IS FLAGGED AND THE ARG IS PRINTED OU
C*****WITH A MESSAGE... THE FLAGGING IS DONE BY SETTING SQROO = 9999.
C*****WITHOUT SUCH A SUBROUTINE THE G20 WILL SIGN YOU OFF IN A HURRY
C*****KEEPING US FROM GETTING TO ANY GOOD DATA
```

C

```
      IF(ARG)10,20,20
10     CONTINUE
      PRINT 15, ARG
15     FORMAT(29H SQRT ENTERED WITH NEG ARG =      ,E13.7)
      SQROC=9999.
      GO TO 30
20     SQROO=SQRT(ARG)
30     RETURN
      END
```

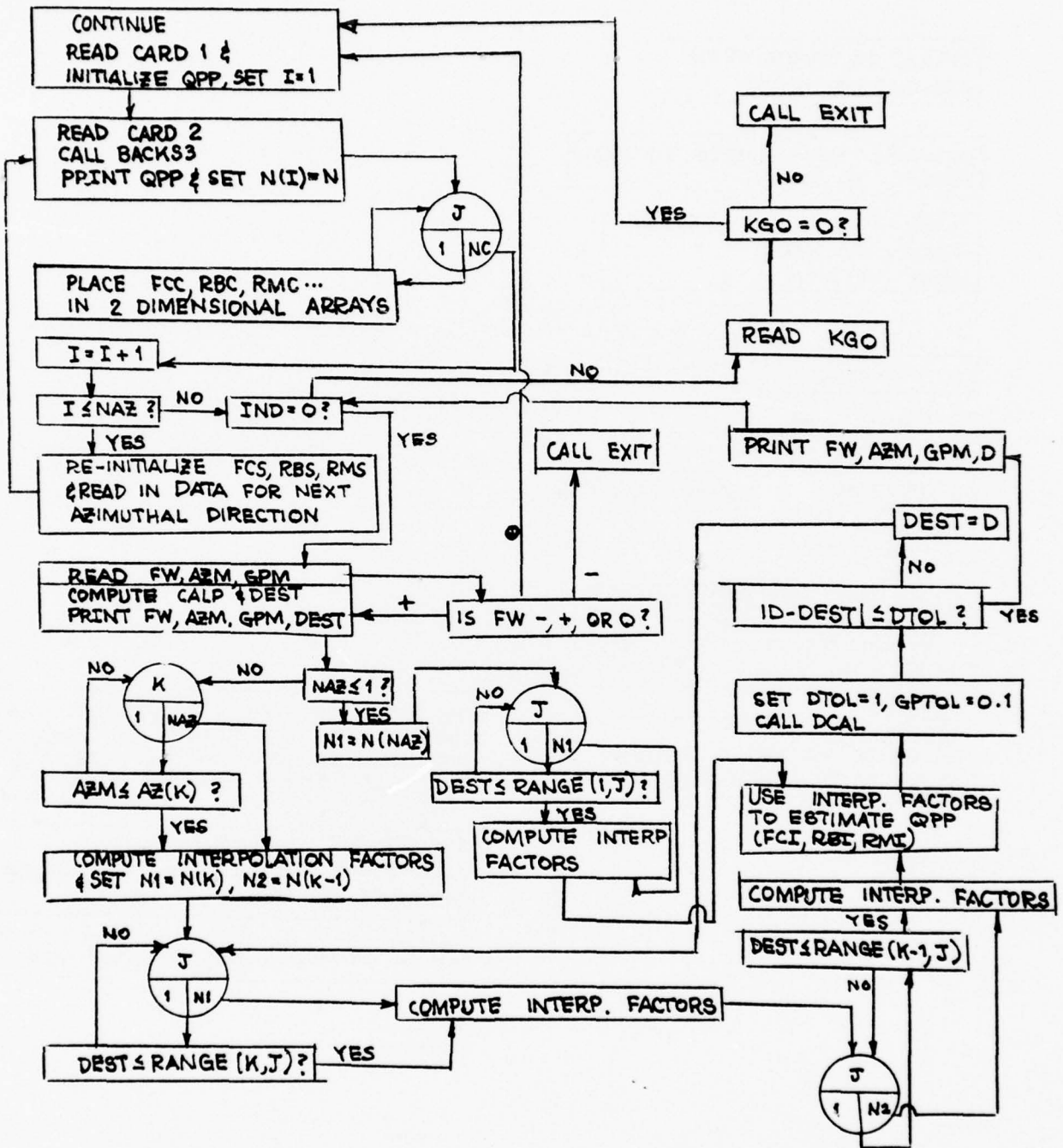


Figure A.3.1. Flow chart for main program.

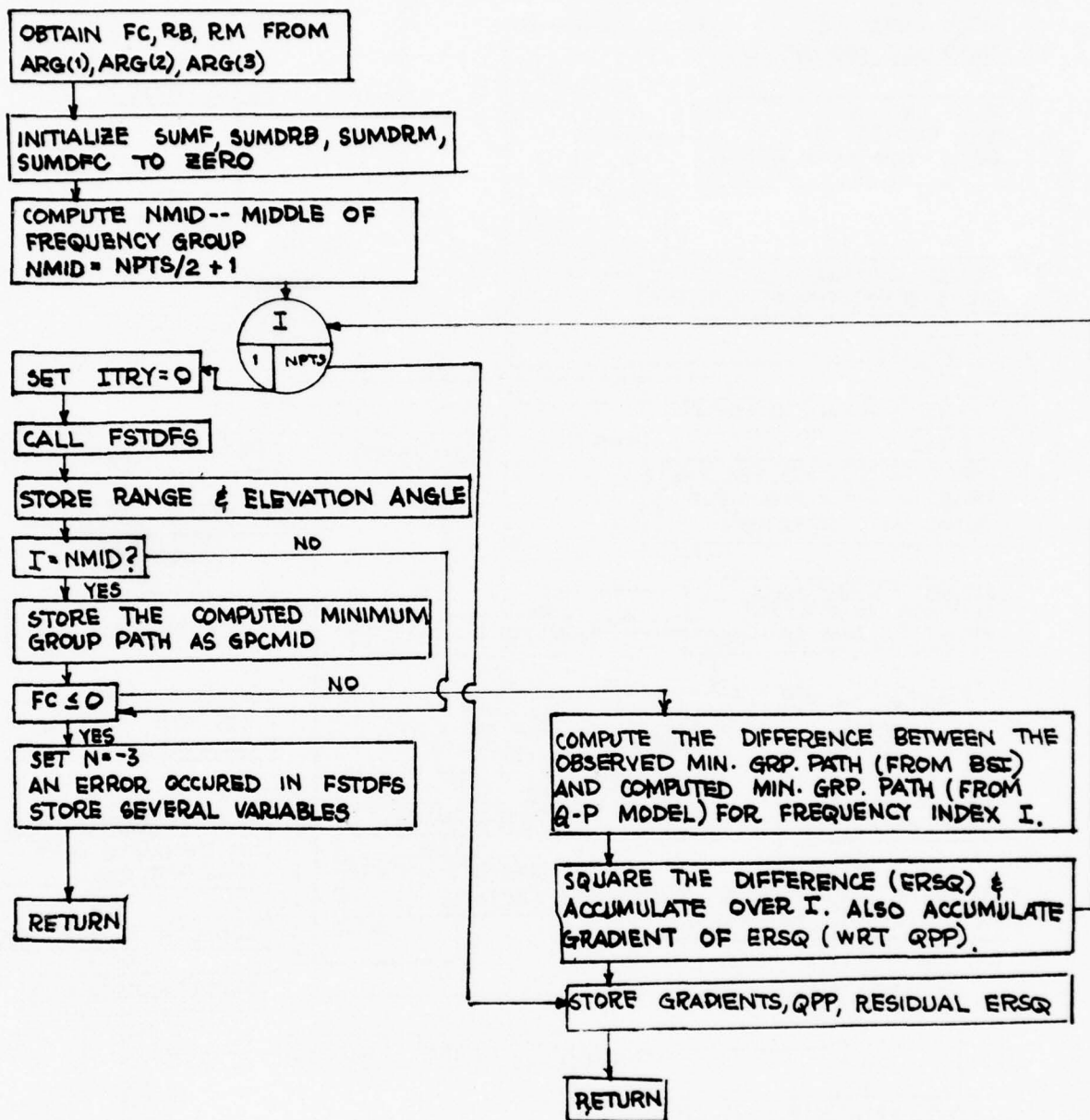


Figure A.3.2. Flow chart for subroutine FUNCT.

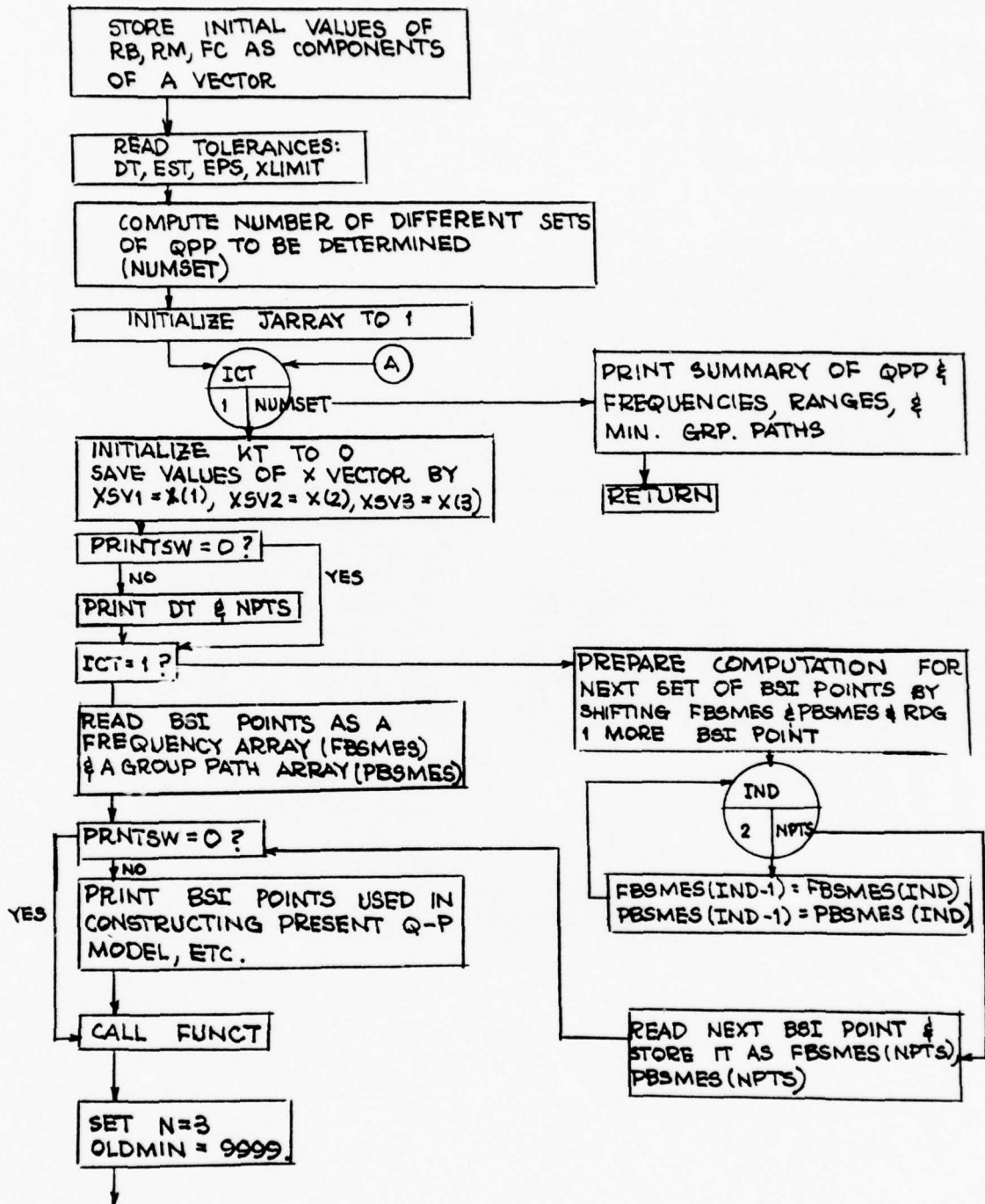


Figure A.3.3.a. Flow chart for subroutine BACKS3 (continued on next figure).

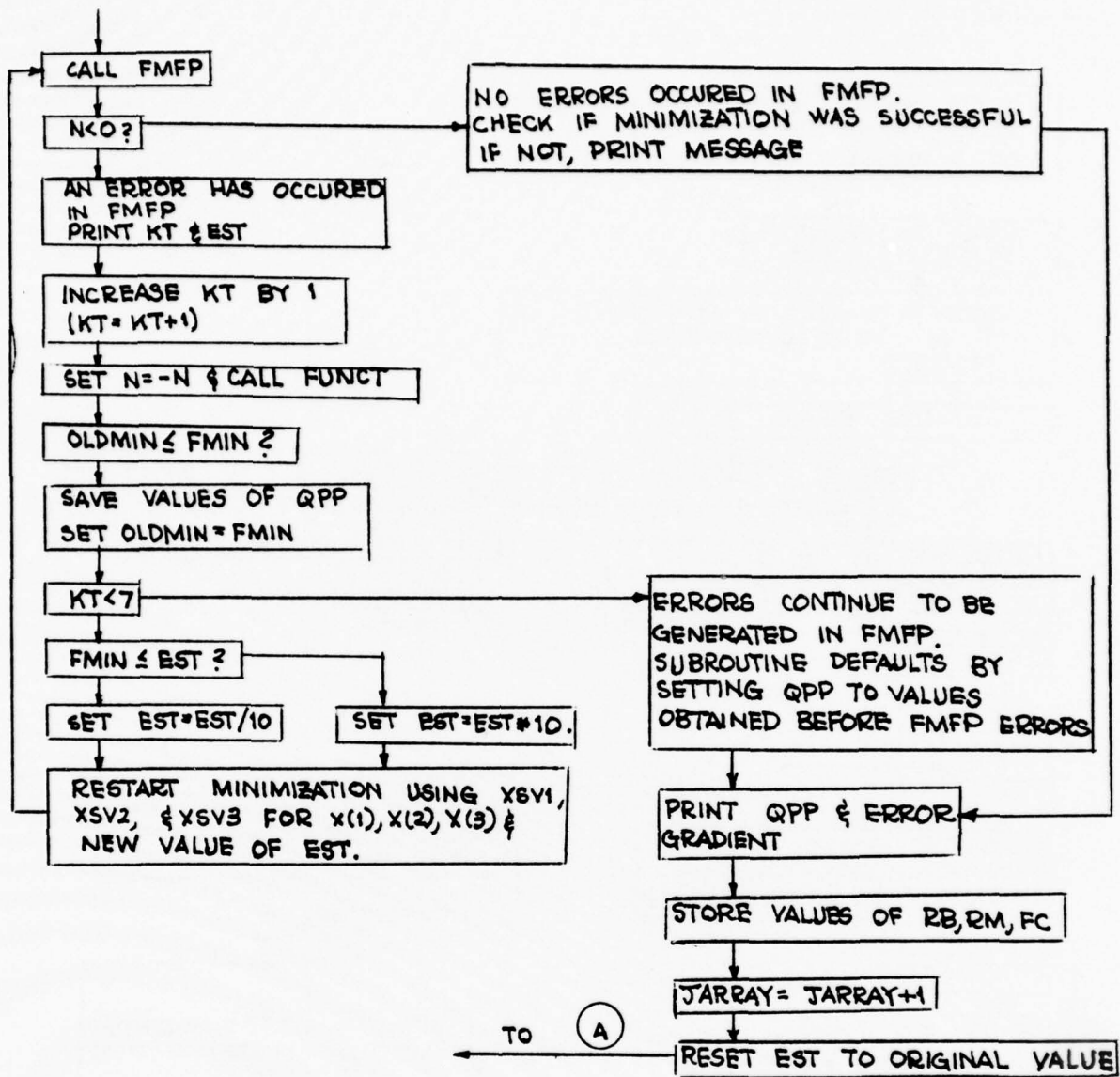


Figure A.3.3.b. Flow chart for subroutine BACKS continuation of Figure A.3.3.a).

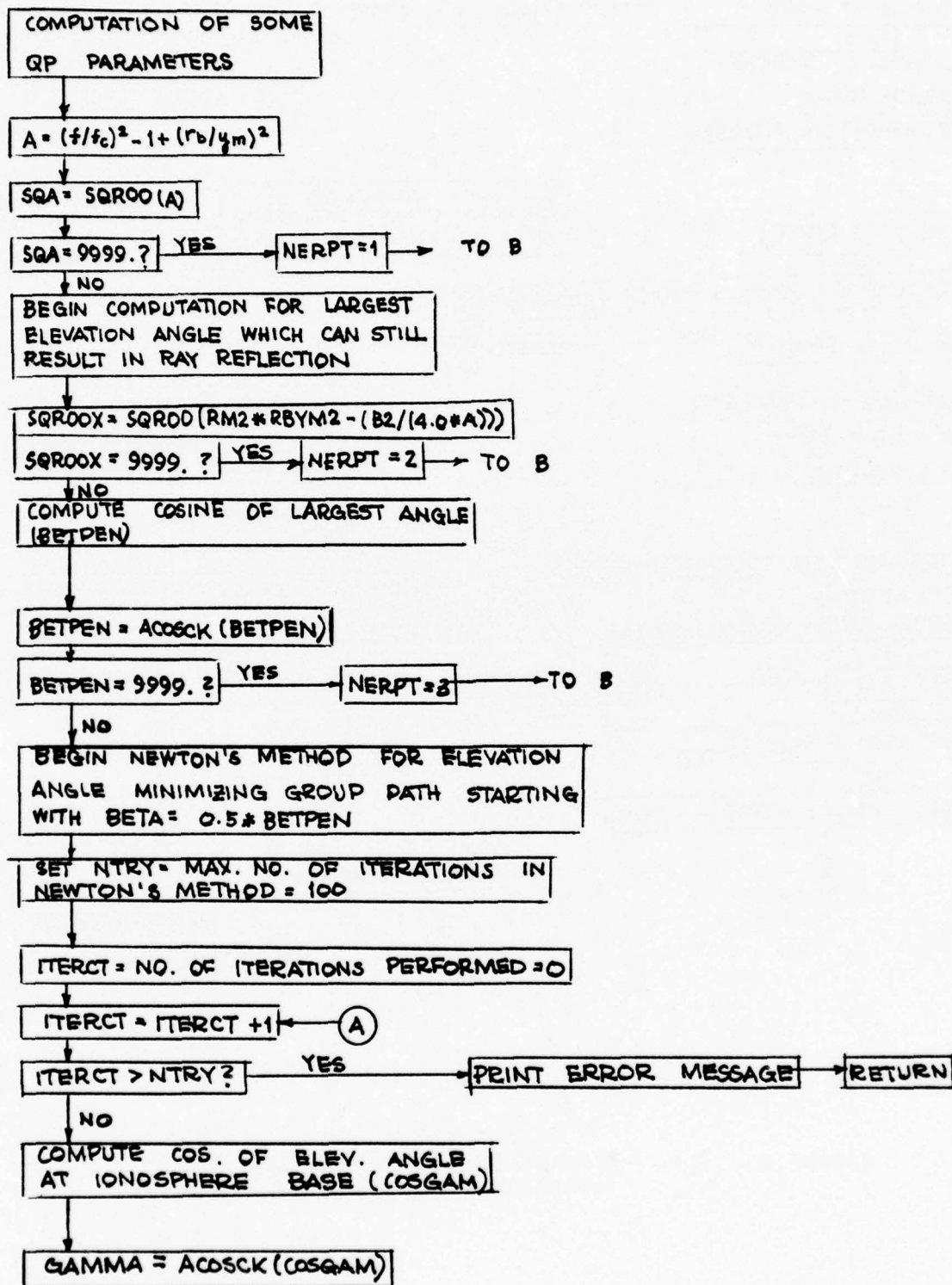


Figure A.3.4.a. Flow chart for subroutine FSTDFS (continued on next figure).

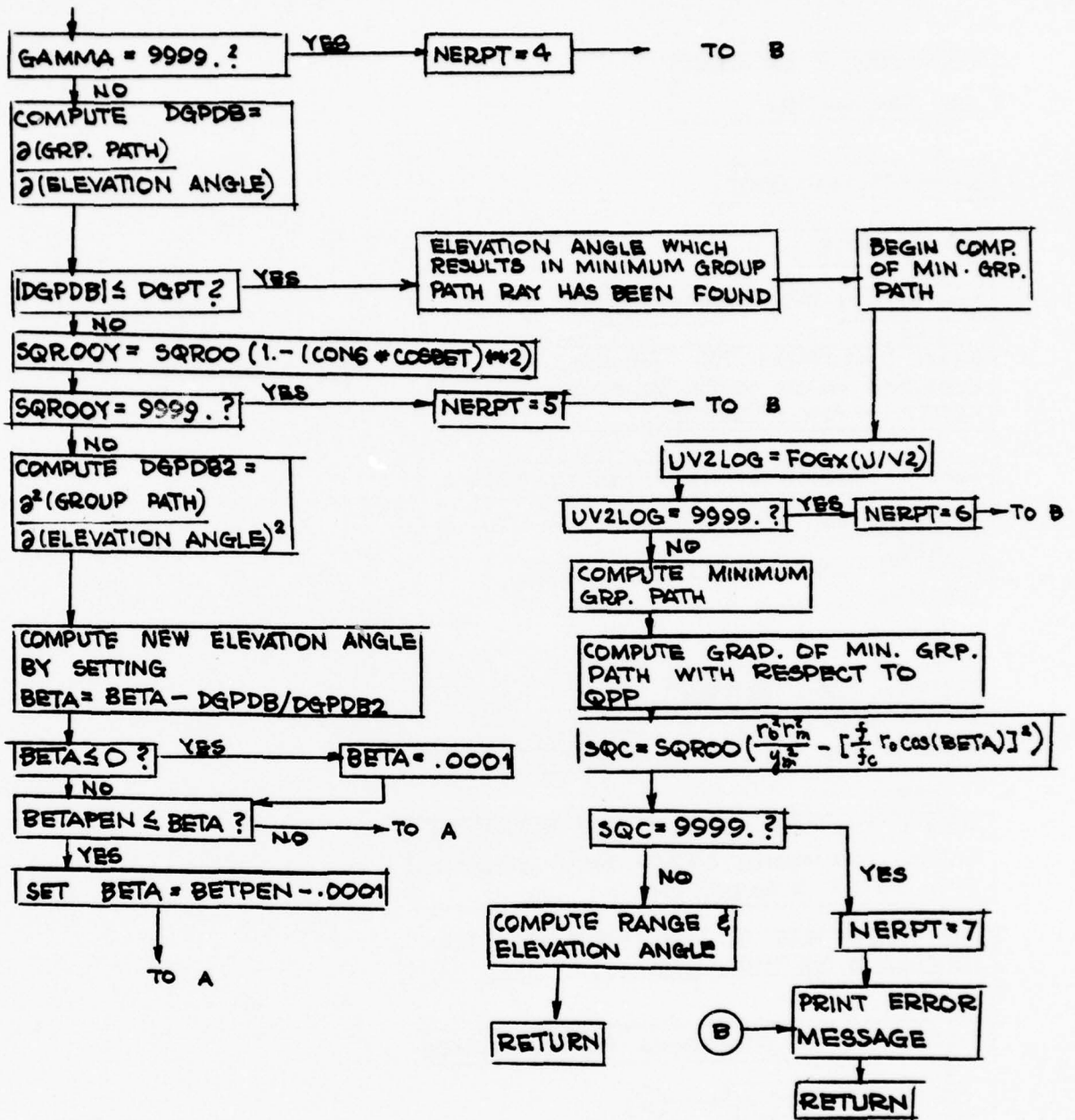


Figure A.3.4.b. Flow chart for subroutine FSTDFS
(continuation of Figure A.3.4.a).

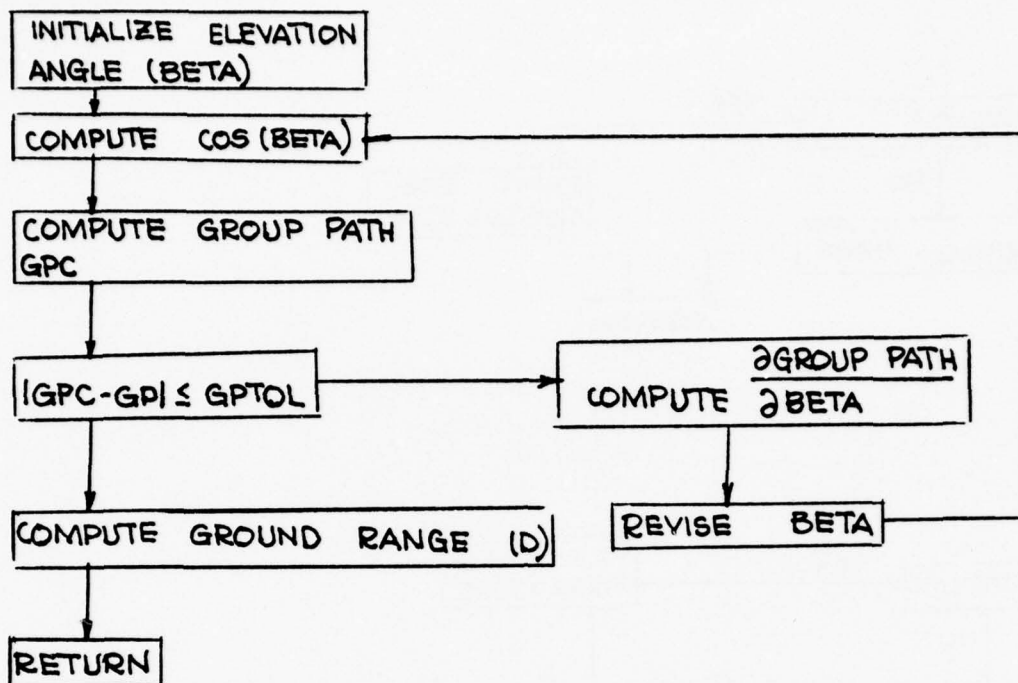


Figure A.3.5. Flow chart for subroutine DCAL.

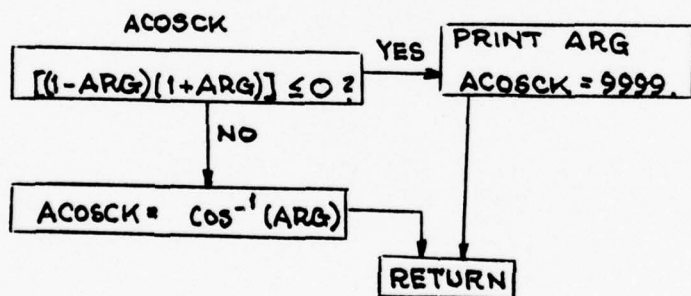
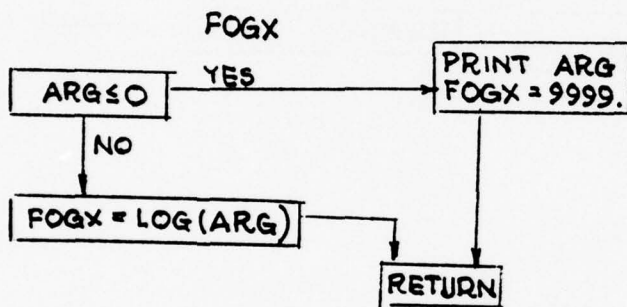
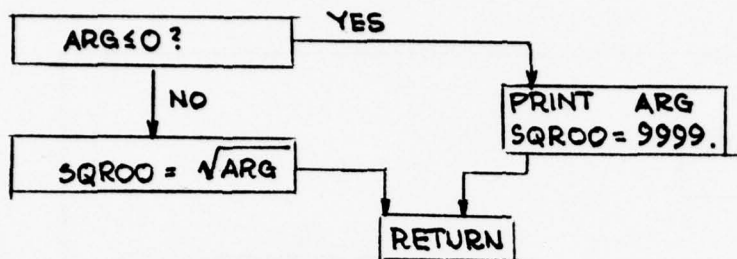


Figure A.3.6. Flow chart for special functions (square root, log, and \cos^{-1}).

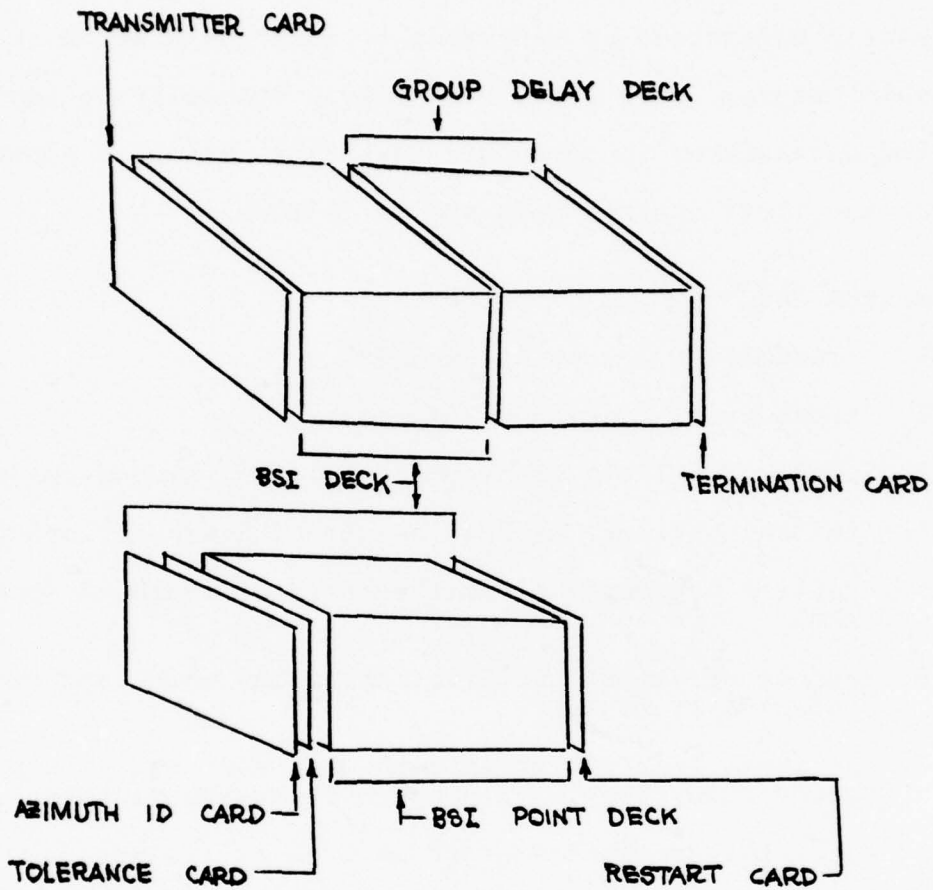


Figure A.3.7. Sequence of data cards.

The program formats are as follows

INPUT:

The input format shown in Figure A.3.7 can, perhaps, be more easily understood by referring to the flow diagram of the main program. The first card serves primarily to identify the backscatter ionogram sounder. The variables appearing on the first control card are as follows.

TRANSMITTER CARD:

1. transmitter latitude (degrees)
2. transmitter longitude (degrees)
3. initial estimate of overhead critical frequency (MHz)
4. initial estimate of base height of overhead ionosphere (km)
5. initial estimate of semithickness of overhead ionosphere (km)
6. number of azimuthal directions along which BSI are obtained (integer)
7. an index (ind) which is zero when the user is supplying group delay deck, and nonzero otherwise (integer)

The format of the transmitter card is 5F10.2, 11, 9X, 11 respectively.

The next set of cards comprise the BSI deck. The first card in this set is the azimuth identification card which contains

AZIMUTH ID CARD:

1. azimuth along which the following set of backscatter ionogram points have been obtained. (degrees)
2. the total number of backscatter ionogram points along the azimuth which will be read in. (integer)
3. the number of consecutive BSI points (less than or equal to the total number of BSI points) which will be considered simultaneously in obtaining a single net of QPP. (integer)

The format of the azimuth card is F10.2, I2, 8X, I2

TOLERANCE CARD:

1. tolerance of the deviation of the group path with respect to elevation angle (typically .05 km/rad.)
2. final step size control for minimization (typically .01)
3. desired final value of error in fitting QPP to measured BSI (typically .05 km/rad.)
4. maximum number of iterations which may be performed in fitting QPP to measured BSI (floating point)

The format of this card is 4F10.5.

BSI POINT DECK (SINGLE AZIMUTH)

There is one card for each measured point on the BSI along the given azimuthal direction. Each card contains:

1. frequency of BSI point (MHz)
2. group path of BSI point (km)

The format is 2F10.0.

USING THE RESTART CARD:

The restart card (format I10) is used only if $IND \neq 0$. When the user sets $IND \neq 0$ (referring to the main program flow chart) the program will not use the QPP to compute the ground range corresponding to a given group path. In fact, the program will go no further than the computation of QPP as performed by subroutine BACKS3. The only information on the restart card is the integer KGO. Setting KGO to zero (or, equivalently, using a blank card) tells the program to read in another batch of cards consisting of

1. TRANSMITTER CARD
2. AZIMUTH ID CARD
3. TOLERANCE CARD
4. BSI POINT DECK

and, if the new transmitter card has $IND=0$

5. GROUP DELAY DECK
6. TERMINATION CARD

Setting $KGO < 0$ will terminate the execution by telling the program that there is no more data to be processed.

NOT USING THE RESTART CARD:

The restart card should not be used when $IND=0$. Also, even when $IND \neq 0$ the restart card should not be used between BSI decks corresponding to the same transmitter card, but different azimuthal angles (multi-azimuth case). In this case, the last card of the BSI point deck is followed immediately by the:

1. AZIMUTH ID CARD
2. TOLERANCE CARD
3. BST POINT DECK

corresponding to the next azimuthal direction, with the data from the first transmitter card being used for all subsequent azimuthal angles. After the BSI point deck corresponding to the last azimuthal angle, the restart card is used to signify end of data ($KGO < 0$), or a new transmitter card ($KGO = 0$).

GROUP DELAY DECK:

The group delay deck provides the program with a specific value of group path from which to compute the ground range.

There is one card for each group path measurement to be used in this manner. Each card in the group delay deck contains:

GROUP DELAY DECK CARD:

1. frequency at which measurement is made (MHz)
2. azimuthal angle at which measurement is made (degrees)
3. measured value of group path (km)

The format is 3F10.0.

TERMINATION CARD:

After the last group delay deck card there must be a termination card, containing the parameter FW in F10.0 format. $FW < 0$ signifies end of data and terminates the program. $FW=0$ tells the program that more data will be read in, starting from the transmitter card and continuing in order to either a restart card or a new termination card.

SUMMARY OF THE BACKSCATTER LEADING EDGE INVERSION
 3 SETS OF n OVERLAPPING SETS WERE SUCCESSIVELY INVERTED

| PB (KM) | RM(KM) | FC (MHZ) | FREQ (MHZ) | RANGE (KM) | MIN GROUP PATH (KM) |
|----------|-----------|-----------|------------|------------|------------------------|
| 6618.919 | 6710.406 | 9.193 | 14.000 | 1061.038 | 1302.247 |
| 6632.230 | 6690.685 | 8.558 | 17.000 | 1449.758 | 1644.938 |
| 6601.425 | 6690.132 | 8.713 | 20.000 | 1877.891 | 2046.869 |
| A | | | | | |
| 9.1927 | 6618.918A | 6710.4062 | 1061.0383 | 1302.2466 | |
| 8.5580 | 6632.2304 | 6690.6846 | 1449.7578 | 1644.9381 | B |
| 8.7130 | 6601.4253 | 6690.1316 | 1877.8905 | 2046.8686 | |
| 16.00 | 52.00 | 1700.00 | 1676.31 | C | |
| 8.64 | 6615.93 | 6690.39 | D | | |
| 1A.00 | 1700.00 | n.00 | 3730.98 | -12739.52 | 8.64 6615.93 6690.39 |
| 1A.00 | 1700.00 | n.16 | 2271.71 | -6004.27 | 8.64 6615.93 6690.39 |
| 1A.00 | 1700.00 | n.25 | 1829.23 | -3462.60 | E 8.64 6615.93 6690.39 |
| 1A.00 | 1700.00 | n.29 | 1714.51 | -2700.21 | 8.64 6615.93 6690.39 |
| 1A.00 | 1700.00 | n.30 | 1700.28 | -2597.05 | 8.64 6615.93 6690.39 |
| 16.00 | 52.00 | 1700.00 | 1676.31 | 1557.09 | F |
| 8.60 | 6624.51 | 6690.55 | D | | |
| 1A.00 | 1700.00 | n.00 | 3780.11 | -12739.53 | 8.60 6624.51 6690.55 |
| 1A.00 | 1700.00 | n.16 | 2286.07 | -6003.18 | 8.60 6624.51 6690.55 |
| 1A.00 | 1700.00 | n.26 | 1832.05 | -3471.20 | E 8.60 6624.51 6690.55 |
| 1A.00 | 1700.00 | n.30 | 1714.65 | -2715.10 | 8.60 6624.51 6690.55 |
| 1A.00 | 1700.00 | n.30 | 1700.27 | -2613.88 | 8.60 6624.51 6690.55 |
| 16.00 | 52.00 | 1700.00 | 1557.09 | 1552.33 | F |
| 8.60 | 6624.85 | 6690.55 | D | | |
| 1A.00 | 1700.00 | n.00 | 3782.03 | -12739.53 | 8.60 6624.85 6690.55 |
| 1A.00 | 1700.00 | n.16 | 2286.62 | -6003.28 | 8.60 6624.85 6690.55 |
| 1A.00 | 1700.00 | n.26 | 1832.14 | -3471.84 | E 8.60 6624.85 6690.55 |
| 1A.00 | 1700.00 | n.30 | 1714.65 | -2716.14 | 8.60 6624.85 6690.55 |
| 1A.00 | 1700.00 | n.30 | 1700.27 | -2615.06 | 8.60 6624.85 6690.55 |
| 16.00 | 52.00 | 1700.00 | 1552.33 | 1552.15 | F |
| 16.00 | 52.00 | 1700.00 | 1552.15 | G | |

OUTPUT FORMAT:

Referring to the sample output which resulted from a single azimuth measurement, subroutine BACKS3 causes block A to be printed. Each row of block A contains RB, RM, FC, frequency, range, and minimum group path. Block B contains the same information as block A (except for frequency) and shows that the variables have been transferred from BACKS3 to the main program. Block C contains frequency, azimuth, measured group path and the first approximation to ground range in the subsequent attempt to compute the ground range from a given value of group path. Block D contains the interpolated values of QPP at the reflection point. Block E is printed out in subroutine DCAL and represents the progress of subroutine DCAL in homing a ray through the QP ionosphere model based upon group path. Each row of block E contains frequency, measured group path, initial elevation angle (β), computed group path, the derivative of group path with respect to β , and the three QPP describing the ionosphere. In the last row of block E, it can be seen that the computed and measured group paths are very close, so DCAL returns to the main program. Upon returning to the main program block F is printed and contains frequency, azimuth, measured group path, estimated ground range, and ground range based upon the homed in value of the initial ray elevation angle. Since these two ground ranges are so different a new interpolation procedure is initiated in the main program to compute the values of QPP at the reflection point of the homed in ray. This interpolation is summarized in block D, and comparing the first block D with

the second block D, we can see that the QPP at the reflection point are indeed different when computed for the homed in ray. This leads to an iterative process which alternates between subroutine DCAL, and the recomputation of the interpolated QPP. The final block F shows, however that the most recent computed ground range, and the ground range from the previous iteration are very close. Thus, block G is printed in the main program and contains the frequency, azimuth, group path and final solution for the ground range.

APPENDIX 4

A Method for Inverting Oblique Sounding Data
in the Ionosphere

by S. I. Chuang and K. C. Yeh

This paper has been submitted to Radio Science.

A METHOD FOR INVERTING OBLIQUE
SOUNDING DATA IN THE IONOSPHERE

S. L. Chuang and K. C. Yeh^{*}
Department of Electrical Engineering
National Taiwan University

We have developed in this paper a method of inverting backscatter leading edge ionograms and fixed distance oblique ionograms to obtain ionization profiles. The problem of ionogram inversion is first formulated in such a way that the Backus-Gilbert technique can be applied. This inversion technique starts by assuming an initial profile based on available knowledge. Oblique group paths are computed by using this initial profile and are compared with the experimental data. The discrepancy in group path is used as a basis for improving the profile and thus an iterative procedure is developed. This iteration is continued until an optimum solution is found. As is well-known, when ionograms are given at discrete frequencies there may exist an infinite number of profiles that will yield the observed group path data. Among this infinite number of solutions there is an optimum one in the sense that its fractional departure from the initially assumed profile is a minimum in terms of value at boundaries and in terms of the profile curvature. The method is then applied to the special vertical incidence case and reasonably fast convergence is obtained. This success demonstrates the promise of this method in inverting oblique sounding data.

* Permanent address: Department of Electrical Engineering, University of Illinois.

1. INTRODUCTION

In ionospheric sounding one usually measures the wave parameters, such as transit time, frequency shift, polarization, power returned, etc. One wishes then to make use of these measured wave parameters to deduce the physical parameters of the ionosphere, such as electron density, temperature, motion, etc. In order to deduce these physical parameters one must make use of a theory, known as the inversion theory, to relate these desired physical parameters to wave parameters. Sometimes the inversion is quite simple; sometimes the inversion can be quite complex. A case in point is the inversion of vertical ionograms, e.g., [Budden, 1961, p. 161], where the virtual height $h'(f)$ as a function of frequency f is measured and the true ionization profile $N(h)$ is desired. From wave propagation studies one realizes that h' is a nonlinear functional of N and as such it is in general very difficult to solve. Fortunately for the case of vertical ionograms with magnetoionic effects ignored, the integral can be put in the form of a convolution type which can then be solved, for example, by Laplace transform, provided that $N(h)$ increases monotonically with height. Now if one wishes to sound obliquely in order to obtain the profile some distance away from the local vertical, the integral is no longer of the convolution type. In this case, since the group delay is a nonlinear functional of $N(h)$, the inversion becomes very difficult. Current techniques are largely numerical and are designed to obtain a model profile that will yield data approximating the measured data.

However, ionospheric investigations have been carried out for several decades. The accumulated knowledge enables us to make a zeroth-order guess about the profile. If this zeroth-order profile does not depart appreciably from the true profile, it is possible to reformulate the problem by a linearization procedure. This reformulated problem is much simpler to deal with

because it is now linear. Many mathematical techniques applicable to linear problems can be used in order to arrive at a solution. Our approach is similar to that used in geophysics for inverting seismic data [Backus and Gilbert, 1967].

2. FORMULATION

For simplicity we will ignore the magnetoionic effects completely. The ionosphere is assumed to be spherically stratified so that the Bouguer's rule applies at any point along the ray, i.e.,

$$r_0 \cos \phi_0 = rn \cos \phi = r_t n_t = \text{constant} \quad (1)$$

where r is the geocentric distance of a point along the ray, $n = n(r)$ is the refractive index and $\phi = \phi(r)$ is the elevation angle of the ray. The earth radius is r_0 at which $\phi_0 = \phi(r_0)$. The ray is reflected with a geocentric distance r_t at which $n_t = n(r_t)$ and $\phi(r_t) = 0$. The group path of an ionospherically reflected signal is

$$P = 2 \int_{r_0}^{r_b} ds + 2 \int_{r_b}^{r_t} ds/n \quad (2)$$

This integral is integrated along the ray from r_0 to the bottom of the ionosphere at r_b in free space and then from r_b to r_t in the ionosphere. In the ionosphere the refractive index is related to the electron density profile $N(r)$ through

$$n^2 = 1 - kN/f^2 \quad (3)$$

where f is the radio frequency and $k = e^2/4\pi^2 m\epsilon_0$ has a numerical value 80.6 in S.I. units. It is easily seen from (2) that P is a nonlinear functional of N . We are not aware of any analytic method that can be used to solve for N .

Therefore, we will adopt a perturbation scheme to linearize the problem. Our approach is similar to that used in inverting teleseismic ray data [Johnson and Gilbert, 1972].

Perturbations in P can come from two sources: perturbations in n and perturbations in ϕ_0 . Taking the variation in (2) and linearizing, we obtain

$$\delta P = 2 \int_{r_b}^{r_t} \frac{-\delta n}{n^2} ds + \frac{\partial P}{\partial \phi_0} \delta \phi_0 \quad (4)$$

In practice two kinds of oblique sounding data can be obtained: backscatter leading edge and oblique ionogram. For a thorough review on the nature of these data, the reader is referred to Davies [1965]. We discuss both of these cases for our purpose in the following.

(i) Backscatter leading edge.

The backscattered leading edge has a minimum time delay. In this case $\partial P / \partial \phi_0 = 0$ and the variation in group path is caused entirely by variations in the refractive index. The variation in n can be related to the variation in N by using (3). Substituting (3) and (1) in (4) yields

$$\delta P = \int_{r_b}^{r_t} K'_1 x \, dr \quad (5)$$

where

$$x = \delta N / N \quad (6)$$

and

$$K'_1 = krN/f^2(1 - kN/f^2)[(1 - kN/f^2)r^2 - r_0^2 \cos^2 \phi_0]^{1/2} \quad (7)$$

The kernel K'_1 can be computed from the model ionosphere and is therefore known. We note in (5) that δP is a linear functional of δN .

(ii) Oblique ionogram

The oblique ionogram gives the group path of ionospherically reflected signals as a function of frequency for a fixed ground distance D . The ground distance is

$$D = 2r_0^2 \cos \phi_0 \left[\int_{r_0}^{r_b} \frac{dr}{r\sqrt{r^2 - r_0^2 \cos^2 \phi_0}} + \int_{r_b}^{r_t} \frac{dr}{r\sqrt{n^2 r^2 - r_0^2 \cos^2 \phi_0}} \right]. \quad (8)$$

As the ionization profile is varied by δN , the initial elevation angle of the ray must also be varied by $\delta \phi_0$ in order to keep D fixed. Take the variation of (8) and set it to zero to produce

$$\delta \phi_0 = \left[2r_0^2 \cos \phi_0 \int_{r_b}^{r_t} \frac{-kr \delta N dr}{2n^2 f^2 r^2 (n^2 r^2 - r_0^2 \cos^2 \phi_0)^{1/2}} \right] / \frac{\partial D}{\partial \phi_0}. \quad (9)$$

Inserting (9) in (4), the variation in group path of an oblique ionogram is found to be

$$\delta P = \int_{r_b}^{r_t} K_2' x dr \quad (10)$$

where the known kernel is

$$K_2' = K_1' \left[1 - \left(r_0^2 \cos \phi_0 / r^2 \right) (\partial P / \partial \phi_0) / (\partial D / \partial \phi_0) \right]. \quad (11)$$

Comparing (5) and (10), one notes that for both kinds of oblique data, the variation in group path is given by

$$\delta P(f) = \int_{r_b}^{r_t} K'(r, f, \phi_0) x(r) dr \quad (12)$$

where for backscatter leading edges $K' = K_1'$, and for oblique ionograms $K' = K_2'$.

The kernel K' is referred to as the Frechet kernel [Backus and Gilbert, 1967; Green, 1975] because δP is obtained by taking the Frechet differential of (2). Our objective is to obtain the optimum x in some sense. We do this by following the Backus-Gilbert approach in the following section.

3. OPTIMIZATION

Suppose the oblique sounding data have been measured experimentally at M frequencies f_i , $i = 1, 2, \dots, M$. The corresponding group paths are P_{mi} , $i = 1, 2, \dots, M$. For the purpose of obtaining the ionization profile $N(r)$ that produces these experimental data, we make use of our knowledge based on past experience to construct a zeroth-order approximation to the true ionization profile. This approximate profile is then used to compute M group paths P_{ci} , for M frequencies f_i , and M initial elevation angles ϕ_{oi} . The departure of the computed group path P_{ci} from the experimentally measured group path P_{mi} is y_i , i.e., $y_i = P_{ci} - P_{mi}$. Then according to (12),

$$y_i(f_i) = \int_{r_b}^{r_p} K_i(r, f_i, \phi_{oi}) x(r) dr \quad i = 1, 2, \dots, M \quad (13)$$

where r_p is the peak height of the ionosphere. The Frechet kernel K_i is given by

$$K_i(r, f_i, \phi_{oi}) = \begin{cases} K_1'(r, f_i, \phi_{oi}) & r_b \leq r \leq r_{ti} \\ 0 & r_{ti} \leq r \end{cases}, \quad (14)$$

for backscatter leading edges, and, for oblique ionograms,

$$K_i(r, f_i, \phi_{oi}) = \begin{cases} K_2'(r, f_i, \phi_{oi}) & r_b \leq r \leq r_{ti} \\ 0 & r_{ti} \leq r \end{cases} \quad (15)$$

where r_{ti} is the geocentric distance of reflection for f_i . In later development K_i will be required to be square integrable. However, since both K_1' and K_2' have singularities at the point of reflection, K_i is obviously not square integrable. This difficulty can be remedied by integrating (13) by parts twice, as suggested by Johnson and Gilbert [1972], to produce

$$y_i = -H_i(r_b)x(r_b) - G_i(r_p)x'(r_p) + \int_{r_b}^{r_p} G_i(r)x''(r) dr \quad (16)$$

$$i = 1, 2, \dots, M$$

where

$$x'(r) = dx/dr$$

$$x''(r) = d^2x/dr^2$$

$$H_i(r) = \int_{r_p}^r K_i(r', f_i, \phi_{oi}) dr'$$

$$G_i(r) = \int_{r_b}^r H_i(r') dr' \quad (17)$$

Now our original nonlinear inversion problem is reduced to the linear problem of (16) in which we have M data points to determine $x''(r)$. In general, the solution to (16) is nonunique. Among this infinite number of solutions is a particular one for which

$$\frac{1}{2} \left\{ x^2(r_b) + x'^2(r_p) + \int_{r_b}^{r_p} [x''(r)]^2 dr \right\} = \text{minimum} \quad (18)$$

This solution, if it exists, is the optimum solution we seek. It is optimum in the sense that the constraint condition (18) is satisfied and that the errors in $x(r_b)$ and $x'(r_p)$ are minimized and the profile $x(r)$ is very smooth since the square of its cumulative curvature over the interval $[r_b, r_p]$ is minimized. Notice that we have chosen to deal with fractional departures of

electron density here as x is defined by (6). But it is possible to introduce any other reasonable weighting function on δN if so desired by modifying the definition of the Frechet kernel as done by Green [1975]. Such weighting may be desirable in cases where parts of data are known a priori more accurately than others, and hence deserve more weight.

The optimum solution can be found easily by introducing Lagrange multipliers v_i . Carrying out the process of minimization, the solutions are found to be

$$x''(r) = \sum_{i=1}^M v_i G_i(r) \quad (19a)$$

$$x'(r_p) = - \sum_{i=1}^M v_i G_i(r_p) \quad (19b)$$

$$x(r_b) = - \sum_{i=1}^M v_i H_i(r_b) \quad (19c)$$

Insertion of (19) into (16) yields

$$y_i = \sum_{j=1}^M v_j \left[H_i(r_b) H_j(r_b) + G_i(r_p) G_j(r_p) + \int_{r_b}^{r_p} G_i(r) G_j(r) dr \right]. \quad (20)$$

Equation (20) can be put in a very compact form if the following vector notations are used. Let the column vectors be

$$\vec{v} = \begin{bmatrix} v_1 \\ v_2 \\ \vdots \\ v_M \end{bmatrix} \quad \vec{y} = \begin{bmatrix} y_1 \\ y_2 \\ \vdots \\ y_M \end{bmatrix} \quad (21)$$

and the symmetric $M \times M$ matrix $A = [A_{ij}]$ have an ij th element

$$A_{ij} = H_i(r_b)H_j(r_b) + G_i(r_p)G_j(r_p) + \int_{r_b}^{r_p} G_i(r)G_j(r) dr \quad (22)$$

Then (20) becomes simply

$$\vec{y} = A\vec{v} \quad (23)$$

For independent data, $\det A \neq 0$, and (23) can be inverted to give \vec{v} . Knowing \vec{v} , (19a) reduces to

$$x''(r) = (A^{-1}\vec{y})\vec{G}(r) \quad (24)$$

where $\vec{G}(r)$ is a column vector whose i th element is $G_i(r)$. Equation (24), together with the boundary conditions (19b) and (19c), enables us to compute $x(r)$ by integrating (24) twice. Once $x(r) = \delta N/N$ is determined, the desired correction δN to the zeroth-order model $N(r)$ is known. Computations can then be started anew by using the new model, $N(r) + \delta N(r)$, to produce eventually a second correction. Thus an iteration procedure is established. By repeated iteration, a final optimum solution can be achieved. At each step we may check the value

$$x^2(r_b) + x'^2(r_p) + \int_{r_b}^{r_p} [x''(r)]^2 dr = \vec{v}^T A \vec{v} \quad (25)$$

When this value is less than a certain specified small value, the iteration procedure may be terminated. The final profile $N(r)$ will be the desired optimum electron density profile for the set of data P_{mi} , $i = 1, 2, \dots, M$.

4. VERTICAL INCIDENCE

As mentioned earlier, the vertical ionogram can be inverted exactly if the ionization profile increases monotonically with height. However, for the sake of completeness, we will also work out our scheme for this particular

case. Since the vertical incidence case is easier to manage analytically, a numerical example will be given in the next section to illustrate the computational procedures involved.

For vertical incidence the initial elevation angle ϕ_0 is 90° . The once-integrated Frechet kernel $H_i(r)$ no longer exists at $r = r_{ti}$ since the singularity of K'_1 at r_{ti} as given by (7) is now of higher order. Close attention must be paid in order not to allow singularities to get out of hand. This can be done by a slight modification. Taking the Frechet differential of (2) as before, except for the vertical incidence case, ds is replaced by dr and one obtains

$$y = \delta P = \int_{r_b}^{r_t} K(r)x(r) dr \quad (26)$$

with

$$x(r) = \delta n / (n + \delta n) \quad (27)$$

$$K(r) = -2/n . \quad (28)$$

Now (26) is identical in form to (13). An identical procedure can be followed by first integrating by parts twice and setting up the minimization process similar to that given in the last section to obtain x . After knowing $x(r)$, (27) and (3) can be used to find the perturbed ionization profile required through

$$\delta N(r) = (1 - kN/f^2)[1 - (1 - x)^{-2}]f^2/k . \quad (29)$$

If one wants, a new model $N(r) + \delta N(r)$ can be used to replace the initial model $N(r)$, and the computations are repeated. Thus an iteration procedure is established as before. This iteration can be terminated when the error is smaller than some specified value.

5. AN EXAMPLE

For purposes of illustration, we shall assume a parabolic layer

$$N_p(z) = N_m [1 - (z - Y)^2/Y^2] \quad 0 < z < 2Y \quad (30)$$

as the true ionization profile. For simplicity the vertical coordinate z starts at the bottom of the ionosphere and the ionosphere has a semithickness Y . In this case the measured group path (equal to twice the group height) is

$$P_m = Y(f/f_c) \ln[(f_c + f)/(f_c - f)] \quad (31)$$

where f_c is the critical frequency.

Suppose as an initial guess of the profile we assume a linear profile

$$N_l(z) = az \quad 0 < z \quad (32)$$

A signal of frequency f incident vertically is reflected at a height $z_t = f^2/ka$. Its corresponding group path is

$$P_c = 4z_t \quad (33)$$

The Frechet kernel (28) becomes, for this initial profile,

$$K(z) = -2/(1 - z/z_t)^{1/2} \quad (34)$$

The corresponding once-integrated and twice-integrated Frechet kernels can be computed easily as

$$H(z) = \int_{z_t}^z K(z) dz = 4z_t(1 - z/z_t)^{1/2} \quad (35)$$

and

$$G(z) = \int_0^z H(z) dz = -(8z_t^2/3)[(1 - z/z_t)^{3/2} - 1] \quad (36)$$

With (36) substituted into (19a), we obtain the solution $x''(z)$. Integrate the resulting expression twice, constrained by the boundary conditions (19b) and (19c), and we obtain

$$x(z) = -\nu(8z_t^2/3) \left[\frac{4z_t^2}{35} \left(1 - \frac{z}{z_t} \right)^{7/2} - \frac{z^2}{2} + (z_t + 1)z + \left(\frac{3}{2z_t} - \frac{4z_t^2}{35} \right) \right]. \quad (37)$$

The Lagrange multiplier ν in (37) is computed from

$$\nu = A^{-1}y \quad (38)$$

where $y = P_c - P_m$ is the difference of time delay in a linear model profile (32) from that in a true parabolic profile (30) at frequency f , and A is computed from the expression

$$A = 16z_t^2 + (64/9)z_t^4 + (16/5)z_t^5 \quad (39)$$

by using formula (22). After knowing $x(z)$, it is then inserted in (29) to produce $\delta N(z)$. Computations can be repeated anew by using $N(z) + \delta N(z)$ as the model profile, except now the corrected model profile is not necessarily linear so that a numerical scheme may have to be developed. One possibility is to use a piecewise linear model.

Let us now adopt some numerical values. We take, for the true (parabolic) profile $Y = 100$ km, $N_m = 10^{12}$ el/m³. Then at a frequency $f = 8.693$ MHz, we obtain from (31) $P_m \cong 400$ km. For the model (linear) profile, we take $a = 1.25 \times 10^{10}$ el/m³/km, which gives $P_c \cong 300$ km at the same frequency. This gives an error in group path of $y = P_c - P_m = -100$ km. Substitute these numerical values in (37) to obtain $x(z)$ which, when inserted in (29), gives us the perturbed $\delta N(z)$ required to reduce the error. The results are shown graphically in Figure 1. It is seen that by using data only at one frequency, the once-iterated profile $N_\ell + \delta N$ approaches the true profile N_p reasonably fast.

6. CONCLUSION

We have outlined in this paper a method whereby ionospheric profiles can be deduced from oblique sounding data. The method starts by assuming a guessed zeroth-order profile based on our past experience and the accumulated knowledge about the ionosphere. An iterative scheme has been worked out to enable us to improve the computed profiles until the errors are smaller than some specified value. As an illustration the method is applied to the vertical incidence case, which shows reasonably fast convergence. Encouraged by this success, we would like to suggest that more extensive numerical computations be carried out.

ACKNOWLEDGEMENT

The major part of this research was carried out while K. C. Yeh was visiting the National Taiwan University with the support of the National Science Council, Republic of China. The work was finished at the University of Illinois with the support of the Deputy for Electronic Technology (RADC-ETEI), Hanscom AFB, MA, under Contract F19628-75-C-0088. Professor Yeh would like to express his appreciation to Professors T. S. Kuo and K. H. Pai of the National Taiwan University for their hospitality.

FIGURE CAPTION

Figure 1. Illustrating convergence of the iterative procedure. The parabolic profile N_p is assumed to be the real profile. The linear profile N_ℓ is the initial guess. The one-iterated profile is $N_\ell + \delta N$.

REFERENCES

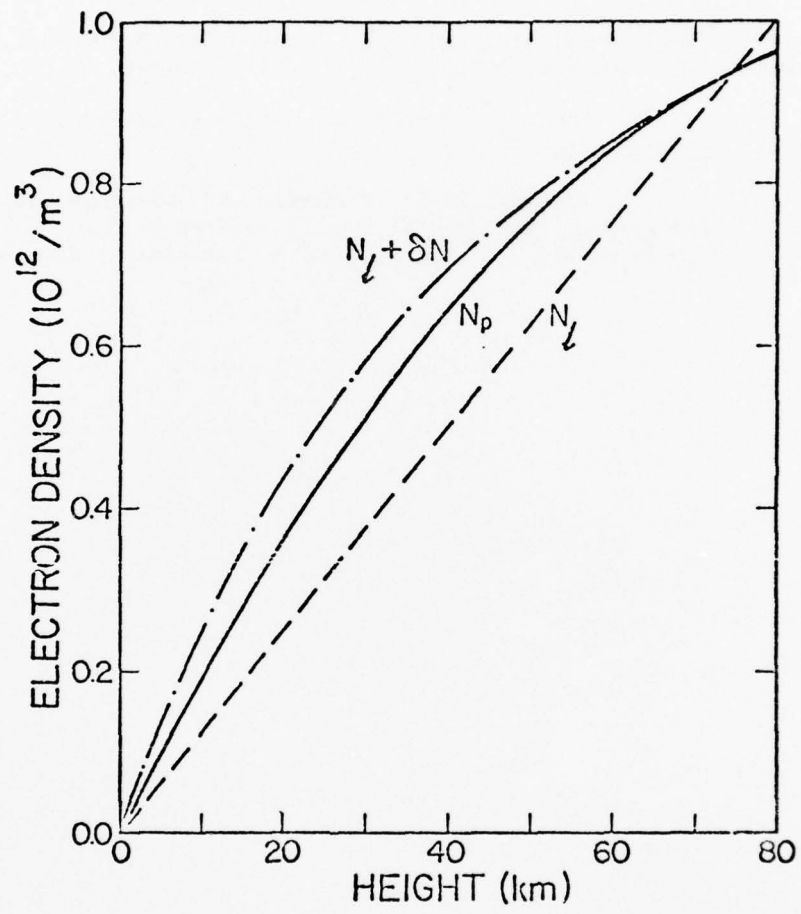
Backus, G. E. and J. F. Gilbert (1967), Numerical application of a formalism for geophysical inverse problems, Geophys. J., 13, 247-276.

Budden, K. G. (1961), Radio Waves in the Ionosphere, Cambridge University Press, New York.

Davies, K. (1965), Ionospheric radio propagation, National Bureau of Standards Monograph 80, U.S. Government Printing Office, Washington, D. C.

Green, W. R. (1975), Inversion of gravity profiles by use of a Backus-Gilbert approach, Geophysics, 40, 763-772.

Johnson, L. E. and F. Gilbert (1972), Inversion and inference for teleseismic ray data, in Methods in Computational Physics, edited by B. A. Bolt, vol. 12: Seismology, Body Waves and Sources, pp. 231-266, Academic Press, New York.



REFERENCES

- Booker, H. G., "Fifty years of the ionosphere. The early years - Electromagnetic theory", J. Atmos. Terr. Phys., 36, 2113-2136, 1974.
- Breit, G. and M. A. Tuve, "A test for the existence of the conducting layer", Phys. Rev., 28, 554-575, 1926.
- Croft, T. A. and H. Hoogasian, "Exact ray calculation in a quasiparabolic ionosphere with no magnetic field", Radio Sci. 3, 69-74, 1968.
- Fletcher, R. and M. J. D. Powell, "A rapidly convergent descent method for minimization", Computer Journal, 6, 163-168, 1963.
- Manning, L. A., "The determination of ionospheric electron distribution", Proc. IRE, 35, 1203-1207, 1947.
- Rao, N. N., "Bearing deviation in HF transionospheric propagation, 1. Exact computations for some ionospheric models with no magnetic field", Radio Sci. 3, 1113-1117, 1968.
- Rao, N. N., "Synthesis of three-dimensional oblique ionograms", Radio Sci., 8, 449-451, 1973.
- Rao, N. N., "Inversion of sweep-frequency sky wave backscatter leading edge for quasiparabolic ionospheric layer parameters", Radio Sci., 9, 845-847, 1974.
- Rao, N. N., "Analysis of discrete oblique ionogram traces in sweep-frequency sky wave high resolution backscatter", Radio Sci., 10, 149-153, 1975.
- Waynick, A. H., "Fifty years of the ionosphere: The early years--Experimental", J. Atmos. Terr. Phys., 2105-2112, 1974.